UNIVERSIDAD NACIONAL AUTÓNOMA DE MÉXICO

DOCTORADO EN CIENCIAS BIOMÉDICAS
INSTITUTO DE FISIOLOGÍA CELULAR

PAPEL DE LAS ESPECIES REACTIVAS DE OXÍGENO EN EL DESARROLLO DE LAS NEURONAS GRANULARES DE CEREBELO

TESIS
QUE PARA OPTAR POR EL GRADO DE:
DOCTOR EN CIENCIAS

PRESENTA:
MAURICIO ALEJANDRO OLGUÍN ALBUERNE

DIRECTOR DE TESIS
DR. JULIO EDUARDO ROQUE MORÁN ANDRADE
INSTITUTO DE FISIOLOGÍA CELULAR
COMITÉ TUTOR
DR. JAIME IVÁN VELASCO VELÁZQUEZ
INSTITUTO DE FISIOLOGÍA CELULAR
DR. VICTOR RAMÍREZ AMAYA
INSTITUTO DE NEUROBIOLOGÍA

MÉXICO, D.F. FEBRERO DE 2015

Este trabajo de investigación se realizó bajo la dirección del Dr. Julio Morán Andrade en la División de Neurociencias del Instituto de Fisiología Celular de la Universidad Nacional Autónoma de México.

Este trabajo fue financiado por donativos otorgados por el Consejo Nacional de Ciencia y Tecnología (CONACyT, 179234), el Programa de Apoyo a Proyectos de Investigación e Innovación Tecnológica de la UNAM (DGAPA-PAPIIT, IN206213/24) y por la beca para estudios de posgrado del CONACyT.

El comité tutoral que asesoró el desarrollo de este trabajo estuvo conformado por:

Dr. Julio Morán Andrade
Dr. Iván Velasco Velázquez
Dr. Víctor Ramírez Amaya

El jurado designado por el Comité Académico del Posgrado en Ciencias Biomédicas estuvo integrado por:

Dra. María Eugenia Gonsebatt Bonaparte
Dr. Julio Morán Andrade
Dra. Clorinda Arias Álvarez
Dra. Lourdes Massieu Trigo
Dra. Susana Castro Obregón

Agradecimientos

A mi tutor, el Dr. Julio Morán Andrade por sus enseñanzas, apoyo y confianza que me dio a lo largo de mi formación en su laboratorio.

A los miembros de mi comité tutoral, el Dr. Jaime Iván Velasco Velásquez y el Dr. Víctor Ramírez Amaya, por sus valiosas aportaciones y apoyo que siempre me otorgaron.

A los miembros del jurado: Dra. María Eugenia Gonsebatt Bonaparte, Dr. Julio Morán Andrade, Dra. Clorinda Arias Álvarez, Dra. Lourdes Massieu Trigo y Dra. Susana Castro Obregón, por su tiempo dedicado a la revisión de este trabajo, su valiosa contribución y asesoría.

A la Maestra en Ciencias Guadalupe Domínguez Macouzet por el apoyo técnico otorgado durante la realización de este trabajo.

A la Dra. Diana Escalante Alcalde por su valiosa contribución a mi formación.

A la Bióloga Teresa Montiel por su apoyo recibido durante la realización de este trabajo.

A mis compañeros de laboratorio y amigos del Instituto

A mi familia.

Índice

Abreviaturas

CRMP2: Proteína mediadora 2 de respuesta a colapsina (collapsin response mediator protein 2)

DIV: días *in vitro*

DPI: Cloruro de difenil iodonio (Diphenyleneiodonium chloride)

ERKs: Cinasas reguladas por señales extracelulares (Extracellular signal-regulated kinases)

ERO: especies reactivas del oxígeno

GPX: Glutatión peroxidasa

GSH: glutatión reducido

GSSG: glutatión oxidado

H_2O_2: peróxido de hidrogeno

HO_2•: Radical hidroperoxilo

MICAL: moléculas que interactúan con CasL (molecules interacting with CasL)

NGC: neuronas granulares del cerebelo

NGF: Factor de crecimiento nervioso (Nerve growth factor)

NOX: NADPH-oxidasas

O_2: Oxígeno molecular

O_2•-: radical anión superóxido

OH•: Radical hidroxilo

PKC: Proteína cinasa C (Protein kinase C)

PRX: Peroxirredoxina

R´SH: Grupo tiol

RO•: Radical alcoxilo

ROO•: Radical peroxilo

R-S-: Grupo tiolato

R-SO_2H: Ácido sulfínico

R-SOH: Ácido sulfénico

R-SS-R´: Enlace disulfuro:

SOD: superóxido dismutasa

TrxS_2: disulfuro de la tiorredoxina

Resumen

Las especies reactivas del oxígeno (ERO) son moléculas que pueden actuar como señales para regular diferentes procesos fisiológicos del sistema nervioso. Específicamente durante el desarrollo del sistema nervioso, las ERO actúan como reguladores de la diferenciación neuronal, de la neuritogenesis y de la muerte celular programada. Sin embargo, no se conocen con exactitud los mecanismos que modulan los niveles y acción de las ERO durante el desarrollo neuronal. Por tal motivo, en el presente estudio nos planteamos el objetivo de estudiar algunos de estos mecanismos que regulan la producción y localización de las ERO así como sus acciones durante el desarrollo de las neuronas granulares (NGC) y sobre las células astrogliales del cerebelo. Para tales propósitos empleamos cultivos primarios de NGC y de astrocitos. En los cultivos de NGC, encontramos que durante los primeros 3 días *in vitro* (DIV) de desarrollo, las NGC gradualmente incrementan los niveles de ERO alcanzando un pico a los 2 y 3 DIV. Posterior a este tiempo los niveles de ERO regresan a los niveles basales y se mantienen sin cambio en los subsecuentes días estudiados (8 DIV). El incremento observado en los niveles de ERO parece estar relacionado con la maduración de las NGC, ya que cuando las NGC se trataron con inhibidores de la enzima NADPH-oxidasa (NOX), una de las principales fuentes de ERO, la expresión de las proteínas Tau y MAP2 disminuyó, sugiriendo que las ERO producidas por la NOX promueven la maduración de las NGC. Por otra parte, los niveles del sistema antioxidante glutatión también se incrementan entre 0 y 1 DIV, precediendo al incremento observado de ERO. Después de 5 DIV, los niveles de glutatión regresan a los niveles basales. El incremento de glutatión parece ser esencial para el desarrollo adecuado de las NGC, ya que cuando el glutatión se eliminó farmacológicamente a los 2 DIV, ocurrió una formación anormal y degeneración de los axones y muerte de las NGC, lo cual no sucedió cuando el glutatión se eliminó en los días posteriores de desarrollo. Concomitante al desarrollo de las NGC, la expresión de NOX2, uno de los homólogos de NOX, incrementa alcanzando su máxima expresión a los 3 DIV, posterior a este tiempo la expresión de NOX2 disminuye. De manera interesante, esta enzima se encuentra localizada en los conos de crecimiento y filopodios de las neuronas en desarrollo, lo cual coincide con los sitios en los que detectamos la producción de peróxido de hidrógeno (H_2O_2). Además, el crecimiento axonal en neuronas deficientes de NOX2 es menor al observado en NGC silvestres. Finalmente, en este estudio también se exploró el papel de las ERO en la muerte de las células astrogliales. Empleando estaurosporina como un inductor de muerte, encontramos que la muerte producida en las células astrogliales depende de las ERO producidas por un homólogo de NOX no identificado. Por otra parte, los cambios morfológicos de las células astrogliales asociados al proceso de muerte no dependen de ERO, aunque la administración exógena de H_2O_2 sí indujo cambios morfológicos similares a los inducidos por el tratamiento de estaurosporina. En su conjunto, nuestros datos sugieren que la regulación de las ERO durante el desarrollo temprano de las NGC, es esencial para la maduración y supervivencia de estas neuronas. Por otra parte, nuestros datos también sugieren que las ERO actúan como reguladoras de la estructura celular, actuando tanto en la formación del axón y la dinámica de los filopodios y conos de crecimiento de las neuronas, así como en la morfología de las células astrogliales.

Abstract

Reactive oxygen species (ROS) are signaling molecules that regulate numerous physiological processes of the nervous system. Specifically, during development, ROS modulate neuronal differentiation, neuritogenesis and programmed cell death. However, the mechanisms that regulate the levels and actions of ROS in developing neurons are not well understood. For this reason, we studied the mechanisms by which ROS are regulated and their actions during cerebellar granule neurons (CGN) development. In this regard, we also evaluated the effects of ROS in astroglial cells. For these purposes, we employed CGN and astrocytic primary cultures. In CGN cultures, we found that during the first 3 days *in vitro* (DIV) of development, CGN gradually increased the levels of ROS, reaching a peak at 2 and 3 DIV. After this time, the levels of ROS returned to the basal levels and remained low in the subsequent DIV. The observed increase of ROS levels, seems to be related to CGN maturation, since CGN treated with inhibitors of the enzyme NADPH-oxidase (NOX), that is a major source of ROS in these cells, the expression of the proteins Tau and MAP2 diminished, suggesting that ROS produced by NOX promote CGN maturation. On the other hand, the levels of the antioxidant glutathione, increased between 0 and 1 DIV, preceding the increase of ROS levels. After 5 DIV, the levels of glutathione returned to basal levels. The increase of glutathione seems to be essential for CGN development, since glutathione depletion at 2 DIV, led to degeneration and abnormal formation of the axons, as well as CGN death, which was not observed when glutathione was depleted in the subsequent days of development. Concomitantly with the development of CGN, the expression of NOX2 increased, reaching its maximum expression at 3 DIV and after this time, the expression of NOX2 diminished. Interestingly, we observed that this enzyme was localized in axonal growth cones and filopodia of developing neurons. This condition is coincident with the sites where hydrogen peroxide is produced (H_2O_2). Furthermore, the extent of axonal growth of CGN devoid of NOX2 was lesser than that observed in wild type CGN. Finally, in this study we also explored the role of ROS in the cell death of cerebellar astrocytes. Using staurosporine as an inducer of cell death in astrocytes, we found that cell death is dependent on ROS produced by a non-identified NOX homologue. On the other hand, the morphological changes associated with the cell death of these cells were not dependent of ROS, although the exogenous administration of H_2O_2 induced similar morphological changes to those produced by staurosporine. Together, these results suggest that the regulation of ROS during CGN development is essential for CGN maturation and survival of these neurons. On the other hand, our observations also suggest that ROS act as regulators of the cellular structure, particularly in the axonal formation and filopodia dynamics during development, as well as in the morphology of astroglial cells.

I. Introducción

Durante el desarrollo del sistema nervioso ocurre una serie de eventos coordinados como la proliferación, migración, diferenciación y muerte celular, los cuales ocurren en un orden estricto en espacio y tiempo. En estos eventos destaca la formación de las neuronas, las cuales se diferencian, maduran y una proporción importante de ellas muere en este proceso. Durante la diferenciación y maduración de las neuronas, éstas desarrollan extensiones o procesos neuríticos, los cuales se diferencian en un axón y una o varias dendritas, constituyendo así la llamada polaridad neuronal (Tahirovic and Bradke, 2009). La polaridad neuronal es la característica más distintiva de las neuronas, el patrón específico de ramificación axonal y dendrítico es esencial para las funciones neuronales, que incluyen la recepción e integración de varias entradas sinápticas en las dendritas, así como la iniciación, conducción y distribución de las señales de salida a través del axón (Cheng and Poo, 2012). El correcto establecimiento de la polaridad neuronal es un evento crítico durante el desarrollo del sistema nervioso, ya que de esto depende el establecimiento adecuado de los circuitos neuronales, que es la base de su funcionalidad (Barnes and Polleux, 2009).

1.1 Cerebelo

El cerebelo es una estructura que participa en la integración de la percepción sensorial, encargada del control motor y el balance, crítica en la adquisición de habilidades motoras y que contribuye a funciones cognitivas como el habla y la memoria espacial (Boyden et al., 2004; Ramnani, 2006; Schmahmann, 2010). Las neuronas del cerebelo se localizan en la corteza cerebelar, la cual está constituida por tres capas compuestas por 8 tipos neuronales que son: neuronas de Purkinje, de Golgi, de Lugaro, en candelero, granulares, en canasta, estrelladas y unipolares en cepillo. Estas neuronas se encuentran distribuidas en un patrón regular a lo largo de la composición foliar de la corteza cerebelar. Este arreglo neuronal característico consiste en un estricto posicionamiento de las neuronas y las fibras aferentes, lo cual da lugar a tres capas principales, siendo la más superficial la capa molecular que corresponde a una zona de baja densidad celular y alta incidencia sináptica y donde se encuentran los arboles dendríticos de las neuronas de Purkinje. La capa más profunda es la capa granular interna, en la cual existe una gran densidad celular que está compuesta en su mayor parte por las neuronas granulares del cerebelo (NGC). En la capa intermedia se encuentran los somas de las neuronas de Purkinje, las cuales se encuentran ordenadas en una hilera única. En esta capa también se encuentra la glía de Bergmann. De los 8 tipos neuronales, únicamente los axones de las neuronas de Purkinje proyectan fuera de la corteza cerebelar, mientras que los otros 7 tipos neuronales son interneuronas que forman parte del circuito local (Sotelo, 2004). Las NGC forman contactos sinápticos con las neuronas de Purkinje, lo cual provee el andamiaje para el circuito primario de la corteza cerebelar. La salida del circuito cerebelar depende de las conexiones entre las NGC y las fibras musgosas provenientes de distintos sitios y las conexiones entre las neuronas de Purkinje con las fibras trepadoras provenientes del núcleo olivar, así como las demás conexiones establecidas con las diferentes interneuronas (Solecki et al., 2006). La organización de la corteza cerebelar con relativamente pocos tipos neuronales, su arreglo

en capas conspicuas y su accesibilidad hacen del cerebelo un modelo ideal para estudios de los procesos del desarrollo del sistema nervioso central (Fig. 1A).

1.1.1 Desarrollo de la corteza cerebelar

Aunque el cerebelo constituye aproximadamente el 10% del volumen total del cerebro, las NGC por si mismas sobrepasan el número de neuronas del resto del cerebro (Solecki et al., 2006). El desarrollo de estas neuronas comienza durante el desarrollo postnatal temprano del cerebelo, cuando los precursores de las NGC proliferan activamente en la parte más externa de la corteza cerebelar, formando así una capa transitoria llamada capa granular externa. Posterior a la última mitosis, las NGC permanecen allí por un periodo de entre 24 y 48 h para posteriormente iniciar su migración a través de la capa molecular. Este proceso comienza con la formación de dos neuritas desiguales, una opuesta a la otra, las cuales están orientadas longitudinalmente al eje del folium. La migración de las neuronas postmitóticas comienza con una migración tangencial que va en dirección del proceso más largo. Para el momento en el que las NGC alargan su soma y extienden una tercera neurita, llamada proceso líder, la cual se sitúa perpendicularmente a las otras dos y con dirección hacia la parte inferior de la capa granular externa, se inicia la transición entre la migración tangencial y la radial. Como resultado de la translocación entre el soma y el proceso líder, se forma un proceso posterior conectado a dos procesos horizontales, los cuales se transformaran en las futuras fibras paralelas. Es en la capa molecular donde las NGC migran radialmente a lo largo de la glía de Bergmann. La correcta migración radial de las NGC, determina la correcta posición de estas células migrantes de la capa molecular a la capa granular interna y por tanto contribuye a la estructuración de las tres capas de la corteza cerebelar.

El movimiento a lo largo de esta capa se caracteriza por fases estacionarias de corta duración en las que las NGC tienen movimientos en dirección hacia delante y hacia atrás, siendo el desplazamiento neto con dirección a la capa de las neuronas de Purkinje. Una vez en esta capa intermedia, la forma de las NGC cambia abruptamente de una forma alargada a una forma esférica, el soma redondeado de las NGC permanece estático en esta capa por un periodo de entre 30 y 220 min. Durante este tiempo se forman lamelipodios y filopodios altamente móviles en la parte distal del proceso líder, sugiriendo que el proceso líder busca activamente moléculas señal que guíen el proceso de migración. Después del período de inmovilidad, el soma se re-extiende junto con el proceso líder y de esta forma continúan migrando las NGC hacia la parte inferior de la capa granular interna, para finalmente disminuir la velocidad de migración. Tan pronto el proceso líder se acerca a la materia blanca, al final de la capa granular interna, el soma se redondea nuevamente, la velocidad de migración disminuye y finaliza una vez que el soma se encuentra en el borde de la capa granular interna y la materia blanca (Fig. 1B) (Komuro and Yacubova, 2003).

Las NGC reciben la influencias glutamatérgicas a lo largo de su trayecto por la capa molecular y en la capa granular interna. Durante su paso por la capa molecular, el glutamato promueve la migración de las NGC. Este glutamato posiblemente proviene de la glía de Bergmann o de las fibras paralelas de las NGC que para ese momento ya han completado el proceso de migración (Komuro and Yacubova, 2003). Una vez que parte de las NGC han completado su migración a la capa granular interna, éstas reciben los primeros contactos sinápticos glutamatérgicos provenientes de las fibras musgosas alrededor del día postnatal 5; sin embargo, estos contactos sinápticos comienzan a ser funcionales entre los días postnatales 10 y 12, tiempo en el cual la mayor parte de las NGC han completado su migración hacia la capa granular interna (Burgoyne and Cambray-Deakin, 1988; Sotelo,

2004). Finalmente, alrededor del 50 % de las NGC formadas, mueren predominantemente mediante apoptosis, lo cual ocurre mayormente en la capa granular externa (Wood et al., 1993; Tanaka and Marunouchi, 1998; Lossi and Gambino, 2008). Durante el desarrollo del sistema nervioso central, la actividad eléctrica promueve la sobrevivencia de las neuronas durante etapas específicas del desarrollo (Mennerick and Zorumski, 2000). En este sentido, se ha sugerido que las influencias presinápticas de las fibras musgosas, promueven la sobrevivencia de las NGC. En experimentos *in vitro*, la influencia presináptica de las fibras musgosas, se mimetiza despolarizando a las NGC con concentraciones elevadas de KCl (25 mM) o con el agonista glutamatérgico NMDA. Durante el desarrollo *in vitro* de las NGC, ocurre una transición en la cual estas neuronas se vuelven dependientes del estado de despolarización, a partir del tercer día *in vitro* (DIV) si las NGC no se encuentran en condiciones despolarizantes, éstas comienzan a morir (Gallo et al., 1987; Balazs et al., 1988). La despolarización también promueve la maduración bioquímica de las NGC (Moran and Patel, 1989b, a) y la maduración de las dendritas (Ramos et al., 2007). En general, los efectos de la despolarización en estas células son visibles después de los 3 DIV, lo cual es coincidente con la formación y maduración de las dendritas (Shalizi et al., 2006). La despolarización activa los canales de calcio sensibles a voltaje, permitiendo la entrada de calcio a las neuronas y con ello la activación de moléculas señal dependientes de calcio, tales como las proteínas cinasas dependientes de Ca^{2+}-Calmodulina y la fosfatasa calcineurina (See et al., 2001; Linseman et al., 2003; Wayman et al., 2004; Sato et al., 2005). Las vías de señalización dependientes de calcio regulan el perfil de expresión génica de las NGC (Kramer et al., 2003; Sato et al., 2005), lo cual se puede ver reflejado en la composición de los receptores $GABA_A$ y NMDA, ya que después de la despolarización la subunidad α6 del receptor $GABA_A$ y la subunidad NR2C del receptor NMDA se sobre-expresan (Mellor et al., 1998; Suzuki et al., 2005).

El proceso de desarrollo de las NGC es dirigido en parte por señales extracelulares, sin embargo, este proceso también responde a un programa genético interno. Por ejemplo, NGC aisladas recapitulan el comportamiento migratorio y la morfología de las NGC en desarrollo *in vivo*, lo cual sucede en ausencia de contactos célula-célula, sugiriendo que el desarrollo de estas neuronas está fuertemente influido por un programa intrínseco (Yacubova and Komuro, 2002). La polaridad neuronal de las NGC también es un proceso que puede ser examinado *in vitro*, ya que las células progenitoras de las NGC una vez aisladas, son capaces de salir del ciclo celular y recapitular fielmente la morfología observada *in vivo* (Powell et al., 1997). El proceso de establecimiento de la polaridad neuronal en las NGC *in vitro*, comienza cuando las células salen del ciclo celular aproximadamente entre 12 y 20 h posteriores al sembrado de las células (Fase 1, células apolares, 24 h), las cuales son obtenidas de ratas de 8 días o 7 días para el caso del ratón. Subsecuentemente, el centrosoma se posiciona en un polo de la célula, a partir del cual protruyen lamelipodios que forman la primera neurita (Fase 2, células bipolares, 24-48 h), en este punto también se localizan el aparato de Golgi y endosomas de reciclamiento tardíos (Zmuda and Rivas, 1998). Posteriormente, el centrosoma se relocaliza en el sitio opuesto al que se formó la primer neurita y a partir de este punto se forma una segunda neurita (Fase 3, 2-3 días), generando así la morfología bipolar característica de las NGC inmaduras. El desarrollo *in vitro* de las NGC, continúa con el crecimiento de una de las dos neuritas, la cual se bifurca, dando lugar así a la morfología característica de las fibras paralelas (Fase 4, 3-4 días); la neurita restante se retrae. A continuación, el axón continúa creciendo y se desarrollan varias dendritas alrededor del soma (Fase 5, células multipolares, 4-5 días) (Fig. 1C) (Powell et al., 1997). Más recientemente, se han identificado

diversos mecanismos moleculares intrínsecos que subyacen la morfogénesis y conectividad de las NGC (Gaudilliere et al., 2004; Konishi et al., 2004; Shalizi et al., 2006; Stegmuller et al., 2006).

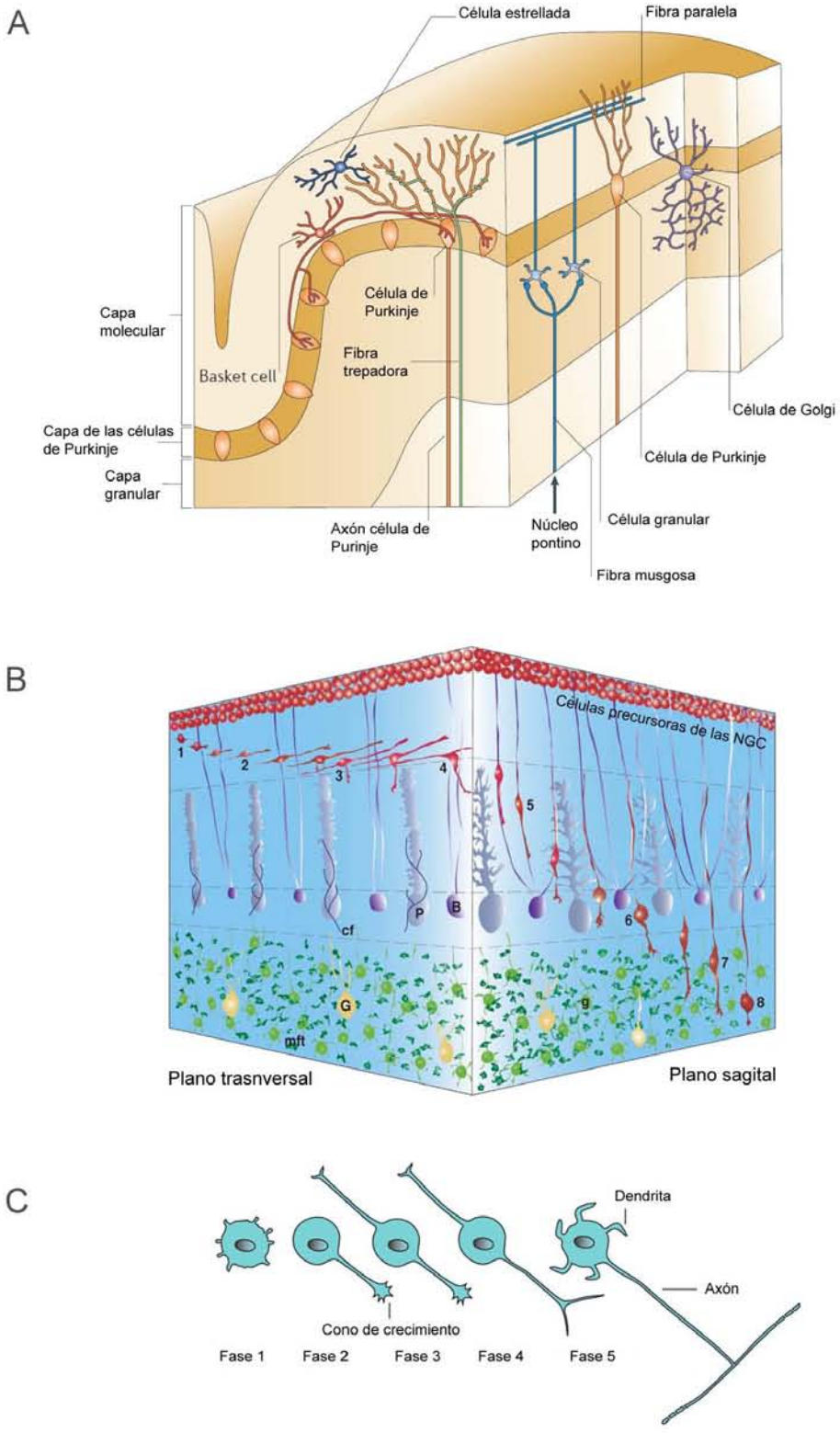

Figura 1. (A) Esquema en el que están representados 6 de los 8 tipos neuronales que constituyen la corteza cerebelar, así como las conexiones que establecen entre ellos y las aferencias que recibe la corteza cerebelar. Se muestran las 3 capas que componen a la corteza del cerebelo adulto: capa molecular, capa de las células de Purkinje y capa granular. Esquema modificado de (Ramnani, 2006). (B) Esquema que representa las diferentes fases del desarrollo de las NGC a lo largo de su migración en corteza cerebelar en desarrollo. Esquema modificado de (Komuro and Yacubova, 2003). (C) Esquema en el que están representadas las distintas fases del desarrollo de las NGC *in vitro.* Esquema modificado de (Powell et al., 1997).

1.3 Especies reactivas del oxígeno

Las especies reactivas del oxígeno (ERO) son moléculas que se originan a partir de la reducción secuencial del oxígeno molecular (O_2). Estas pueden dividirse en dos grupos principales: los radicales libres y las moléculas no radicales. La reducción univalente del O_2 genera al radical anión superóxido ($O_2^{\bullet -}$), el cual es considerado una ERO primaría ya que a partir de esta molécula se forman ERO secundarias de importancia biológica como pueden ser el peróxido de hidrógeno (H_2O_2) y los radicales hidroxilo (OH•), peroxilo (ROO•), alcoxilo (RO•) e hidroperoxilo (HO_2•) (Valko et al., 2007; Pourova et al., 2010). De entre las distintas ERO producidas en las células, el H_2O_2 es la ERO de mayor relevancia en la fisiología celular, ya que posee distintas propiedades que la hacen una molécula propicia para la señalización, incluyendo su relativa alta capacidad de difundir a través de las membranas biológicas, su relativamente baja reactividad y una vida media relativamente más larga que otras ERO. Además, es capaz de modificar la función de distintas proteínas a través de su oxidación (Kamata and Hirata, 1999; Droge, 2002).

1.3.1 Señalización redox

La oxidación de proteínas involucradas en la señalización celular representa una regulación critica post-traduccional (Cross and Templeton, 2006). Diversos estudios han descrito numerosos procesos fisiológicos en los cuales el H_2O_2 actúa como regulador de la función celular, lo cual ocurre a través de la oxidación especifica de proteínas, lo que a su vez lleva a una modificación de su estado de activación, lo cual subsecuentemente afecta vías de señalización específicas, modificando de esta forma la función celular. Esto ocurre principalmente a través de la oxidación de aminoácidos específicos como pueden ser cisteínas, tirosinas y triptófanos (Droge, 2002). El H_2O_2 induce la activación de varias proteínas cinasas, como la JNK, etc. así como la activación o inactivación de varias proteínas fosfatasas, lo cual es mediado exclusivamente por la oxidación especifica de cisteínas (Kamata and Hirata, 1999; Tonks, 2005; Valko et al., 2007; Pourova et al., 2010).

La función de una gran variedad de proteínas es afectada por una serie de reacciones reversibles que son controladas por el estado redox de las células. En este sentido, la oxidación de cisteínas por el H_2O_2 constituye un mecanismo fundamental en la regulación oxidativa de las proteínas. Para que esto ocurra, una vez que un tiolato de alguna cisteína reactiva interactúa con el H_2O_2, ésta es convertida en ácido sulfénico (R-SOH). A partir de aquí, diferentes reacciones pueden ocurrir en ausencia de glutatión, tiorredoxina y glutarredoxina. El ácido sulfénico que es altamente reactivo puede reducir a un grupo tiol adyacente y de esta manera se forma un enlace disulfuro. Alternativamente, el ácido sulfénico puede ser posteriormente oxidado por otra molécula de H_2O_2, lo cual forma al ácido sulfínico ($R\text{-}SO_2H$). La formación de este grupo es importante en la regulación redox de algunas proteínas como ocurre en el caso de las peroxirredoxinas. A pesar de la estabilidad de este grupo, éste puede ser reducido a ácido sulfénico por las sulfirredoxinas y sestrinas (Jonsson and Lowther, 2007; Day et al., 2012) o bien puede ser oxidado por otra molécula de H_2O_2 y formar ácido sulfónico ($R\text{-}SO_3H$), del cual hasta este momento no se conoce ninguna reacción enzimática que reduzca este grupo a ácido sulfínico (Finkel, 2011; Lo Conte and Carroll, 2013).

Por otra parte, el ácido sulfénico puede también formar un enlace disulfuro entre la molécula de glutatión reducido y el residuo de cisteína, lo cual forma a una proteína glutationilada; por el contrario, si el glutatión se encuentra en su forma oxidada, este puede establecer un enlace disulfuro con el tiolato de un residuo de cisteína. Los enlaces disulfuro formados pueden ser reducidos por tiorredoxina o glutarredoxina, lo cual forma un enlace disulfuro entre la proteína y tiorredoxina o glutarredoxina. Ambos procesos son relevantes para la regulación de diversas proteínas como son ASK1 y CRMP2. Finalmente, los enlaces formados entre proteína-tiorredoxina y proteína-glutarredoxina pueden ser rotos por H_2O_2, lo cual forma un ciclo de reacciones oxido-reducción en el que la función de las proteínas es afectada por el estado redox de la célula (Figura 2) (Forman et al., 2004; Rinna et al., 2006; Forman et al., 2014).

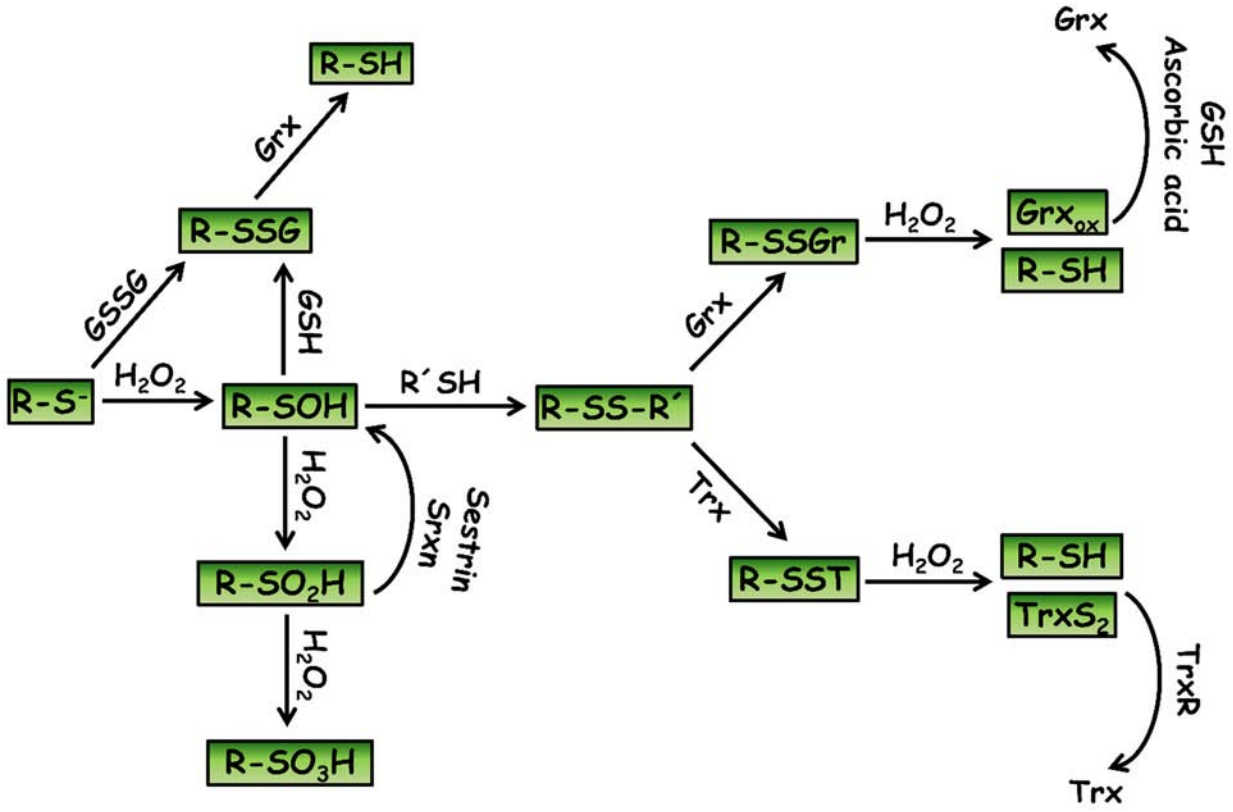

Figura 2. Mecanismos de oxidación de cisteínas involucrados en la señalización redox. La reacción entre el H_2O_2 y una cisteína reactiva de un grupo tiolato ($R\text{-}S^-$) produce ácido sulfénico (R-SOH), el cual incrementa la probabilidad de generar un enlace disulfuro (R-SS-R´) con un grupo tiol (R´SH) adyacente. Si R-SOH es oxidado por H_2O_2, entonces se forma el ácido sulfínico ($R\text{-}SO_2H$), el cual puede ser reducido a R-SOH por las sestrinas y sulforredoxinas. Cuando el H_2O_2 oxida a $R\text{-}SO_2H$, se forma ácido sulfónico ($R\text{-}SO_3H$). La presencia de glutatión reducido (GSH) y proteínas que contienen un grupo R-SOH, genera la glutationilización de proteínas (R-SSG), sin embargo, si el glutatión se encuentra en su forma oxidada (GSSG), este se une al grupo tiolato de los residuos de cisteínas, formando así R-SSG. Las distintas tiorredoxinas y glutaredoxinas pueden reducir los enlaces disulfuro entre las proteínas oxidadas a través de la formación de enlaces disulfuro intermoleculares, los cuales a su vez pueden ser disociados por el H_2O_2. Tomado de (Olguín-Albuerne et al., 2014)

1.3.2 Producción de especies reactivas del oxígeno

Las ERO son formadas dentro de las células a través de diferentes mecanismos, de entre los cuales la cadena de transporte de electrones de la mitocondria ha sido considerado tradicionalmente como una de las más

importante. Aquí los electrones obtenidos a partir de moléculas reducidas pasan a un aceptor final que es la molécula de oxígeno, generándose un gradiente de protones que será utilizado en la generación de moléculas de ATP. Durante este proceso los electrones fluyen a través de una cadena de complejos enzimáticos I-IV, en donde al final las moléculas de oxígeno son reducidas completamente a H_2O. Sin embargo, durante el proceso puede ocurrir una fuga de electrones en los complejos I y III, los cuales reducen parcialmente al O_2, produciéndose el $O_2^{\bullet -}$. Se ha estimado que el porcentaje de electrones fugados en las mitocondrias de mamíferos ocurre en alrededor de un 0.16% a un 2%**,** sin embargo, estos valores pueden cambiar dependiendo del tipo de tejido, el organismo y otros factores. Además, dentro de la mitocondria las ERO también se generan por diferentes enzimas como las monoamino oxidasas y p66shc (Fridovich 2004, Dröge 2002, Kamata 1999).

En años recientes las NADPH-oxidasas (NOX 1-5) y las oxidasas duales (DUOX 1-2), producen $O_2^{\bullet -}$ y H_2O_2 como su principal función y no como un subproducto. Se activan en respuesta a factores de crecimiento, citosinas, agonistas de receptores acoplados a proteínas G, neurotrofinas y receptores glutamatérgicos tipo NMDA. Su actividad está regulada por diferentes subunidades acopladoras y activadoras, sin embargo, NOX 4 presenta una actividad constitutiva, mientras que NOX 5 y DUOX 1 y 2 son reguladas por calcio. Se expresan en diferentes tejidos y su distribución subcelular es diversa, pudiéndose encontrar en núcleo, retículo endoplasmático, endosomas, lamelipodios, caveolas y balsas lipídicas de la membrana plasmática (Brown 2009, Bedard 2005, Sorce 2009).

La enzima NOX2, ha sido la más ampliamente estudiada, la cual fue caracterizada en macrófagos y neutrófilos, donde esta enzima es responsable del llamado estallido respiratorio. NOX2 está constituida por dos subunidades membranales, gp91phox y p22phox, de las cuales gp91phox constituye la subunidad catalítica. Además de estas subunidades, existen diversas subunidades reguladoras citoplásmaticas, las cuales son p40phox, p47phox, p67phox y Rac 1/2 (Lambeth, 2004). La activación de este complejo enzimático inicia cuando p47phox es fosforilada en 8-9 serinas por alguna cinasa como puede ser PKC, ERK 1/2, p38 MAPK, Pak1 y Akt. Las serinas 370 y 359 de p47phox son fosforiladas inicialmente y subsecuentemente se fosforila la serina 379, exponiendo así el dominio SH3, el cual interactúa con una región rica en prolinas de p22phox facilitando de esta forma su translocación. Finalmente, se fosforilan las serinas 303 y 304, llevando así a la completa activación de p47phox. Es a partir de este momento cuando p40phox y p67phox se translocan, proporcionando así el sitio de unión para Rac 1/2 y con ello, formando al complejo activo (Brown and Griendling, 2009)

1.3.3 Regulación de las especies reactivas del oxígeno

Los niveles intracelulares de H_2O_2 están regulados por diferentes sistemas antioxidantes, cuya finalidad es degradar a esta molécula en agua y al mismo tiempo mantener el ambiente reducido de la célula. Existen diferentes enzimas que se encargan de dismutar al peróxido de hidrógeno en agua y oxigeno molecular. Su distribución dentro de la célula es específica. Tal es el caso de la catalasa que se localiza en los peroxisomas y la glutatión peroxidasa (GPX) y la peroxirredoxina (PRX) que se encuentran en el citoplasma y las mitocondrias (Salmon 2010, Tamara 2006). Tanto la glutatión peroxidasa como la peroxirredoxina emplean al glutatión reducido (GSH) y a la tiorredoxina para catalizar la dismutación del peróxido de hidrógeno a agua. El resultado es la formación de las formas disulfuro del glutatión o glutatión oxidado (GSSG) y al disulfuro de la tiorredoxina ($TrxS_2$). Tanto el glutatión oxidado como la tiorredoxina disulfuro vuelven a sus formas reducidas a través de las enzimas reductasa de glutatión y reductasa de

tiorredoxina (Dröge 2002, Kamata 1999). El glutatión además de ser un co-sustrato obligado de la glutatión peroxidasa, es una molécula que por sí misma es un antioxidante capaz de degradar una gran variedad de ERO (Franco and Cidlowski, 2009; Lubos et al., 2011). Además, cambios en los pares GSH/GSSG son considerados determinantes para el ambiente redox y para la señalización redox en las células (Schafer and Buettner, 2001; Jones, 2006; Franco and Cidlowski, 2012). Por lo tanto, las acciones de las ERO durante el desarrollo del sistema nervioso muy probablemente son influenciadas por el sistema antioxidante del glutatión. En particular, durante el desarrollo del cerebelo existe muy poca información y la existente es un tanto controvertida. Se sabe que durante la segunda semana de desarrollo cerebelar en rata, ocurre un continuo incremento de los niveles de glutatión, los cuales permanecen inalterados incluso después de la tercer semana de desarrollo (Rice and Russo-Menna, 1998); sin embargo, un estudio distinto, indica que los niveles de glutatión incrementan transitoriamente durante la primera semana de desarrollo y después regresan a los niveles basales, permaneciendo sin cambios en los siguientes estados de desarrollo (Nanda et al., 1996).

1.4 Acciones fisiológicas de las ERO en el sistema nervioso

Las ERO actúan como moléculas señal que regulan diferentes procesos tanto del cerebro adulto como del cerebro en desarrollo (Munnamalai and Suter, 2009; Le Belle et al., 2011; Morinaka et al., 2011; Coyoy et al., 2013; Munnamalai et al., 2014a). Sin embargo, es importante notar que la mayor parte de la información que existe hasta el momento se ha descrito en eventos del desarrollo (Tsatmali et al., 2006; Le Belle et al., 2011; Coyoy et al., 2013). Durante el desarrollo de las células neurales, las ERO son reguladoras de la proliferación de las células precursoras neurales y de la diferenciación neuronal (Munnamalai and Suter, 2009; Le Belle et al., 2011; Morinaka et al., 2011; Coyoy et al., 2013; Munnamalai et al., 2014a). Por otra parte, las ERO producidas durante el desarrollo pueden actuar como morfógenos; por ejemplo, en un modelo de *Drosophila* en el cual la enzima superóxido dismutasa (SOD) mitocondrial está mutada, los niveles de ERO mitocondriales se incrementan, lo cual lleva a aberraciones en la formación del cerebro y anormalidades en la orientación de los axones. Estás moscas también presentan grupos de núcleos localizados en el neuropilo del cerebro central, lo cual no sucede en las moscas silvestres (Celotto et al., 2012).

En mamíferos, durante el desarrollo postnatal del cerebelo de rata, se producen ERO en ciertas regiones de la corteza cerebelar, lo cual ocurre de forma transitoria en diferentes etapas del desarrollo. Acompañando a estas ERO, ocurre una expresión diferencial de diferentes homólogos NOX y si estás enzimas son inhibidas o si las ERO son disminuidas con un antioxidante, se altera el patrón de foliación cerebelar y el comportamiento motor (Coyoy et al., 2013). En este modelo las condiciones antioxidantes no modificaron la muerte celular programada, aunque cabe la posibilidad de que las condiciones antioxidantes sí modifiquen la muerte programada de un tipo celular específico, ya que en este estudio se analizó la muerte programada en un tiempo regiones en las cuales la mayor parte de las células que mueren corresponden a neuronas (Krueger et al., 1995), lo cual no excluye que estos tratamientos si modifiquen in vivo la muerte de otros tipos celulares en otros tiempos y/o regiones de la corteza cerebelar en desarrollo. Además, es posible que otros procesos del desarrollo como son la proliferación de las células precursoras de las NGC y/o la diferenciación neuronal, sean responsables de los efectos vistos; por otra parte tampoco se descarta que las ERO actúen sobre las células astrogliales que son otro de los principales tipos celulares de la corteza cerebelar, sin embargo, ninguno de estos procesos se ha explorado en algún modelo de

desarrollo de la corteza cerebelar. Estos estudios sugieren que la regulación correcta de las ERO durante eventos críticos del desarrollo del sistema nervioso es crucial para que se lleve a cabo el desarrollo normal del cerebro. En particular, la corteza cerebelar en desarrollo representa un modelo ideal para el estudiar el papel fisiológico de las ERO durante el desarrollo.

1.4.1 Proliferación

Diferentes estudios sugieren que las ERO promueven la proliferación de células neurales. Por ejemplo, se sabe que las células precursoras neurales derivadas del hipocampo embrionario generan ERO bajo condiciones basales y que los antioxidantes e inhibidores de la enzima NOX promueven una disminución de la proliferación de estas células. (Yoneyama et al., 2010). Además, la administración del antioxidante ácido α-lipoico reduce la proliferación celular en la zona subgranular dentada del hipocampo (Limoli et al., 2004). En este sentido, Le Belle y colaboradores (2011) demostraron que en cultivos de neuroesferas obtenidos de la zona subventricular, el H_2O_2 (2-4 μM) promueve la capacidad de auto-renovación de estas células. Cuando se reducen los niveles de ERO, el número de neuroesferas también disminuye, lo cual es reestablecido con la adición de H_2O_2 exógeno. Consistentemente, se han detectado altos niveles de ERO en diferentes regiones neurogénicas como son la zona subventricular, la capa glomerular del bulbo olfatorio y la zona subgranular del hipocampo (Tsatmali et al., 2006; Le Belle et al., 2011).

Las ERO pueden ser producidas en las células en respuesta a diferentes factores; en el caso de los progenitores neurales, la adición de BDNF incrementa los niveles de ERO, lo cual incrementa la capacidad de auto-renovación de estas células, sin embargo, estos efectos no son observados en células derivadas de ratones deficientes de NOX2, lo cual indica que el BDNF promueve la activación de esta enzima que a su vez genera ERO que promueven la capacidad de auto-renovación de estas células. Estos resultados son corroborados por demostraciones *in vivo* que demuestran que los ratones deficientes de NOX2 poseen menos células proliferativas en la zona subventricular en comparación a los ratones silvestres y que la inhibición farmacológica de NOX disminuye tanto la generación de ERO como la proliferación en la zona subventricular. Estos resultados en conjunto muestran que BDNF induce la proliferación de progenitores neurales de forma dependiente de ERO producido por NOX2 (Le Belle et al., 2011). En este mismo modelo, el H_2O_2 induce la oxidación de PTEN, mientras que en otros modelos el H_2O_2 activa la vía PI3K/Akt/mTOR a través de la inactivación oxidativa de PTEN (Leslie, 2006). Consistente con esta observación, se demostró que en los ratones deficientes de PTEN el H_2O_2 o BDNF no puede estimular la formación de neuroesferas, lo cual sugiere que los efectos de las ERO están mediados por la inactivación redox de PTEN (Le Belle et al., 2011).

1.4.2 Diferenciación neuronal

Las ERO son determinadores críticos de la diferenciación neuronal en varios modelos experimentales. Parte de esta idea es apoyada por observaciones *in vivo* en donde se aprecia que las ERO son producidas en respuesta a factores tróficos como son el NGF o el BDNF, los cuales inducen diferenciación neuronal en regiones específicas del sistema nervioso (Tsatmali et al., 2006; Le Belle et al., 2011; Coyoy et al., 2013). En todos estos modelos el proceso de diferenciación es retardado o disminuido cuando las ERO son disminuidas por antioxidantes o inhibidores de las fuentes de producción de ERO en las células. La mayor parte de los estudios sobre los efectos

de las ERO durante la diferenciación neuronal se han llevado a cabo en la línea celular PC12. Cuando se trata a estas células con la neurotrofina NGF, éstas desarrollan neuritas y expresan diferentes marcadores neuronales como son βIII-tubulina, GAP-43 y neurofilamento L, entre otros. Este proceso comienza con la activación del receptor TrkA por NGF, lo cual lleva a la activación de PLCγ-PKC-Raf y la subsecuente activación de la vía de señalización Ras-Raf-MEK-ERK. La activación sostenida de ERKs es necesaria y suficiente para inducir la adquisición de características tipo neuronales en las células PC12 (Kaplan and Miller, 2000; Patapoutian and Reichardt, 2001).

En este modelo, la diferenciación neuronal de las células PC12 depende de ERO. Por ejemplo, tan solo basta promover la generación de ERO a través de inductores no tróficos para inducir la formación de neuritas a través de la activación sostenida de ERKs (Katoh et al., 1999). Esta activación de ERKs se afecta por las ERO en diferentes puntos de la cascada de señalización; por ejemplo, las ERO inducen la fosforilación del receptor TrkA a través de la inhibición de proteínas fosfatasas de tirosina, también promueve la activación de PLCγ y PI3K así como la formación de complejos del receptor con las proteínas acopladoras Shc, Grb2 Sos, los cuales son indispensables para la activación de la vía de las MAPKs (Kamata et al., 2005). Las ERO se producen en las células PC12 en respuesta a NGF, a los 10 min posteriores al tratamiento con esta neurotrofina se induce un pico de ERO. Esta producción de ERO se inhibe por DPI, un inhibidor de NOX, y se inhibe también mediante la expresión de una mutante dominante negativa de RAC1, la cual se requiere para la activación de NOX1-2, sugiriendo que NOX es la fuente de generación de ERO en respuesta a NGF (Suzukawa et al., 2000). Por otra parte, el tratamiento de NGF produce una reducción de la expresión de NOX2 a las 48 h junto con un incremento en la expresión de NOX1. Después de 72 h post-tratamiento de NGF, hay un segundo pico de ERO que es producido por NOX1, ya que la eliminación de NOX1 remueve por completo este pico. Después de 48 h post-tratamiento de NGF, si las ERO se inhiben mediante inhibidores NOX o por el antioxidante Euk-8, se incrementa la longitud de las neuritas y la expresión de βIII-tubulina, sin embargo, cuando Euk-8 se aplica desde el principio junto con NGF, la diferenciación neuronal se inhibe (Ibi et al., 2006). Estos experimentos sugieren que la generación de ERO por diferentes fuentes productoras, tienen distintos efectos sobre las células PC12. Durante el primer pico de ERO, el cual es producido probablemente por NOX2, las ERO son críticas para iniciar el proceso de diferenciación, mientras que el segundo pico de ERO, el cual es producido por NOX1, regula negativamente el crecimiento de las neuritas (Figura 3).

Por su parte, los sistemas antioxidantes también parecen desempeñar una función importante durante la diferenciación neuronal de las células PC12. El tratamiento con NGF induce la expresión de los antioxidantes glutatión peroxidasa y catalasa después de los 3 días post-tratamiento (Sampath et al., 1994). La regulación de estos sistemas antioxidantes permite a las células contender con el H_2O_2 producido crónicamente por NGF (Jackson et al., 1994). En este sentido, como fue mencionado anteriormente, el NGF induce la fosforilación de ERKs a los 10 min, lo cual es crucial para inducir la expresión y actividad de la MnSOD mitocondrial, para así inducir la diferenciación de las células PC12. Además, la MnSOD es necesaria para inducir la fosforilación de ERKs a los 180 min, lo cual ocurre a través de la conversión de $O_2^{\bullet -}$ en H_2O_2 el cual es indispensable para inducir la fosforilación a largo plazo de ERKs y la diferenciación neuronal (Figura 3) (Cassano et al., 2010).

No es del todo claro como el H_2O_2 promueve la fosforilación de ERKs; sin embargo, algunos estudios se han enfocado en tratar de descifrar los distintos elementos regulados por H_2O_2 durante la diferenciación neuronal de las células PC12. Gopalakrishna y colaboradores (Gopalakrishna et al., 2008) emplearon al $CoCl_2$ como un sistema

oxidante de proteínas, el cual induce la diferenciación neuronal de las células PC12 así como la expresión de GAP-43, SCG10 y neurofilamento-L. La diferenciación es inducida por oxidación de PKC, ya que los inhibidores no selectivos calfostina y queleritrina redujeron el crecimiento neurítico inducido por $CoCl_2$. El tratamiento con $CoCl_2$ indujo la translocación de PKC del citoplasma a la membrana plasmática y redujo la capacidad de PKC de unir esteres de forbol, lo cual puede ser explicado por una modificación redox del dominio regulador de PKC. En este estudio, el inhibidor de MEK PD98059 no tuvo efecto alguno en la activación de PKCε, pero si disminuyó la activación de ERKs, CREB y el crecimiento neurítico inducido por $CoCl_2$. Lo cual sugiere que PKCε acopla la señal oxidativa con la activación de ERKs. En el contexto del tratamiento con NGF, las ERO producidas durante los primeros minutos en respuesta a NGF, activan PKCε, lo cual indica que la oxidación de PKCε es un evento importante en la diferenciación neuronal inducida por NGF (Figura 3) (Gopalakrishna et al., 2008).

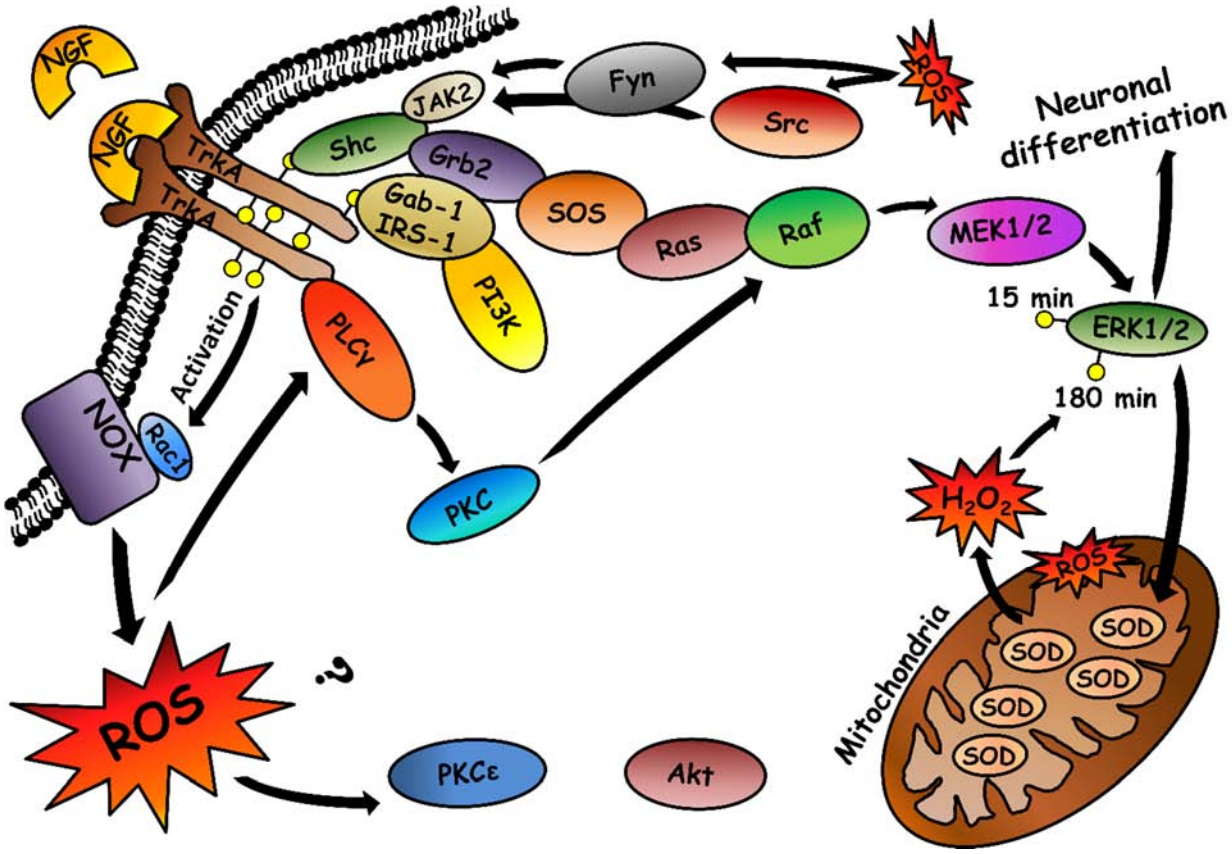

Figura 3. Regulación redox en la diferenciación neuronal de las células PC12. Cuando se trata a las células PC12 con NGF ocurre la transfosforilación del receptor TrkA, el cual induce el reclutamiento de proteínas adaptadoras, llevando así a la activación de la vía de señalización Ras-Raf-MEKs-ERKs y la subsecuente diferenciación. Por otra parte, se ha propuesto que las ERO producidas por NOX, inducen la máxima fosforilación de ERKs a los 15 min posteriores al tratamiento de NGF, lo cual es crucial para inducir la expresión y actividad de la MnSOD que se requiere para la conversión del $O_2^{\bullet-}$ a H_2O_2. La generación de H_2O_2 es necesaria para generar un segundo pico en la fosforilación de ERKs a los 180 min posteriores al tratamiento de NGF. Por otra parte, las ERO generadas por NOX, pueden inducir la activación de PKC, acoplando de esta forma la señal oxidante a la activación de ERKs. La unión de NGF a su receptor TrkA también lleva a la activación de la vía de señalización PLCγ-PKC-Raf y la subsecuente activación de ERKs. Las ERO pueden activar a Fyn y de esta forma acoplar la vía de señalización Shc-Ras-Raf-MEKs-ERKs. También se ha sugerido que PKC y Akt inducen la activación de NOX. Tomado de (Olguín-Albuerne et al., 2014)

En cultivos primarios de células progenitoras neurales obtenidas de la corteza, las ERO controlan el destino neuronal ya que las células que producen mayor cantidad de ERO se diferencian a neuronas. (Tsatmali et al., 2005). Lo mismo ocurre en cultivos primarios de células progenitoras neurales obtenidas de la zona subventricular, en donde la administración exógena de H_2O_2 produce un aumento en el número de neuronas diferenciadas. Por el contrario, la inhibición de NOX o PI3K, produjo una disminución del número de neuronas, mientras que la aplicación exógena de H_2O_2 no indujo un mayor número de neuronas al inhibir farmacológicamente a PI3K. En correspondencia con estos resultados, los cultivos derivados de ratones deficientes de NOX2, desarrollaron significativamente menos neuronas que los cultivos obtenidos de ratones silvestres (Le Belle et al., 2011).

Por otra parte, la diferenciación neuronal de los precursores neurales corticales es también influenciada por las ERO en múltiples aspectos. Cuando las células precursoras son seleccionadas de acuerdo a la producción de ERO, aquellas que produjeron niveles de ERO más altas, generaron neuronas, mientras que las células que produjeron bajos niveles de ERO generaron astrocitos, oligodendrocitos y neuronas. Estas neuronas fueron clasificadas en dos tipos, el tipo 1 con morfología piramidal, múltiples neuritas y con capacidad para disparar potenciales de acción únicos. El tipo 2, menor en proporción (alrededor del 35%), con una morfología redondeada, pocas neuritas y con capacidad para disparar potenciales de acción múltiples. Cuando las células productoras de bajos niveles de ERO fueron incubadas con antioxidantes, la proporción de neuronas entre los tipos 1 y 2 fue revertida, incrementando el número de neuronas tipo 2 (alrededor del 80%) (Tsatmali et al., 2006). En su conjunto estos resultados resaltan la importancia de las ERO durante la diferenciación neuronal en diferentes regiones del cerebro.

1.4.3 Dirección y crecimiento axonal

La presencia de las ERO se ha estudiado en los conos de crecimiento axónico y es precisamente en estas estructuras del axón en donde se han descrito diferentes funciones de las ERO. En los conos de crecimiento axónico de neuronas de *Aplysia* se han detectado altos niveles de ERO, las cuales promueven el crecimiento del axón, ya que si estas ERO se disminuyen con tratamientos antioxidantes o con inhibidores de los productores de ERO NOX y lipoxigenasa, se disminuye la longitud de los axones. Las ERO modulan diferentes aspectos de la dinámica del citoesqueleto de actina en los conos de crecimiento, lo cual va en función de la fuente de generación. Los niveles fisiológicos de ERO promueven el ensamble y formación de protrusiones de filamentos de actina en los conos de crecimiento, mientras que la inhibición de NOX previene estos procesos. Por otra parte, la inhibición de la enzima lipoxigenasa modifica el ensamble de actina y la formación de arcos de actina, pero no modifica la formación de filopodios (Munnamalai and Suter, 2009).

En estudios posteriores, Munnamalai y colaboradores (Munnamalai et al., 2014b) determinaron que NOX2 está localizada en la membrana plasmática de los conos de crecimiento axónico. La activación de NOX2 lleva a un incremento de las ERO en el dominio P, mientras que la inhibición farmacológica de NOX2 altera la dinámica de la actina y el crecimiento de los axones. Interesantemente, la localización de NOX2 activa, es muy alta en los haces de F-actina, lo cual es interrumpido con citocalasina B. Esto sugiere que la actividad de NOX2 es influenciada por el citoesqueleto; además cuando las neuronas fueron crecidas en camas de apCAM, la cuales evocan crecimiento axonal, también promovieron actividad de NOX2, por lo que se sugiere que la relación entre NOX2 y el citoesqueleto de actina es bidireccional (Munnamalai et al., 2014a).

La función de las ERO en los conos de crecimiento axónico pueden regular diferentes aspectos de la dinámica y función de estas estructuras celulares. Zhang y colaboradores (Zhang and Forscher, 2009) caracterizaron en neuronas de Aplysia una relación entre las ERO y el calcio. En este modelo el calcio es elevado en los conos de crecimiento axónico en respuesta a serotonina de manera dependiente de las ERO producidas por NOX. En condiciones normales, cerca del 13% de las neuronas incrementan los niveles de calcio en respuesta a serotonina, lo cual es incrementado a un 80% cuando las células expresan una forma constitutivamente activa de Rac1. La forma constitutivamente activa de Rac1 promueve el movimiento de los microtúbulos y las pozas de Ca^{2+} del retículo endoplasmático hacia el dominio P del cono de crecimiento axónico. Al mismo tiempo y de forma independiente, la forma constitutivamente activa de Rac1 promueve la formación de ERO en respuesta a serotonina, mientras que la forma dominante negativa tiene un efecto opuesto. Cuando las ERO se eliminaron con antioxidantes en presencia de la forma constitutivamente activa, el incremento de calcio evocado por serotonina se bloquea completamente. Por el contrario, cuando se agrega H_2O_2 de forma exógena, la liberación de calcio se restaura en presencia de la forma dominante negativa de Rac1. Este efecto del H_2O_2 es dependiente de los receptores IP_3, ya que el bloqueo de estos receptores con xestopongina C, bloquea el efecto del H_2O_2 exógeno sobre la liberación de calcio (Zhang and Forscher, 2009). Este efecto podría estar mediado por una regulación oxidativa de los receptores IP_3, los cuales responden a ERO modificando su apertura (Joseph et al., 2006). Los efectos funcionales de este proceso podrían tener grandes implicaciones en la dinámica de los conos de crecimiento, ya que se sabe que el calcio posee efectos pleiotrópicos en la movilidad de los conos de crecimiento (Henley and Poo, 2004).

La regulación de la motilidad axonal es de gran relevancia, ya que de esto depende que las neuronas establezcan los contactos sinápticos de forma adecuada. Estos movimientos son regulados en respuesta a señales extracelulares que guían a los axones. Las semaforinas son un grupo de proteínas que guían el crecimiento axonal, cuyos mecanismos de acción requieren de la activación de receptores específicos (Sharma et al., 2012), los cuales acoplan vías de señalización que regulan la dirección del axón y la migración neuronal. En las neuronas del ganglio de la raíz dorsal, la semaforina3A induce el colapso del cono de crecimiento axónico a través de la regulación de CRMP2 (Proteína mediadora 2 de respuesta a colapsina). La fosforilación de CRMP2 por GSK3-β y Cdk5 promueve el desensamble de los microtúbulos, lo cual produce el colapso del cono de crecimiento axónico (Zhou et al., 2008). En estas neuronas, Morinaka y colaboradores (Morinaka et al., 2011) encontraron que la fosforilación de CRMP2 se regula específicamente por H_2O_2, ya que la semaforina3A induce la generación de H_2O_2 en el cono de crecimiento axónico a través de la fuente de ERO MICAL (moléculas que interactúan con CasL), lo cual oxida a CRMP2 e induce la formación transitoria de un enlace disulfuro homodímero entre las cisteínas 504 de dos moléculas de proteínas CRMP2. En este punto el homodímero se reduce por tiorredoxina, formando un enlace disulfuro entre una molécula de CRMP2 y tiorredoxina. Este complejo es posteriormente fosforilado por GSK3-β, lo cual produce el colapso del cono de crecimiento en estas neuronas (Morinaka et al., 2011). En su conjunto estos estudios demuestran la importancia de la producción localizada y regulada de las ERO en los conos de crecimiento axónico y su función como moléculas señal que regula la dinámica de estas estructuras, lo cual es trascendental para el desarrollo adecuado del sistema nervioso y el establecimiento adecuado de los circuitos sinápticos.

1.5 Células astrogliales

En el cerebro humano las células gliales sobrepasan diez veces en número a las neuronas. Esta proporción se reduce en los mamíferos con cerebros de menor tamaño (Oberheim et al., 2006). La astroglía es un tipo celular muy importante tanto en el cerebro adulto como en el cerebro en desarrollo. Su morfología es muy variada, pudiendo cambiar en determinadas condiciones, tal como ocurre durante la activación, proceso caracterizado por cambios en la expresión génica, la hipertrofia y proliferación (Belanger and Magistretti, 2009). En condiciones normales, estas células extienden procesos que entretejen una compleja comunicación con distintos tejidos como los vasos sanguíneos, lo que constituye la barrera hematoencefálica (Anderson and Nedergaard, 2003). Otros procesos pueden contactar los somas y procesos de las neuronas y de esta forma pueden controlar la formación de las sinapsis en el desarrollo y su modulación en el adulto (Jessen, 2004). Además, estas células pueden proveer un suporte estructural y metabólico muy importante para el sistema nervioso central. Se sabe que las células astrogliales ayudan a regular el exceso de K^+ extracelular que puede ocurrir con la actividad neuronal (Wallraff et al., 2006), también participan en la regulación del pH extracelular (Majumdar et al., 2008) y en la recaptura del glutamato y GABA (Rothstein et al., 1996; Haberg et al., 2001), entre otras funciones.

1.5.1 Células astrogliales y ERO

El sistema nervioso central de mamíferos es particularmente susceptible de los efectos tóxicos de las ERO, lo cual se debe al alto índice de actividad metabólica oxidativa y al alto contenido de ácidos grasos presentes en la mielina y otras membranas plasmáticas. Los enlaces insaturados carbono-carbono requeridos para asegurar la fluidez de las cadenas de ácidos grasos de los fosfolípidos son los más susceptibles al estrés oxidante por ERO (Halliwell and Gutteridge, 1999). Los niveles de ERO pueden incrementarse durante eventos fisiológicos que ocurren principalmente durante el desarrollo del sistema nervioso (Olguín-Albuerne et al., 2014) y en distintas neuropatologías y enfermedades neurodegenerativas tales como alguno desórdenes psicopatológicos, problemas cerebrovasculares, excitotoxicidad por glutamato y en las enfermedades del Parkinson, Alzheimer, Esclerosis Lateral Amiotrófica y Huntington, entre otras (Barnham et al., 2004; Sorce and Krause, 2009; Uttara et al., 2009; Sorce et al., 2010; Valencia et al., 2013).

Las implicaciones de los efectos de las ERO en las células astrogliales durante el desarrollo no se han descrito, no obstante, en los eventos patológicos se han abordado ampliamente. Alteraciones en la función de las células astrogliales pueden conducir a distintos eventos patológicos, sin embargo, también se sabe que las células astrogliales poseen cualidades neuroprotectoras (Belanger and Magistretti, 2009; Stobart and Anderson, 2013). La capacidad neuroprotectora de las células astrogliales puede deberse en parte a que estas células poseen una mayor capacidad antioxidante. Por ejemplo, las células astrogliales poseen mayores niveles de glutatión en comparación a las neuronas (Rice and Russo-Menna, 1998) y también muestran una incrementada actividad de las enzimas glutatión S-transferasa, glutatión peroxidasa y catalasa (Wilson, 1997; Dringen et al., 1999). Por otra parte, las ERO producidas por NOX, conducen a los cambios morfológicos de estas células (Zhu et al., 2009) y la desregulación de las ERO en la astroglía puede conducir a la muerte celular (Jacobson and Duchen, 2002; Wang et al., 2009). Además, durante el desarrollo del cerebelo se presenta un episodio de muerte celular programada alrededor del día P7, en el cual aproximadamente el 50 al 70 % de las células que mueren corresponden a células astrogliales (Krueger et al., 1995). Sin embargo, hasta el momento no se ha determinado que la muerte programada

de células astrogliales este asociada a la generación ERO, tal como ocurre en el caso de las NGC cultivadas, donde las ERO guían el proceso de muerte celular apoptótica (Valencia and Moran, 2004; Ramiro-Cortes and Moran, 2009; Ramiro-Cortes et al., 2011).

II. Planteamiento del problema

Los efectos de las ERO en el sistema nervioso han sido ampliamente estudiados en distintas patologías y enfermedades neurodegenerativas. Sin embargo, muy pocos estudios se han enfocado en el entendimiento de las ERO como moléculas señal que regulan la fisiología del sistema nervioso. La mayor parte de los estudios que han abordado este aspecto, se han centrado en modelos de líneas celulares en las cuales un estímulo induce la adquisición de características del tipo neuronal. Estos estudios han sido fundamentales para nuestro entendimiento sobre la regulación de la señalización redox que ocurre durante la adquisición de características neuronales. Otros estudios han abordado la relevancia de las ERO en células neurales, en las cuales se ha determinado que las ERO pueden actúan como reguladores de la proliferación de las células precursoras neurales y como reguladores de la diferenciación neuronal. Por otra parte, otros trabajos han descrito como las ERO pueden regular la dinámica del citoesquelo, lo cual también se ha demostrado que ocurre durante la guía y el crecimiento de los axones de las neuronas en desarrollo. Finalmente, estudios previos de nuestro grupo sugieren que la corteza cerebelar en desarrollo es un sitio importante de generación de ERO, además, estos mismos estudios indican que las ERO pueden actuar como morfógenos en el desarrollo de la corteza cerebelar. Sin embargo, en este modelo no se conoce con exactitud sobre qué procesos del desarrollo actúan las ERO y si es que los efectos de estas actúan sobre las neuronas y/o células astrogliales.

A lo largo de estos estudios se han descrito distintos mecanismos por los cuales actúan las ERO, sin embargo, la información acumulada hasta el momento es muy escasa, por lo que resulta pertinente realizar más estudios que nos permitan expandir nuestro conocimiento sobre las funciones fisiológicas de las ERO durante el desarrollo del sistema nervioso. Un aspecto crítico de estos estudios, es que gran parte de la información con la que contamos hasta el momento, está centrada en fases iniciales de la diferenciación neuronal, sin embargo, muy poco se sabe sobre los efectos de las ERO en la maduración neuronal. Por otro parte, poco se sabe acerca de los mecanismos por los cuales las ERO se regulan durante los procesos del desarrollo del sistema nervioso. Por estas razones, en el presente estudio, nosotros nos planteamos estudiar los mecanismos que regulan a las ERO y su función sobre el desarrollo y la maduración neuronal, así como el papel de las ERO sobre las células astrogliales del cerebelo en desarrollo. Para esto, nosotros empleamos un modelo de desarrollo de las NGC, que resulta ideal para el estudio de distintos procesos del desarrollo neuronal y cultivos de células astrogliales obtenidos del cerebelo en desarrollo.

III. Hipótesis

1.-, Durante el desarrollo de las NGC en cultivo, los homólogos NOX generan ROS de manera regulada, las cuales participan en la sobrevivencia, maduración y neuritogénesis de estas células.

2.- Las ERO tienen un papel relevante en la regulación de la morfología y muerte de las células astrogliales.

IV. Objetivos

Determinar la producción de ERO durante el desarrollo de las NGC.

Analizar el efecto de las ERO en el desarrollo de las NGC.

Determinar la fuente de generación de las ERO y el sistema antioxidante que las regula.

Determinar si el H_2O_2 regula el desarrollo de las NGC.

Examinar el efecto de la manipulación experimental de los sistemas antioxidantes y pro-oxidantes sobre el desarrollo de las NGC.

Estudiar el papel de las ERO en la muerte de astroglía y si la inducción de ERO modula la morfología y muerte de las células astrogliales.

V. Métodos

5.1 Cultivo celular

Todos los animales empleados para experimentación en el presente estudio, fueron tratados de acuerdo con los estándares de cuidado animal y con los procedimientos aprobados por el Comité de Investigación y Ética del Instituto de Fisiología Celular de la Universidad Nacional Autónoma de México.

Los cultivos de NGC y células astrogliales fueron preparados a partir de ratas Wistar postnatales de 8 días y de ratones C57 black de 7 días postnatales silvestres y deficientes en NADPH-oxidasa 2 y 3 para el caso de las células astrogliales tal como fue reportado por Morán y Patel (Moran and Patel, 1989a). Las neuronas granulares fueron sembradas a una densidad de 265 $\times 10^3$ células/cm^2 en cajas Petri o cubreobjetos tratados con poli-$_L$-lisina (5 µg/ml), mientras que las células astrogliales fueron sembradas a una densidad 135 $\times 10^3$ células/cm^2. Las células fueron cultivadas en medio basal Eagle suplementado con10% (v/v) de suero fetal bovino (inactivado por calor),

glutamina (2 mM), KCL (20 mM), penicilina (50 U/ml) y estreptomicina (50 mg/ml). Las NGC se cultivaron bajo estas condiciones en periodos que abarcaron de 0 a 8 DIV y las células astrogliales fueron cultivadas por un periodo de 15 DIV. Los cajas de cultivo fueron incubadas a 37ºC en una atmosfera humidificada de CO2/aire (5%/95%). Con la finalidad de impedir el crecimiento de células gliales, se agregó citosina arabinosa (10 µM) a las 24h posteriores al sembrado de las células. Los cultivos contienen aproximadamente un 95% de neuronas. Las colonias de ratones deficientes de NADPH-oxidasa 2 (gp91phox) y NADPH-oxidasa 3 se adquirieron de los laboratorios Jackson y se mantuvieron en el biotério del instituto.

5.2 Viabilidad celular

Las NGC fueron incubadas con calceína (10 µM) y ioduro de propidio (5 µM) durante 15 min a 37ºC. Las células fueron fotografiadas en un microscopio de epifluorescencia utilizando los filtros con las siguientes características: filtro de excitación/espejo dicroico/filtro de barrera 450-490/500/515 nm y 510-560/565/590 nm para calceína y ioduro de propidio respectivamente. Por lo menos dos fotografías diferentes se tomaron para cada condición. Los resultados se expresaron como el porcentaje de células viables (células positivas a calceína) respecto al total de células (células positivas a calceína más las células positivas a ioduro de propidio) por campo.

5.3 Actividad metabólica

La actividad metabólica fue determinada por la conversión de MTT a cristales de formazan. Para esto las células fueron sembradas durante diferentes días en una misma caja con pozos múltiples. Se agregó MTT (0.5 mg/ml) a las células y este se incubó en oscuridad durante 15 min a 37 ºC. Los cristales de formazán fueron extraídos con DMSO (100%) y cuantificados espectrofotométricamente a 560 nm.

5.4 Detección de ERO

Las NGC fueron sembradas durante diferentes días en una misma caja de cultivo con pozos múltiples. En el caso de las células astrogliales, éstas fueron tratadas con estaurosporina (0.5 µM) durante diferentes tiempos. Las células se lavaron dos veces con medio Locke (154 mM NaCl, 25 or 5 mM KCl, 3.6 mM NaHCO3, 2.3 mM CaCl, 5.6 mM glucosa y 10 mM Hepes) y posteriormente se incubaron con dihidroetidina (3.17 µM) durante 35 min. Posteriormente las células se lavaron dos veces con medio Locke y se fotografiaron en un microscopio de epifluorescencia empleando el filtro con las siguientes características: filtro de excitación/espejo dicroico/filtro de barrera 510-560/565/590 nm. Se adquirieron dos fotografías, una correspondiente al contraste de fases y la segunda a la fluorescencia. Los registros de fluorescencia se realizaron trazando una región de interés que delimitó el soma, los trazos se realizaron considerando únicamente el canal del contraste de fases y el valor del canal de fluorescencia de 15 neuronas se promedió. A cada medición se le restó el valor de fluorescencia del fondo. Se tomaron al menos dos fotografías por cada condición. Se midió la fluorescencia de 15 células por fotografía y se tomaron dos fotografías por pozos, y el promedio de 4 pozos por experimento fue considerado como n=1. Los resultados están expresados como valores absolutos o datos normalizados respecto a 2 DIV.

5.5 Determinación del contenido de glutatión intracelular

El contenido de glutatión intracelular se determinó por el método del reciclamiento enzimático en una modificación para cajas de múltiples pozos (Tietze, 1969; Rahman et al., 2006). Para esto, las NGC se cultivaron en cajas de 35 mm durante 0 a 8 DIV. Las células fueron lavadas con PBS y sonicadas en 0.1% Tritón X-100 (0.1%) y ácido sulfosalicílico (0.6%) en KPE (0.1 M buffer de fosfatos de potasio y 5 mM EDTA, pH 7.5). Las muestras se mezclaron en volúmenes iguales de DNTB y glutatión reductasa, después de 30 segundos se agregó β-NADPH y se registró una cinética de la absorbancia a 412 nm durante 15 min. Con la finalidad de determinar el glutatión oxidado, las muestras se pre-incubaron con 2.5% de vinilpiridina por 60 min y posteriormente se neutralizaron con triethanolamina. Se emplearon curvas de concentración tanto de glutatión reducido como oxidado para determinar la concertación real de las muestras. El glutatión reducido se calculó a partir de la resta del glutatión oxidado del glutatión total.

5.6 Western Blot

Las NGC se cultivaron en cajas de 60 mm de 0 a 3 DIV en la presencia y ausencia de los antioxidantes Ebselen (10 µM) y Euk-134 (20 µM) y de los inhibidores de la NADPH oxidasa AEBSF (50 µM) y Apocinina (400 µM) en tiempos de incubación de 24 h a los tiempos 1, 2 y 3 DIV. Las células se lavaron dos veces en PBS frio y se realizaron homogenados con una solución de lisis (25 mM Trizma, 50 mM NaCl, 2% Igepal, 0.2% SDS y Complete (Roche ®), pH 7.4). Se determinó la concentración de proteína de las muestras por el método de Lowry. Un total de 60 µg de proteína se corrieron en geles de acrilamida para ser electro-transferidos a membranas PVDF. Posteriormente las membranas fueron bloqueadas en leche libre de grasas (5%) diluida en una solución TTBS (100 mM Trizma, 150 mM NaCl y 0.1% Tween, pH 7.4). Posteriormente las membranas se incubaron toda la noche con alguno de los siguientes anticuerpos primarios: anti-GAPDH (1:3000) (Millipore mab374), anti-Tau (1:500) (Cell Signaling mab4019) y anti-MAP2 (1:500) (Cell Signaling 4542). En los experimentos correspondientes a las células astrogliales, éstas fueron tratadas con estaurosporina (0.5 µM), MnTMPyP (50 µM) y DPI (0.52 µM). Las membranas PVDF fueron incubadas con los anticuerpos anti β-tubulina (1:200) (Sigma T6199) y anti α-actina (1:200).

5.7 Actividad NADPH-oxidasa en células vivas

La actividad NADPH-oxidasa se determinó por la producción extracelular de anión superóxido, determinado mediante la reducción de citocromo c. Para esto, las NGC se sembraron durante diferentes días de cultivo en una misma caja de pozos múltiples; las células se lavaron dos veces con medio Locke y posteriormente se incubaron con 100 µl de medio Locke que contenía citocromo c (250 µM) y β-NADPH (200 µM). Se registró la reducción del citocromo c midiendo la absorbancia a 550 nm a 37^{o}C in un lector Synergy HT. La cantidad del radical anión superóxido se calculó empleando un coeficiente de extinción de 21 mM^{-1} cm^{-1}. Se consideró una distancia de 300 µm como el volumen que ocupan 100 µl en un pozo más la base de la caja de pozos múltiples.

5.8 RT-PCR en tiempo real

El RNA total fue extraído de NGC cultivadas de 0 a 5 DIV, utilizando Trizol de acuerdo a las instrucciones del fabricante. La calidad del RNA extraído fue determinada mediante por absorbancia en un equipo Nanodrop y

mediante electroforesis en geles de agarosa. Un µg del RNA total de cada muestra fue transcrito en cDNA empleando la Transcriptasa reversa M-MLV con el cebador oligo (dT)12-18. Un µg del cDNA fue empleado para determinar la expresión relativa de los genes, lo cual fue hecho en el termociclador Rotor-gene 6000, empleando el Master Mix de Taqman y las pruebas específicas para NOX1 (Rn00586652_m1), NOX2 (Rn00576710_m1) y GAPDH (Rn01775763_g1). Los niveles relativos del mRNA amplificados se normalizaron con el gen GAPDH. El promedio de los valores *C*t del control endógeno (GAPDH) de cada muestra, fueron sustraídos del valor *C*t de cada gen blanco, resultando en el valor ΔC_T. Los cambios se calcularon empleando el método del $2^{-\Delta\Delta CT}$ en donde el umbral ($\Delta\Delta C_T$) se definió como la diferencia entre ΔC_T de 1 a 5 DIV menos el ΔC_T del día en el cual se alcanzó la máxima expresión.

5.9 Inmunocitoquímica

Las células se crecieron durante 0 a 3 DIV en cubre objetos bañados en poli-$_L$-lisina, en algunos casos las células se sembraron a una densidad de $50X10^3$ células/cm^2. Las células se lavaron dos veces en PBS y se fijarón con paraformaldehido (4%) durante 20 min. Posteriormente las células se bloquearon y permeabilizarón en una solución de bloqueo (PBS, 0.5 % Tritón X-100 y 10% suero normal de cabra) durante toda la noche a 4ºC. Más adelante las células se incubaron en la misma solución de bloque con el anticuerpo primario anti-NOX2 (1:250 (0.4 µg/ml)) (Abcam ab31092). El anticuerpo primario se detectó con el anticuerpo secundario Alexa Fluor® 488 Cabra Anti-Conejo IgG (H+L) (1:1000), el cual se incubó durante dos horas a temperatura ambiente. El anticuerpo primario anti-Tau se detectó con un anticuerpo secundario IgG (H+L) Dylight 594 (1:1000), el cual fue incubado por 2 horas a temperatura ambiente. En los experimentos correspondientes a las células astrogliales, se empleó el anticuerpo primar anti α-tubulina (1:200) y la rodamina-faloidina (1 unidad) (Molecular Probes R415). Los cubre objetos fueron montados empleando el medio de montaje Vectashield con DAPI. Las imágenes se capturaron en un microscopio confocal Oympus FV10i-LIV, mientras que para las inmunofluorescencias de las células astrogliales se empleó un microscopio de epifluorescencia. Las NGC incubadas sin el anticuerpo primario o con IgG de conejo (1:50 (10 µg/ml)) no mostraron tinción.

5.10 Medición de la localización de H_2O_2 en células vivas

Las NGC se transfectaron antes de sembrarse con 5 µg del plásmido HyPer-cyto (Evrogene), mediante la técnica de nucleofectación empleando el programa C-13 y el kit Amaxa VP1003. Este plásmido es un sensor fluorescente genéticamente codificado que está diseñado para detectar H_2O_2 citoplasmático. Las NGC fueron visualizadas en un microscopio Axiovert 200M con un sistema Lambda DG-4 y un sistema PECON para cultivo celular y microscopía. Se empleó un objetivo Fluar 40x/1.30 Oil M27 para visualizar a las células. La fluorescencia se adquirió en dos canales diferentes: C1 (excitación 460-480 nm, espejo dicroico 493 nm, emisión 505-530) y C2 (excitación 379-395 nm, espejo dicroico 410 nm, emisión 465-555) en intervalos de tiempo. Las imágenes presentadas están expresadas como el índice de C1 y C2 menos sus respectivas fluorescencias de fondo. Los índices más altos corresponden a mayores niveles de H_2O_2. Con la finalidad de determinar las regiones en las cuales hubo mayores niveles de H_2O_2, se registró una región de interés y los valores se registraron durante distintos fotogramas, se promedió el valor en el tiempo y se normalizó con respecto al valor medio de la fluorescencia del soma. Únicamente se consideraron los fotogramas en los cuales la región de interés se encontraba plenamente en

foco. La medición de cada estructura representa n=1. El análisis de las imágenes fue realizado con los programas AxioVision 4.8.2 e Image J.

5.11 Determinación de la morfología axonal

Las NGC se tiñeron con el marcador de membranas PKH67 (3 µM) (Sigma PKH67GL-1KT) en una proporción de $10X10^3$ células teñidas y de $18X10^3$ de células no teñidas. El PH67 es un marcador de membranas, el cual está compuesto por un marcador verde fluorescente que posee una larga cola alifática que se intercala en las regiones lipídicas de las membranas celulares (Wallace et al., 2008). Las células se trataron con el inhibidor de la síntesis del glutatión BSO (100 µM) al momento de sembrarse, en algunos experimentos las células se trataron con el antioxidante Euk-134 (10 µM) durante 24 h después del sembrado. Las células se visualizaron y fotografiaron en un microscopio de fluorescencia. La morfología de los axones se clasificó en tres diferentes categorías que fueron, no alterados, con esferoides múltiples y colapsados. La proporción de neuronas categorizadas en estos tres tipos morfológicos fue determinada por experimento y posteriormente promediada en experimentos independientes.

5.12 Crecimiento axonal

Las NGC se tiñeron antes de sembrarse con PKH-67 (3 µM) a temperatura ambiente durante 5 min. Se empleó un volumen igual de albumina (1%) disuelta en PBS para bloquear la reacción. Las células teñidas se centrifugaron a 400 g por 8 min a temperatura ambiente. Posteriormente se re-suspendieron en medio de cultivo en una proporción de 10×10^3 células teñidas y 18×10^6 células no teñidas. Las neuritas se midieron manualmente y solo aquellas neuritas más largas que el diámetro de la célula y que no establecieron contactos con otras células teñidas se consideraron para promediar. En el caso de las NGC bipolares, solo se consideró la neurita de mayor tamaño. La medición de cada proceso neurítico representa n=1. Las mediciones se hicieron con Image J con la extensión Neuron J.

5.13 Análisis estadístico

El análisis estadístico se realizó con el programa SigmaPlot 12.1. Los datos están expresados como medias ± error estándar o desviación estándar según es especificado. Se realizó un análisis de varianza (ANOVA) seguido de la prueba post-hoc Holm-Sidak. En algunos casos se realizó una ANOVA no paramétrica. Las diferencias estadísticas en las comparaciones realizadas entre dos grupos fueron hechas mediante la prueba de T o la U de Mann-Whitney según es especificado. Para las comparaciones realizadas en el tiempo, se empleó una prueba de T pareada. Únicamente los valores p menores a 0.05 fueron considerados como estadísticamente significativos.

VI. Resultados

6.1 Desarrollo de las NGC in vitro

Con la finalidad de determinar si durante el desarrollo de las NGC, existen cambios en la producción basal de ERO, realizamos cultivos de NGC, los cuales se mantuvieron tanto en concentraciones despolarizantes (K25)

como no despolarizantes (K5) de KCl, (25 mM y 5 mM, respectivamente). Este procedimiento experimental nos permitió contrastar una condición en la cual las NGC son capaces de completar su desarrollo *in vitro* (K25), con una condición en la cual estas células no son capaces de completar su desarrollo *in vitro* (K5) (Schulz et al., 1996). Bajo estas condiciones, medimos la viabilidad celular y la actividad metabólica de las NGC durante los primeros 5 DIV, con la finalidad de determinar el tiempo durante el cual la sobrevivencia neuronal se compromete durante el desarrollo de las NGC. En correspondencia con lo reportado por Gallo y colaboradores (Gallo et al., 1987), la sobrevivencia de las NGC medida por la incorporación de calceína y ioduro de propidio depende del estado de despolarización después de 3 DIV. La Figura 4 muestra que cuando las NGC fueron cultivadas en K5, la viabilidad celular disminuyó significativamente desde el 4 DIV, mientras que en K25 la viabilidad celular permaneció inalterada durante los primeros 5 DIV (Figuras 4A y B). Por otra parte, la actividad metabólica se midió como la transformación de MTT durante los mismos tiempos, encontrándose que en K5, ésta se mantuvo sin cambios a lo largo del tiempo y fue menor aproximadamente en un 30% con respecto a K25 en el 5 DIV; en contraste, la actividad metabólica de las NGC crecidas en K25 mostró un incremento sostenido durante los primeros 5 DIV (Figura 4C).

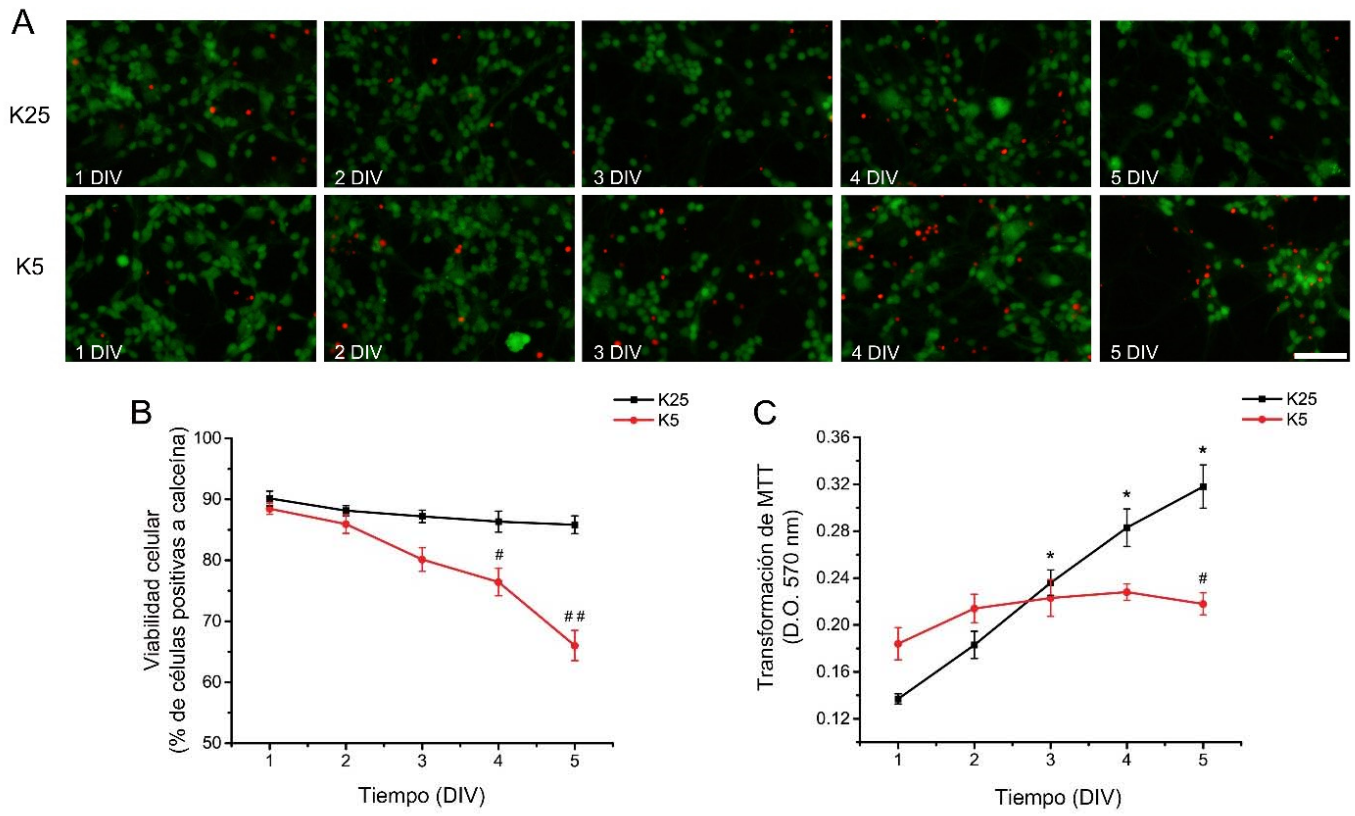

Figura 4. Viabilidad celular de las NGC disminuye en condiciones no despolarizantes. (A) Imágenes representativas de NGC en condiciones despolarizantes (K25) y no despolarizantes (K5) de 1 a 5 DIV. Las células positivas a calceína están marcadas en color verde y las células positivas a ioduro de propidio están marcadas en color rojo (La barra de escala equivale a 100 µm). (B) La viabilidad celular está expresada como el porcentaje de células positivas a calceína del total de células que corresponde a la suma de las células positivas a calceína más las células positivas a ioduro de propidio. En las neuronas crecidas en K5, la

viabilidad celular fue menor a 4 y 5 DIV en comparación a las neuronas crecidas en K25 a las mismas edades (# $p<0.01$, ## $p<0.001$, ANOVA, n=6). Los datos son la media ± error estándar. (C) La actividad metabólica se determinó por la transformación de MTT por NGC crecidas en K25 o K5 de 1 a 5 DIV. En las NGC crecidas en K25, la actividad metabólica incrementó a los 3, 4 y 5 DIV comparado con 1 DIV (⋆ $p<0.001$, ANOVA, n=6). En NGC crecidas en K5, la actividad metabólica fue menor a 5 DIV en comparación a 5 DIV en K25 (⋆ $p<0.001$, ANOVA, n=6). Los datos son la media ± error estándar.

6.2 Los niveles de ERO cambian diferencialmente durante el desarrollo de las NGC

Una vez determinado el tiempo durante el cual disminuye la viabilidad celular en las NGC, se midió la producción de ERO mediante la oxidación de dihidroetidina. Encontramos que cuando las NGC se cultivaron en K5, los niveles de ERO fueron idénticos a los encontrados en las NGC cultivadas en K25, durante los primeros 3 DIV, sin embargo, a 4 y 5 DIV, los niveles de ERO continuaron incrementando (Figura 5B). Por otra parte, cuando las NGC se cultivaron en K25, los niveles incrementaron paralelamente conforme al desarrollo. De 0 a 1 DIV, los niveles de ERO incrementaron alrededor de 160% y de 1 a 2 DIV incrementaron aproximadamente un 110% (Figura 5C). El máximo nivel de ERO alcanzado a los 2 DIV, se mantuvo hasta los 3 DIV, para posteriormente descender a los niveles basales de ERO observados a 1 DIV, los cuales permanecieron inalterados hasta los 8 DIV. Estos resultados indican que los niveles de ERO cambian durante el desarrollo de las NGC, existiendo un punto en el cual se alcanzan los mayores niveles de ERO (2 y 3 DIV) a partir del cual diverge la producción de ERO de acuerdo al estado de despolarización de las neuronas: bajo despolarización, las neuronas disminuyen sus niveles de ERO mientras que en condiciones no despolarizantes sucede lo contrario, las ERO continúan incrementando.

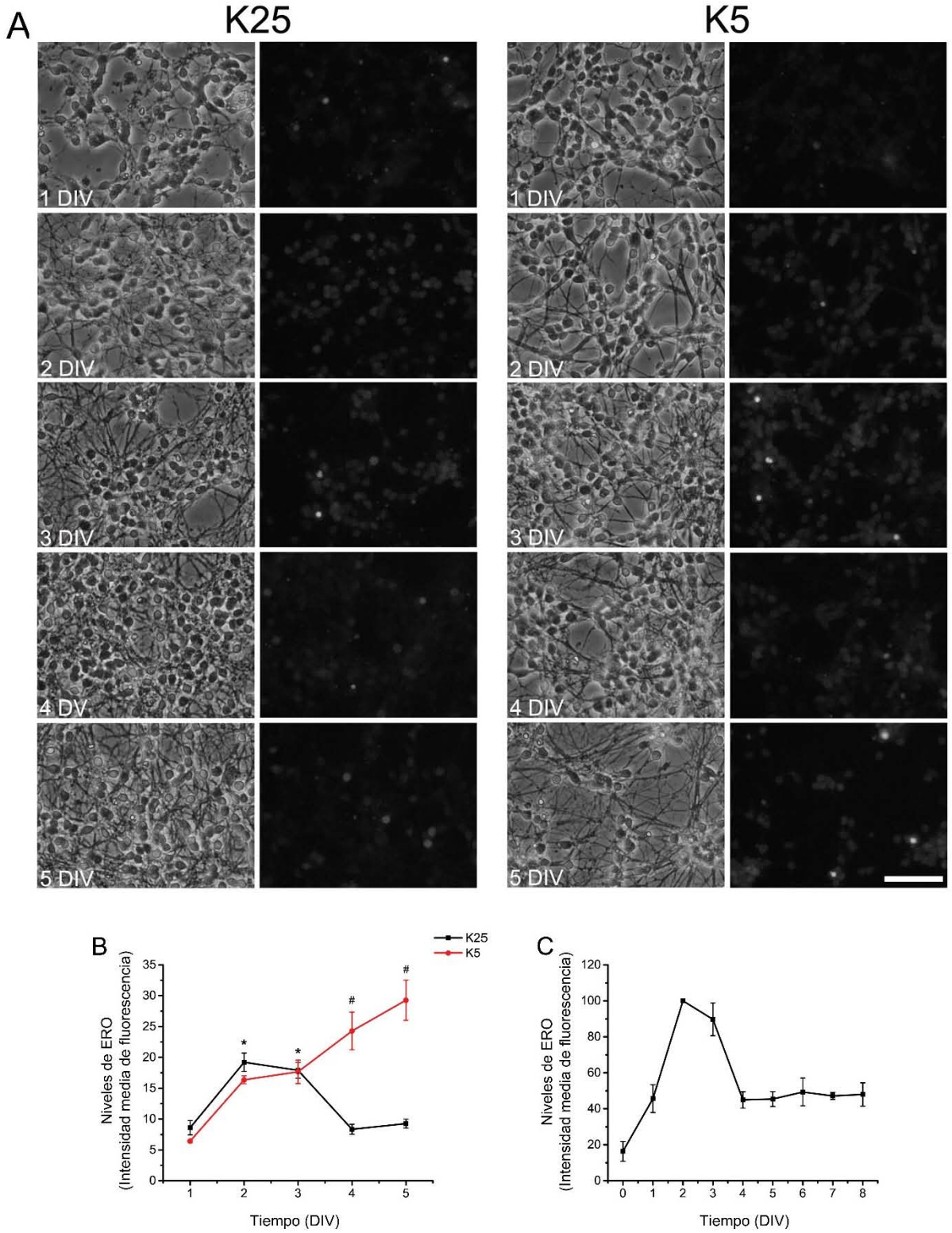

Figura 5. Regulación de las ERO durante el desarrollo de las NGC. (A) Imágenes de contraste de fases y fluorescencia de NGC crecidas en K25 o K5 de 1 a 5 DIV (la barra de escala representa 100 µm). (B) Los niveles de ERO están expresados como los valores de la intensidad de fluorescencia media del catión etidio, que es el producto de la oxidación de la dihidroetidina. En NGC crecidas en K25, los niveles de ERO producidos a 2 y 3 DIV, incrementaron en comparación a 1 DIV (⋆ $p<0.05$, ANOVA, n=4). En NGC crecidas en K5, los niveles de ERO producidos a 4 y 5 DIV fueron mayores en comparación a las NGC crecidas en K25 a las mismas edades (# $p<0.001$, ANOVA, n=4). Los datos son la media ± error estándar. (C) Niveles de ERO de las NGC crecidas en K25 de 0 a 8 DIV. Los niveles de ERO producidos de 1 8 DIV fueron mayores que aquellos producidos a 0 DIV

(p<0.001, ANOVA, n=3-9). Los niveles de ERO producidos a 2 y 3 días fueron mayores que aquellos producidos a 0, 1, 4-8 DIV (p<0.001, ANOVA, n=3-9). Los datos están normalizados con respecto a 2 DIV y son la media ± desviación estándar.

6.3 Papel del glutatión durante el desarrollo de las NGC

Como se mencionó, los niveles de ERO en las células se mantienen estables debido a un equilibrio entre la producción de ERO por las distintas fuentes productoras y por los niveles y actividad de los sistemas antioxidantes (Halliwell, 2009). De entre los numerosos sistemas antioxidantes, el glutatión se destaca por ser uno de los sistemas más relevantes y como se explicó, los niveles de este antioxidante se incrementan durante el desarrollo (Nanda et al., 1996; Rice and Russo-Menna, 1998), en un tiempo que coincide con la diferenciación y maduración de las NGC (Komuro and Yacubova, 2003). Todo esto sugiere que el glutatión podría estar implicado en la regulación de las ERO producidas durante el desarrollo de las NGC, razón por la cual evaluamos los niveles de glutatión durante el desarrollo de las NGC con la finalidad de encontrar una posible relación entre este sistema antioxidante y los niveles detectados ERO.

En la Figura 6A, se muestra que cuando las NGC fueron crecidas en K25, el contenido de glutatión reducido se incrementó durante los primeros 2 DIV. El mayor incremento ocurrió de 0 a 1 DIV (~90 %) y de 1 a 2 DIV incrementó alrededor de un 10 %. Los altos niveles de glutatión reducido permanecieron altos hasta el 5 DIV. A 8 DIV, los niveles de glutatión reducido disminuyeron significativamente y estos fueron similares a los valores encontrados en 0 DIV (Fig. 7B). Cuando las células fueron crecidas en K5, el incremento de los niveles de glutatión reducido fue similar al observado en las NGC crecidas en K25, de 0 a 2 DIV; sin embargo, después de 3 DIV, los niveles de glutatión reducido disminuyeron y fueron significativamente distintos de K25 a los 5 DIV (Fig. 7A). Por otra parte, los niveles de glutatión oxidado no cambiaron significativamente a lo largo de las diferentes fases de desarrollo de las NGC y no se encontraron diferencias entre las células sembradas en K25 y K5 (Fig. 6A).

Considerando que los niveles de glutatión incrementaron en correspondencia con los niveles de ERO, nosotros razonamos que el glutatión reducido podría estar involucrado en la protección de las NGC contra las ERO que se producen durante los primeros 3 DIV. Este planteamiento se basa en numerosos estudios que correlacionan altos niveles de ERO con muerte celular. Por otra parte, es posible que la disminución de glutatión reducido en las NGC cultivadas en K5, que se observó después de 3 DIV, pueda relacionarse con el proceso de muerte, lo cual puede ser en dos formas distintas: a) el contenido de glutatión intracelular se agota debido al proceso de muerte celular que se observa en K5 después de los 3 DIV, lo cual explicaría la bajada de glutatión como una consecuencia del proceso de muerte; b) que ocurra lo opuesto, ya que se sabe que la disminución de los niveles de glutatión, puede llevar al proceso de muerte apoptótica, lo cual explicaría que la disminución de los niveles de glutatión son la causa del proceso de muerte apoptótica (Franco and Cidlowski, 2009, 2012).

Con la finalidad de responder estas preguntas, decidimos evaluar el papel del glutatión en la sobrevivencia de las NGC en desarrollo, disminuyendo los niveles de glutatión en tratamientos de 24 y 48 h, con butationin sulfoximina (BSO), que es un inhibidor de la enzima ɣ-glutamilcisteina sintetasa, la cual es la enzima limitante en la biosíntesis del glutatión. Las Figuras 6C-F muestran que los tratamientos con BSO durante 48 h, redujeron significativamente los niveles de glutatión a 2, 3, 5 y 8 DIV. De manera similar, el contenido de glutatión oxidado disminuyó con los tratamientos de BSO a las mismas edades (Figuras 6C-F).

Cuando la viabilidad celular se evaluó, encontramos que los tratamientos con BSO durante 24 h, no afectaron la sobrevivencia de las NGC a ninguna edad (Fig. 6G). Sin embargo, cuando los cultivos se trataron por

48 h con BSO, observamos una reducción total de la viabilidad celular a 2 DIV (Fig. 6H). El efecto del BSO se previno completamente cuando se cultivaron a las NGC durante las últimas 24 h con el antioxidante Euk-134 (Fig. 2I,J), sugiriendo que la muerte celular inducida por BSO a 2 DIV se debe probablemente a un estrés oxidante inducido por la reducción de los niveles de glutatión. Es importante resaltar, que bajo estos mismos tratamientos, la viabilidad celular no se afectó en NGC de 3 a 8 DIV, lo cual indica que las NGC son más vulnerables a la inducción de muerte celular mediada por estrés oxidante a los 2 DIV, en contraste con NGC que se encuentran en estados de desarrollo relativamente más maduros (edades posteriores a 3 DIV). La determinación de los niveles de glutatión a 2 DIV, también se hizo en presencia del antioxidante Euk-134, esto se realizó con la finalidad de asegurarnos que los niveles estimados de glutatión a 2 DIV en tratamientos de BSO a 48 h, no estuviera sesgada por los bajos niveles de proteína encontrados en el tiempo en el que casi la totalidad de las NGC ha muerto (Fig. 6C).

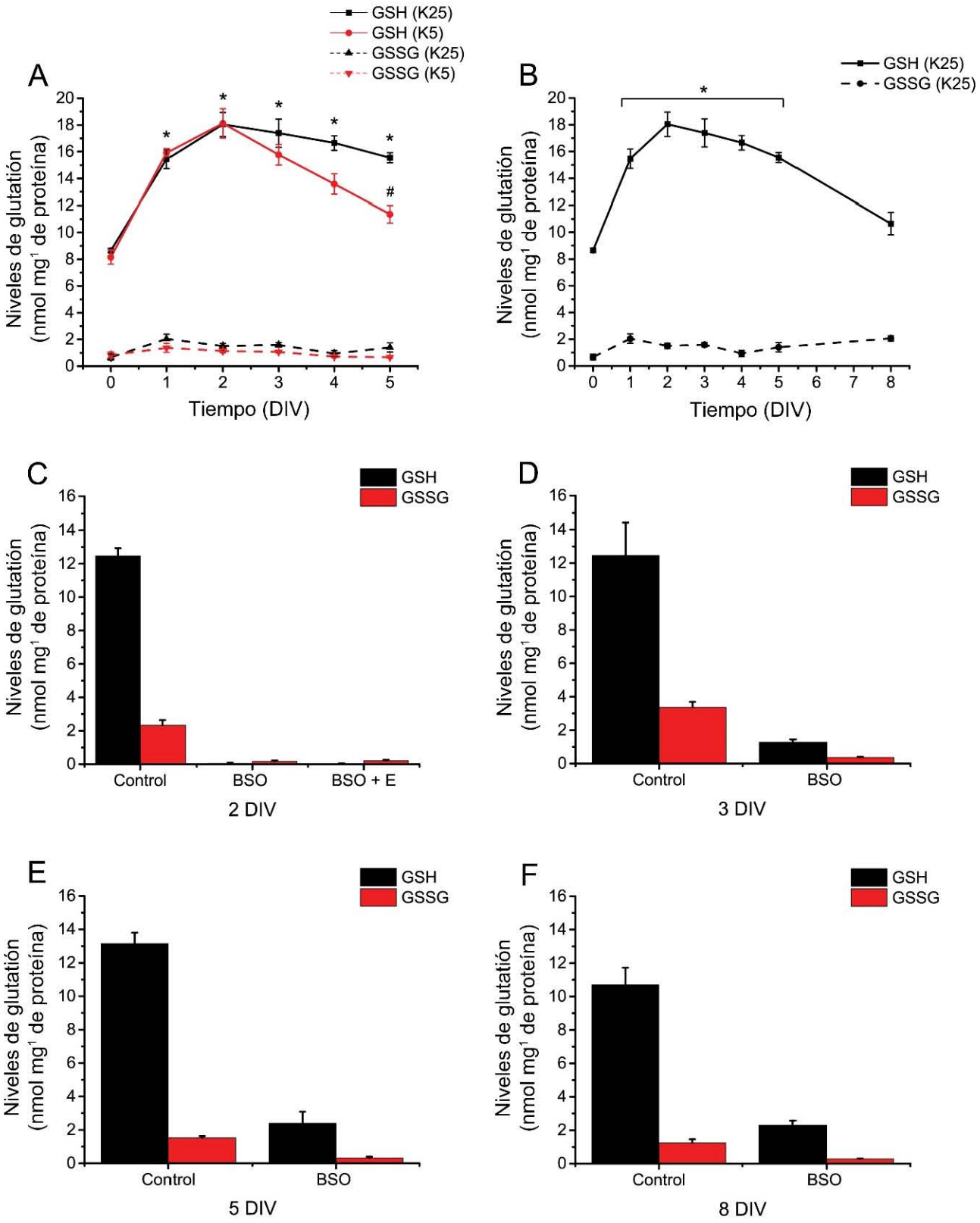
A
GSH (K25)
GSH (K5)
GSSG (K25)
GSSG (K5)
Niveles de glutatión (nmol mg¹ de proteína)
Tiempo (DIV)
B
GSH (K25)
GSSG (K25)
Niveles de glutatión (nmol mg¹ de proteína)
Tiempo (DIV)
C
GSH
GSSG
Niveles de glutatión (nmol mg¹ de proteína)
Control
BSO
BSO + E
2 DIV
D
GSH
GSSG
Niveles de glutatión (nmol mg¹ de proteína)
Control
BSO
3 DIV
E
GSH
GSSG
Niveles de glutatión (nmol mg¹ de proteína)
Control
BSO
5 DIV
F
GSH
GSSG
Niveles de glutatión (nmol mg¹ de proteína)
Control
BSO
8 DIV

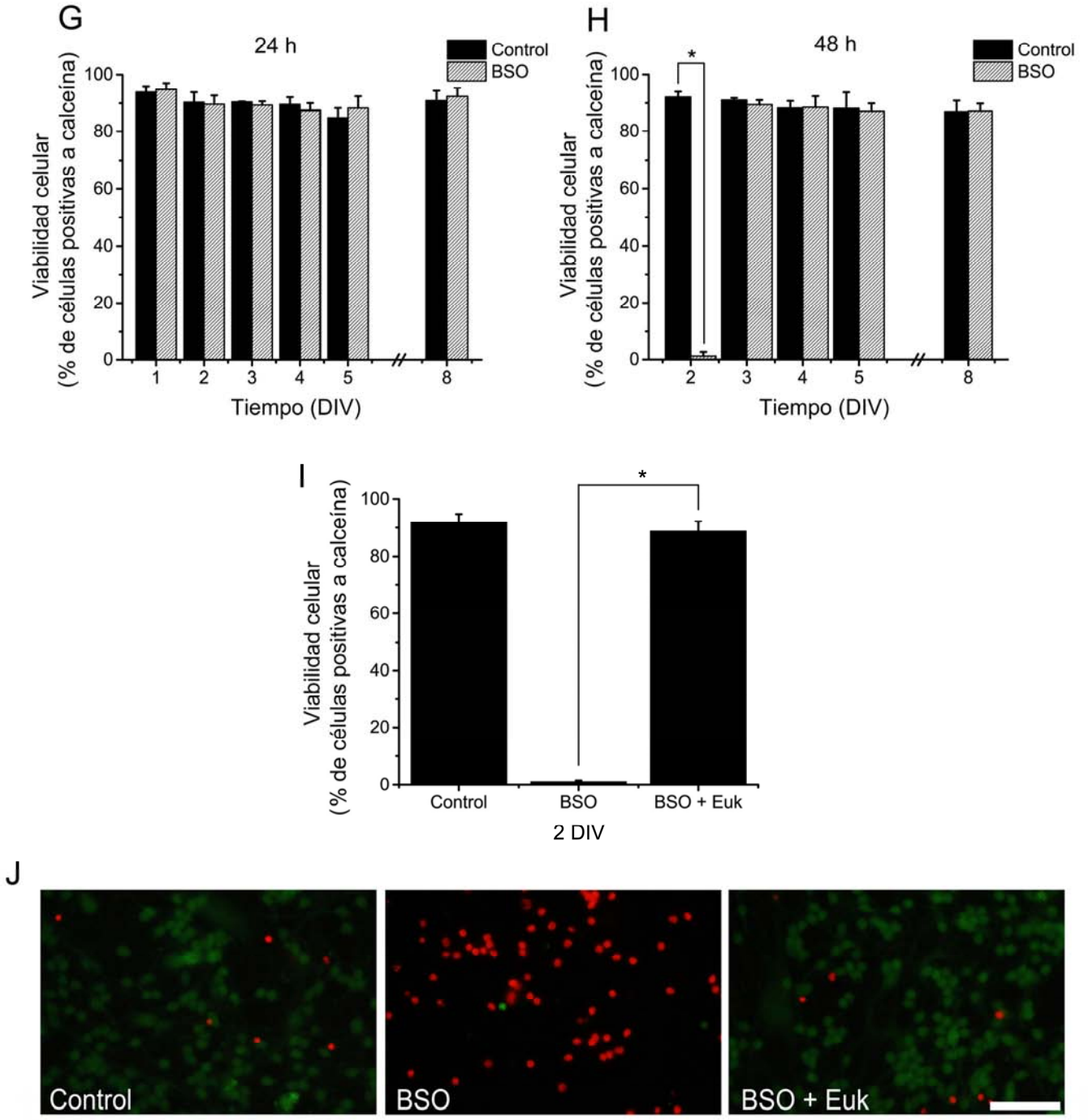

Figura 6. La regulación del glutatión se requiere para la sobrevivencia de las NGC. (A,B) Los niveles de glutatión reducido (GSH) y oxidado (GSSG) se determinaron en NGC crecidas entre 0 y 8 DIV. (A) En NGC crecidas en K25, los niveles de GSH de 1 a 5 DIV fueron mayores en comparación a 0 DIV (⋆ P<0.001, ANOVA, n=4). Los datos son la media ± el error estándar. (B) En NGC crecidas en K25 de 0 a 8 DIV, los niveles de GSH de 1 a 5 DIV fueron más altos en comparación a 0 DIV (⋆ P<0.001, ANOVA, n=4). Los datos son la media ± el error estándar. (C-F) Los niveles de GSH y GSSG se determinaron en NGC crecidas en K25 y tratadas con BSO (100 µM) por 48 h y con Euk-134 (10 µM) por 24 h. El tratamiento con BSO redujo los niveles de GSH y GSSG en todos los casos (P<0.001, Prueba de T, n=5, n=4, n=4 respectivamente). (G-I) La viabilidad celular se determinó por calceína y ioduro de propidio. Los datos están expresados como el porcentaje de células positivas a calceína del total de células que corresponde a la suma de las células positivas a calceína más las células positivas a ioduro de propidio. (G) La viabilidad celular se determinó en NGC crecidas en K25 y tratadas con BSO (100 µM) por 24 h a 1, 2, 3, 4, 5 y 8 DIV (no se encontraron diferencias, ANOVA, n=4). (H) La viabilidad celular se determinó en NGC crecidas en K25 y tratadas con BSO (100 µM). El BSO disminuyó la viabilidad celular a 2 DIV (⋆ p<0.001, ANOVA, n=4). (I) La viabilidad celular fue determinada en NGC crecidas en K25 y tratadas con BSO (100 µM) por 48 h y con Euk-134 (10 µM) por 24 h. La viabilidad celular disminuyó por el BSO, pero completamente se rescató por Euk-134 (⋆ p<0.001, ANOVA, n=4). Los datos son la media ± el error estándar. (J)

Imágenes representativas de NGC crecidas en K25 y tratadas con BSO (100 µM) por 48 h y con Euk-134 (10 µM) por 24 h. Las células positivas a calceína están marcadas en verde y las células positivas a ioduro de propidio están marcadas en rojo (la barra de escala equivale a 100 µm).

6.4 Las ERO promueven la maduración de las NGC

Diferentes estudios sugieren que las ERO regulan la maduración celular durante periodos críticos del desarrollo del sistema nervioso (Tsatmali et al., 2006; Le Belle et al., 2011; Celotto et al., 2012; Coyoy et al., 2013). Con la finalidad de determinar la relevancia de las ERO durante el desarrollo de las NGC, probamos el efecto de dos antioxidantes y dos inhibidores de la NOX, sobre la expresión de Tau y MAP2. Los antioxidantes que se emplearon son Euk-134, que es un mimético de SOD y catalasa (Baker et al., 1998), y Ebselen, el cual es un mimético de la glutatión peroxidasa (Parnham and Kindt, 1984). Los inhibidores de NOX1/2 empleados, son AEBSF y Apocinina (Diatchuk et al., 1997; Cheret et al., 2008; Hernandez-Enriquez et al., 2011; Dvoriantchikova et al., 2012; Lu et al., 2012)

Se sabe que la expresión de las proteínas Tau y MAP2, puede ser empleada como indicador de la maduración neuronal (Dehmelt and Halpain, 2004). Bajo estas condiciones, determinamos la expresión de Tau y MAP2 en NGC de 0 a 3 DIV, así como en astrocitos aislados de cerebelo empleados como un control negativo de la expresión de estas dos proteínas. Encontramos una correlación entre el incremento de ambas proteínas conforme a la maduración de las NGC. Para ambas proteínas, el mayor incremento ocurrió entre 1 y 2 DIV (Fig. 7A). Cuando las NGC se trataron con Ebselen y Euk-134 a 0 DIV, durante 24h, no se observaron efectos en los niveles de Tau y MAP2; sin embargo, AEBSF y Apocinina disminuyeron los niveles de Tau aproximadamente un 50%, mientras que AEBSF, pero no Apocinina, disminuyó la expresión de MAP2 aproximadamente un 70% (Fig. 7B). Cuando las NGC se trataron durante 24 h a 1 DIV, ninguno de los antioxidantes tuvo efecto en los niveles de Tau, pero sí disminuyeron la expresión de MAP2 alrededor de un 30%. En contraste, AEBSF y Apocinina, disminuyeron significativamente la expresión de Tau y MAP2 en un 60% y 30% respectivamente (Fig. 7C). Finalmente, cuando las NGC se trataron de 2 a 3 DIV, ninguno de los tratamientos tuvo efecto alguno en los niveles de las proteínas Tau y MAP2 (Fig 7D). Estos resultados sugieren que la maduración de las NGC se promueve por las ERO generadas por NOX. (Tau y MAP-2 tienen isoformas propias del desarrollo. La MAP2 de células jóvenes es la MAP2c y es de menor peso molecular, muy parecido a Tau. Muchas veces más que cambios en la expresión ocurren cambios en la fosforilación lo que permite un mayor dinamismo de los microtúbulos. Qué anticuerpos usaste para Tau? Por otro lado MAP2 es muy susceptible a degradación durante el proceso de daño neuronal calcio/dependiente, así que un bajo contenido puede indicar que la proteína se está degradando).

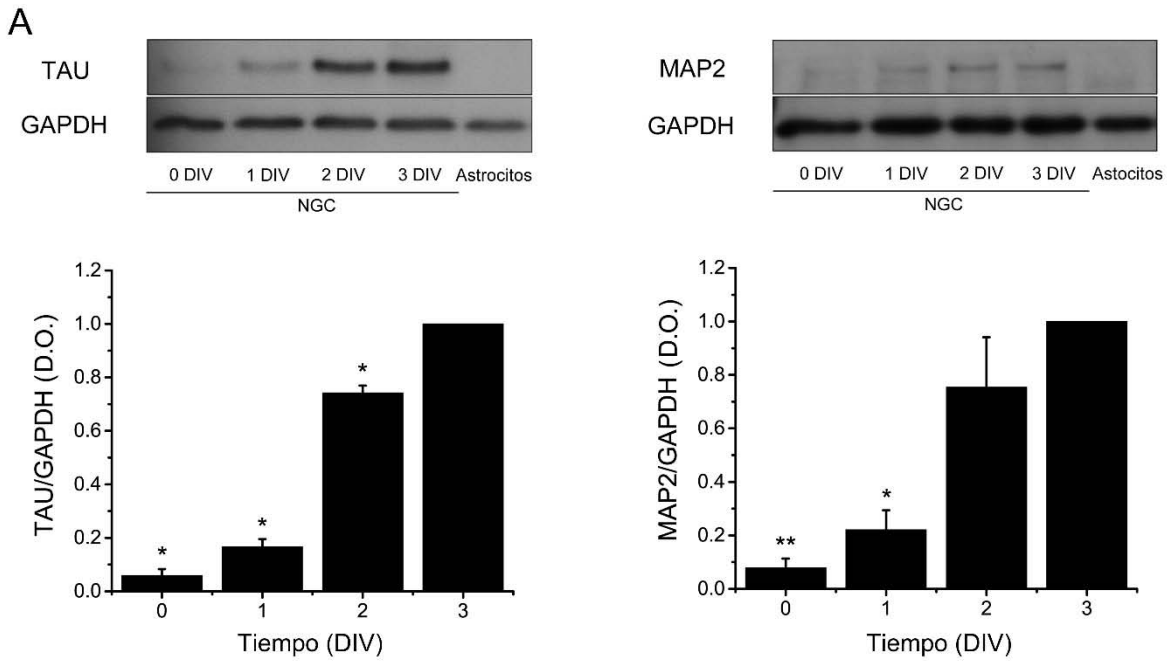
A
TAU
GAPDH
0 DIV
1 DIV
2 DIV
3 DIV
Astrocitos
NGC
MAP2
GAPDH
0 DIV
1 DIV
2 DIV
3 DIV
Astocitos
NGC
TAU/GAPDH (D.O.)
Tiempo (DIV)
MAP2/GAPDH (D.O.)
Tiempo (DIV)

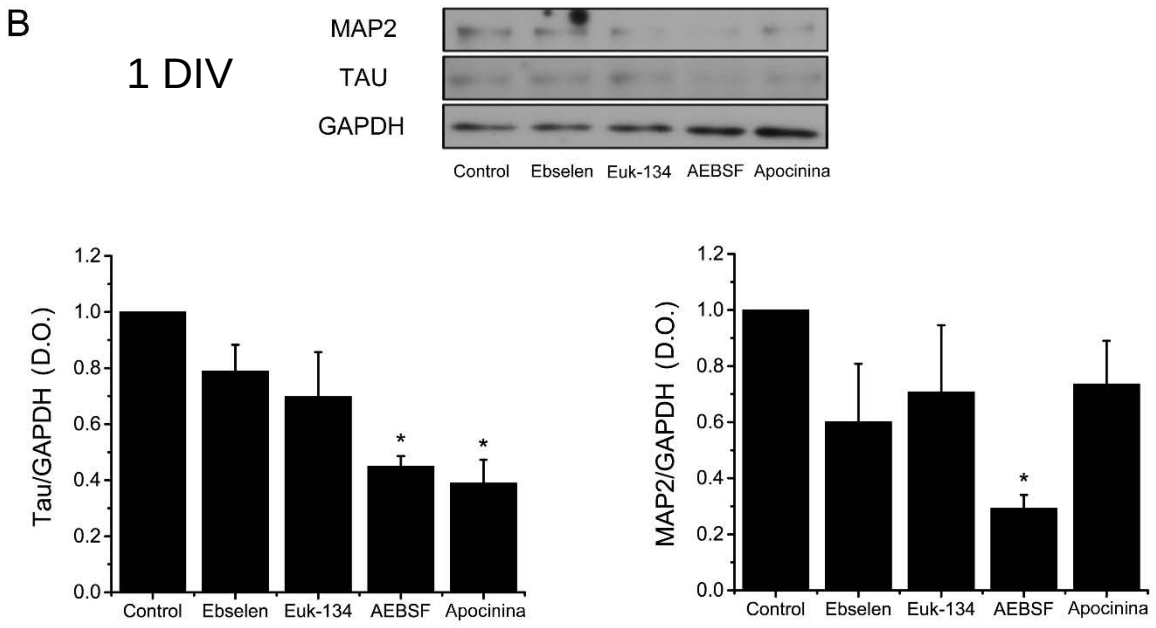
B
1 DIV
MAP2
TAU
GAPDH
Control
Ebselen
Euk-134
AEBSF
Apocinina
Tau/GAPDH (D.O.)
MAP2/GAPDH (D.O.)
Control
Ebselen
Euk-134
AEBSF
Apocinina

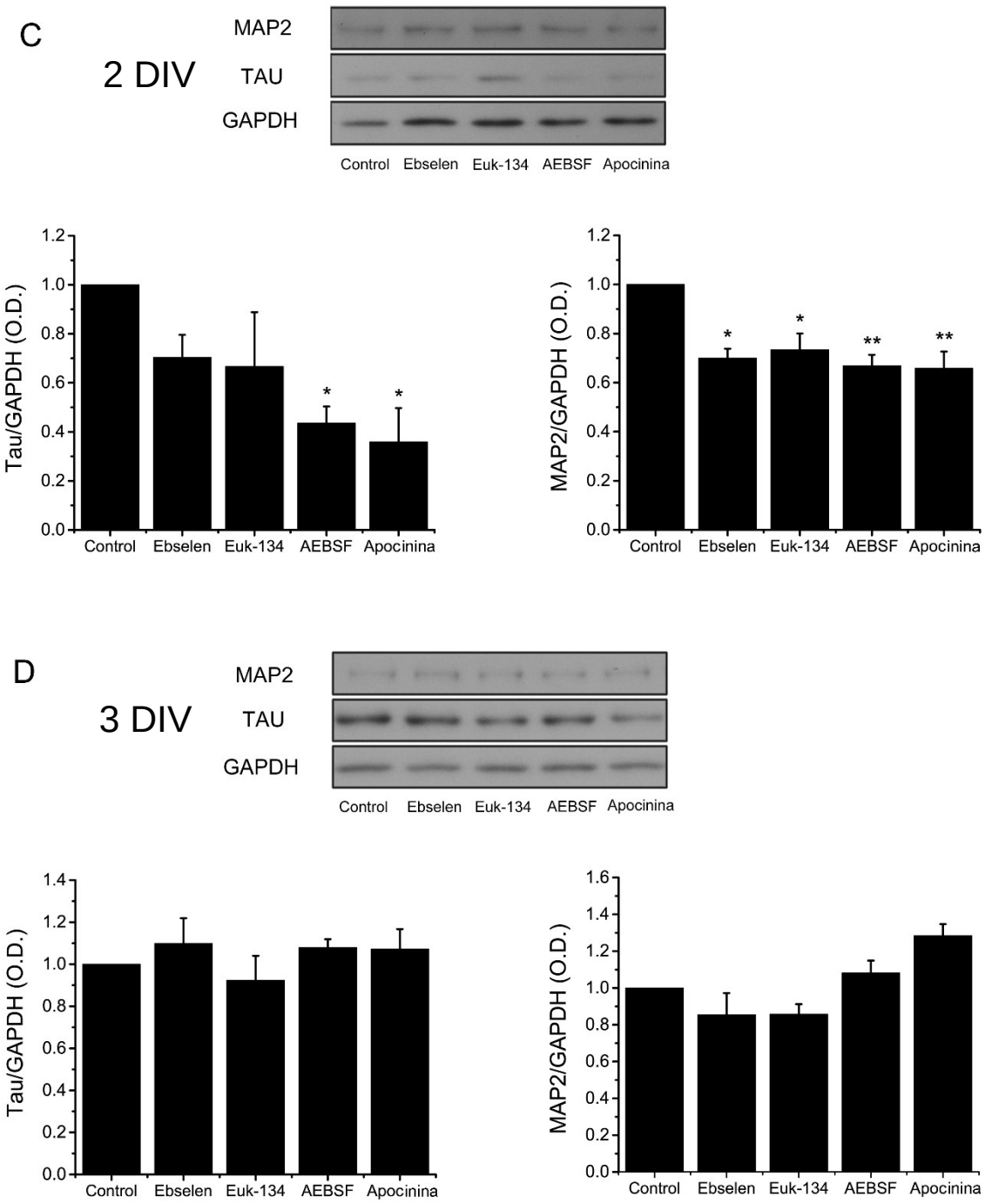

Figura 7. Las ERO promueven la maduración de las NGC. Los niveles de Tau y MAP2 se determinaron por Western Blot en homogenados de NGC crecidas en K25 de 0 a 3 DIV y en cultivos de astrocitos de cerebelo. (A) Blots representativos de Tau (~70 kDa) y MAP2 (~280 kDa) con sus respectivos análisis densitométricos de Tau (⋆ $p<0.001$, ANOVA, n=3) y MAP2 (⋆⋆ $p<0.005$, ⋆ $p<0.001$, ANOVA, n=4). Los datos están normalizados respecto a 3 DIV y son la media ± error estándar. (B-D) Blots representativos de Tau y MAP2 con sus respectivos análisis densitométricos de células tratadas con los antioxidantes Ebselen (10 µM) y Euk-134 (20 µM) o con los inhibidores NOX, AEBSF (50 µM) y Apocinina (400 µM) por 24 h. (B) NGC a 1 DIV, Tau (⋆ $P<0.001$, ANOVA, n=5) y MAP2 (⋆ $p=<0.01$, ANOVA, n=4). (C) NGC a 2 DIV, Tau (⋆ $p<0.05$, ANOVA, n=4) y MAP2 (⋆ $p<0.01$, ⋆⋆ $p<0.001$, ANOVA, n=4). (D) NGC a 3 DIV, Tau ($p=0.604$, ANOVA, n=5) y MAP2 ($p<0.01$, ANOVA, n=5). Los valores de las densitometrías son el índice de Tau/GAPDH y MAP2/GAPDH y están normalizados con respecto al control. Los datos sona la media ± error estándar.

6.5 Papel de la NOX durante el desarrollo de las NGC

Los resultados anteriores, sugieren que la producción de ERO durante el desarrollo de las NGC, es un proceso altamente regulado, el cual posiblemente se encuentra relacionado a los eventos de maduración y muerte de las NGC. En este sentido, se sabe que las enzimas NOX son fuentes de generación de ERO muy importantes en diferentes tipos celulares (Bedard and Krause, 2007; Sorce and Krause, 2009). Considerando que los inhibidores NOX interfirieron con la maduración de las NGC, nosotros hipotetizamos que miembros de la familia NOX probablemente están mediando la generación de ERO. Por tales motivos, nosotros medimos la actividad NOX, mediante la reducción extracelular de citocromo c por $O_2^{\bullet -}$ producido por NOX (Fig. 8A). Nosotros encontramos que la actividad NOX, incrementó gradualmente de 1 a 3 DIV (~50%) y que después de 3 DIV, la actividad disminuyó a los niveles encontrados a 2 DIV, lo cual asemeja la producción ERO de 1 a 5 DIV en células crecidas en K25.

Con la finalidad de evaluar la importancia especifica de los homólogos NOX durante el desarrollo de las NGC, nosotros medimos la expresión de dos homólogos NOX que se han descritos en el sistema nervioso: NOX1 y NOX2. Esto se realizó en NGC cultivadas en K25 de 0 a 5 DIV mediante ensayos cuantitativos de RT-PCR en tiempo real (Figuras 8B-E). Encontramos que ambos homólogos se expresan en las NGC, ambos presentaron su menor expresión al 0 DIV. NOX1 alcanzó su máxima expresión a 1 DIV, disminuyendo gradualmente durante los días subsecuentes (2-5 DIV) (Figura 8B). Por otra parte, NOX2 presentó un marcado incremento de 1 a 2 DIV y un incremento menor de 2 a 3 DIV, posteriormente, los niveles de NOX2 disminuyeron abruptamente de 3 a 4 DIV (Figura 8C). Con la intención de determinar la relativa importancia de estos dos homólogos, se comparó la expresión relativa de estos dos homólogos, con lo cual se estableció que NOX2 presenta una mayor expresión tanto en el día en el que NOX1 alcanzó su máximo nivel de expresión, como en el día en el que NOX2 lo alcanzó (Figuras 8D,E).

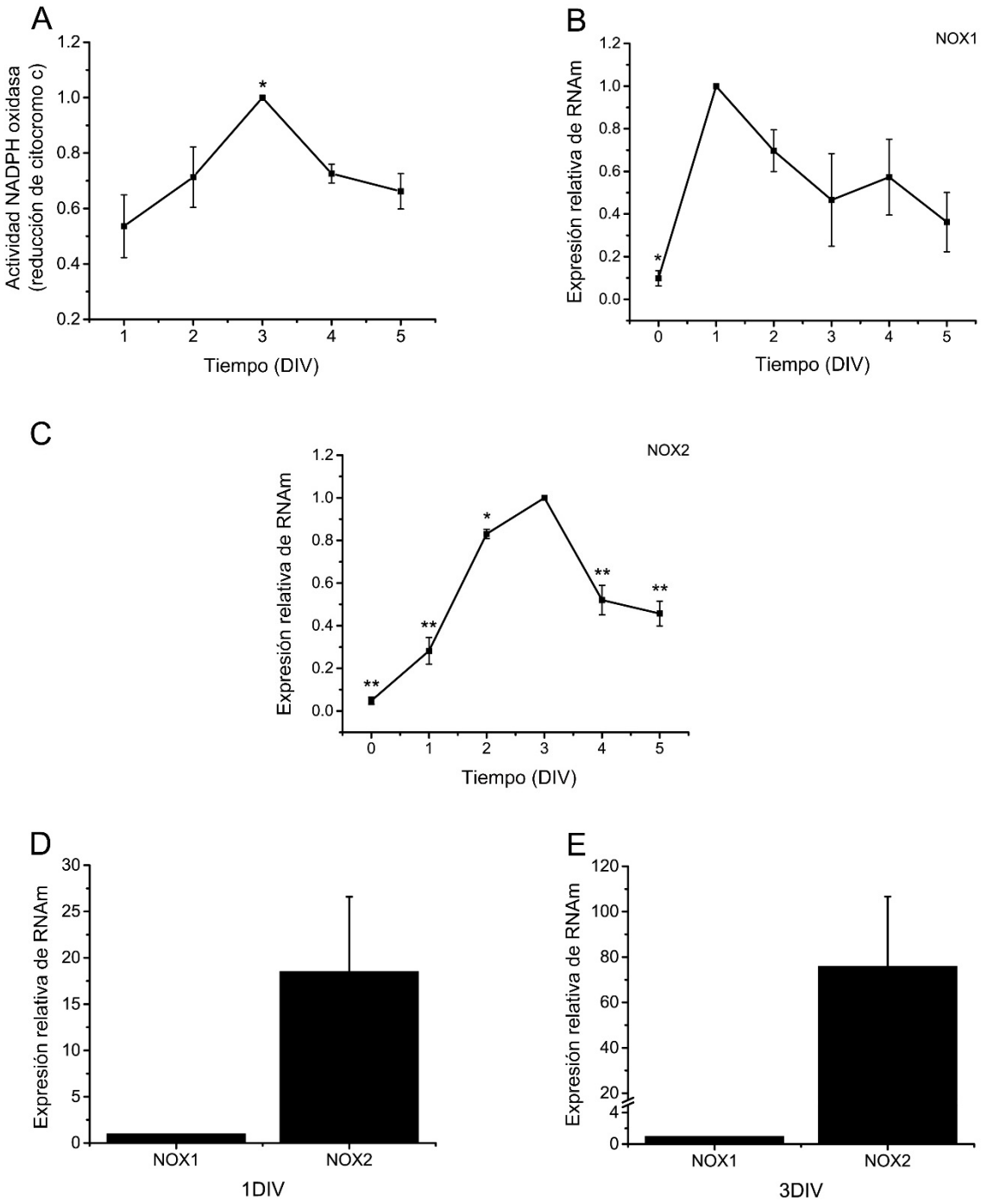

Figura 8. NOX1 y NOX2 se expresan diferencialmente durante el desarrollo de las NGC. (A) La actividad de NOX se determinó en NGC de 1 a 5 DIV por la reducción de citocromo c tal como es detallado en métodos. La actividad de NOX es significativamente más elevada a 3 DIV comparándolo con 1 DIV ($p<0.01$, ANOVA, n=5). Los datos se expresan en nmol min^{-1} y están normalizados con respecto a 3 DIV y están presentados como la media ± error estándar. (B-E) Los niveles relativos del RNAm de NOX1 y NOX2, se determinaron en NGC de 0 a 5 DIV por el método de cuantificación relativa $2^{-\Delta\Delta Ct}$ tal como fue detallado en métodos. Los datos están normalizados con respecto al tiempo en el cual la expresión alcanzó su máximo nivel. (B) Los niveles del RNAm de NOX1 a 0 DIV fueron significativamente diferentes de 1 DIV (⋆ $p<0.01$, ANOVA, n=3). Los datos son la media ± error estándar. (C) Los niveles del RNAm de NOX2 a 0, 1, 2, 4 y 5 DIV fueron significativamente diferentes de 3 DIV (⋆ $p<0.05$, ⋆⋆ $p<0.001$, ANOVA, n=3). Los datos son la media ± error estándar. (D) Los niveles del RNAm de NOX2 a 1 DIV, fueron más altos en comparación de los niveles del RNAm de NOX1 (⋆ $p<0.05$, U de Mann-Whitney, n=4). Los datos son la media ± error estándar. (E) Los niveles del RNAm de NOX2 a 3 DIV fueron más altos que los niveles de NOX1 en comparación con los niveles de RNAm de NOX1 (⋆ $p<0.05$, U de Mann-Whitney, n=4). Los datos son la media ± error estándar.

6.6 Localización de las ERO y NOX2 en las NGC en desarrollo

Algunos estudios resaltan la importancia de la compartimentalización de la producción de ERO en las células (Mishina et al., 2011b), lo cual se piensa permite la activación de eventos de señalización redox en regiones específicas de las células (Ushio-Fukai, 2009b). Por esta razón, estudiamos la localización de NOX2 en NGC en desarrollo que se crecieron en K25, lo cual se sustenta en el hallazgo que demuestra que NOX2 es el homólogo estudiado en nuestro sistema, cuya expresión es la más abundante (Figura 8,E). La figura 9 muestra que NOX2 se distribuye mayormente en las neuritas y que se asocia estrechamente con los conos de crecimiento. Particularmente a 0 DIV, NOX2 se localiza en los conos de crecimiento de la mayor parte de las neuritas en desarrollo (Figura 9A), mientras que en estados más avanzados de desarrollo (3DIV), NOX2 se encontró abundantemente en filopodios, varices axonales y conos de crecimiento (Figura 9B).

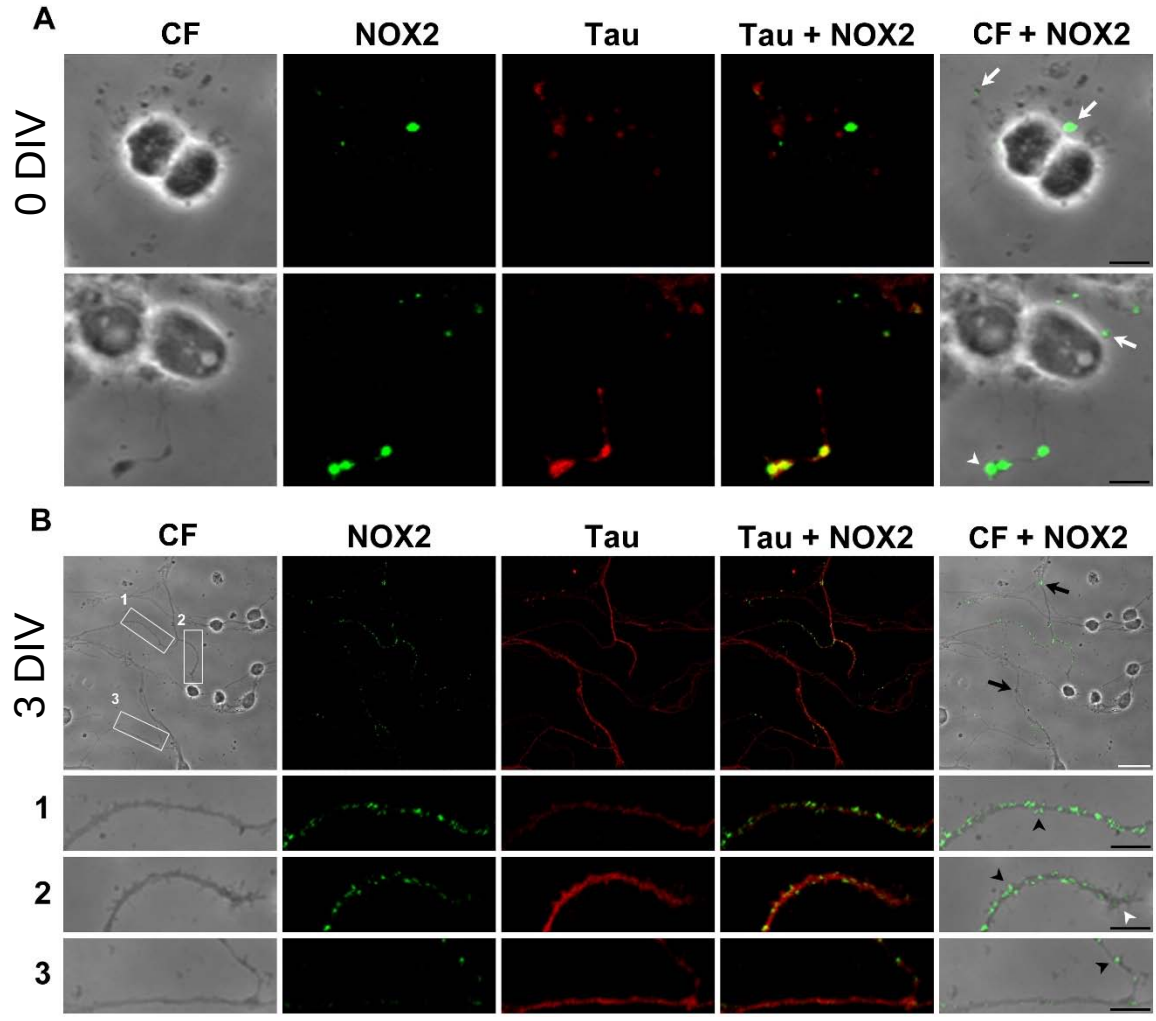

Figura 9. NOX2 se encuentra expresada en filopodios y conos de crecimiento axónico. Imágenes representativas de la distribución de NOX2 (en verde) y contraste de fases (CF), Tau (en rojo) y de contraste de fases de NGC de 0 y 3 DIV. (A) Se muestran dos imágenes representativas de NGC a 0 DIV. Las flechas blancas indican pequeñas protrusiones y las cabezas de flecha blancas indican conos de crecimiento. (B) Se muestra una imagen representativa de NGC a 3 DIV. Los recuadros blancos (1-3) se muestran en imágenes magnificadas más abajo. Las NGC se sembraron a baja densidad. Las cabezas de flecha blancas indican conos de crecimiento, las cabezas de flecha negras indican filopodios y las flechas negras indican varices axonales (La barra de escala blanca representa 20 µm; las barras de escala negras equivalen a 5 µm).

Dado que NOX2 se localiza específicamente en las NGC en desarrollo y considerando que algunos estudios señalan que en los conos de crecimiento se producen ERO (Munnamalai and Suter, 2009; Morinaka et al., 2011; Munnamalai et al., 2014b), decidimos evaluar la producción localizada de ERO en tiempo real mediante una técnica altamente sensible en espacio y tiempo. Esto se logró transfectando a las NGC con el plásmido HyPer, el cual es un sensor fluorescente genéticamente codificado, diseñado para detectar H_2O_2 citoplasmático (Belousov et al., 2006), y que ha sido sugerida como la ERO más importante en la señalización redox. Este sensor radiométrico posee dos picos de excitación, uno a 420 nm y otro a 500 nm y un único pico de emisión a 516 nm. La fluorescencia de emisión cambia conforme a la exposición a H_2O_2, mientras el pico de excitación a 420 nm disminuye, el pico a 500 nm incrementa, lo cual nos permitió determinar diferencias en los niveles de H_2O_2 en diferentes regiones de la neurona, independientemente de la cantidad de proteína expresada. Encontramos que el H_2O_2 se distribuye heterogéneamente en las NGC de 1 a 3 DIV crecidas en K25 (Datos no mostrados). Únicamente se emplearon NGC de 2 DIV, esto fue debido a que en este tiempo se consigue la máxima expresión del plásmido y es un tiempo que también corresponde al momento en el que se produce mayor cantidad de ERO medidas por dihidroetidina (Figuras 5B,C).

En la Figura 10 se aprecia como la proteína expresada por el plásmido HyPer, responde a cambios en la concentración de H_2O_2, cuando a las NGC se les agregó H_2O_2 exógenamente, la eficiencia de fluorescencia del canal 480 aumentó, mientras que la del canal 395 disminuyó (Fig. 10A). Del mismo modo el índice entre los canales 480/395 incrementó en presencia de H_2O_2 (500 µM), confirmando que nuestro sistema es capaz de detectar cambios en los niveles de H_2O_2. Por otro lado, se registró la misma neurona en la región del axón en un tiempo previo a la perfusión de H_2O_2, con lo cual se lograron comparar los niveles relativos de una región en la cual se producen altos niveles de H_2O_2 (axón), con una región de bajos niveles de producción de H_2O_2 (soma) y el incremento en esta última al ser expuesta a H_2O_2 exógeno. Encontramos que los niveles de H_2O_2 producidos en el cono de crecimiento axónico, son equiparables a la perfusión de 500 µM de H_2O_2, sin embargo, la producción de H_2O_2 en el cono de crecimiento axónico fue alta durante todo el tiempo de registro, aunque esta fluctuó continuamente (Fig. 10C).

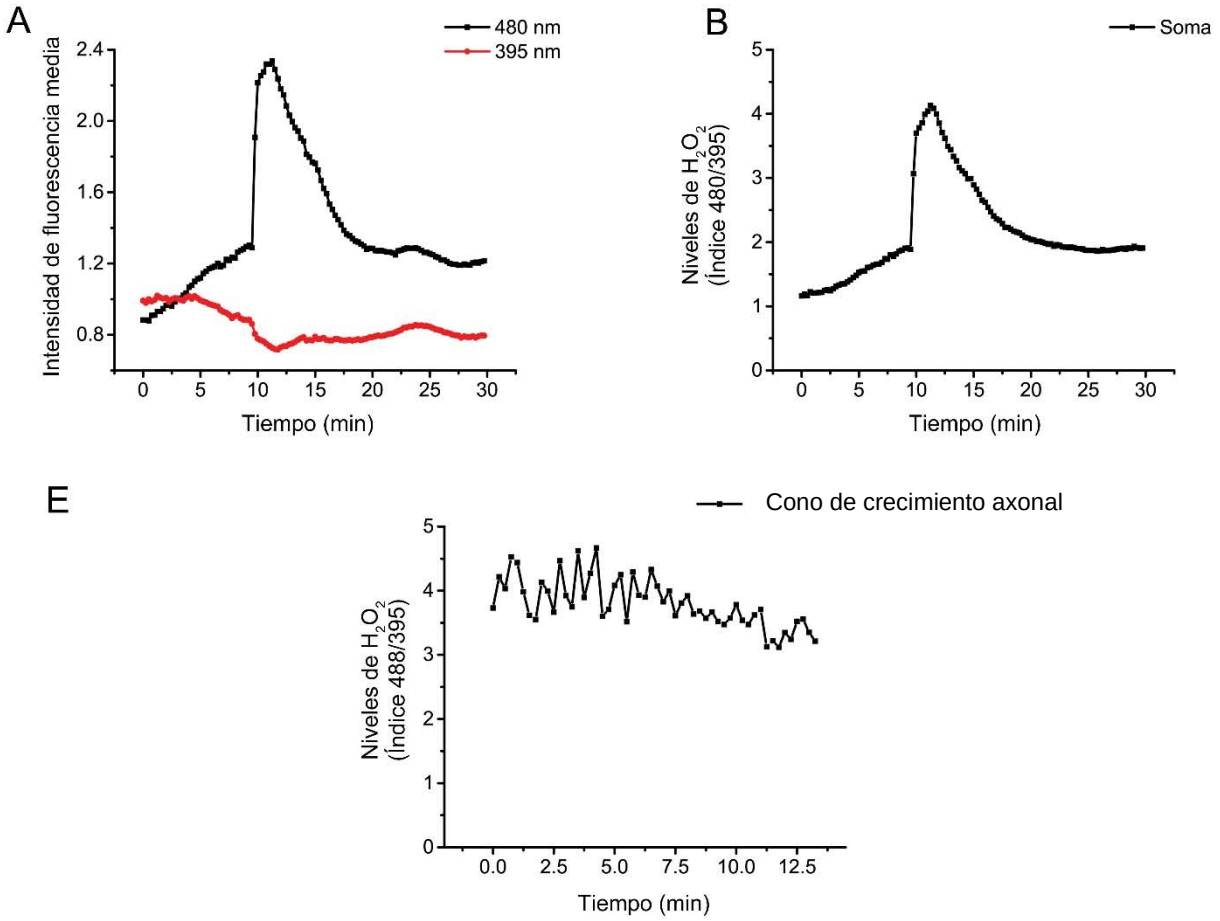
A
480 nm
395 nm
Intensidad de fluorescencia media
Tiempo (min)
B
Soma
Niveles de H2O2 (Índice 480/395)
Tiempo (min)
E
Cono de crecimiento axonal
Niveles de H2O2 (Índice 488/395)
Tiempo (min)
C
F
5
4.1
3.1
2.1
1.1
0.1

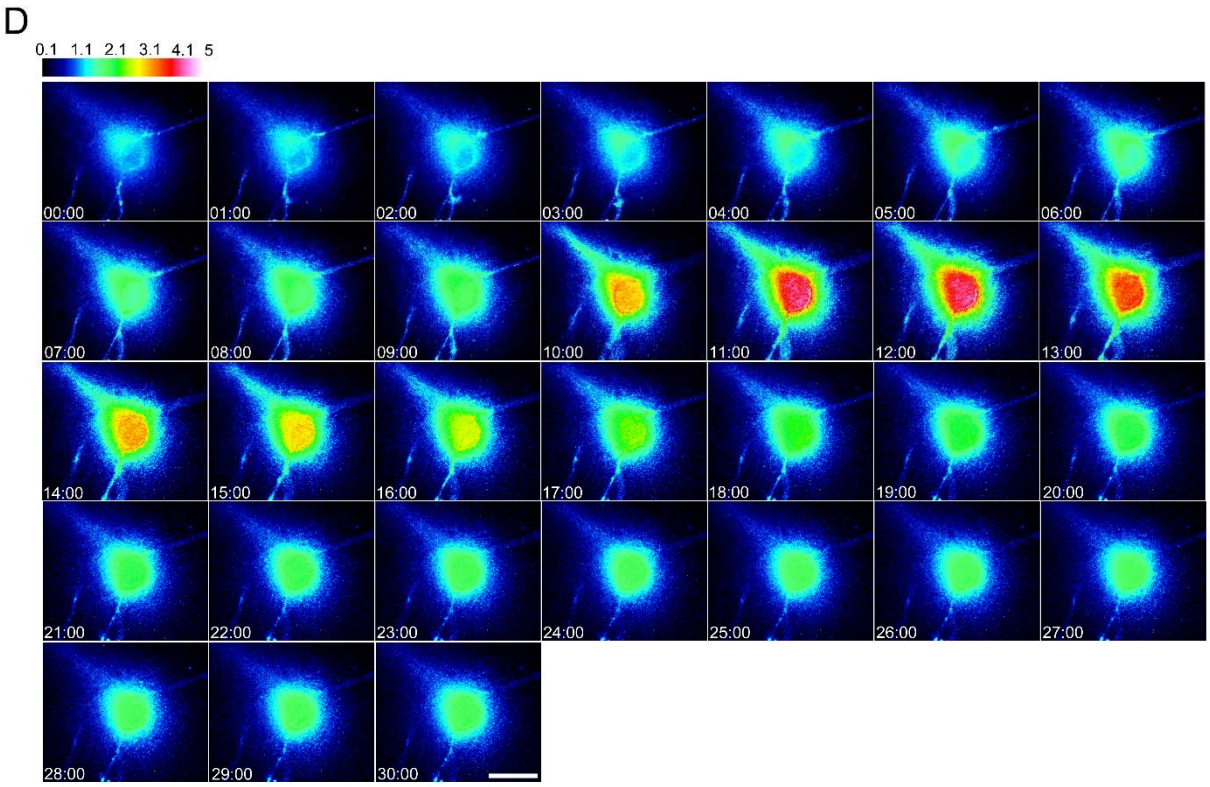

Figura 10. La fluorescencia de HyPer cambia en respuesta a cambios en la concentración de H_2O_2. (A-F) Las NGC de 2 DIV se transfectaron con el plásmido HyPer y se detectaron los niveles de H_2O_2 como se detalla en métodos. (A) La emisión de fluorescencia de las longitudes de onda de excitación 480 nm y 395 nm, corresponden a una región de interés trazada en el soma de una neurona administrada con H_2O_2 (500 µM). Los datos se normalizaron con respecto al promedio de los 10 primeros puntos registrados. (B,E) El índice de fluorescencia de las longitudes de excitación 480 nm y 395 nm se registró en una región de interés dentro del soma (B) o en el cono de crecimiento axónico (E) de una misma neurona. (C,F) Son imágenes del soma y del axón de una misma neurona transfectada con el plásmido HyPer. La imagen mostrada en (F) se registró antes de la administración de H_2O_2 (la barra de escala equivale a 50 µm) (D) Se muestra una serie de imágenes amplificadas del soma de la neurona mostrada en (C) durante la administración de H_2O_2.

En nuestros estudios registramos 42 neuronas, a partir de las cuales determinamos las regiones de las NGC donde se producen los niveles relativos de H_2O_2 más altos. Las Figuras 11 A-F, muestran que aunque hay niveles basales de H_2O_2 en todas las estructuras de la neurona, existe una clara diferencia entre algunas regiones del axón y las dendritas con respecto al soma, donde los niveles de H_2O_2 se encuentran uniformemente distribuidos y son relativamente bajos (Fig. 11A,C,E). Los niveles de H_2O_2 en el soma no son modificados en el tiempo bajo condiciones basales, a menos que se aplique H_2O_2 exógenamente. En contraste con esta observación, los niveles de H_2O_2 a lo largo del axón son variables, en algunas áreas la concentración es ligeramente más baja que la observada en el soma, pero en algunas otras áreas es más alta. En promedio, la producción de H_2O_2 en el axón es igual a la del soma, sin embargo, este promedio está calculado únicamente para aquellas regiones del axón donde no hay ni filopodios, ni varices axonales (Figuras 11A-H). Interesantemente, las zonas del axón que mostraron los niveles más altos de H_2O_2 corresponden a regiones de la neurona con alta actividad de re-modelamiento y crecimiento, tales como son los conos de crecimiento y filopodios (Figuras 11B,C,D,F). En todos los casos estás zonas mostraron niveles de H_2O_2 alrededor del doble del soma o de otras regiones del axón (Fig. 11H). Observamos que independientemente de la magnitud del movimiento en los conos de crecimiento axónico, estas

regiones siempre mostraron altos niveles de H_2O_2.También se encontraron altos niveles de H_2O_2 en los conos de crecimiento dendrítico (Figuras 11A,C,H). Los altos niveles de H_2O_2 no solo se encontraron en zonas altamente mótiles, sino que también en regiones estáticas que corresponde a las varices axonales (Figuras 11D,H).

Además encontramos que en las regiones del eje axónico donde se encuentran localizados los filopodios, existen altos niveles de H_2O_2 (Fig. 11F-H), esta observación fue más evidente en algunas neuronas en las cuales hallamos regiones donde los filopodios están en continuo re-modelamiento, a dichas regiones las denominamos zonas dinámicas. En estas zonas encontramos claras variaciones en los niveles de H_2O_2, constituyendo así micro-dominios del eje del axón donde los filopodios están creciendo y retrayéndose. Durante la formación de filopodios, observamos un incremento en los niveles de H_2O_2 que ocurrió inmediatamente antes de la formación de filopodios, el cual alcanzó los niveles máximos durante el tiempo de formación del filopodio, para disminuir a los niveles basales iniciales una vez completada la retracción del filopodio. En algunos casos, los filopodios en formación presentaron altos niveles de H_2O_2 dentro de éstos mismos, lo cual ocurrió en gran proporción cuando los filopodios eran muy largos o cuando estos presentaron otras protrusiones (Fig. 11G,J). Esto se ilustra claramente en la Figura 11G, donde es mostrada una serie de magnificaciones de una zona dinámica, en donde se aprecia cómo en una región del eje del axón en donde no hay un filopodio presente, comienza a haber una generación de H_2O_2 que antecede a la formación del filopodio y que perdura durante el tiempo que está presente el filopodio, una vez completada la retracción del filopodio, la producción de H_2O_2 cesa.

Todas las mediciones de la fluorescencia, se calcularon como el promedio de la fluorescencia en una región determinada en el tiempo. En algunas estructuras este promedio abarcó una serie de eventos en una escala del orden de minutos (como sucedió en los conos de crecimiento axónico, el axón, el soma y varices axonales) o en el rango de segundos (tal como ocurrió en el caso de conos de crecimiento dendrítico, las zonas dinámicas y filopodios). Las Figuras 10E,F muestran que los niveles de H_2O_2 en los conos de crecimiento son altos y relativamente estables en el tiempo, sin embargo estos presentan pequeñas fluctuaciones en el tiempo. Las escalas de fluorescencia de las Figuras 10E,F son distintas de las Figuras 11C y F para poder medir adecuadamente los niveles de H_2O_2 durante la perfusión.

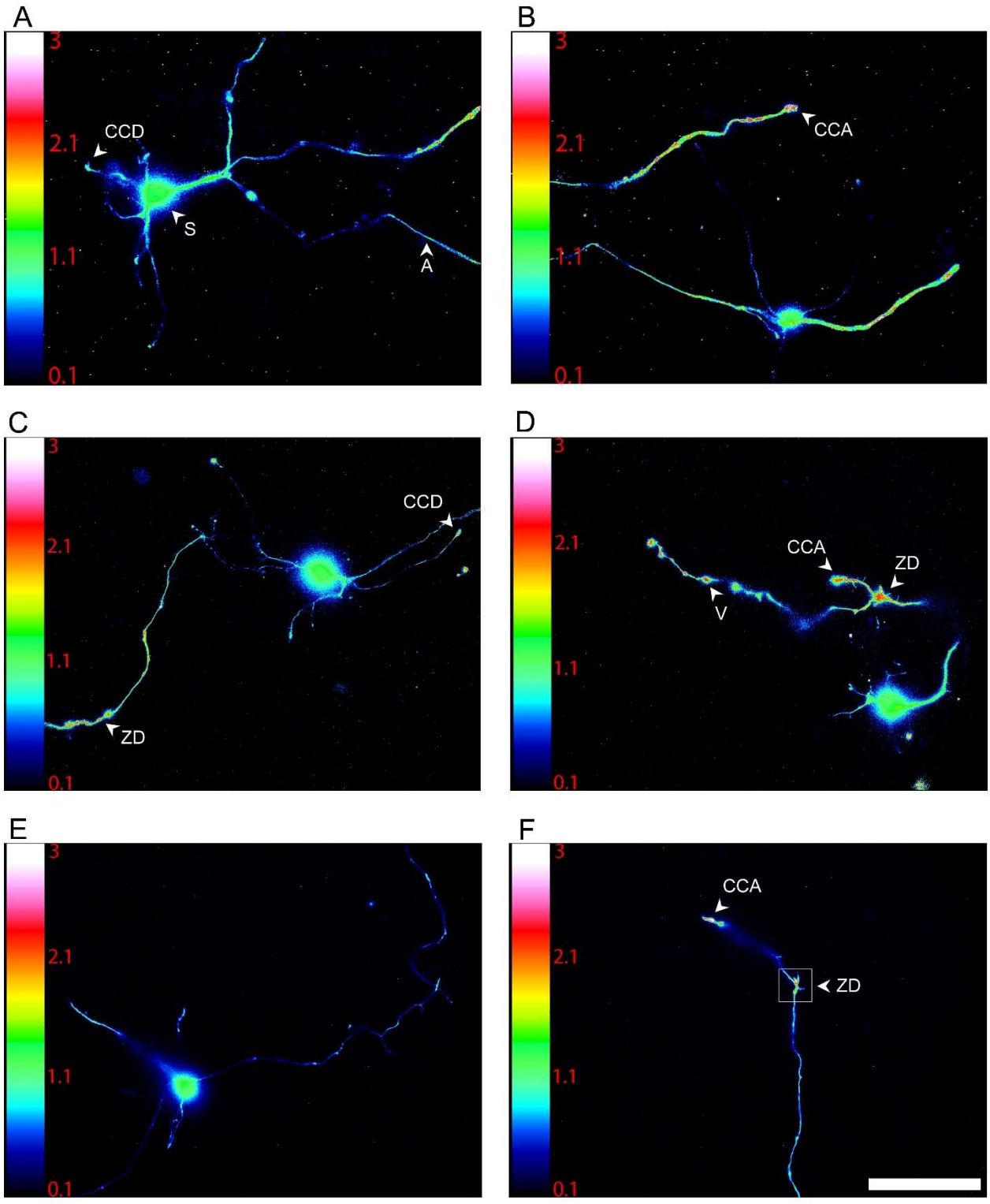
A
3
2.1
1.1
0.1
CCD
S
A
B
3
2.1
1.1
0.1
CCA
C
3
2.1
1.1
0.1
CCD
ZD
D
3
2.1
1.1
0.1
CCA
ZD
V
E
3
2.1
1.1
0.1
F
3
2.1
1.1
0.1
CCA
ZD

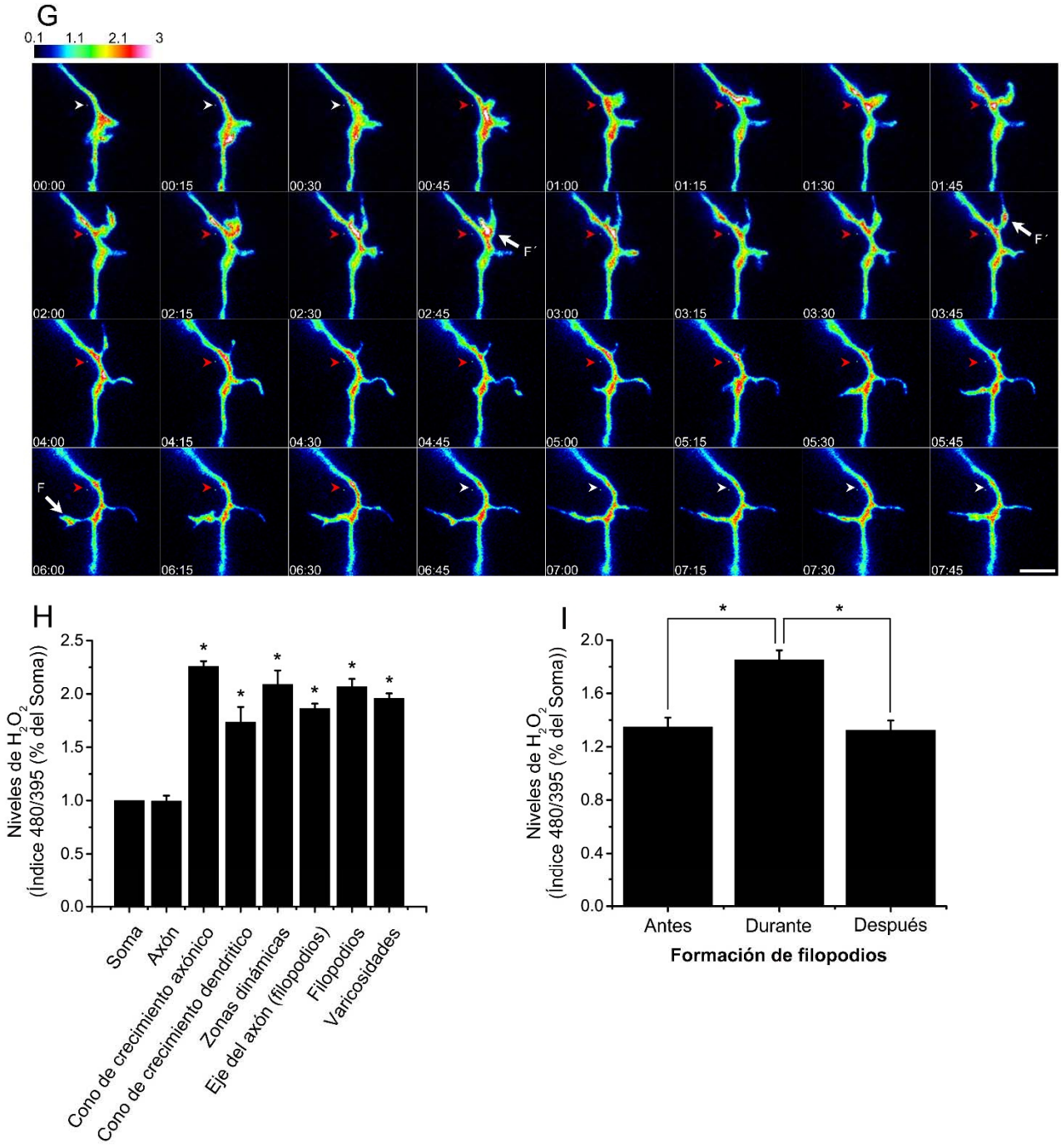

Figura 11. H_2O_2 es producido en regiones específicas de las NGC. (A-F) Imágenes representativas de NGC de 2 DIV transfectadas con el plásmido HyPer y los niveles de H_2O_2 se detectaron como se detalla en métodos. La emisión de fluorescencia se registró a partir de las longitudes de excitación 480 nm y 395 nm en series de imágenes. Las barras de escala de color, representan el índice entre las longitudes de excitación 480 nm y 395 nm. Las cabezas de flecha indican: soma (S), axón (A), cono de crecimiento axónico (CCA), cono de crecimiento dendrítico (CCD), zona dinámica (ZD) y varices axonales (V) (La barra de escala equivale a 50 µm). (G) Imágenes magnificadas de la zona dinámica remarcada en (F). (A) es el soma de (B). (E) es el soma de (F). (F) se capturó previamente a la administración de H_2O_2 mostrada en (F). (F) Las flechas blancas indican una región de interés del eje del axón, previamente o posterior a la formación del filopodio. Las flechas rojas indican una región de interés del eje del axón donde el filopodio está presente y que además corresponde a altos niveles de H_2O_2. La flecha blanca indica a un filopodio (F´) con altos niveles de H_2O_2 (la barra de escala equivale a 5 µm). (H) Cuantificación de los niveles de H_2O_2 normalizados con respecto al soma ($\star$ $p<0.05$, ANOVA no paramétrica, n=42 (A), n=52 (AGC), n=12 (DGC), n=14 (DZ), n=106 (ASF), n=26 (F), n=93 (V)). Los datos son la media ± error estándar de 42 neuronas registradas en series de imágenes. (I) Cuantificación de la fluorescencia registrada durante la formación de filopodios, la cual está normalizada con respecto al

soma. La fluorescencia se midió en el eje del axón de la región donde se establece el filopodio, antes, durante y después de la presencia del filopodio. La fluorescencia media es más alta cuando el filopodio se encuentra presente al momento anterior a la formación del filopodio y al momento posterior a la retracción del mismo (⋆ $p<0.001$, Prueba de T pareada, n=21).

6.7 El glutatión promueve la integridad axonal durante el desarrollo temprano de las NGC

Altos niveles de ERO se relacionan con una alteración de la fisiología celular y daño estructural, lo cual lleva a la muerte celular (Ryter et al., 2007). Como se mencionó previamente, el glutatión es uno de los sistemas antioxidantes más importantes en el sistema nervioso. Basados en que la depleción del glutatión conduce a la muerte de las NGC en una ventana de tiempo específica en la que los niveles de H_2O_2 son altos en los axones en desarrollo, decidimos evaluar el efecto de la depleción del glutatión en la integridad estructural y analizar los niveles de H_2O_2 en los axones de las NGC en desarrollo. Para poder visualizar los axones de forma aislada, teñimos una población parcial de NGC con el colorante de membranas plasmáticas PKH67, lo cual nos permitió visualizar en detalle y de forma individual, la estructura de los axones (Figura 12). En la Figura 13A se muestra que cuando las células se tratan con BSO durante las primeras 42 h de desarrollo, los axones de las NGC presentan alteraciones en la estructura del axón. Algunas células presentaron axones con múltiples estructuras tipo esferoides (Figura 13A). En otras células, estas estructuras incrementaron en tamaño y número, llevando a la apariencia del axón del tipo colapsado (Figura 13A). No se encontraron alteraciones evidentes en la estructura de los somas. Los efectos observados del tratamiento con BSO están mediados por ERO, ya que la presencia del antioxidante Euk-134 previno completamente las alteraciones mencionadas (Figuras 13A,B). La cuantificación de las alteraciones morfológicas inducidas por el tratamiento con BSO, se muestra en la figura 14C. Alrededor del 40% de las células tratadas con BSO mostraron una estructura del axón del tipo colapsado y alrededor del 50% de las células presentaron una estructura del axón del tipo múltiples esferoides. Además, alrededor del 10% de las células con múltiples esferoides no se rescataron por el tratamiento con Euk-134, mientras que la totalidad de las células con axones con una estructura del tipo colapsada, se rescataron por completo, lo cual sugiere que la formación de pequeños esferoides, precede a la formación de los axones con una estructura del tipo colapsado y que las neuronas presentan una susceptibilidad distinta a la depleción del glutatión.

Por otra parte, cuando se transfectaron las células con el plásmido HyPer se trataron con BSO durante las primeras 42 h de desarrollo. Observamos que prácticamente todas las estructuras tipo esferoides contuvieron altos niveles de H_2O_2, lo cual fue más evidente en los axones del tipo colapsados. No se observaron incrementos evidentes en los niveles de H_2O_2 en los somas (Figura 13D). Además observamos que la continuidad axonal no se perdió en los axones del tipo colapsado, ya que fue posible observar la continuidad del axón en las neuronas transfectadas con HyPer (dato no mostrado).

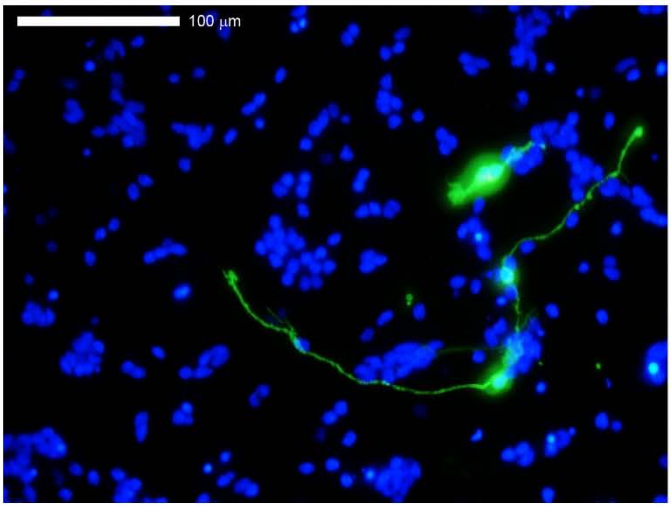

Figura 12. Visualización de NGC de forma aislada. Las NGC a 1 DIV muestran las neuritas teñidas con PKH67 (en verde) y los núcleos teñidos con DAPI (en azul).

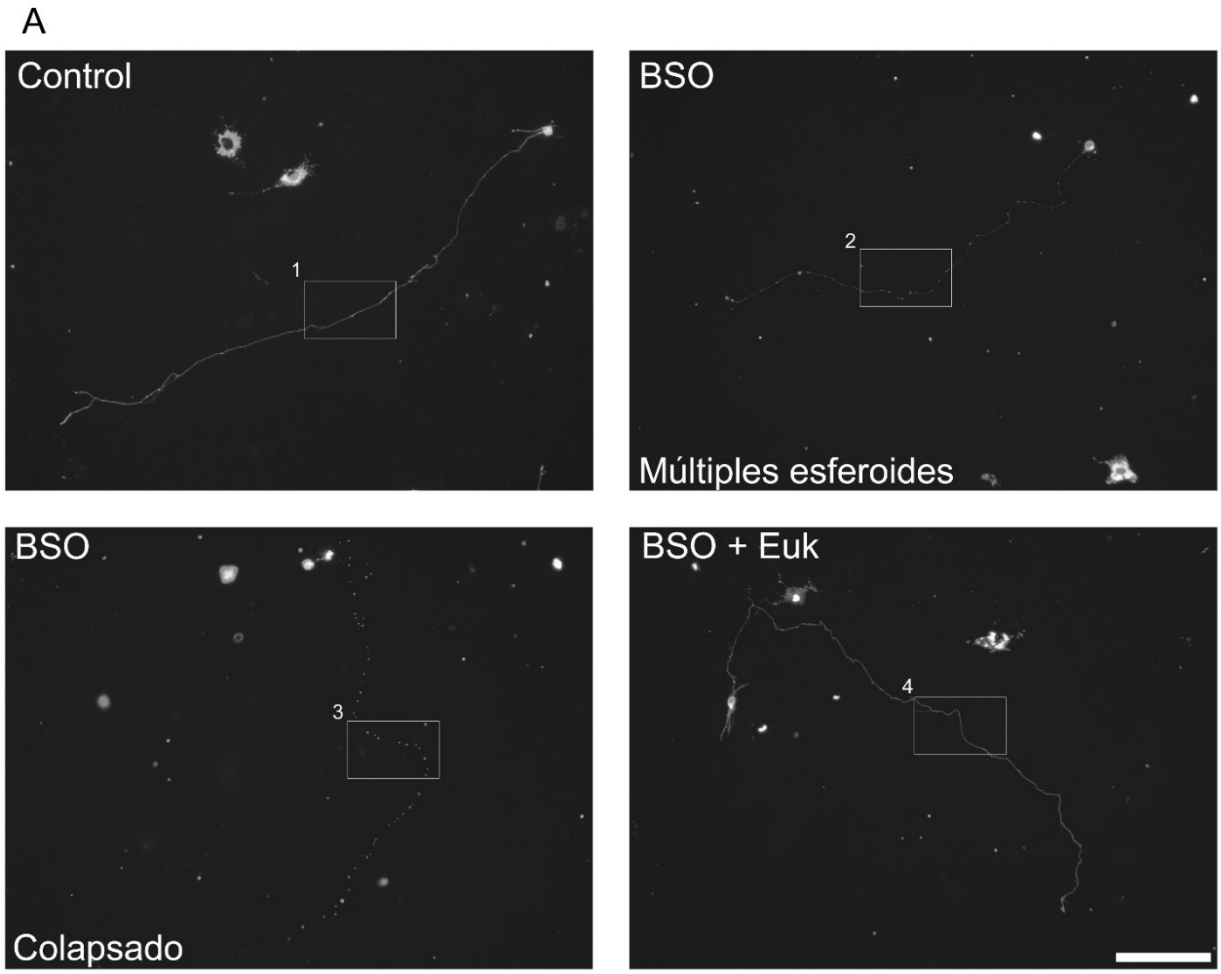

B

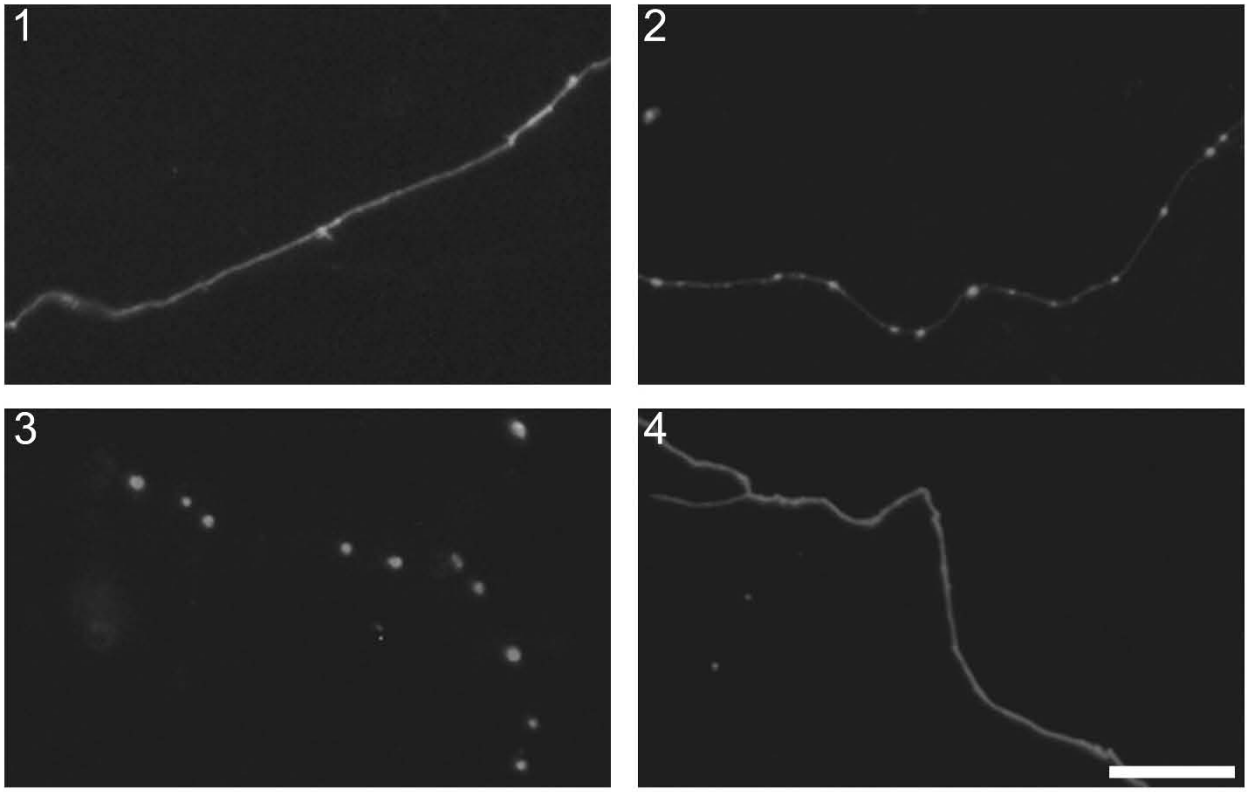
1
2
3
4

C

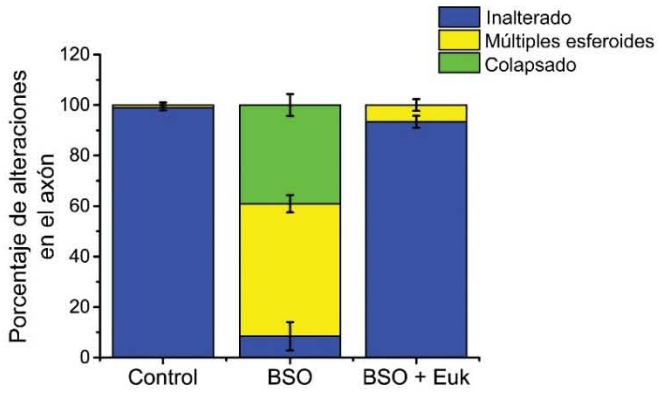
Inalterado
Múltiples esferoides
Colapsado
Porcentaje de alteraciones en el axón
120
100
80
60
40
20
0
Control
BSO
BSO + Euk

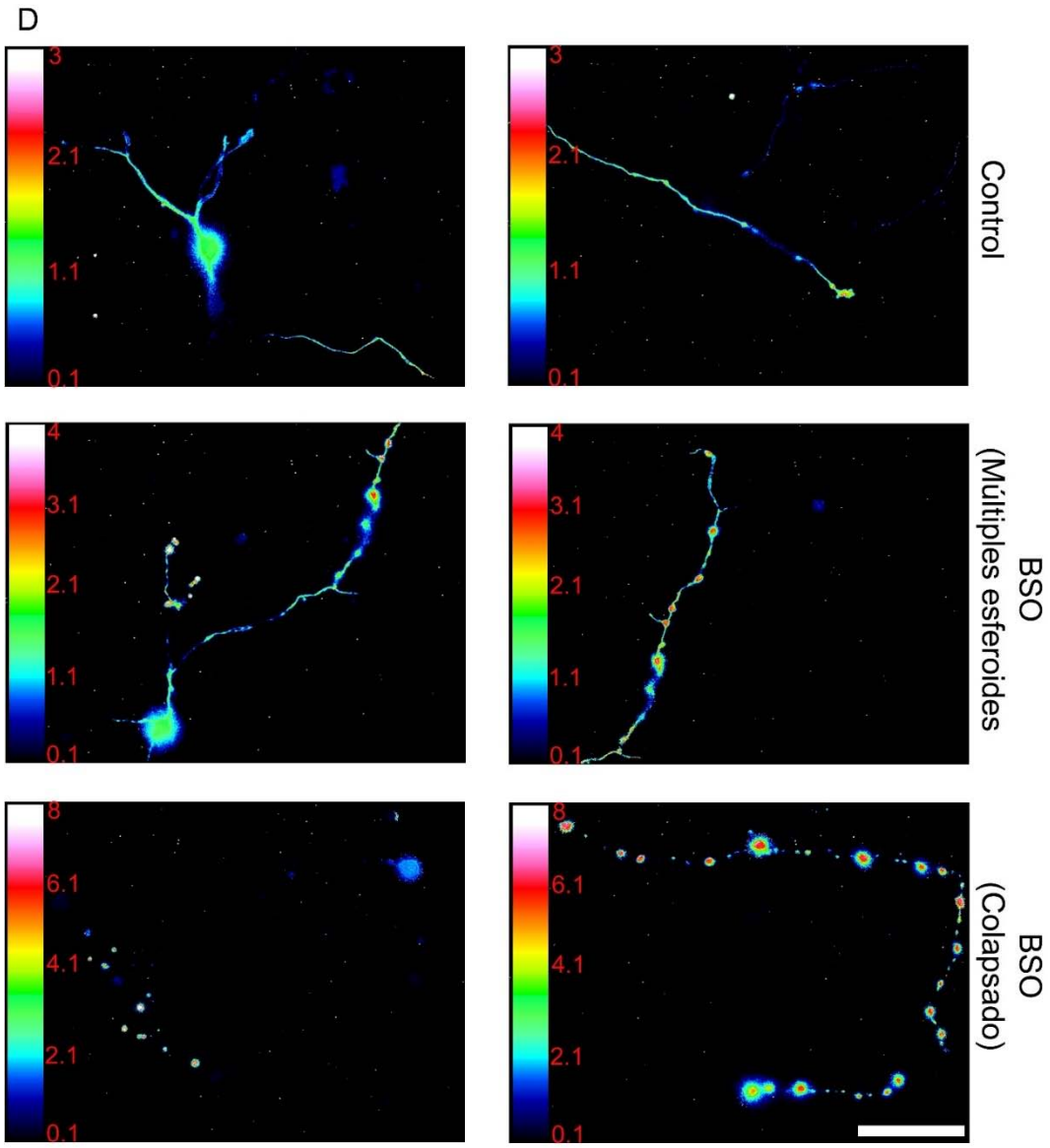

Figura 13. La depleción del glutatión induce alteraciones en la morfología del axón. (A) Imágenes representativas de NGC a 2 DIV tratadas con BSO (100 µM) por 42 h y con Euk-134 (10 µM) por 18 h. Las células se tiñeron con PKH67 (3 µM) previamente al sembrado de las mismas y las neuritas se visualizaron como se describe en métodos. Dos diferentes morfologías del axón se detectaron en las células tratadas con BSO: axones con esferoides múltiples y axones colapsados (La barra de escala equivale a 100 µm). (B) Imágenes magnificadas de las áreas indicadas por cuadrantes en (A) (la barra de escala corresponde a 20 µm). (C) Cuantificación de los axones con morfologías alteradas por la depleción de glutatión. Las NGC tratadas con BSO mostraron un mayor porcentaje de axones con morfologías alteradas en comparación al control y en comparación a las células tratadas con BSO + Euk-134 ($p<0.05$, ANOVA no paramétrica, n=4). (D) Imágenes representativas de NGC transfectadas con el plásmido HyPer tal como está detallado en métodos. Las NGC se trataron con BSO por 42 h y la fluorescencia de estás se registró en series de imágenes en el tiempo (la barra de escala equivale a 50 µm).

6.8 NOX2 regula el crecimiento neurítico de las NGC

Ya que NOX2 está expresado en los conos de crecimiento axónico y por otra parte, los inhibidores NOX redujeron parcialmente la expresión de Tau y MAP2, pensamos que NOX2 podría estar involucrado en el desarrollo neurítico de las NGC. Con la finalidad de responder esto, medimos la longitud de los axones y los niveles generales de ERO en NGC obtenidas de ratones deficientes de NOX2 y de ratones silvestres (Figura 14). En estas

condiciones, no observamos aparentes diferencias en las NGC tanto silvestres como KO NOX2 observadas por microscopía de contraste de fases (Figura 14C). Cuando las NGC fueron teñidas con PKH67 y la longitud de los axones se midió, encontramos en cambio que las neuritas provenientes de ratones silvestres, mostraron un incremento consistente de alrededor de tres veces entre 1 y 2 DIV (Figuras 14A,B). En contraste, el crecimiento neurítico de las NGC deficientes de NOX2, fue menor en alrededor de un 25% a 1 DIV y menor en alrededor de un 20% a 2 DIV (Figuras 14A,B). Al comparar los niveles de ERO en NGC silvestres y KO, encontramos que los niveles de ERO incrementaron alrededor de dos veces entre 1 y 2 DIV en ambos (Figuras 14C-E). Cuando comparamos los niveles de ERO entre las NGC silvestres y KO, no encontramos diferencias ni a 1 DIV, ni a 2 DIV (Figura 14F).

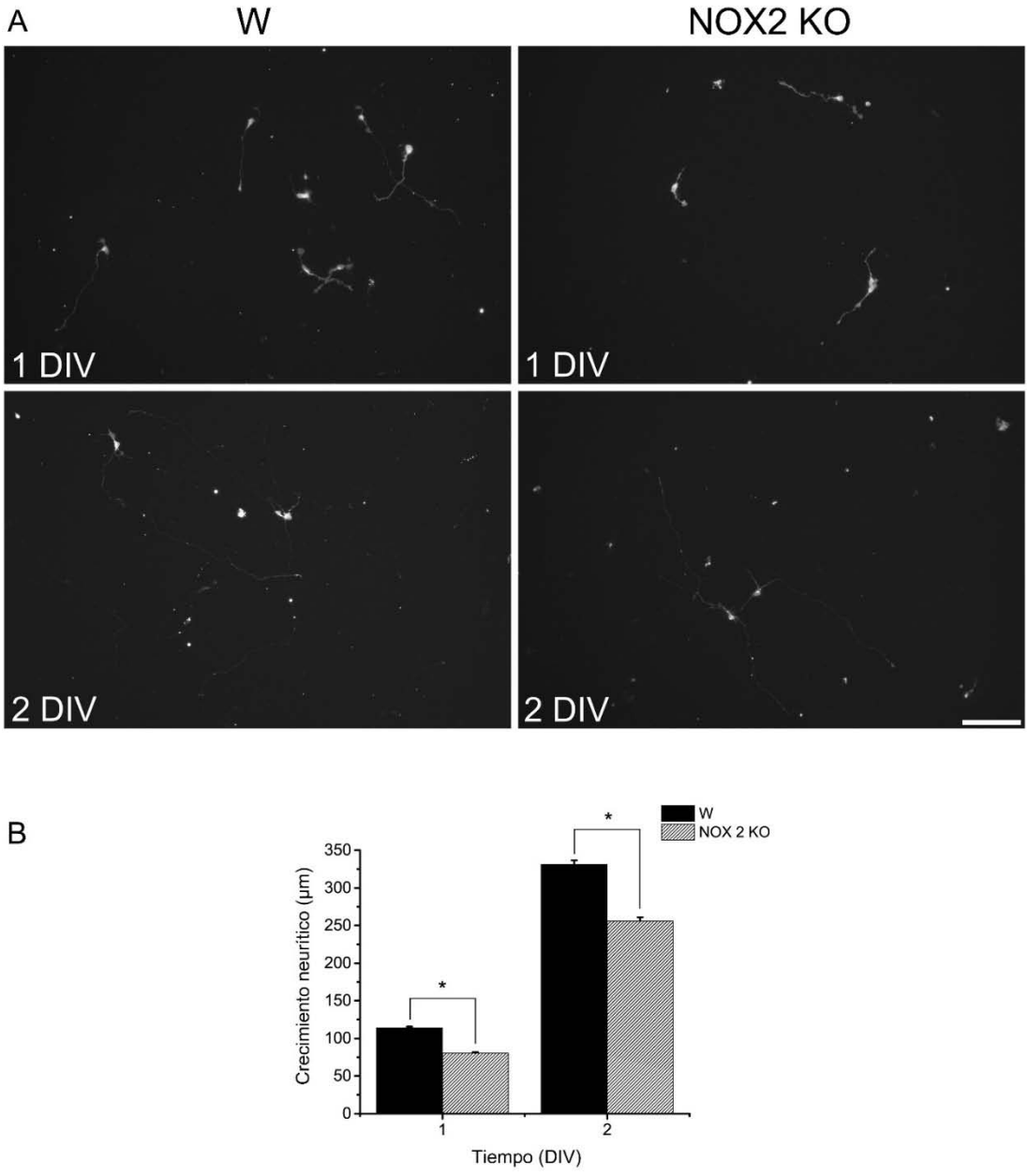

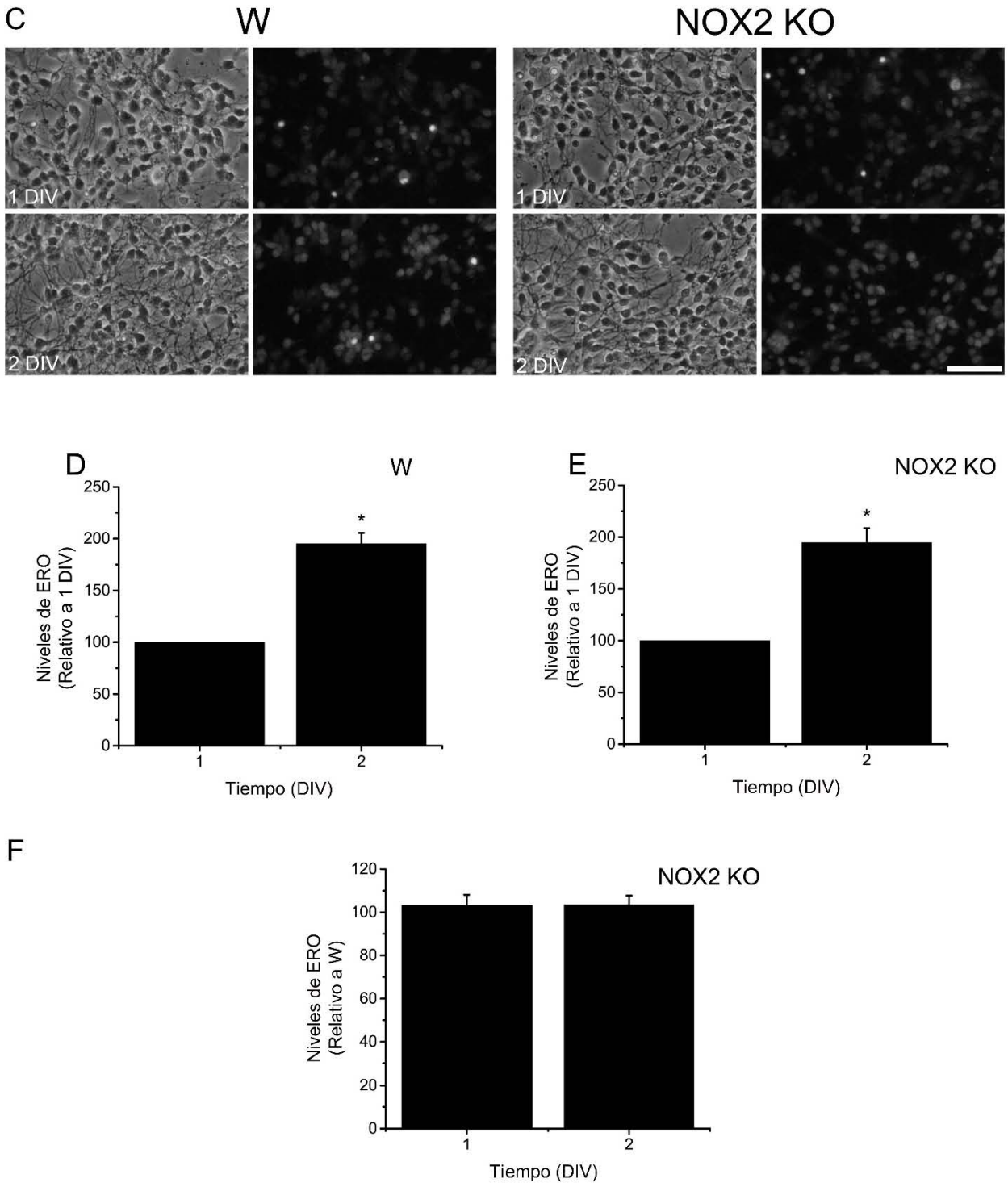

Figura 14. NOX2 regula el desarrollo neurítico de las NGC. (A) Imágenes representativas de NGC silvestres (W) y deficientes de NOX2 (KO NOX2) teñidas con PKH67 (3 µM) a 1 y 2 DIV (la barra de escala equivale a 100 µm). (B) Cuantificación del crecimiento neurítico de NGC W y KO NOX2. El crecimiento neurítico de las NGC en las NGC KO NOX2 a 1 y a 2 DIV fue menor que el de las NGC W a las mismas edades (⋆ $p<0.001$, U de Mann-Whitney, n=2067 and n=1151, respectivamente). Los datos son la media ± error estándar. (C) Imágenes representativas de NGC W y KO NOX2 incubadas con DHE a 1 y 2 DIV (la barra de escala equivale a 100 µm). (D,E) Cuantificación de los niveles de ERO en las NGC W y KO NOX2 a 1 y 2 DIV (⋆ $p<0.05$, Mann-Whitney U Test, n=4) Los datos se normalizaron con respecto a 1 DIV y son la media ± error estándar. (F) Los niveles de ERO

de las NGC KO NOX2 tanto a 1 como a 2 DIV, se compararon con respecto a W (no se encontraron diferencias, U de Mann-Whitney, n=5). Los datos se normalizaron con respecto a W y son la media ± error estándar.

6.9 Efecto de las ERO sobre las células astrogliales de la corteza cerebelar en desarrollo

La segunda pregunta abordada en esta tesis, está relacionada con el efecto de las ERO sobre las células astrogliales. Todos los experimentos realizados en esta sección se realizaron con la colaboración de la Maestra en Ciencias Guadalupe Domínguez Macouzet. El sustento para realizar estos experimentos se basa en que las células astrogliales desempeñan un papel importante durante el desarrollo y la fisiología de la corteza cerebelar (Hoogland and Kuhn, 2010) y que durante el desarrollo de la corteza cerebelar existe una ocurrencia de muerte programada de la astroglía (Krueger et al., 1995). En este sentido, se sabe que existe una coincidencia entre la muerte astroglial en cerebelo (Krueger et al., 1995) y los altos niveles de ERO en la corteza cerebelar (Coyoy et al., 2013). Aunque en este último estudio no identificamos a las células astrogliales como células productoras de ERO, es probable que las ERO producidas por las neuronas tengan algún efecto en las células astrogliales, por lo que resulta pertinente investigar las posibles consecuencias de las ERO sobre este tipo de células. Para esto, empleamos cultivos de astrocitos obtenidos de la corteza cerebelar del día P8, los cuales son correspondientes en edad a los cultivos de las NGC realizados a lo largo de este estudio.

Con la finalidad de inducir la generación de ERO, empleamos el inhibidor general de PKC, estaurosporina, puesto que se sabe induce la muerte apoptótica de las NGC de una forma dependiente de la producción de ERO a través de NOX2 (Guemez-Gamboa and Moran, 2009). Decidimos probar si la estaurosporina induce la muerte celular de las células astrogliales de forma dependiente de ERO. Para esto, primero evaluamos si el tratamiento con estaurosporina induce la generación de ERO en las células astrogliales a lo largo del tiempo. La figura 15A muestra que el tratamiento con estaurosporina disminuyó la viabilidad celular alrededor de un 50 % a las 24 horas post-tratamiento (esta figura se obtuvo de la tesis de Maestría de Guadalupe Domínguez Macouzet (Dominguez, 2011)) y se muestra con el fin de servir de antecedente a esta investigación. El tratamiento con estaurosporina indujo también la producción de ERO en estas células, alcanzando su máximo nivel a las 2 horas (Figura 15B). Como se aprecia en la figura 15B, se alcanzó un máximo en la generación de ERO a las dos horas post-tratamiento. Esta producción de ERO se debe una enzima NOX, ya que la actividad NOX coincide con el tiempo en que se alcanzaron los máximos niveles de ERO. Además, el uso del inhibidor AEBSF, disminuyó los niveles de ERO a este mismo tiempo (Figuras 15C,D respectivamente. La Figura 15C se obtuvo de la tesis de Maestría de Guadalupe Domínguez Macouzet (Dominguez, 2011)) y se muestra con el fin de servir de antecedente a los experimentos posteriores.

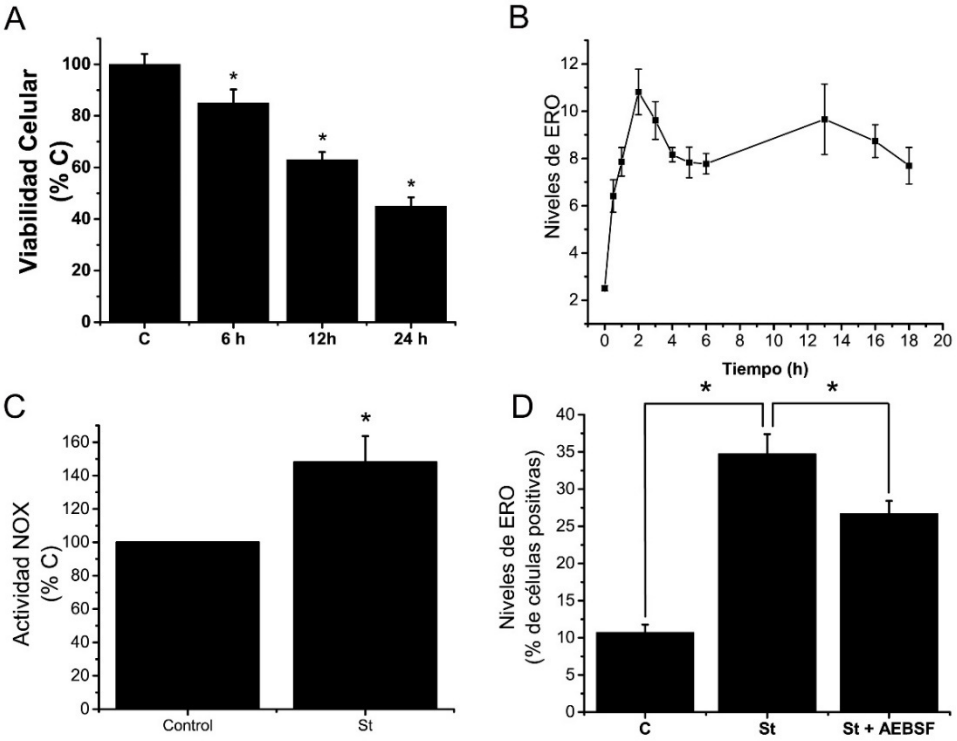

Figura 15. La estaurosporina reduce la viabilidad de células astrogliales de manera dependiente de ERO. (A) Los astrocitos de cerebelo fueron tratados con estaurosporina (0.5 µM) por 6, 12 y 24 horas y la viabilidad celular fue medida por la transformación de MTT. La viabilidad celular disminuyó con el tratamiento de estaurosporina a todos los tiempos (⋆ $p<0.05$, ANOVA, n=4). Los datos son la media ± error estándar. Tomado de (Dominguez, 2011). (B) Los niveles de ERO se determinaron por la oxidación de dihidroetidina en células astrogliales tratadas con estaurosporina (0.5 µM), analizándose por la intensidad de fluorescencia media. El tratamiento con estaurosporina incrementó los niveles de ERO en todos los tiempos observados (⋆ $p<0.001$, ANOVA, n=4). Los datos son la media ± error estándar. (C) La actividad de NOX se midió en células astrogliales tratadas con estaurosporina (0.5 µM) durante dos horas. La actividad de NOX fue mayor en las células tratadas con estaurosporina (⋆ $p<0.05$, Prueba de T, n=5). Los datos son la media ± error estándar y están normalizados respecto al Control. Tomado de (Dominguez, 2011). (D) Los niveles de ERO se determinaron por el conteo de células positivas a dihidroetidina en células astrogliales tratadas con estuarosporina (0.5 µM) y/o AEBSF (50 µM). El tratamiento con AEBSF redujo los niveles de ERO en estas células tratadas con estaurosporina (⋆ $p<0.05$ ANOVA, n=3). Los datos son la media ± error estándar.

Por otra parte, decidimos explorar si la muerte celular observada en las células astrogliales, se relaciona con la producción de ERO mediada por NOX. Empleamos el inhibidor AEBSF, el cual rescató la viabilidad celular (Figura 16A). Sin embargo, el uso de este inhibidor no nos permite discernir cuál es el homólogo específico de NOX que está mediando dicho proceso, por lo que decidimos emplear animales deficientes en NOX2 y NOX3. Encontramos que la viabilidad celular disminuyó de igual forma en los animales silvestres y en los animales deficientes en NOX2 y NOX3, por lo que establecimos que la muerte celular inducida por estaurosporina no está mediada por estos homólogos (Figuras 16B-D).

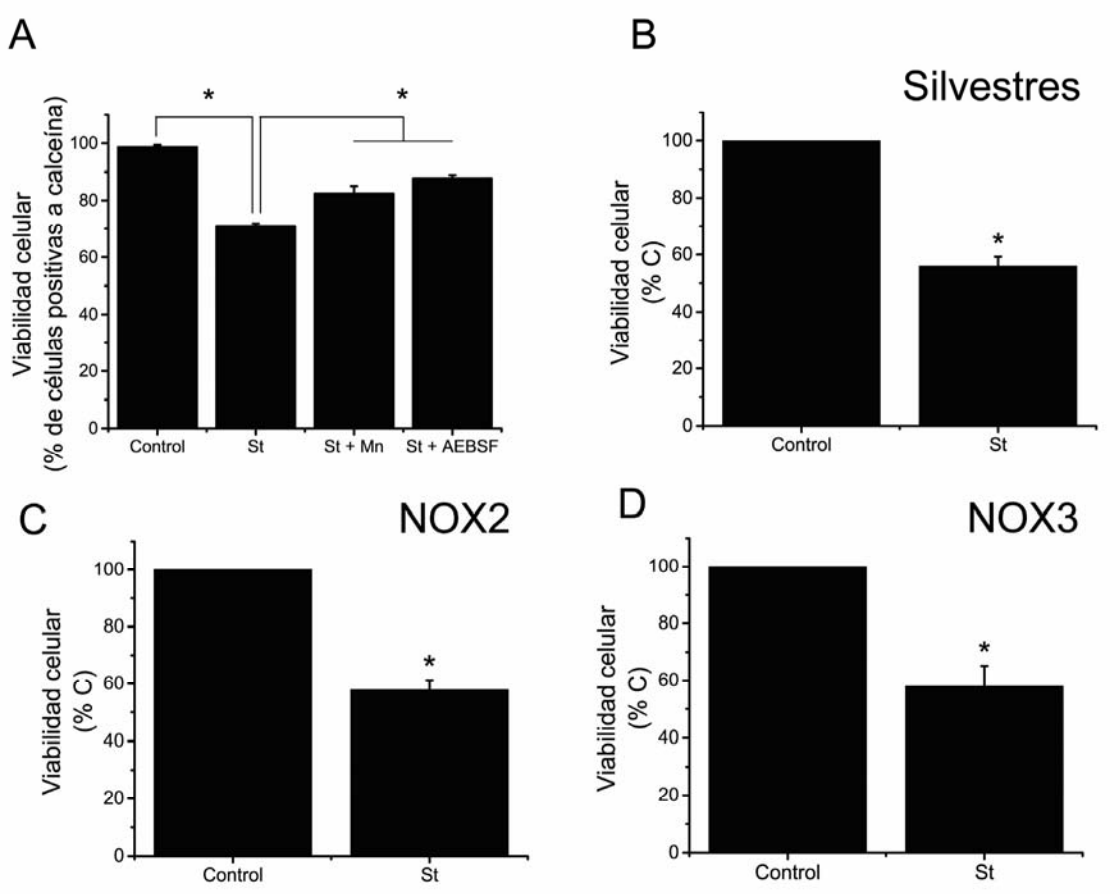

Figura 16. La muerte celular inducida por estaurosporina no depende de NOX2 y NOX3. (A) Se determinó la viabilidad de las células tratadas con estaurosporina (0.5 µM) y/o con el antioxidante MnTMPyP (50 µM) o con el inhibidor de NOX, AEBSF (50 µM) por 24 horas, mediante la técnica de calceína y ioduro de propidio. Los tratamientos MnTMPyP y AEBSF rescataron la sobrevivencia de las células astrogliales tratadas con estaurosporina (⋆ P<0.05, ANOVA, n=3). Los datos son la media ± error estándar. (B-D) La viabilidad celular se determinó por transformación de MTT en células astrogliales obtenidas de animales deficientes de NOX2 (C) y NOX3 (D) tratadas con estaurosporina (0.5 µM) durante 24 horas. La estaurosporina redujo la viabilidad celular en todos los casos (⋆ P<0.05, Prueba de T, n=5). Los datos son la media ± error estándar.

En la figura 17A se aprecia que el tratamiento con estaurosporina indujo cambios drásticos en la morfología de las células astrogliales, ya que éstas la cambian drásticamente con el tratamiento con estaurosporina, el cual provoca la compactación de los somas celulares e induce la extensión de largos procesos, asemejando así a células astrogliales reactivas con una morfología estrellada. En las células no tratadas, el citoesqueleto de actina se distribuye en haces difusos a lo largo de toda la célula, estos haces son compactados y se extienden a lo largo del proceso en formación bajo el tratamiento de estaurosporina. Por otra parte el citoesqueleto de tubulina se extiende semejando una malla que se compacta bajo el tratamiento con estaurosporina. Resulta evidente que la red del citoesqueleto de tubulina, está extendida en la misma magnitud que los filamentos de actina. En la Figura 18A se aprecia que los filamentos de actina se extienden aún más lejos que la red de microtúbulos. Estos cambios están asociados a una re-estructuración del citoesqueleto de actina y tubulina y no a un cambio en la expresión de estas proteínas, ya que los niveles de las proteínas actina y tubulina no cambiaron bajo el tratamiento con estaurosporina ni con los tratamientos antioxidantes o utilizando los inhibidores de la NOX (Figura 17B).

A

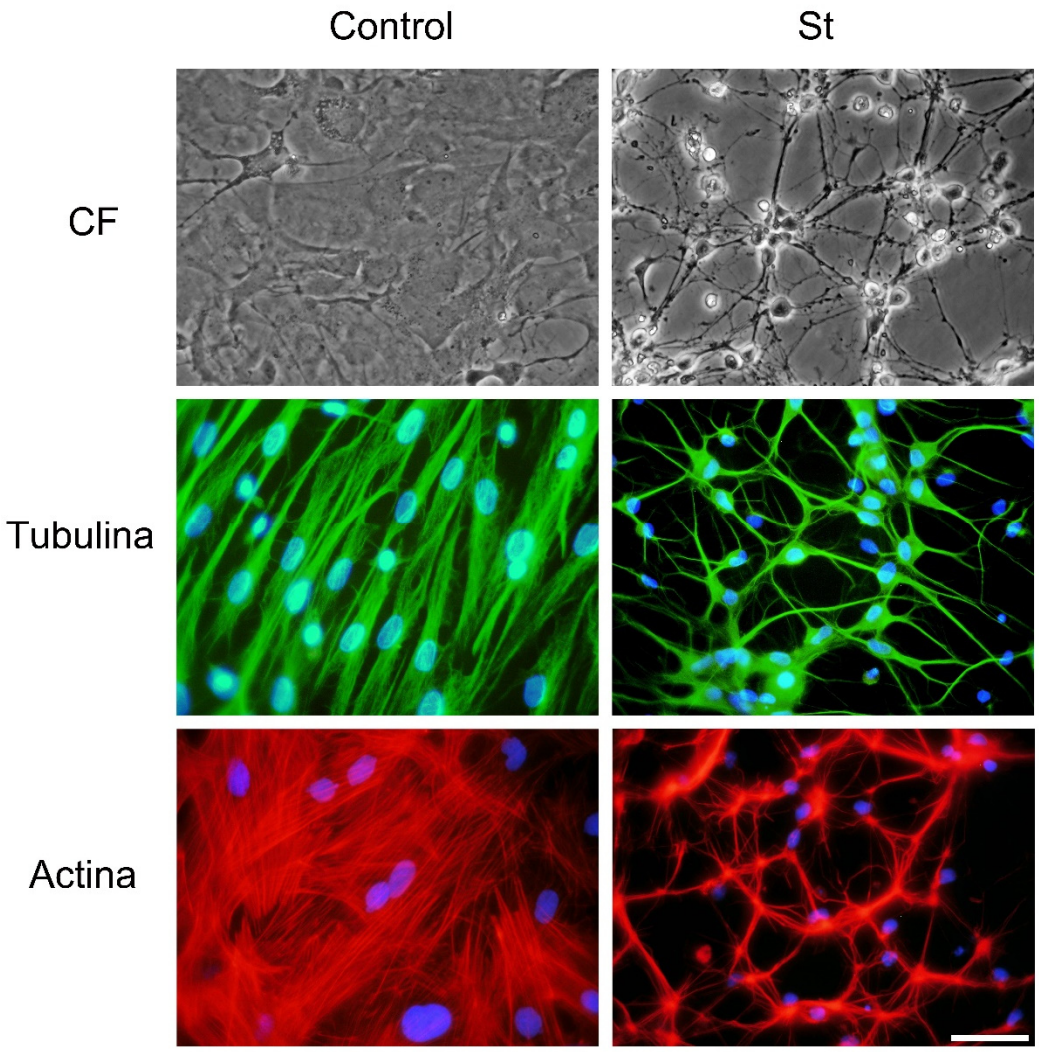

B

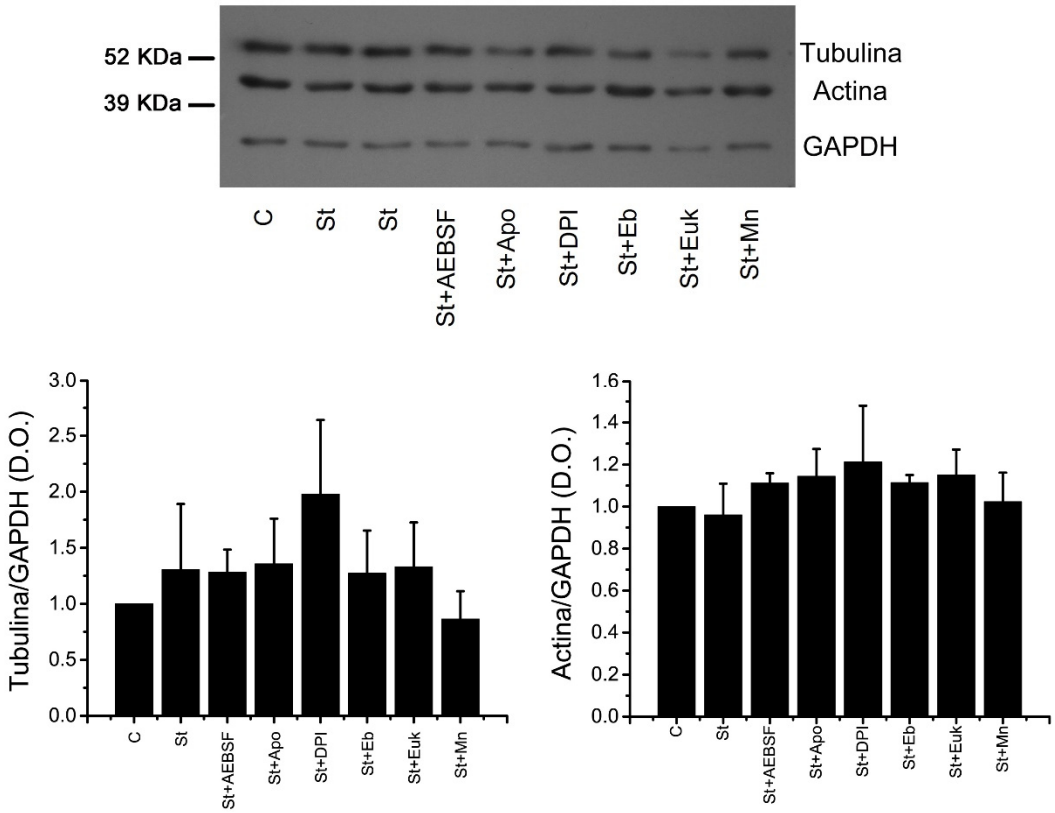

Figura 17. Los cambios morfológicos de las células astrogliales están mediados por el re-arreglo del citoesqueleto. (A) Las células astrogliales se trataron con estaurosporina (0.5 µM) durante 12 horas y posteriormente se realizó la inmunotinción contra tubulina y la tinción con rodamina y faloidina para actina (la barra de esquela equivale a 50 µm). (B) Se detectaron los niveles de las proteínas actina y tubulina bajo el tratamiento con estaurosporina más los antioxidantes Ebselen (10 µM), Euk-134 (20 µM) y MnTMPyP (50 µM) y más los inhibidores de NOX, DPI (520 nm) y AEBSF (50 µM). No se encontraron diferencias estadísticas entre los tratamientos. Los datos son la media ± error estándar.

Es importante mencionar que diferentes morfologías de la glía de Bergmann se han documentado a lo largo de distintos trabajos en diferentes mutaciones que afectan la función del cerebelo (Rakic and Sidman, 1973; Bignami and Dahl, 1974; Terashima et al., 1985), sugiriendo que la morfología de estas células afecta su propia función. Razón por la cual, decidimos explorar si la producción de ERO estaba asociada a los cambios morfológicos de las células astrogliales que fueron inducidos por el tratamiento con estaurosporina. Por otra parte, como se mostró en la figura 11I, el H_2O_2 promueve la formación de filopodios, los cuales son estructuras altamente reguladas por el citoesqueleto, además, se sabe que las ERO son reguladoras del citoesqueleto y la morfología celular (Alexandrova et al., 2006). Por estas razones decidimos tratar a las células astrogliales con los antioxidantes MnTMPyP y Euk-134 y con los inhibidores AEBSF y DPI, sin embargo, ninguna de estas condiciones antioxidantes logró prevenir los cambios morfológicos inducidos por estaurosporina (Figuras 18A,B). Aunque nuestra hipótesis no resultó ser cierta, sí identificamos al H_2O_2 como un regulador de los cambios morfológicos de las células astrogliales, ya que el tratamiento por H_2O_2 sí indujo cambios morfológicos de estas células, los cuales se previnieron completamente con la presencia del antioxidante Euk-134, corroborando así, que las concentraciones empleadas de este antioxidante fueron capaces de prevenir la acción oxidante del H_2O_2 pero no los cambios

inducidos por estaurosporina (Figura 18B). Los efectos del H_2O_2 sobre la morfología de las células astrogliales es específica de esta molécula, ya que el sistema de generación de $O_2^{\bullet -}$, xantina/xantina oxidasa, no produjo cambios morfológicos en estas células (dato no mostrado).

A

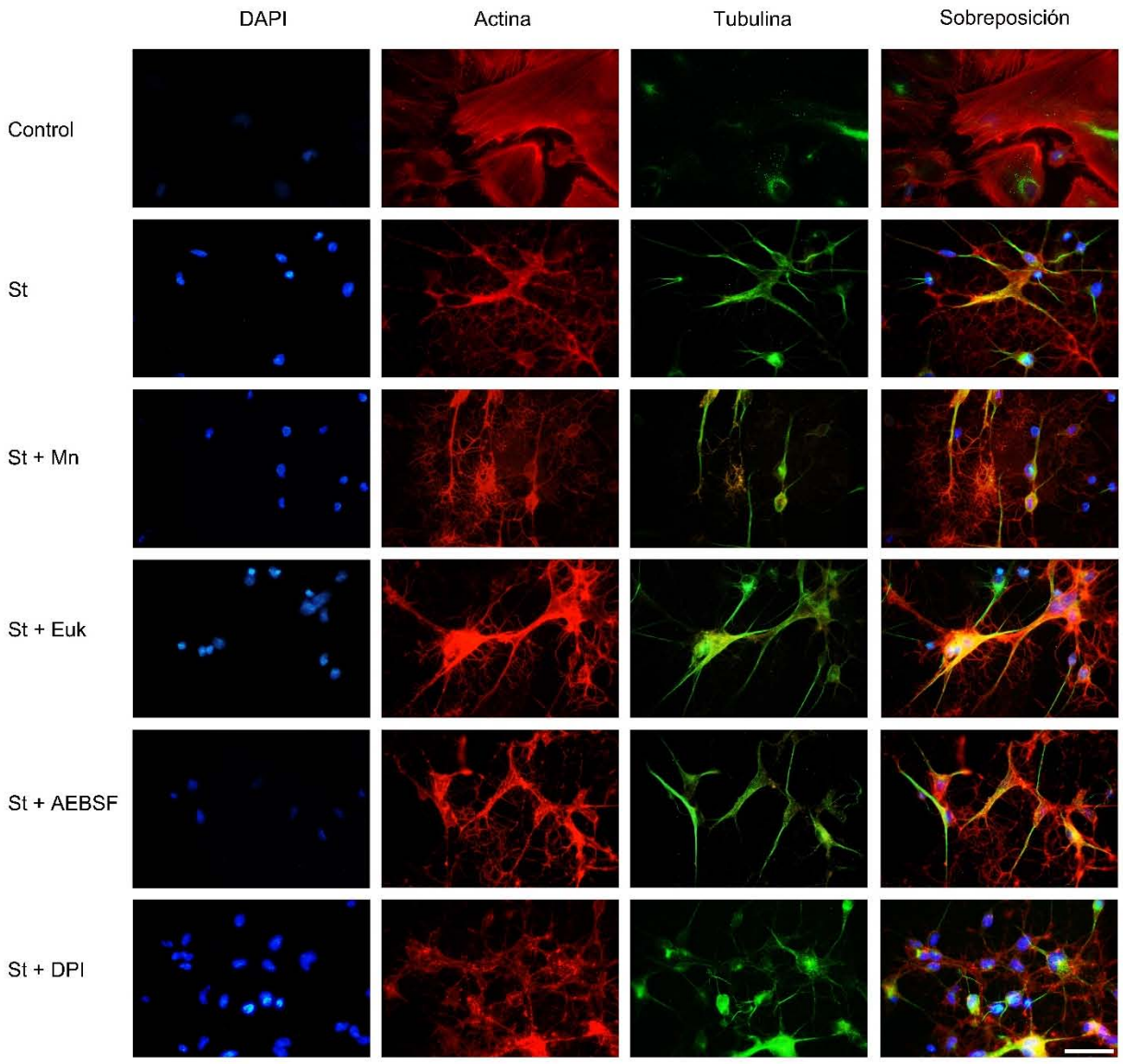

B

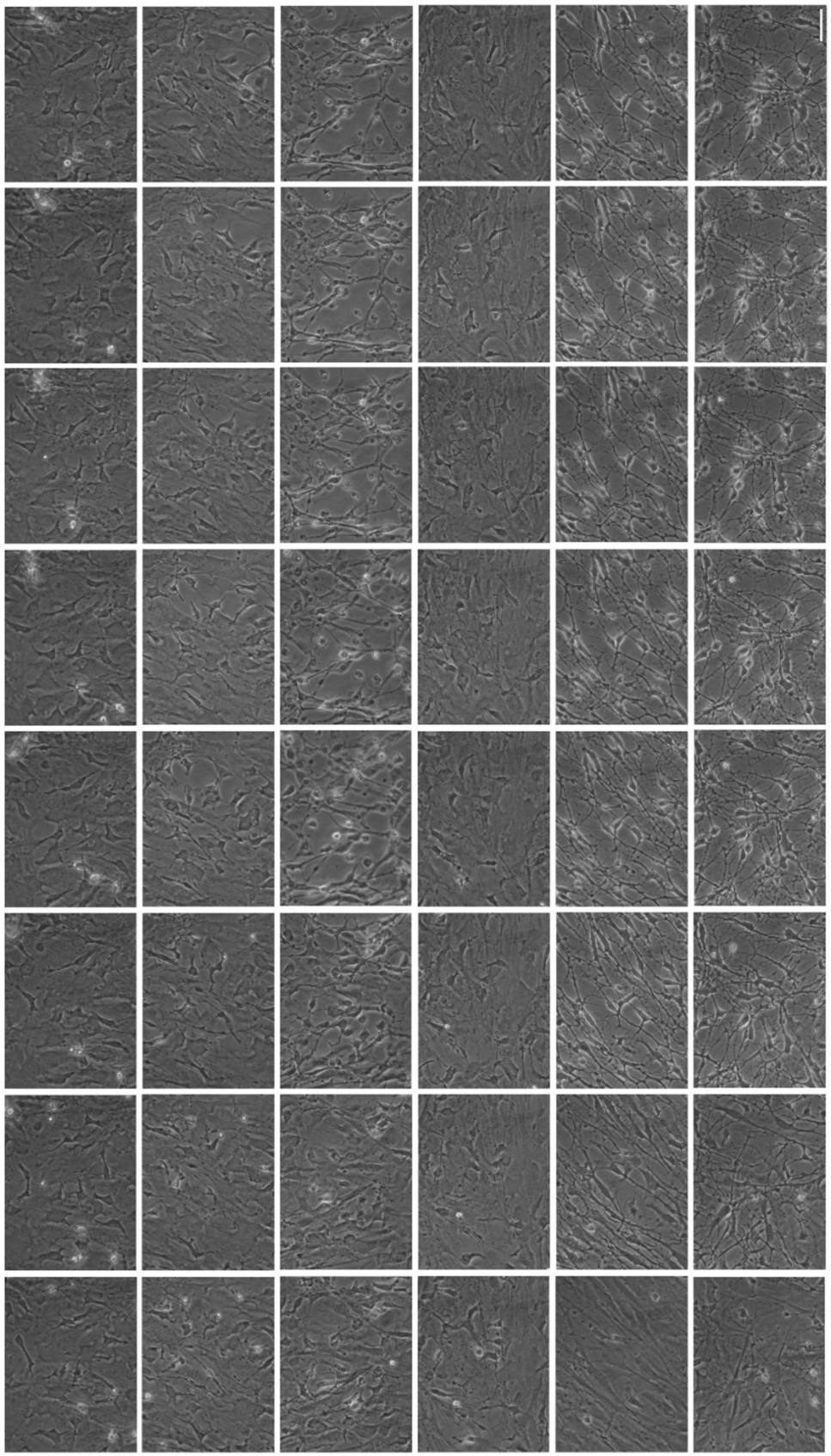
0 min
15 min
45 min
75 min
105 min
135 min
165 min
195 min
Control
Euk
H2O2
H202 +Euk
St
St +Euk

Figura 18. Los cambios morfológicos inducidos por estaurosporina no son dependientes de las ERO. (A) Las células astrogliales se trataron con estaurosporina (0.5 µM) durante 2 horas en la presencia y ausencia de los antioxidantes MnTMPyP (50 µM) y Euk-134 (20 µM) y de los inhibidores NOX, DPI (520 nm) y AEBSF (50 µM). En azul se marcan los núcleos celulares, en verde se marca la tubulina y en rojo la actina (la barra de escala equivale a 50 µm). (B) Secuencias de imágenes en el tiempo de células astrogliales tratadas con estuarosporina (0.5 µM), con H_2O_2 (200 µM) en la presencia o ausencia de Euk-134 (20 µM) (la barra de escala equivale a 50 µm).

VII. Discusión

7.1 ERO y NOX durante el desarrollo de las NGC

En el presente estudio encontramos que la producción de ERO varía a lo largo del desarrollo de las NGC. Al respecto, proponemos que el desarrollo de las NGC puede ser dividido en dos fases distintas. En la primera fase, las ERO incrementan durante los primeros 2 DIV y permanecen elevadas hasta el 3 DIV, lo cual ocurre independientemente del estado de despolarización de las neuronas. En la segunda fase, los niveles de ERO dependen del estado de despolarización: en condiciones despolarizantes, los niveles de ERO disminuyen a partir del 4 DIV y permanecen bajos en los subsecuentes días, mientras que en condiciones no despolarizantes, los niveles de ERO continúan incrementando a 4 y 5 DIV. Durante estas dos fases, las NGC llevan a cabo diferentes procesos del desarrollo. Durante la primer fase, las NGC inician los procesos de maduración bioquímicos (Gallo et al., 1987) y morfológicos (Powell et al., 1997). Mientras que a los 3 DIV, la mayoría de las NGC han desarrollado el axón y múltiples dendritas (de la Torre-Ubieta et al., 2010). La segunda fase coincide con la dependencia al estado de despolarización y la sobrevivencia celular (Gallo et al., 1987) y la maduración de las dendritas (Shalizi et al., 2006; Ramos et al., 2007).

Nuestros resultados muestran que a pesar de que hay niveles altos de ERO a los 2 y 3 DIV, la viabilidad de las neuronas no se compromete, lo cual es independiente del estado de despolarización. En contraste, durante la segunda fase, estos datos muestran una correlación entre los bajos niveles de ERO y la sobrevivencia de las NGC en condiciones despolarizantes. Al parecer en condiciones no despolarizantes, los altos niveles de ERO están asociados con una actividad metabólica reducida y con la sobrevivencia celular. En este sentido, nuestro grupo ha mostrado en trabajos previos que las ERO pueden ser señales que desencadenan el proceso de muerte apoptótica en NGC a 8 DIV, cuando las células se cambian de una condición despolarizante a una no despolarizante (Ramiro-Cortes and Moran, 2009; Ramiro-Cortes et al., 2011). En su conjunto, estos resultados sugieren que la regulación de los niveles de ERO durante el desarrollo de las NGC, puede ser crítica para la sobrevivencia durante la segunda fase del desarrollo.

7.2 Regulación del glutatión durante el desarrollo de las NGC

También exploramos la posibilidad de que el glutatión pudiera ser responsable de modificar los niveles de ERO durante el desarrollo. Esto fue apoyado por la hecho que sostiene que el balance entre la producción de ERO y la actividad y expresión de los sistemas antioxidantes, determinan los niveles de ERO en las células. Por otra parte, se sabe que durante el desarrollo del sistema nervioso, las neuronas y las células gliales contienen glutatión y que alrededor del día postnatal 5, la mayor parte de las neuronas disminuyen los niveles de glutatión, sin embargo, las células granulares y mitrales olfatorias, las NGC y las neuronas del ganglio de la raíz dorsal,

consistentemente retienen altos niveles de glutatión a lo largo del desarrollo y en el estado adulto (Beiswanger et al., 1995). Además, los ratones deficientes de glutatión, mueren antes del día embrionario 8.5 mediante apoptosis masiva (Shi et al., 2000) y la ausencia de la glutatión peroxidasa 4 (GPx4) provoca que los ratones mueran en el día embrionario 8, también por un incremento anormal de la muerte apoptótica (Yant et al., 2003). Interesantemente, mientras que la GPx4 se expresa en neuronas, las células gliales carecen de esta enzima (Savaskan et al., 2007). Además, se ha sugerido que el cerebro constituye el sitio más importante de expresión de la GPx4, lo cual queda de manifiesto cuando se suprime la GPx4 específicamente entre los días embrionarios 7.5 y 10.5, lo cual conduce a la microcefalia y al desarrollo anormal del rombonecéfalo (Borchert et al., 2006).

En este estudio, encontramos cambios importantes en los niveles de glutatión durante el desarrollo de las NGC. Durante la primera fase de desarrollo de las NGC, cuando los niveles de ERO son relativamente altos, el contenido de glutatión incrementa y se establece también en los niveles más altos del desarrollo. Una posibilidad para explicar esta observación, es que probablemente existe un mecanismo encargado del balance de las ERO, requerido para una correcta señalización redox y a su vez, también para prevenir los efectos nocivos de las ERO. El mayor incremento de glutatión, ocurre entre los 0 y 1 DIV, lo cual precede el mayor incremento de ERO durante la primera fase. Estos resultados, sugieren que los cambios en el contenido de glutatión en las NGC, responden a un programa genético intrínseco de las células, lo cual probablemente es independiente tanto de las condiciones tróficas como de los niveles de ERO. Está idea es apoyada por el hecho de que *in vivo*, el contenido de glutatión en el cerebelo en desarrollo, incrementa en el tiempo en el cual los precursores de las NGC comienzan su proceso de diferenciación (Nanda et al., 1996; Rice and Russo-Menna, 1998; Komuro and Yacubova, 2003).

También se sabe que el tratamiento crónico con BSO y oxígeno en ratas neonatas, lleva a un alto índice de apoptosis en el hipocampo, el cerebelo y el estriado (Taglialatela et al., 1998). En este sentido, nuestros resultados demuestran que el incremento del contenido de glutatión, es necesario para permitir la sobrevivencia durante el desarrollo de las NGC, ya que la eliminación del contenido de glutatión a los 2 DIV, drásticamente reduce la sobrevivencia de las NGC, pero no afecta su sobrevivencia en estadios posteriores del desarrollo. Este proceso puede explicarse por dos mecanismos de acción del glutatión: a) la interacción del glutatión con las proteínas, lo cual modifica las vías de señalización durante las variaciones en la homeostasis de las ERO (Grek et al., 2013); b) las acciones antioxidantes del glutatión. El hecho de que el antioxidante Euk-134 rescate la viabilidad de las NGC bajo condiciones de depleción del glutatión, sugiere fuertemente que el efecto de la ausencia del glutatión en la sobrevivencia de las NGC, se debe a sus propiedades antioxidantes.

Durante la segunda fase, los niveles de glutatión dependen del estado de despolarización de las neuronas. En condiciones despolarizantes, el contenido de glutatión permanece elevado entre los 3 y 5 DIV, lo cual corresponde a un tiempo en el que los niveles de ERO disminuyen marcadamente. En contraste, en condiciones no despolarizantes, el contenido de glutatión disminuye desde el 4 DIV, lo cual correlaciona con la disminución de la sobrevivencia de las NGC y los altos niveles de ERO. Esta disminución del glutatión, puede considerarse como una marca de la progresión de la muerte celular (Franco and Cidlowski, 2012). Con la finalidad de descartar que la disminución del contenido de glutatión es responsable de la muerte celular observada durante la segunda fase en condiciones no despolarizantes, disminuimos los niveles de glutatión con BSO, sin embargo, aunque el contenido de glutatión disminuyó importantemente, la viabilidad celular bajo condiciones despolarizantes no se alteró a los 5 DIV, indicando que una disminución del contenido de glutatión no es suficiente para desencadenar la muerte celular

en las NGC en desarrollo y que la disminución del contenido de glutatión durante la segunda fase en condiciones no despolarizantes es probablemente una consecuencia del proceso de muerte.

7.3 ROS y NOX en la maduración de las NGC

La posibilidad de que las ERO se requieran para el desarrollo de las NGC en la primera fase, se sostiene en nuestros resultados que muestran que las condiciones antioxidantes disminuyen marcadamente los niveles de las proteínas Tau y MAP2. Interesantemente, encontramos que los antioxidantes Ebselen y Euk-134 redujeron el contenido de MAP2 a los 2 DIV, mientras que los inhibidores NOX, AEBSF y Apocinina, disminuyeron los niveles de Tau y MAP2 a los 2 DIV y parcialmente a 1 DIV sugiriendo una acción más específica de las ERO producidas por la actividad de NOX durante el proceso de maduración. Ninguno de estos tratamientos disminuyó la expresión de estas proteínas a los 3 DIV, lo cual puede explicarse por el hecho de que entre 2 y 3 DIV los niveles de Tau y MAP2 no incrementaron considerablemente en condiciones control y/o porque para este tiempo, el proceso de maduración de las NGC no depende de las ERO.

Es importante mencionar que basados en los mecanismos de inhibición del AEBSF y la Apocinina, su blanco primario son las homólogos NOX1 y NOX2 (Jaquet et al., 2009). Sin embargo, ya que el efecto de estos inhibidores fue únicamente parcial, en este estudio no podemos excluir la contribución de otros homólogos NOX y/o otras fuentes de producción de ERO que actúen durante el desarrollo de las NGC. Aunque no podemos descartar que parte de los efectos observados por AEBSF y Apocinina se deban a acciones inespecíficas de estos fármacos, sus efectos se validan con el uso de un segundo inhibidor de NOX (ya sea AEBSF o Apocinina). Por lo tanto, pensamos que los resultados obtenidos utilizando separadamente ambos inhibidores con resultados similares, indican que las enzimas NOX están involucradas en la producción de ERO, las cuales se requieren para la maduración de las NGC.

Parte de nuestros resultados se basan en observaciones previas de otros estudios, los cuales proponen que las enzimas NOX probablemente actúan como moléculas señal en la regulación de la diferenciación neuronal de las células PC12. Se sabe que en estas células la neurotrofina NGF induce la expresión de marcadores de diferenciación como son βIII-tubulina, GAP-43 y neurofilamento L, lo cual ocurre a través de la activación del receptor TrkA, que a su vez activa la vía de señalización Ras/Raf/MEK/ERKs (Kaplan and Miller, 2000; Patapoutian and Reichardt, 2001). Además, el NGF induce un incremento de los niveles de ERO producidos por NOX (Suzukawa et al., 2000). Estas ERO inducen la fosforilación de ERKs a través de la formación de complejos con las proteínas de andamiaje Shc, Grb2 y Sos (Kamata et al., 2005). Por otra parte, el NGF induce la expresión y la activación de la MnSOD, la cual a su vez induce la formación de H_2O_2 que es esencial para la activación sostenida de ERKs, induciendo la diferenciación neuronal (Cassano et al., 2010).

Otros estudios han mostrado que las enzimas NOX median la diferenciación neuronal en distintos modelos (Wang et al., 2007; Kennedy et al., 2010; Nitti et al., 2010; Le Belle et al., 2011). En el presente estudio, encontramos que la actividad de NOX es similar a los niveles de ERO observadas tanto en primera fase como en la segunda en condiciones despolarizantes. Diferentes homólogos de NOX podrían contribuir a la actividad de NOX observada, por tal motivo exploramos la expresión de dos homólogos de NOX, NOX1 y NOX2, los cuales se inhiben por AEBSF y Apocinina. Nuestros resultados indican que la expresión de estos homólogos se regula significativamente a lo largo del desarrollo de las NGC. En general, durante la primera fase los niveles de RNAm

tanto de NOX1 como de NOX2 presentan sus mayores niveles, mientras que en la segunda fase, la expresión de ambos disminuye. Estos resultados sugieren que estas enzimas probablemente participan de manera diferencial durante el desarrollo de las NGC.

Es importante mencionar que la expresión de NOX2 se asocia más estrechamente a la actividad de NOX y a los niveles de ERO en comparación con NOX1. Además, los niveles de RNAm de NOX2 son considerablemente más abundantes que los niveles de RNAm de NOX1. Por lo tanto, consideramos que el homólogo NOX2 puede ser la fuente principal de producción de ERO producidas durante el desarrollo de las NGC. Sin embargo, no encontramos diferencias en los niveles de ERO entre las NGC obtenidas de animales deficientes de NOX2 y silvestres a 1 y 2 DIV. Esto podría significar que la enzima NOX2 no es responsable del incremento de ERO que ocurre durante la primera fase del desarrollo. Sin embargo, no descartamos un posible mecanismo compensatorio en las NGC deficientes de NOX2, ya que se ha demostrado en otras preparaciones que existe una sobre-expresión de NOX4 en animales deficientes de NOX2 y en células donde se ha silenciado el gen de NOX2 (Pendyala et al., 2009). Lo anterior también se ha demostrado cuando se induce de manera indirecta una menor expresión de NOX2 (Sedeek et al., 2010).

A pesar del hecho de que los niveles de ERO en las NGC KO NOX2 no fueron menores que aquellos de las NGC silvestres, encontramos que la longitud de los axones de las NGC KO NOX2, sí fueron menores a la de los axones de las NGC silvestres a 1 y 2 DIV, lo cual corrobora la importancia de NOX2 durante el desarrollo de las NGC. Este resultado, concuerda con otros estudios realizados en neuronas de *Aplysia*, donde se ha mostrado que la inhibición de NOX2 reduce el flujo y ensamblaje de actina en la parte más distal del cono de crecimiento, conduciendo así a una disminución del crecimiento neurítico (Munnamalai and Suter, 2009). La regulación de NOX2 en los conos de crecimiento axonal de las neuronas de *Aplysia*, parece ser una relación bidireccional en la que NOX2 produce H_2O_2 que regula a la dinámica de la F-actina y al crecimiento neurítico. Por otra parte, la estimulación del crecimiento neurítico induce la proximidad de la subunidad citoplasmática de NOX2, p40phox hacia la subunidad catalítica, gp91phox, indicando que la regulación de la dinámica del citoesquelo afecta la actividad de NOX2 (Munnamalai et al., 2014b).

La relevancia de NOX2 en el desarrollo del sistema nervioso también se ha demostrado mediante observaciones de la fisiología del cerebro de ratones deficientes de NOX2. Estos animales poseen una menor cantidad de células proliferantes en la zona subventricular, menos células migrantes y menor diferenciación neuronal en el bulbo olfatorio, en comparación con los animales silvestres (Le Belle et al., 2011) .Además estos animales muestran deficiencias en la plasticidad sináptica del hipocampo así como ciertas deficiencias en la función cognitiva y deficiencias en el aprendizaje motor (Kishida et al., 2006), que pueden ser atribuidas a una función alterada ya sea de la corteza cerebelar o de los núcleos cerebelares profundos (Caston et al., 1995). Hasta el momento no se ha estudiado si las alteraciones en el comportamiento motor de los animales deficientes de NOX2 se relacionan con la formación de los circuitos cerebelares y/o alteraciones de la función y plasticidad sináptica. Al respecto, en un estudio previo de nuestro grupo, se encontró que la administración de Apocinina o de un antioxidante en ratas postnatales, produce alteraciones en el patrón de foliación cerebelar al igual que una deficiencia en el comportamiento motor (Coyoy et al., 2013). Basados en lo anterior, especulamos que la deficiencia del crecimiento axonal que observamos en los NGC deficientes de NOX2, puede tener implicaciones en la formación de los circuitos de la corteza cerebelar.

7.4 H_2O_2 y la localización de NOX2

En este trabajo estudiamos analizamos la posibilidad de que el H_2O_2 sea producido localmente durante el desarrollo de las NGC, así como la posible contribución del glutatión como un regulador del contenido del H_2O_2. Aunque no se conoce con exactitud cómo ocurre la señalización redox, existe evidencia que indica que las funciones fisiológicas del H_2O_2 ocurren por la activación específica de vías de señalización a través de modificaciones redox reversibles de proteínas en compartimentos específicos de la célula (Chen et al., 2009; Ushio-Fukai, 2009a; Gough and Cotter, 2011; Mishina et al., 2011a; Kaludercic et al., 2014). Interesantemente, encontramos diferentes regiones de los axones y de las dendritas en desarrollo, donde el H_2O_2 se produce continuamente. Estas regiones aparentemente corresponden a las regiones donde NOX2 está expresada. Por ejemplo, NOX2 se expresa abundantemente en filopodios, tanto en la base del filopodio, como en la parte interna, lo cual coincide con micro-dominios donde el H_2O_2 es continuamente producido, sugiriendo que tanto NOX2 como el H_2O_2 probablemente están asociados a la regulación de la dinámica de estas estructuras. Además, observamos que el incremento de H_2O_2 dentro de los filopodios, precede al alargamiento del mismo y posterior a la retracción del filopodio los niveles de H_2O_2 retornan los niveles basales. En su conjunto, estos resultados sugieren fuertemente que el H_2O_2 está involucrado en la formación de filopodios y que NOX2 probablemente es una posible fuente de producción de H_2O_2. Esta idea se apoya por diferentes estudios que indican que las ERO controlan la dinámica del citoesquelo de actina (Munnamalai and Suter, 2009; Sakai et al., 2012; Lee et al., 2013; Munnamalai et al., 2014b). En neutrófilos, los niveles fisiológicos de H_2O_2 producidos por NOX2, regulan negativamente la polimerización de la actina, lo cual ocurre a través de la glutationilización de la actina, mientras que el aumento de la expresión de glutarredoxina 1 (enzima que cataliza la desglutationilización), lleva a la formación de seudópodios (Sakai et al., 2012). En macrófagos, la formación de filopodios y la polimerización de actina, son procesos regulados por la oxidación reversible de dos residuos de metionina a través de MICAL1 y MICAL2. La oxidación de estos residuos lleva al desensamble de actina, mientras que la reducción de estos residuos por la sulfoxido-R-metionina reductasa B, lleva al ensamble de actina, lo cual en su conjunto orquesta la dinámica de la actina y la función del macrófago (Lee et al., 2013). Por tanto, especulamos que las reacciones redox posiblemente controlan la formación de filopodios en las NGC.

Por otra parte, la localización de NOX2 en los conos de crecimiento axonales, también correlaciona con sitios de elevada producción de H_2O_2. Este resultado sugiere que el H_2O_2 probablemente está asociado con la dinámica de los conos de crecimiento y que el H_2O_2 probablemente es producido por NOX2, lo cual es acorde con nuestra observación de que las NGC deficientes de NOX2 tienen un menor crecimiento axonal en comparación a las NGC silvestres. Esta observación ha sido previamente examinada en las neuronas de Aplysia, donde el H_2O_2 producido por NOX2, modula la dinámica de la F-actina y promueve el crecimiento axonal (Munnamalai et al., 2014b). Por otra parte, también se sabe que el H_2O_2 regula negativamente el crecimiento axonal. En neuronas del ganglio de la raíz dorsal, la semaforina3A induce el colapso del cono de crecimiento axónico a través de la regulación oxidativa de CRMP2 (Morinaka et al., 2011). Aunque no se conoce con exactitud como el H_2O_2 regula la dinámica del cono de crecimiento axónico, parece ser que múltiples fuentes generadoras de H_2O_2, se localizan en esta estructura, por lo que es probable que las ERO poseen distintas funciones en dicha estructura.

También, exploramos la posibilidad de que la integridad del axón pudiese alterarse en ausencia de glutatión. Interesantemente, no encontramos alteraciones en los somas, pero sí observamos severas aberraciones en los axones de las NGC tratadas con BSO, las cuales son seguidas por la muerte celular, sugiriendo que los niveles de ERO son críticos tanto para la formación del axón como para su integridad. Las estructuras tipo esferoides con se forman bajo el tratamiento con BSO, probablemente se originan por un desbalance de la producción de H_2O_2 en el axón, ya que estas estructuras contienen altos niveles de H_2O_2 y su formación drásticamente se inhibe por la administración de un antioxidante exógeno. Estas estructuras tipo esferoides formadas bajo los tratamientos con BSO, asemejan a las estructuras encontradas en modelos clásicos de degeneración axonal. Esto podría tener implicaciones clínicas importantes, ya que los axones degeneran antes que los somas en diferentes enfermedades neurodegenerativas como son la enfermedad del Alzheimer, el Parkinson, la enfermedad de Huntington y la esclerosis lateral amiotrófica, entre otras (Coleman, 2005; Conforti et al., 2014). Estas mismas enfermedades se han relacionado a procesos de estrés oxidante (Barnham et al., 2004). Por lo tanto, especulamos que la desregulación de los mecanismos que regulan las ERO durante el desarrollo neuronal, podría equiparase a aquellas alteraciones que actúan durante el desarrollo de distintas enfermedades neurodegenerativas.

7.5 Efecto de las ERO sobre la viabilidad y morfología de las células gliales

Por otra parte, estudiamos el papel de las ERO sobre la sobrevivencia y morfología de las células astrogliales ya que se sabe que, tanto en el desarrollo como en la fisiología de la corteza cerebelar, estas células desempeñan funciones muy importantes (Krueger et al., 1995) y, particularmente, estos procesos son regulados por las ERO en otras preparaciones (Jacobson and Duchen, 2002; Zhu et al., 2009). De acuerdo a estudios realizados por nuestro grupo en neuronas (Guemez-Gamboa and Moran, 2009; Ramiro-Cortes and Moran, 2009), encontramos que la viabilidad celular se compromete por la generación de ERO a través de un homólogo de NOX el cual no fue identificado en el presente estudio y que por exclusión, podría tratarse de NOX1 o NOX4. En concordancia con el proceso de muerte celular, las células astrogliales experimentan cambios morfológicos inducidos por el tratamiento con estaurosporina, los asociamos a la redistribución de las proteínas del citoesqueleto actina y tubulina y no a cambios en el contenido de las mismas. Se sabe que las células astrogliales presentan una gran plasticidad en su morfología tanto en eventos del desarrollo como en eventos patológicos (Yamada and Watanabe, 2002). Estas células son capaces de cambiar su morfología por la interacción con otros tipos celulares (Mi et al., 2001) y en respuesta al daño del sistema nervioso central (Eddleston and Mucke, 1993). Considerando lo anterior, hipotetizamos que las ERO producidas por las células astrogliales en respuesta a estaurosporina, están relacionadas a los cambios morfológicos de estas células, considerando que las ERO son moléculas reguladoras de distintos elementos del citoesqueleto y la morfología celular (Alexandrova et al., 2006; Moldovan et al., 2006; Chiarugi and Fiaschi, 2007). Sin embargo, no encontramos que los cambios morfológicos y el re-arreglo del citoesqueleto estuvieran mediados por las ERO producidas por NOX, por lo que probablemente los cambios morfológicos responden a la inhibición de Rho por estaurosporina, ya que los miembros de esta familia son reguladores de la dinámica del citoesqueleto de actina y por ende de la morfología celular (Hall, 1998; Rouach et al., 2006; Kim et al., 2012). Aunque los cambios morfológicos inducidos por estaurosporina no se asocian a las ERO, nosotros sí encontramos que el H_2O_2 desencadena cambios morfológicos semejantes a los producidos por

estaurosporina, los cuales probablemente ocurren a través de la regulación de los elementos del citoesqueleto, y esto parece coincidir con nuestros hallazgos obtenidos en NGC.

Es importante mencionar que aunque nuestros hallazgos realizados en células astrogliales pudieran no tener implicación tangible y directa en los procesos del desarrollo de la corteza cerebelar y en el desarrollo de las NGC, existe la posibilidad de que en condiciones patológicas (en las cuales exista una desregulación de los niveles de las ERO), algunos de estos procesos pudieran ser recapitulados. Lo anterior es importante, ya que estudios *in vitro* e *in vivo* han demostrado que la glía de Bergmann es esencial para la migración de las NGC hacia su destino final durante el desarrollo (Hatten, 1999). Además, la estructura de la glía de Bergmann es también esencial para la correcta migración radial de las NGC (Rakic, 1971). La inadecuada migración de las NGC, conlleva usualmente a la disfunción motora y a la ataxia, lo que es recurrente en numerosas condiciones patológicas (Xu et al., 2013). Por lo que nuestros hallazgos podrían tener implicaciones en el estudio de las diversas patologías relacionadas a la formación de la corteza cerebelar.

VIII. Conclusiones

En el presente estudio aportamos evidencias que sugieren que el contenido de las ERO se asocia a diferentes estadios de maduración morfológica de las NGC. Durante los primeros 3 DIV de desarrollo, las ERO incrementan, lo cual se asoció con la maduración de las NGC. Si la producción de estas moléculas no se regula correctamente en los subsecuentes días de desarrollo debido a las condiciones tróficas (i.e. bajas concentración de KCl), los niveles de ERO aumentan conduciendo a la muerte celular. Antecediendo al primer incremento fisiológico de ERO, los niveles de glutatión incrementan, lo cual se requiere para el desarrollo adecuado de las NGC, ya que la disminución farmacológica del glutatión conduce a la muerte celular. La mayor parte de las ERO producidas durante esta etapa, se originan muy probablemente por la actividad de la NOX2, que se encuentra localizada principalmente en filopodios y conos de crecimiento. Estas estructuras corresponden a micro-regiones en las que se produce continuamente el H_2O_2.

En correspondencia con estos resultados, el crecimiento neurítico es menor en las NGC deficientes de NOX2, lo cual sugiere que NOX2 es importante durante las etapas tempranas del desarrollo de las NGC. Por otra parte, la depleción farmacológica del glutatión, demuestra la importancia de esta molécula en la regulación del H_2O_2 producido en los axones de las NGC y la importancia de las ERO en la morfogénesis axonal.

En conjunto estos resultados sugieren que el H_2O_2 generado por NOX2 y su regulación por el glutatión, participan en el control de la morfogénesis axonal en las NGC en desarrollo. Estos resultados contribuyen al conocimiento de los mecanismos que operan durante el desarrollo neuronal.

Finalmente, demostramos que las ERO producidas por un homólogo NOX no determinado, promueven la muerte celular de las células astrogliales, pero no modulan los cambios morfológicos de éstas, sin embargo, el H_2O_2 sí induce cambios morfológicos en estas células.

IX. Bibliografía

Alexandrova AY, Kopnin PB, Vasiliev JM, Kopnin BP (2006) ROS up-regulation mediates Ras-induced changes of cell morphology and motility. Experimental cell research 312:2066-2073.

Anderson CM, Nedergaard M (2003) Astrocyte-mediated control of cerebral microcirculation. Trends in neurosciences 26:340-344; author reply 344-345.

Baker K, Marcus CB, Huffman K, Kruk H, Malfroy B, Doctrow SR (1998) Synthetic combined superoxide dismutase/catalase mimetics are protective as a delayed treatment in a rat stroke model: a key role for reactive oxygen species in ischemic brain injury. The Journal of pharmacology and experimental therapeutics 284:215-221.

Balazs R, Jorgensen OS, Hack N (1988) N-methyl-D-aspartate promotes the survival of cerebellar granule cells in culture. Neuroscience 27:437-451.

Barnes AP, Polleux F (2009) Establishment of axon-dendrite polarity in developing neurons. Annual review of neuroscience 32:347-381.

Barnham KJ, Masters CL, Bush AI (2004) Neurodegenerative diseases and oxidative stress. Nat Rev Drug Discov 3:205-214.

Bedard K, Krause KH (2007) The NOX family of ROS-generating NADPH oxidases: physiology and pathophysiology. Physiol Rev 87:245-313.

Beiswanger CM, Diegmann MH, Novak RF, Philbert MA, Graessle TL, Reuhl KR, Lowndes HE (1995) Developmental changes in the cellular distribution of glutathione and glutathione S-transferases in the murine nervous system. Neurotoxicology 16:425-440.

Belanger M, Magistretti PJ (2009) The role of astroglia in neuroprotection. Dialogues in clinical neuroscience 11:281-295.

Belousov VV, Fradkov AF, Lukyanov KA, Staroverov DB, Shakhbazov KS, Terskikh AV, Lukyanov S (2006) Genetically encoded fluorescent indicator for intracellular hydrogen peroxide. Nature methods 3:281-286.

Bignami A, Dahl D (1974) The development of Bergmann glia in mutant mice with cerebellar malformations: reeler, staggerer and weaver. Immunofluorescence study with antibodies to the glial fibrillary acidic protein. The Journal of comparative neurology 155:219-229.

Borchert A, Wang CC, Ufer C, Schiebel H, Savaskan NE, Kuhn H (2006) The role of phospholipid hydroperoxide glutathione peroxidase isoforms in murine embryogenesis. The Journal of biological chemistry 281:19655-19664.

Boyden ES, Katoh A, Raymond JL (2004) Cerebellum-dependent learning: the role of multiple plasticity mechanisms. Annual review of neuroscience 27:581-609.

Brown DI, Griendling KK (2009) Nox proteins in signal transduction. Free radical biology & medicine 47:1239-1253.

Burgoyne RD, Cambray-Deakin MA (1988) The cellular neurobiology of neuronal development: the cerebellar granule cell. Brain research 472:77-101.

Cassano S, Agnese S, D'Amato V, Papale M, Garbi C, Castagnola P, Ruocco MR, Castellano I, De Vendittis E, Santillo M, Amente S, Porcellini A, Avvedimento EV (2010) Reactive oxygen species, Ki-Ras, and mitochondrial superoxide dismutase cooperate in nerve growth factor-induced differentiation of PC12 cells. The Journal of biological chemistry 285:24141-24153.

Caston J, Vasseur F, Stelz T, Chianale C, Delhaye-Bouchaud N, Mariani J (1995) Differential roles of cerebellar cortex and deep cerebellar nuclei in the learning of the equilibrium behavior: studies in intact and cerebellectomized lurcher mutant mice. Brain research Developmental brain research 86:311-316.

Celotto AM, Liu Z, Vandemark AP, Palladino MJ (2012) A novel Drosophila SOD2 mutant demonstrates a role for mitochondrial ROS in neurodevelopment and disease. Brain and behavior 2:424-434.

Coleman M (2005) Axon degeneration mechanisms: commonality amid diversity. Nature reviews Neuroscience 6:889-898.

Conforti L, Gilley J, Coleman MP (2014) Wallerian degeneration: an emerging axon death pathway linking injury and disease. Nature reviews Neuroscience 15:394-409.

Coyoy A, Olguin-Albuerne M, Martinez-Briseno P, Moran J (2013) Role of reactive oxygen species and NADPH-oxidase in the development of rat cerebellum. Neurochemistry international 62:998-1011.
Cross JV, Templeton DJ (2006) Regulation of signal transduction through protein cysteine oxidation. Antioxidants & redox signaling 8:1819-1827.
Chen K, Craige SE, Keaney JF, Jr. (2009) Downstream targets and intracellular compartmentalization in Nox signaling. Antioxid Redox Signal 11:2467-2480.
Cheng PL, Poo MM (2012) Early events in axon/dendrite polarization. Annual review of neuroscience 35:181-201.
Cheret C, Gervais A, Lelli A, Colin C, Amar L, Ravassard P, Mallet J, Cumano A, Krause KH, Mallat M (2008) Neurotoxic Activation of Microglia Is Promoted by a Nox1-Dependent NADPH Oxidase. Journal of Neuroscience 28:12039-12051.
Chiarugi P, Fiaschi T (2007) Redox signalling in anchorage-dependent cell growth. Cellular signalling 19:672-682.
Day AM, Brown JD, Taylor SR, Rand JD, Morgan BA, Veal EA (2012) Inactivation of a peroxiredoxin by hydrogen peroxide is critical for thioredoxin-mediated repair of oxidized proteins and cell survival. Molecular cell 45:398-408.
de la Torre-Ubieta L, Gaudilliere B, Yang Y, Ikeuchi Y, Yamada T, DiBacco S, Stegmuller J, Schuller U, Salih DA, Rowitch D, Brunet A, Bonni A (2010) A FOXO-Pak1 transcriptional pathway controls neuronal polarity. Genes & development 24:799-813.
Dehmelt L, Halpain S (2004) Actin and microtubules in neurite initiation: are MAPs the missing link? Journal of neurobiology 58:18-33.
Diatchuk V, Lotan O, Koshkin V, Wikstroem P, Pick E (1997) Inhibition of NADPH oxidase activation by 4-(2-aminoethyl)-benzenesulfonyl fluoride and related compounds. The Journal of biological chemistry 272:13292-13301.
Dominguez G (2011) Papel de la NADPH-IXIDASA en la muerte de astrocitos en cultivo. In: UNAM, Instituto de Fisiología Celular,, p 62. México D.F.: Universidad Nacional Autónoma de México.
Dringen R, Kussmaul L, Gutterer JM, Hirrlinger J, Hamprecht B (1999) The glutathione system of peroxide detoxification is less efficient in neurons than in astroglial cells. Journal of neurochemistry 72:2523-2530.
Droge W (2002) Free radicals in the physiological control of cell function. Physiol Rev 82:47-95.
Dvoriantchikova G, Grant J, Santos ARC, Hernandez E, Ivanov D (2012) Neuronal NAD(P)H Oxidases Contribute to ROS Production and Mediate RGC Death after Ischemia. Investigative ophthalmology & visual science 53:2823-2830.
Eddleston M, Mucke L (1993) Molecular profile of reactive astrocytes--implications for their role in neurologic disease. Neuroscience 54:15-36.
Finkel T (2011) Signal transduction by reactive oxygen species. The Journal of cell biology 194:7-15.
Forman HJ, Fukuto JM, Torres M (2004) Redox signaling: thiol chemistry defines which reactive oxygen and nitrogen species can act as second messengers. American journal of physiology Cell physiology 287:C246-256.
Forman HJ, Ursini F, Maiorino M (2014) An overview of mechanisms of redox signaling. Journal of molecular and cellular cardiology.
Franco R, Cidlowski JA (2009) Apoptosis and glutathione: beyond an antioxidant. Cell death and differentiation 16:1303-1314.
Franco R, Cidlowski JA (2012) Glutathione efflux and cell death. Antioxid Redox Signal 17:1694-1713.
Gallo V, Kingsbury A, Balazs R, Jorgensen OS (1987) The role of depolarization in the survival and differentiation of cerebellar granule cells in culture. The Journal of neuroscience : the official journal of the Society for Neuroscience 7:2203-2213.
Gaudilliere B, Konishi Y, de la Iglesia N, Yao G, Bonni A (2004) A CaMKII-NeuroD signaling pathway specifies dendritic morphogenesis. Neuron 41:229-241.
Gopalakrishna R, Gundimeda U, Schiffman JE, McNeill TH (2008) A direct redox regulation of protein kinase C isoenzymes mediates oxidant-induced neuritogenesis in PC12 cells. The Journal of biological chemistry 283:14430-14444.
Gough DR, Cotter TG (2011) Hydrogen peroxide: a Jekyll and Hyde signalling molecule. Cell death & disease 2:e213.

Grek CL, Zhang J, Manevich Y, Townsend DM, Tew KD (2013) Causes and consequences of cysteine S-glutathionylation. The Journal of biological chemistry 288:26497-26504.
Guemez-Gamboa A, Moran J (2009) NOX2 mediates apoptotic death induced by staurosporine but not by potassium deprivation in cerebellar granule neurons. Journal of neuroscience research 87:2531-2540.
Haberg A, Qu H, Saether O, Unsgard G, Haraldseth O, Sonnewald U (2001) Differences in neurotransmitter synthesis and intermediary metabolism between glutamatergic and GABAergic neurons during 4 hours of middle cerebral artery occlusion in the rat: the role of astrocytes in neuronal survival. Journal of cerebral blood flow and metabolism : official journal of the International Society of Cerebral Blood Flow and Metabolism 21:1451-1463.
Hall A (1998) Rho GTPases and the actin cytoskeleton. Science 279:509-514.
Halliwell B (2009) The wanderings of a free radical. Free radical biology & medicine 46:531-542.
Halliwell B, Gutteridge JMC (1999) Free radicals in biology and medicine, 3rd Edition. Oxford

New York: Clarendon Press ;

Oxford University Press.
Hatten ME (1999) Central nervous system neuronal migration. Annual review of neuroscience 22:511-539.
Henley J, Poo MM (2004) Guiding neuronal growth cones using Ca2+ signals. Trends in cell biology 14:320-330.
Hernandez-Enriquez B, Guemez-Gamboa A, Moran J (2011) Reactive oxygen species are related to ionic fluxes and volume decrease in apoptotic cerebellar granule neurons: role of NOX enzymes. Journal of neurochemistry 117:654-664.
Hoogland TM, Kuhn B (2010) Recent developments in the understanding of astrocyte function in the cerebellum in vivo. Cerebellum 9:264-271.
Ibi M, Katsuyama M, Fan C, Iwata K, Nishinaka T, Yokoyama T, Yabe-Nishimura C (2006) NOX1/NADPH oxidase negatively regulates nerve growth factor-induced neurite outgrowth. Free radical biology & medicine 40:1785-1795.
Jackson GR, Sampath D, Werrbach-Perez K, Perez-Polo JR (1994) Effects of nerve growth factor on catalase and glutathione peroxidase in a hydrogen peroxide-resistant pheochromocytoma subclone. Brain research 634:69-76.
Jacobson J, Duchen MR (2002) Mitochondrial oxidative stress and cell death in astrocytes--requirement for stored Ca2+ and sustained opening of the permeability transition pore. Journal of cell science 115:1175-1188.
Jaquet V, Scapozza L, Clark RA, Krause KH, Lambeth JD (2009) Small-Molecule NOX Inhibitors: ROS-Generating NADPH Oxidases as Therapeutic Targets. Antioxid Redox Sign 11:2535-2552.
Jessen KR (2004) Glial cells. The international journal of biochemistry & cell biology 36:1861-1867.
Jones DP (2006) Redefining oxidative stress. Antioxid Redox Signal 8:1865-1879.
Jonsson TJ, Lowther WT (2007) The peroxiredoxin repair proteins. Sub-cellular biochemistry 44:115-141.
Joseph SK, Nakao SK, Sukumvanich S (2006) Reactivity of free thiol groups in type-I inositol trisphosphate receptors. The Biochemical journal 393:575-582.
Kaludercic N, Deshwal S, Di Lisa F (2014) Reactive oxygen species and redox compartmentalization. Frontiers in physiology 5:285.
Kamata H, Hirata H (1999) Redox regulation of cellular signalling. Cellular signalling 11:1-14.
Kamata H, Oka S, Shibukawa Y, Kakuta J, Hirata H (2005) Redox regulation of nerve growth factor-induced neuronal differentiation of PC12 cells through modulation of the nerve growth factor receptor, TrkA. Archives of biochemistry and biophysics 434:16-25.
Kaplan DR, Miller FD (2000) Neurotrophin signal transduction in the nervous system. Current opinion in neurobiology 10:381-391.
Katoh S, Mitsui Y, Kitani K, Suzuki T (1999) Hyperoxia induces the neuronal differentiated phenotype of PC12 cells via a sustained activity of mitogen-activated protein kinase induced by Bcl-2. The Biochemical journal 338 (Pt 2):465-470.

Kennedy KA, Ostrakhovitch EA, Sandiford SD, Dayarathna T, Xie X, Waese EY, Chang WY, Feng Q, Skerjanc IS, Stanford WL, Li SS (2010) Mammalian numb-interacting protein 1/dual oxidase maturation factor 1 directs neuronal fate in stem cells. The Journal of biological chemistry 285:17974-17985.

Kim M, Song K, Jin EJ, Sonn J (2012) Staurosporine and cytochalasin D induce chondrogenesis by regulation of actin dynamics in different way. Experimental & molecular medicine 44:521-528.

Kishida KT, Hoeffer CA, Hu D, Pao M, Holland SM, Klann E (2006) Synaptic plasticity deficits and mild memory impairments in mouse models of chronic granulomatous disease. Molecular and cellular biology 26:5908-5920.

Komuro H, Yacubova E (2003) Recent advances in cerebellar granule cell migration. Cellular and molecular life sciences : CMLS 60:1084-1098.

Konishi Y, Stegmuller J, Matsuda T, Bonni S, Bonni A (2004) Cdh1-APC controls axonal growth and patterning in the mammalian brain. Science 303:1026-1030.

Kramer D, Fresu L, Ashby DS, Freeman TC, Genazzani AA (2003) Calcineurin controls the expression of numerous genes in cerebellar granule cells. Molecular and cellular neurosciences 23:325-330.

Krueger BK, Burne JF, Raff MC (1995) Evidence for large-scale astrocyte death in the developing cerebellum. The Journal of neuroscience : the official journal of the Society for Neuroscience 15:3366-3374.

Lambeth JD (2004) NOX enzymes and the biology of reactive oxygen. Nature reviews Immunology 4:181-189.

Le Belle JE, Orozco NM, Paucar AA, Saxe JP, Mottahedeh J, Pyle AD, Wu H, Kornblum HI (2011) Proliferative neural stem cells have high endogenous ROS levels that regulate self-renewal and neurogenesis in a PI3K/Akt-dependant manner. Cell Stem Cell 8:59-71.

Lee BC, Peterfi Z, Hoffmann FW, Moore RE, Kaya A, Avanesov A, Tarrago L, Zhou Y, Weerapana E, Fomenko DE, Hoffmann PR, Gladyshev VN (2013) MsrB1 and MICALs regulate actin assembly and macrophage function via reversible stereoselective methionine oxidation. Molecular cell 51:397-404.

Leslie NR (2006) The redox regulation of PI 3-kinase-dependent signaling. Antioxidants & redox signaling 8:1765-1774.

Limoli CL, Rola R, Giedzinski E, Mantha S, Huang TT, Fike JR (2004) Cell-density-dependent regulation of neural precursor cell function. Proceedings of the National Academy of Sciences of the United States of America 101:16052-16057.

Linseman DA, Bartley CM, Le SS, Laessig TA, Bouchard RJ, Meintzer MK, Li M, Heidenreich KA (2003) Inactivation of the myocyte enhancer factor-2 repressor histone deacetylase-5 by endogenous Ca(2+) //calmodulin-dependent kinase II promotes depolarization-mediated cerebellar granule neuron survival. The Journal of biological chemistry 278:41472-41481.

Lo Conte M, Carroll KS (2013) The redox biochemistry of protein sulfenylation and sulfinylation. The Journal of biological chemistry 288:26480-26488.

Lossi L, Gambino G (2008) Apoptosis of the cerebellar neurons. Histology and histopathology 23:367-380.

Lu Q, Wainwright MS, Harris VA, Aggarwal S, Hou YL, Rau T, Poulsen DJ, Black SM (2012) Increased NADPH oxidase-derived superoxide is involved in the neuronal cell death induced by hypoxia-ischemia in neonatal hippocampal slice cultures. Free Radical Bio Med 53:1139-1151.

Lubos E, Loscalzo J, Handy DE (2011) Glutathione peroxidase-1 in health and disease: from molecular mechanisms to therapeutic opportunities. Antioxid Redox Signal 15:1957-1997.

Majumdar D, Maunsbach AB, Shacka JJ, Williams JB, Berger UV, Schultz KP, Harkins LE, Boron WF, Roth KA, Bevensee MO (2008) Localization of electrogenic Na/bicarbonate cotransporter NBCe1 variants in rat brain. Neuroscience 155:818-832.

Mellor JR, Merlo D, Jones A, Wisden W, Randall AD (1998) Mouse cerebellar granule cell differentiation: electrical activity regulates the GABAA receptor alpha 6 subunit gene. The Journal of neuroscience : the official journal of the Society for Neuroscience 18:2822-2833.

Mennerick S, Zorumski CF (2000) Neural activity and survival in the developing nervous system. Molecular neurobiology 22:41-54.

Mi H, Haeberle H, Barres BA (2001) Induction of astrocyte differentiation by endothelial cells. The Journal of neuroscience : the official journal of the Society for Neuroscience 21:1538-1547.

Mishina NM, Tyurin-Kuzmin PA, Markvicheva KN, Vorotnikov AV, Tkachuk VA, Laketa V, Schultz C, Lukyanov S, Belousov VV (2011a) Does cellular hydrogen peroxide diffuse or act locally? Antioxid Redox Signal 14:1-7.
Mishina NM, Tyurin-Kuzmin PA, Markvicheva KN, Vorotnikov AV, Tkachuk VA, Laketa V, Schultz C, Lukyanov S, Belousov VV (2011b) Does Cellular Hydrogen Peroxide Diffuse or Act Locally? Antioxidants & redox signaling 14:1-7.
Moldovan L, Mythreye K, Goldschmidt-Clermont PJ, Satterwhite LL (2006) Reactive oxygen species in vascular endothelial cell motility. Roles of NAD(P)H oxidase and Rac1. Cardiovascular research 71:236-246.
Moran J, Patel AJ (1989a) Effect of potassium depolarization on phosphate-activated glutaminase activity in primary cultures of cerebellar granule neurons and astroglial cells during development. Brain research Developmental brain research 46:97-105.
Moran J, Patel AJ (1989b) Stimulation of the N-methyl-D-aspartate receptor promotes the biochemical differentiation of cerebellar granule neurons and not astrocytes. Brain research 486:15-25.
Morinaka A, Yamada M, Itofusa R, Funato Y, Yoshimura Y, Nakamura F, Yoshimura T, Kaibuchi K, Goshima Y, Hoshino M, Kamiguchi H, Miki H (2011) Thioredoxin mediates oxidation-dependent phosphorylation of CRMP2 and growth cone collapse. Sci Signal 4:ra26.
Munnamalai V, Suter DM (2009) Reactive oxygen species regulate F-actin dynamics in neuronal growth cones and neurite outgrowth. Journal of neurochemistry 108:644-661.
Munnamalai V, Weaver CJ, Weisheit CE, Venkatraman P, Agim ZS, Quinn MT, Suter DM (2014a) Bidirectional interactions between NOX2-type NADPH oxidase and the F-actin cytoskeleton in neuronal growth cones. Journal of neurochemistry.
Munnamalai V, Weaver CJ, Weisheit CE, Venkatraman P, Agim ZS, Quinn MT, Suter DM (2014b) Bidirectional interactions between NOX2-type NADPH oxidase and the F-actin cytoskeleton in neuronal growth cones. Journal of neurochemistry 130:526-540.
Nanda D, Tolputt J, Collard KJ (1996) Changes in brain glutathione levels during postnatal development in the rat. Brain research Developmental brain research 94:238-241.
Nitti M, Furfaro AL, Cevasco C, Traverso N, Marinari UM, Pronzato MA, Domenicotti C (2010) PKC delta and NADPH oxidase in retinoic acid-induced neuroblastoma cell differentiation. Cellular signalling 22:828-835.
Oberheim NA, Wang X, Goldman S, Nedergaard M (2006) Astrocytic complexity distinguishes the human brain. Trends in neurosciences 29:547-553.
Olguín-Albuerne M, Zaragoza-Campillo MA, J. M (2014) Role of Reactive Oxygen Species As Signaling Molecules in the Regulation of Physiological Processes of the Nervous System. In: Reactive Oxygen Species, Lipid Peroxidation and Protein Oxidation (Angel C, ed), p 284. New York: Nova Science
Parnham MJ, Kindt S (1984) A novel biologically active seleno-organic compound--III. Effects of PZ 51 (Ebselen) on glutathione peroxidase and secretory activities of mouse macrophages. Biochemical pharmacology 33:3247-3250.
Patapoutian A, Reichardt LF (2001) Trk receptors: mediators of neurotrophin action. Current opinion in neurobiology 11:272-280.
Pendyala S, Gorshkova IA, Usatyuk PV, He D, Pennathur A, Lambeth JD, Thannickal VJ, Natarajan V (2009) Role of Nox4 and Nox2 in hyperoxia-induced reactive oxygen species generation and migration of human lung endothelial cells. Antioxid Redox Signal 11:747-764.
Pourova J, Kottova M, Voprsalova M, Pour M (2010) Reactive oxygen and nitrogen species in normal physiological processes. Acta Physiol (Oxf) 198:15-35.
Powell SK, Rivas RJ, Rodriguez-Boulan E, Hatten ME (1997) Development of polarity in cerebellar granule neurons. Journal of neurobiology 32:223-236.
Rahman I, Kode A, Biswas SK (2006) Assay for quantitative determination of glutathione and glutathione disulfide levels using enzymatic recycling method. Nat Protoc 1:3159-3165.
Rakic P (1971) Neuron-glia relationship during granule cell migration in developing cerebellar cortex. A Golgi and electronmicroscopic study in Macacus Rhesus. The Journal of comparative neurology 141:283-312.
Rakic P, Sidman RL (1973) Sequence of developmental abnormalities leading to granule cell deficit in cerebellar cortex of weaver mutant mice. The Journal of comparative neurology 152:103-132.

Ramiro-Cortes Y, Moran J (2009) Role of oxidative stress and JNK pathway in apoptotic death induced by potassium deprivation and staurosporine in cerebellar granule neurons. Neurochemistry international 55:581-592.
Ramiro-Cortes Y, Guemez-Gamboa A, Moran J (2011) Reactive oxygen species participate in the p38-mediated apoptosis induced by potassium deprivation and staurosporine in cerebellar granule neurons. The international journal of biochemistry & cell biology 43:1373-1382.
Ramnani N (2006) The primate cortico-cerebellar system: anatomy and function. Nature reviews Neuroscience 7:511-522.
Ramos B, Gaudilliere B, Bonni A, Gill G (2007) Transcription factor Sp4 regulates dendritic patterning during cerebellar maturation. Proceedings of the National Academy of Sciences of the United States of America 104:9882-9887.
Rice ME, Russo-Menna I (1998) Differential compartmentalization of brain ascorbate and glutathione between neurons and glia. Neuroscience 82:1213-1223.
Rinna A, Torres M, Forman HJ (2006) Stimulation of the alveolar macrophage respiratory burst by ADP causes selective glutathionylation of protein tyrosine phosphatase 1B. Free radical biology & medicine 41:86-91.
Rothstein JD, Dykes-Hoberg M, Pardo CA, Bristol LA, Jin L, Kuncl RW, Kanai Y, Hediger MA, Wang Y, Schielke JP, Welty DF (1996) Knockout of glutamate transporters reveals a major role for astroglial transport in excitotoxicity and clearance of glutamate. Neuron 16:675-686.
Rouach N, Pebay A, Meme W, Cordier J, Ezan P, Etienne E, Giaume C, Tence M (2006) S1P inhibits gap junctions in astrocytes: involvement of G and Rho GTPase/ROCK. The European journal of neuroscience 23:1453-1464.
Ryter SW, Kim HP, Hoetzel A, Park JW, Nakahira K, Wang X, Choi AM (2007) Mechanisms of cell death in oxidative stress. Antioxid Redox Signal 9:49-89.
Sakai J, Li J, Subramanian KK, Mondal S, Bajrami B, Hattori H, Jia Y, Dickinson BC, Zhong J, Ye K, Chang CJ, Ho YS, Zhou J, Luo HR (2012) Reactive oxygen species-induced actin glutathionylation controls actin dynamics in neutrophils. Immunity 37:1037-1049.
Sampath D, Jackson GR, Werrbach-Perez K, Perez-Polo JR (1994) Effects of nerve growth factor on glutathione peroxidase and catalase in PC12 cells. Journal of neurochemistry 62:2476-2479.
Sato M, Suzuki K, Yamazaki H, Nakanishi S (2005) A pivotal role of calcineurin signaling in development and maturation of postnatal cerebellar granule cells. Proceedings of the National Academy of Sciences of the United States of America 102:5874-5879.
Savaskan NE, Borchert A, Brauer AU, Kuhn H (2007) Role for glutathione peroxidase-4 in brain development and neuronal apoptosis: specific induction of enzyme expression in reactive astrocytes following brain injury. Free radical biology & medicine 43:191-201.
Schafer FQ, Buettner GR (2001) Redox environment of the cell as viewed through the redox state of the glutathione disulfide/glutathione couple. Free Radical Bio Med 30:1191-1212.
Schmahmann JD (2010) The role of the cerebellum in cognition and emotion: personal reflections since 1982 on the dysmetria of thought hypothesis, and its historical evolution from theory to therapy. Neuropsychology review 20:236-260.
Schulz JB, Weller M, Klockgether T (1996) Potassium deprivation-induced apoptosis of cerebellar granule neurons: a sequential requirement for new mRNA and protein synthesis, ICE-like protease activity, and reactive oxygen species. The Journal of neuroscience : the official journal of the Society for Neuroscience 16:4696-4706.
Sedeek M, Callera G, Montezano A, Gutsol A, Heitz F, Szyndralewiez C, Page P, Kennedy CR, Burns KD, Touyz RM, Hebert RL (2010) Critical role of Nox4-based NADPH oxidase in glucose-induced oxidative stress in the kidney: implications in type 2 diabetic nephropathy. American journal of physiology Renal physiology 299:F1348-1358.
See V, Boutillier AL, Bito H, Loeffler JP (2001) Calcium/calmodulin-dependent protein kinase type IV (CaMKIV) inhibits apoptosis induced by potassium deprivation in cerebellar granule neurons. FASEB journal : official publication of the Federation of American Societies for Experimental Biology 15:134-144.
Shalizi A, Gaudilliere B, Yuan Z, Stegmuller J, Shirogane T, Ge Q, Tan Y, Schulman B, Harper JW, Bonni A (2006) A calcium-regulated MEF2 sumoylation switch controls postsynaptic differentiation. Science 311:1012-1017.

Sharma A, Verhaagen J, Harvey AR (2012) Receptor complexes for each of the Class 3 Semaphorins. Frontiers in cellular neuroscience 6:28.
Shi ZZ, Osei-Frimpong J, Kala G, Kala SV, Barrios RJ, Habib GM, Lukin DJ, Danney CM, Matzuk MM, Lieberman MW (2000) Glutathione synthesis is essential for mouse development but not for cell growth in culture. Proceedings of the National Academy of Sciences of the United States of America 97:5101-5106.
Solecki DJ, Govek EE, Tomoda T, Hatten ME (2006) Neuronal polarity in CNS development. Genes & development 20:2639-2647.
Sorce S, Krause KH (2009) NOX enzymes in the central nervous system: from signaling to disease. Antioxid Redox Signal 11:2481-2504.
Sorce S, Schiavone S, Tucci P, Colaianna M, Jaquet V, Cuomo V, Dubois-Dauphin M, Trabace L, Krause KH (2010) The NADPH oxidase NOX2 controls glutamate release: a novel mechanism involved in psychosis-like ketamine responses. The Journal of neuroscience : the official journal of the Society for Neuroscience 30:11317-11325.
Sotelo C (2004) Cellular and genetic regulation of the development of the cerebellar system. Progress in neurobiology 72:295-339.
Stegmuller J, Konishi Y, Huynh MA, Yuan Z, Dibacco S, Bonni A (2006) Cell-intrinsic regulation of axonal morphogenesis by the Cdh1-APC target SnoN. Neuron 50:389-400.
Stobart JL, Anderson CM (2013) Multifunctional role of astrocytes as gatekeepers of neuronal energy supply. Frontiers in cellular neuroscience 7:38.
Suzukawa K, Miura K, Mitsushita J, Resau J, Hirose K, Crystal R, Kamata T (2000) Nerve growth factor-induced neuronal differentiation requires generation of Rac1-regulated reactive oxygen species. The Journal of biological chemistry 275:13175-13178.
Suzuki K, Sato M, Morishima Y, Nakanishi S (2005) Neuronal depolarization controls brain-derived neurotrophic factor-induced upregulation of NR2C NMDA receptor via calcineurin signaling. The Journal of neuroscience : the official journal of the Society for Neuroscience 25:9535-9543.
Taglialatela G, Perez-Polo JR, Rassin DK (1998) Induction of apoptosis in the CNS during development by the combination of hyperoxia and inhibition of glutathione synthesis. Free radical biology & medicine 25:936-942.
Tahirovic S, Bradke F (2009) Neuronal polarity. Cold Spring Harbor perspectives in biology 1:a001644.
Tanaka M, Marunouchi T (1998) Immunohistochemical analysis of developmental stage of external granular layer neurons which undergo apoptosis in postnatal rat cerebellum. Neuroscience letters 242:85-88.
Terashima T, Inoue K, Inoue Y, Mikoshiba K, Tsukada Y (1985) Observations on Golgi epithelial cells and granule cells in the cerebellum of the reeler mutant mouse. Brain research 350:103-112.
Tietze F (1969) Enzymic method for quantitative determination of nanogram amounts of total and oxidized glutathione: applications to mammalian blood and other tissues. Anal Biochem 27:502-522.
Tonks NK (2005) Redox redux: revisiting PTPs and the control of cell signaling. Cell 121:667-670.
Tsatmali M, Walcott EC, Crossin KL (2005) Newborn neurons acquire high levels of reactive oxygen species and increased mitochondrial proteins upon differentiation from progenitors. Brain research 1040:137-150.
Tsatmali M, Walcott EC, Makarenkova H, Crossin KL (2006) Reactive oxygen species modulate the differentiation of neurons in clonal cortical cultures. Molecular and cellular neurosciences 33:345-357.
Ushio-Fukai M (2009a) Compartmentalization of redox signaling through NADPH oxidase-derived ROS. Antioxid Redox Signal 11:1289-1299.
Ushio-Fukai M (2009b) Compartmentalization of Redox Signaling Through NADPH Oxidase-Derived ROS. Antioxid Redox Sign 11:1289-1299.
Uttara B, Singh AV, Zamboni P, Mahajan RT (2009) Oxidative stress and neurodegenerative diseases: a review of upstream and downstream antioxidant therapeutic options. Curr Neuropharmacol 7:65-74.
Valencia A, Moran J (2004) Reactive oxygen species induce different cell death mechanisms in cultured neurons. Free Radical Bio Med 36:1112-1125.

Valencia A, Sapp E, Kimm JS, McClory H, Reeves PB, Alexander J, Ansong KA, Masso N, Frosch MP, Kegel KB, Li X, DiFiglia M (2013) Elevated NADPH oxidase activity contributes to oxidative stress and cell death in Huntington's disease. Hum Mol Genet 22:1112-1131.

Valko M, Leibfritz D, Moncol J, Cronin MT, Mazur M, Telser J (2007) Free radicals and antioxidants in normal physiological functions and human disease. The international journal of biochemistry & cell biology 39:44-84.

Wallraff A, Kohling R, Heinemann U, Theis M, Willecke K, Steinhauser C (2006) The impact of astrocytic gap junctional coupling on potassium buffering in the hippocampus. The Journal of neuroscience : the official journal of the Society for Neuroscience 26:5438-5447.

Wang CC, Fang KM, Yang CS, Tzeng SF (2009) Reactive oxygen species-induced cell death of rat primary astrocytes through mitochondria-mediated mechanism. Journal of cellular biochemistry 107:933-943.

Wang N, Xie K, Huo S, Zhao J, Zhang S, Miao J (2007) Suppressing phosphatidylcholine-specific phospholipase C and elevating ROS level, NADPH oxidase activity and Rb level induced neuronal differentiation in mesenchymal stem cells. Journal of cellular biochemistry 100:1548-1557.

Wayman GA, Kaech S, Grant WF, Davare M, Impey S, Tokumitsu H, Nozaki N, Banker G, Soderling TR (2004) Regulation of axonal extension and growth cone motility by calmodulin-dependent protein kinase I. The Journal of neuroscience : the official journal of the Society for Neuroscience 24:3786-3794.

Wilson JX (1997) Antioxidant defense of the brain: a role for astrocytes. Canadian journal of physiology and pharmacology 75:1149-1163.

Wood KA, Dipasquale B, Youle RJ (1993) In situ labeling of granule cells for apoptosis-associated DNA fragmentation reveals different mechanisms of cell loss in developing cerebellum. Neuron 11:621-632.

Xu H, Yang Y, Tang X, Zhao M, Liang F, Xu P, Hou B, Xing Y, Bao X, Fan X (2013) Bergmann glia function in granule cell migration during cerebellum development. Molecular neurobiology 47:833-844.

Yacubova E, Komuro H (2002) Intrinsic program for migration of cerebellar granule cells in vitro. The Journal of neuroscience : the official journal of the Society for Neuroscience 22:5966-5981.

Yamada K, Watanabe M (2002) Cytodifferentiation of Bergmann glia and its relationship with Purkinje cells. Anatomical science international 77:94-108.

Yant LJ, Ran Q, Rao L, Van Remmen H, Shibatani T, Belter JG, Motta L, Richardson A, Prolla TA (2003) The selenoprotein GPX4 is essential for mouse development and protects from radiation and oxidative damage insults. Free radical biology & medicine 34:496-502.

Yoneyama M, Kawada K, Gotoh Y, Shiba T, Ogita K (2010) Endogenous reactive oxygen species are essential for proliferation of neural stem/progenitor cells. Neurochemistry international 56:740-746.

Zhang XF, Forscher P (2009) Rac1 modulates stimulus-evoked Ca(2+) release in neuronal growth cones via parallel effects on microtubule/endoplasmic reticulum dynamics and reactive oxygen species production. Mol Biol Cell 20:3700-3712.

Zhou Y, Gunput RA, Pasterkamp RJ (2008) Semaphorin signaling: progress made and promises ahead. Trends in biochemical sciences 33:161-170.

Zhu D, Hu C, Sheng W, Tan KS, Haidekker MA, Sun AY, Sun GY, Lee JC (2009) NAD(P)H oxidase-mediated reactive oxygen species production alters astrocyte membrane molecular order via phospholipase A2. Biochem J 421:201-210.

Zmuda JF, Rivas RJ (1998) The Golgi apparatus and the centrosome are localized to the sites of newly emerging axons in cerebellar granule neurons in vitro. Cell motility and the cytoskeleton 41:18-38.

X. Publicaciones

Hindawi Publishing Corporation
Oxidative Medicine and Cellular Longevity
Volume 2014, Article ID 678371, 13 pages
http://dx.doi.org/10.1155/2014/678371

Research Article

Effect of Staurosporine in the Morphology and Viability of Cerebellar Astrocytes: Role of Reactive Oxygen Species and NADPH Oxidase

Mauricio Olguín-Albuerne, Guadalupe Domínguez, and Julio Morán

División de Neurociencias, Instituto de Fisiología Celular, Universidad Nacional Autónoma de México, Apartado Postal 70-253, 04510 México, DF, Mexico

Correspondence should be addressed to Julio Morán; jmoran@ifc.unam.mx

Received 20 March 2014; Revised 20 June 2014; Accepted 23 June 2014; Published 17 August 2014

Academic Editor: Felipe Dal-Pizzol

Cell death implies morphological changes that may contribute to the progression of this process. In astrocytes, the mechanisms involving the cytoskeletal changes during cell death are not well explored. Although NADPH oxidase (NOX) has been described as being a critical factor in the production of ROS, not much information is available about the participation of NOX-derived ROS in the cell death of astrocytes and their role in the alterations of the cytoskeleton during the death of astrocytes. In this study, we have evaluated the participation of ROS in the death of cultured cerebellar astrocytes using staurosporine (St) as death inductor. We found that astrocytes express NOX1, NOX2, and NOX4. Also, St induced an early ROS production and NOX activation that participate in the death of astrocytes. These findings suggest that ROS produced by St is generated through NOX1 and NOX4. Finally, we showed that the reorganization of tubulin and actin induced by St is ROS independent and that St did not change the level of expression of these cytoskeletal proteins. We conclude that ROS produced by a NOX is required for cell death in astrocytes, but not for the morphological alterations induced by St.

1. Introduction

Apoptotic cell death plays a key role in the shaping of the nervous system during development and in the etiology and progression of certain neurodegenerative disorders [1, 2]. Apoptosis is a highly regulated process that involves several morphological alterations, including cell shrinkage and chromatin condensation. These morphological changes are accompanied by a number of biochemical changes [3], including the activation of a group of proteases known as caspases [4] that act on many substrates, including cytoskeletal molecules [5–9].

Previous studies have shown the mechanisms involved in the morphological changes occurring during the apoptotic death of neurons and how these changes contribute to the overall progression of apoptosis in neurons [2, 4, 10]. In cerebellar and hippocampal neurons, apoptotic cell death has been associated with cytoskeletal disruption [9, 11–17]. In some studies, cytoskeletal disruptors such as nocodazole promote apoptosis of neuronal cells, suggesting that cytoskeletal alteration could be a signal during the initial phases of apoptosis [13–17]. We have previously shown in cerebellar neurons that cytoskeletal proteins undergo a differential reorganization depending on the apoptotic condition [8]; also, cytoskeletal breakdown has been shown to be involved in neuronal apoptosis [9]. Although the morphological changes related to apoptosis are documented in neurons, the precise mechanisms involving the cytoskeletal changes during the progression of apoptosis are not well explored in astrocytes. In these cells, the actin cytoskeleton is known to play a role in the regulation of a variety of cellular actions such as cell attachment, motility, and morphological changes [18].

It is known that staurosporine (St) induces apoptosis in several cell types, including cerebellar astrocytes [19], a condition that involves changes in cell morphology from a flat to a stellate shape. Staurosporine is a competitive

inhibitor of protein kinases that binds to kinases with high affinity and little selectivity [20]. This alkaloid has been demonstrated to inhibit cell cycle in different cell lines [21]. It also induces cell differentiation [22] and morphological changes in apoptotic cardiomyocytes [23] and hippocampal neurons [24]. Staurosporine has been considered a valuable tool for the study of apoptosis [25]. Its mechanisms of action include the activation of caspases through JNK1 and AP-1 activation in cell lines [26] or the p38 pathway activation in cerebellar granule neurons [27].

On the other hand, a large body of evidence has shown that during the process of neuronal death a generation of reactive oxygen species (ROS) [28–31] occurs. Moreover, it has been demonstrated that antioxidants prevent cell death, suggesting a key role of ROS in the death process. In cultured neurons, ROS have been shown to act as early signaling molecules in the death of cerebellar neurons induced by St or potassium deprivation [28, 29]. During spinal cord development, the physiological elimination of motoneurons is also regulated by ROS [30]. In addition, the redox regulation of several members of the MAPK pathway has been shown to be critical in the cell death mechanisms [27, 31, 32].

Although ROS can be generated by several sources, it has been suggested that NADPH oxidase (NOX) could be critical in the production of ROS involved in cell death. It is known that NOX has several homologues termed NOX 1 to 5 and DUOX 1 and 2, which are widely distributed in vertebrate tissues, including the nervous system [29, 33–38]. NOX2 was originally described in phagocytic cells, where it is responsible for the respiratory burst [39]. Many studies have shown that the inhibition of NOX activity remarkably protects neurons from cell death; however, in contrast to neurons, studies about the participation of ROS and NOX in the cell death of astrocytes are limited. In a previous study, NOX was shown to be the source for ROS involved in cell death and astrocyte survival [40]. Astrocytes exposed to acute H_2O_2 increased ROS levels, decreased glutamate uptake, and underwent oxidative damage and cell death [41]. The role of the oxidation of cytoskeletal proteins during the death of astrocytes is still not well understood.

Cytoskeleton alteration plays a key role in the regulation of diverse physiological processes. This alteration implies changes in the expression and/or reorganization of proteins such as actin, tubulin, and the proteins associated with the cytoskeletal proteins. On the other hand, ROS, particularly those produced by a NOX, have been implicated in the regulation of cytoskeletal remodeling [42]. For example, the oxidation of the actin binding protein cofilin stimulates apoptosis [43] and impairs cytoskeletal function in T cells [44]. Also, a redox imbalance modifies the actin cytoskeleton of cortical astrocytes [45] and H_2O_2 alters astrocyte cytoskeleton through the activation of the p38 MAPK pathway [46].

In the present study, we assessed the participation of ROS in the death of cultured rat cerebellar astrocytes using St as death inducer. Specifically, we examined the ROS generation and NOX activity induced by St and the involvement of ROS generated by NOX in the astrocytic death induced by St. We also studied the possible participation of ROS and a NOX in the alteration of the morphology and cytoskeletal proteins of astrocytes treated with St.

2. Materials and Methods

2.1. Chemicals and Materials. Fetal calf serum, penicillin/streptomycin, and Trizol reagent were from GIBCO (Grand Island, NY, USA). Poly-L-lysine (mol. wt. > 300,000), trypsin, DNAse, MTT (3-(4,5-dimethylthiazol-2-yl)-2,5-diphenyltetrazolium bromide), propidium iodide (PI), cytochrome c, staurosporine, and 4-(2-aminoethyl)-benzenesulfonyl fluoride (AEBSF) were from Sigma (St. Louis, MO, USA). Dihydroethidium and calcein-AM were purchased from Molecular Probes, Invitrogen (Carlsbad, CA, USA). Mouse anti-actin monoclonal antibodies were from Chemicon Int., anti-β-tubulin monoclonal antibodies were from Sigma-Aldrich, and FITC-goat anti-mouse IgG conjugated were from Zymed Laboratories Inc. All other chemicals were of the purest grade available from regular commercial sources. The colonies of NOX2 (gp91phox) knockout mice and NOX3 knockout mice on a C57BL6 background were purchased from the Jackson Laboratory (Bar Harbor, ME, USA) and were bred in the animal house of our institute.

2.2. Cell Cultures. All animals used for this experimentation were treated in accordance with the accepted standards of animal care and the procedures were approved by the Local Committee of Research and Ethics of the Instituto de Fisiología Celular, Universidad Nacional Autónoma de México. The protocol used followed the Guidelines for the Care and Use of Mammals in Neuroscience and the guidelines released by the Mexican Institutes of Health Research and the National Institutes of Health guide for the care and use of laboratory animals. All efforts were made to minimize animal suffering and to reduce the number of animals used.

Astrocytes were obtained from 8-day-old Wistar rats and 7-day-old $NOX2^{-/-}$, $NOX3^{-/-}$, or wild type mice as previously described by Moran and Patel [47]. Briefly, the dissociated cells suspensions from rat or mouse cerebella were plated at a density of 1×10^6 cells/cm^2. The culture medium consisted of basal Eagle's medium supplemented with 10% heat-inactivated fetal calf serum, 8 mM glucose, 2 mM glutamine, 50 U/mL penicillin, and 50 μg/mL streptomycin. The culture dishes were incubated at 37°C in a humidified 5% CO_2/95% air atmosphere. After 2 weeks in culture, cells were pretreated with antioxidants or NADPH oxidase inhibitors for 1 h and then treated with St (500 nM) for the indicated times and cells were used for different purposes. For immunofluorescence assays, cells were cultured on cover slips as indicated above. Morphology of astrocytes was evaluated by observations under a phase contrast microscope coupled to a digital camera.

2.3. Cell Viability. Cell viability was estimated by using calcein AM and propidium iodide (PI) to identify living and dead cells, respectively. Calcein enters viable cells and emits green fluorescence and when it is cleaved by esterases it can no longer permeate cell membranes. PI is not permeable

to cell membranes and only dying cells are stained. After treatment, cells were incubated with calcein (1 μM) for 15 min and with PI (40 μM) for 5 min at 37°C and cells were observed in an epifluorescence microscope, using an excitation wavelength of 485–520 nm for calcein and 450–510 nm wavelengths for PI and the number of labeled cells with calcein and PI were counted.

Cell viability was also estimated at 6, 12, and 24 h after treatment by the conversion of 3-(4,5-dimethylthiazol-2-yl)-diphenyltetrazolium bromide (MTT) to formazan blue. MTT (0.25 mg/mL) was added to astrocyte cultures and incubated for 10 min at 37°C in 5% CO_2-95% air atmosphere. After removal of the medium, 100% DMSO was added to the dishes and formazan blue formed was quantified spectroscopically at 570 nm excitation wavelength. A correspondence between the ability of cells to form formazan blue and the number of cells and DNA content [48] has been shown.

2.4. RT-PCR. Total RNA was isolated from cultured astrocytes with the single-step method based on guanidine isothiocyanate/phenol/chloroform extraction using Trizol reagent (Gibco-BRL). RNA concentration was determined by absorbance at 260 nm and its integrity was verified by electrophoresis on 1.1% denaturing agarose gels in the presence of 2.2 M formaldehyde. Total RNA was reverse transcribed to synthesize single strand cDNA. Four microliters of RT reaction was subjected to PCR in order to amplify NOX1, NOX2, and NOX4. The sequences of the primers for NOX1 were 5′-[CCT TCT GGG AAA CCT GCC TTT AG]-3′ in the sense primer and 5′-[TGT TGG TCA CAC TGG ATG ATA AGC]-3′ in the antisense; to NOX2 they were 5′-[TGG AGT GGT GTG TGA ATG CCA GAG]-3′ in the sense primer and 5′-[CGG ACA GCG ACT GCT GA]-3′ in the antisense; and to NOX4 they were 5′-[AGC CAA GAT TCT GAG ATT CTG CC]-3′ in the sense primer and 5′-[CCG AGG ACG CCC AAT AAA AAG]-3′ in the antisense. Forty-five microliters of PCR products was separated in 1.5% agarose gel and was stained with ethidium bromide. The image was captured under a UV transilluminator with a Type 665 negative film (Polaroid Co). The intensity of bands was quantified by densitometry using the Image J Program (NIH Image version 1.38x).

2.5. ROS Levels. ROS levels were measured with dihydroethidine (DHE). Cells were plated on coverslips and after treatments cells were incubated for 30 min with 1 μM DHE in culture medium at 37°C. After incubation, cells were washed three times with PBS, fixed with 3% formaldehyde at 4°C for 15 minutes, washed with PBS, and mounted with PBS-glycerol 1 : 1 v/v. Preparations were observed under an epifluorescence microscope (Nikon Diaphot TMD, Nikon Corp., Japan) using a rhodamine filter (excitation filter wavelength/dichromatic mirror cut-on wavelength/barrier filter wavelengths of 510–560/565/590 nm). Results are expressed as mean fluorescence intensity.

2.6. NADPH Oxidase (NOX) Activity. NOX activity was evaluated as superoxide produced by NOX, which was measured in a quantitative kinetic assay based on the SOD-inhibitable reduction of cytochrome c [29]. Cultured cells were homogenized in a saline buffer (150 mM K, Na-phosphate, pH 7.4 supplemented with 1 mM $MgCl_2$, 1 mM EGTA, and 2 mM NaN_3). Cell homogenates were incubated with a reaction mixture containing 65 mM K, Na-phosphate, pH 6.8, 1 mM $MgCl_2$, 1 mM EGTA, 2 mM NaN_3, 0.1 mM cytochrome c, 10 mM FAD, and 0.1 mM SDS. The reaction started with the addition of 0.2 mM NADPH to the reaction mixture. The reference cuvette additionally contained 300 U/mL SOD. Reduction of cytochrome c was measured at 550 nm. Results are expressed as the difference between reduced and oxidized cytochrome c per hour per milligram of protein.

2.7. Immunofluorescence. Astrocytes were grown on poly-L-lysine-coated glass slides and treated with St (0.5 μM) for different periods of time to induce cell death. Cells were immediately fixed with 4% paraformaldehyde for 20 min. After blocking with PBS (containing 1% BSA), the samples were incubated with mouse anti-actin (1 : 100 dilution), anti-β-tubulin (1 : 200 dilution), or anti-α-tubulin (1 : 200 dilution, Sigma-Aldrich, cat.T6199) monoclonal antibodies. Primary antibodies were incubated for 1 h at room temperature, followed by 1 h incubation with FITC-goat anti-mouse IgG conjugated (1 : 250 dilution) at room temperature. Coverslips were mounted using Vectashield mounting media with DAPI (Vector Labs). Stained cells were visualized under an epifluorescence microscope using a 40x objective (Nikon Diaphot-TMD) and their digitalized fluorescence images were captured.

2.8. Statistical Analysis. Data are presented as mean ± SEM and statistical significance of the results was determined by one-way analysis of variance (ANOVA) followed by Bonferroni's test. The statistical significance in the comparisons between wild type and NOX2 KO/NOX3 KO mice was determined by Student's t-test. P values less than 0.05 were considered statistically significant. Statistical significance of data from Figure 2(a) was determined by a nonparametric analysis followed by Dunnett's post hoc test.

3. Results

3.1. Staurosporine Induces Death of Astrocytes. Figure 1 shows that St induces a reduction in cell viability of astrocytes, measured as the MTT transformation, in a time- and concentration-dependent manner. Treatment with St during 24 h induced a 22% reduction of cell viability at a concentration of 0.1 μM and by 55% at 0.5 μM (Figure 1(a)). When astrocytes were subjected to 0.5 μM St treatment, cell viability was decreased by 40% and 55% at 12 and 24 h, respectively (Figure 1(b)). These results were supported by the morphological appearance of astrocytes observed by phase contrast microscopy (Figures 2(b) and 6).

3.2. St Induced Cell Death Is Dependent on ROS Production. It was previously reported [27–32] that some apoptotic conditions induce the generation of ROS in neuronal cells.

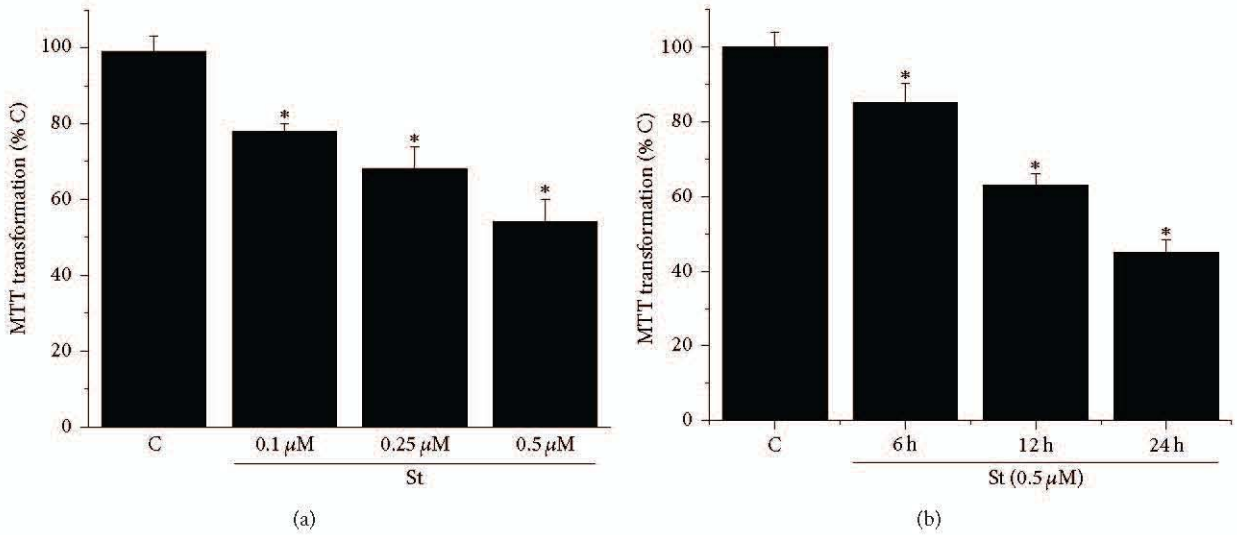

FIGURE 1: Staurosporine reduces cerebellar astrocytes viability. (a) Cerebellar astrocytes were treated with staurosporine 0.1 μM, 0.25 μM, and 0.5 μM for 24 h and the cell viability was measured by MTT transformation as detailed in Section 2. (b) Cerebellar astrocytes were treated with staurosporine 0.5 μM for 6, 12, and 24 h and the cell viability was measured by MTT transformation as detailed in Section 2. Data are presented as mean ± SEM of four independent experiments. * is significantly different from control ($P < 0.05$).

Therefore, we evaluated the ROS production in astrocytes treated with St (0.5 μM). Figure 2(a) shows that St induced ROS generation, which were measured as dihydroethidium- (DHE-) derived fluorescence (fluorescence intensity). ROS levels increased after 1 h of treatment with St, reaching a maximal level at 2 h. At this time, ROS decreased and from 6 h to 18 h ROS levels remained relatively high without change.

In order to evaluate the roles of ROS and NOX in the death of astrocytes induced by St, we tested the effects of the antioxidant MnTMPyP and the nonspecific inhibitor of NOX (Figures 2(b) and 2(c)). Under these conditions, both, the antioxidant and the NOX inhibitor AEBSF, significantly reduced cell death by 45%. Similarly, the presence of the NOX inhibitor markedly inhibited cell death by 65% (Figure 2(c)). These results were confirmed by the morphological changes of the astrocytes observed in the phase contrast microscopy (Figure 2(b)).

3.3. Astrocytes Express NOX Subunits and St Induces NOX Activity. The expression of NOX was evaluated by RT-PCR analysis in astrocytes by using specific oligonucleotides for NOX1, NOX2, and NOX4. Figure 3 shows that astrocytes cultured for 2 weeks expressed mRNA of all three NOX homologues tested. We also measured the NOX activity induced by St in astrocytes after 2 h of treatment, when the maximal production of ROS was observed. Under these conditions, NOX activity was increased by 50% (Figure 4(a)). In addition, the observed increase of ROS production induced by St was partially inhibited by the NOX inhibitor AEBSF (Figure 4(b)).

3.4. Cell Death Induced by St Is Not Reduced in NOX2- and NOX3-Deficient Astrocytes. In order to evaluate the role of specific NOX homologues in the death induced by St in cerebellar astrocytes, we tested the effect of St in cultured astrocytes obtained from NOX2 KO and NOX3 KO mice as described in Section 2. Figure 5 shows that St induced more than 50% cell death after 24 h of St treatment in wild type astrocytes. Similar results were found when cell viability was measured in NOX2 KO and NOX3 KO astrocytes treated with St.

3.5. Rearrangement of the Cytoskeleton during the Cell Death Induced by St. Astrocytes showed morphological changes during cell death induced by St. After 12 h of St treatment cells showed somatic shrinkage and the formation of neurite-like processes with an apparent reticular aspect (Figure 6) that eventually fragmented and practically disappeared after 24 h (not shown). In order to explore the relationship between cytoskeleton and the morphological changes induced by St described above, we studied the immunofluorescent patterns of actin and tubulin organization after St treatment. Figure 6 shows that, under control conditions, actin, α-tubulin, and β-tubulin (Figure 8) were homogeneously distributed in the soma and organized in fibers running longitudinally. After 12 h of St treatment, these proteins markedly compacted following the morphological changes described above. Particularly, α-tubulin was equally distributed in both soma and processes, but actin showed a tendency to be located in the processes (Figure 6).

In order to evaluate the role of ROS in the morphology and cytoskeleton rearrangement, we first studied the action of a prooxidant condition in the astrocytic morphology. Figure 7 shows that the presence of 200 μM H_2O_2 induced morphological changes after 45 min of treatment. The observed changes in the cell morphology were similar to those observed in astrocytes treated with St, that is, cell body shrinkage and formation of thin processes. The observed

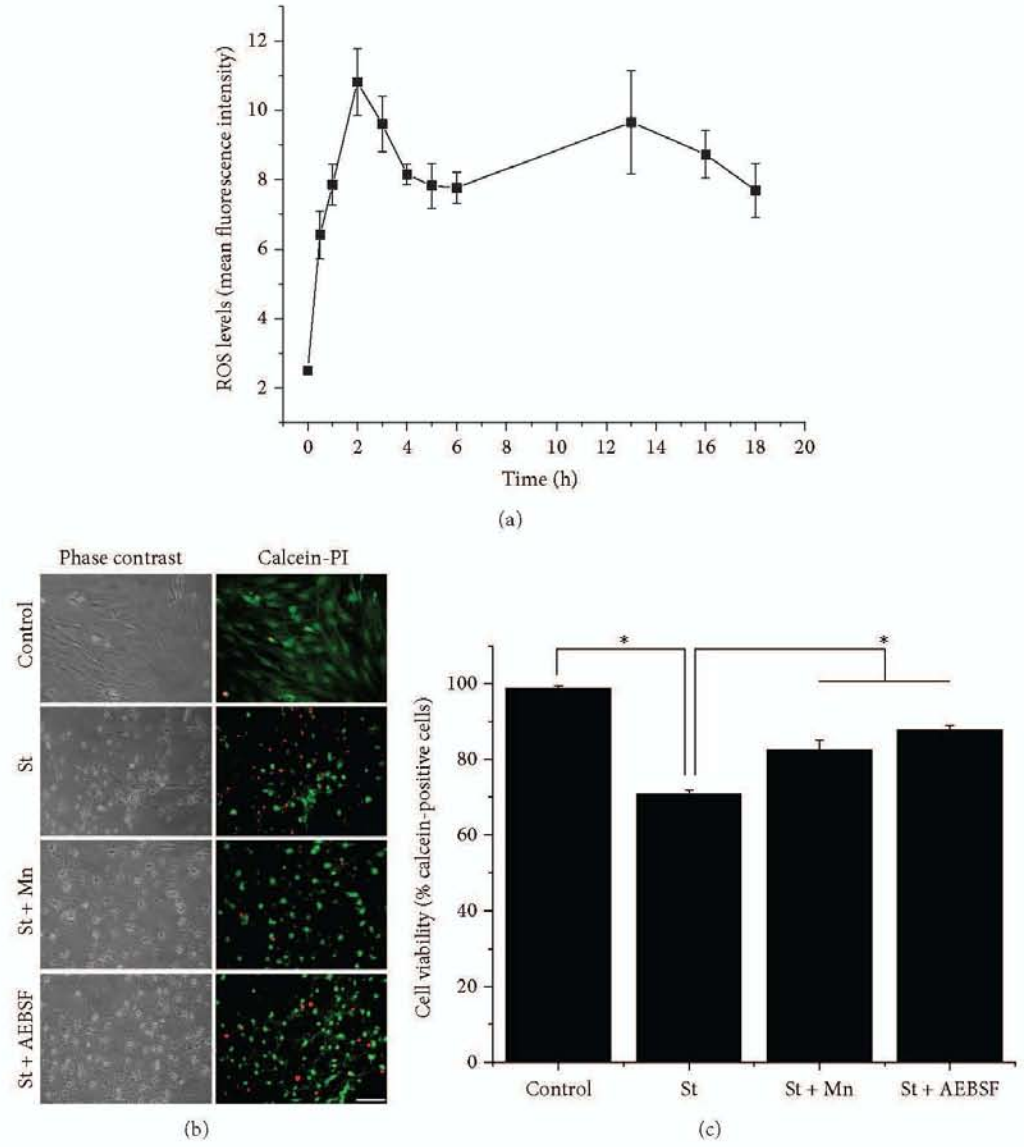

FIGURE 2: Reactive oxygen species are involved in cerebellar astrocytes death induced by St. (a) The levels of ROS were measured during different times by the oxidation of dihydroethidium (1 μM) as detailed in Section 2. Data are presented as mean ± SEM of four independent experiments. All points are significantly different from control (0 h) ($P < 0.001$). (b) Representative micrographs of cerebellar astrocytes treated with St (0.5 μM) for 24 in the presence or absence of MnTMPyP (50 μM) or AEBSF (50 μM). Cells were marked with calcein (green) and propidium iodide (red). Scale bar represents 50 μm. (c) Cell viability was determined by the percentage of calcein-positive cells from the total number of cells (calcein-positive cells plus propidium iodide-positive cells). Data are presented as mean ± SEM of three independent experiments.

changes in astrocytes were evident after 15 min of treatment (Figure 7). Although the prooxidant condition also induced a cell shrinkage, the formation of process-like extensions was less evident and they did not form the reticular structure observed with St. More importantly, astrocytes treated simultaneously with the antioxidants EUK and H_2O_2 did not show any morphological change. In contrast, the treatment with the antioxidants EUK did not affect the changes induced by St (Figure 7).

In order to further examine the participation of ROS in the cytoskeletal organization, under the apoptotic conditions previously described, we evaluated the effect of antioxidants and NOX inhibitors on the organization of actin and tubulin in astrocytes. Under these conditions, we found that neither the antioxidants MnTPMyP and EUK nor the NOX inhibitors DPI and AEBSF induced any significant change in the rearrangement of α-tubulin or actin induced by St (Figure 8).

3.6. Expression of Tubulin and Actin during Apoptotic Death of Astrocytes Induced by St. We evaluated by Western blot analysis the effect of St on the levels of actin and α-tubulin in astrocytes. We found that this condition did not change neither α-tubulin nor actin expression levels (Figure 9(a)).

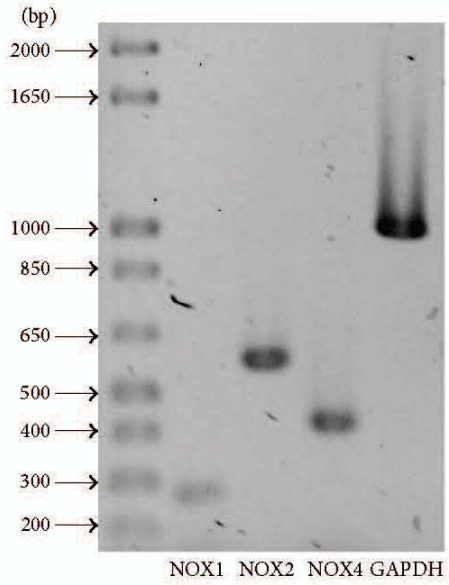

FIGURE 3: NOX subunits are expressed in cerebellar astrocytes. NOX subunits expression was determined by RT-PCR assays in cultured astrocytes as detailed in Section 2 for NOX1 (268 bp), NOX2 (558 bp), and NOX4 (408 bp). Three independent assays were performed.

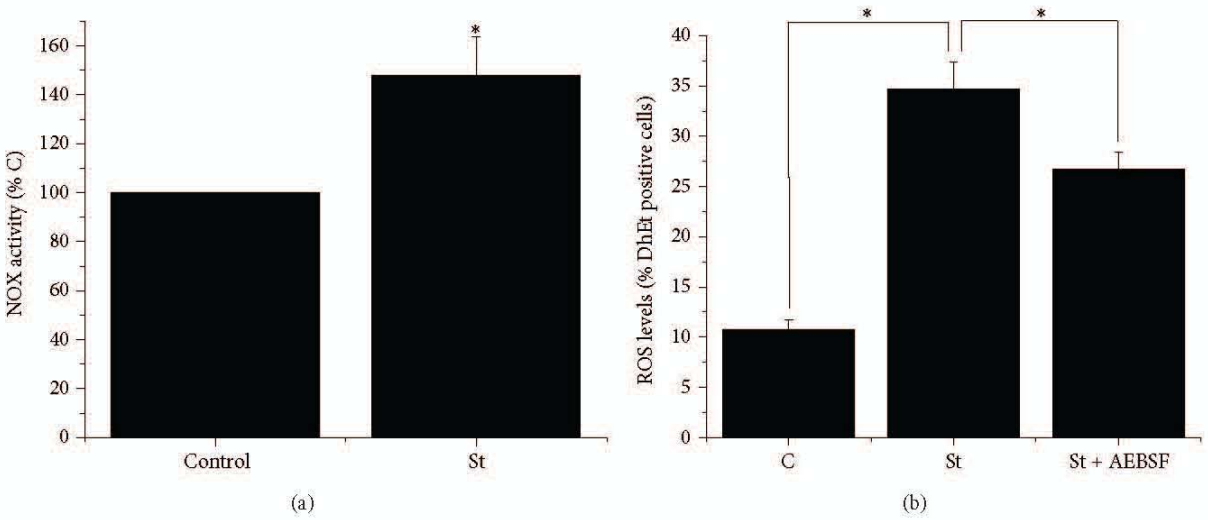

FIGURE 4: Staurosporine induces NOX activity. (a) NOX activity was evaluated at 2 h as detailed in Section 2. Data are presented as mean ± SEM of five independent experiments. * is significantly different from control ($P < 0.05$). (b) ROS levels were determined in cerebellar astrocytes treated with St (0.5 μM) for 2 h in the presence or absence of AEBSF (50 μM) by measuring the oxidation of dihydroethidium (1 μM) as detailed in Section 2. Data are presented as mean ± SEM of three independent experiments.

On the other hand, we also found that any antioxidant or NOX inhibitor tested induced changes in the protein levels of these two cytoskeletal proteins (Figure 9(a)). Densitometric analysis shows that neither St nor the antioxidants, EUK, MnTPMyP, and Ebselen, nor the NOX inhibitors, AEBSF, apocynin, and DPI, had any effect in the observed expression of α-tubulin (Figure 9(b)) and actin (Figure 9(c)).

4. Discussion

A large body of evidence has shown that ROS regulate cell death under pathological and physiological conditions. In cerebellar neurons, apoptotic death involves ROS generation [27–29, 31] that plays a central role in the initiation and execution of neuronal apoptosis [28, 49–51], probably acting as an early signal. On the other hand, we also demonstrated an active role of NOX in the apoptotic death of cerebellar neurons [29]. Although ROS has been proposed to play a central role in neurons, there is a lack of information about the action of ROS in the apoptotic death of astrocytes. We, therefore, evaluated the role of ROS and the possible participation of NOX as a source of ROS in the death of cerebellar astrocytes and their involvement in the morphological and cytoskeletal changes associated with this process.

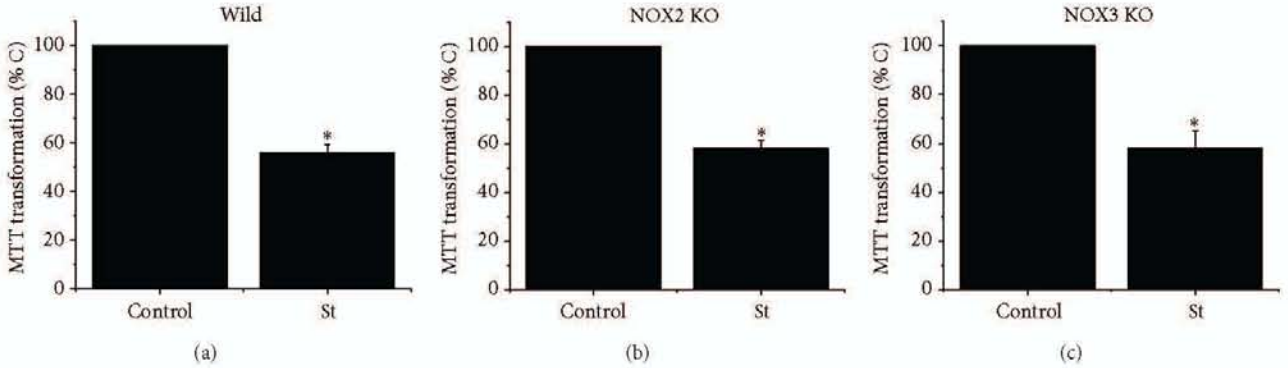

FIGURE 5: Cell death induced by St is not mediated by NOX2 and NOX3. Cerebellar astrocytes were obtained from wild type mice and NOX2 KO and NOX3 KO mice. Cells were treated with St (0.5 μM) for 24 h and the cell viability was estimated as MTT transformation as detailed in Section 2. Data are presented as mean ± SEM of five independent experiments. * is significantly different from control ($P < 0.05$).

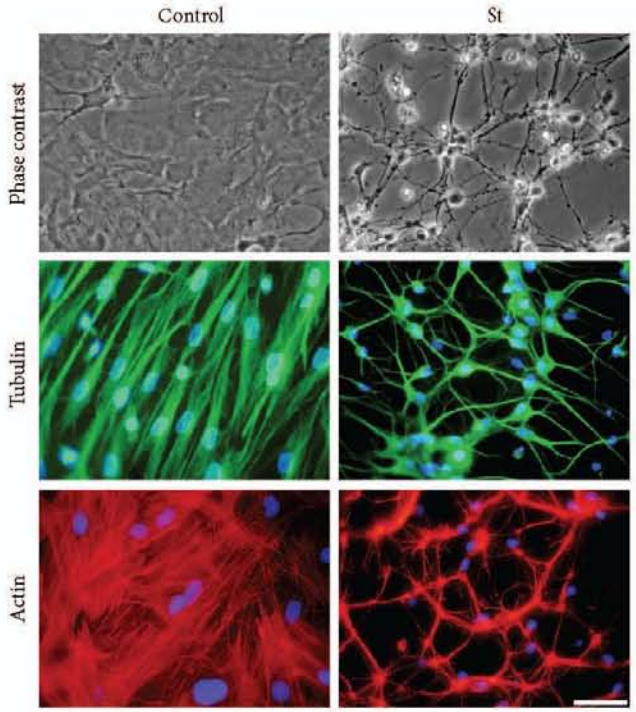

FIGURE 6: Morphological changes of astrocytes induced by St are evidenced by the rearrangement of cytoskeletal proteins. Astrocytes were treated with St (0.5 μM) for 12 hours and then were labelled with rhodamine-phalloidin or immunostained for tubulin as detailed in Section 2. Representative images of phase contrast, rhodamine-phalloidin, and tubulin are shown in control and St treated astrocytes. Scale bar represents 50 μm.

Cultured astrocytes have been shown to be an appropriate model for the study of cell death [52]. Also, St has been considered a useful tool to induce apoptosis [25]. In particular, there are several reports showing that St induces apoptotic death of astroglial cells in culture [53–57]. In the present study, we found in cerebellar astrocytes that St induced cell death in a time- and concentration-dependent manner. We also found that St treatment induced a differential ROS generation. After 1 h of treatment, it was observed that there was a significant increase of ROS and the highest ROS levels were detected after 2 h of treatment. This result coincides with previous observations in other preparations showing a transient ROS production before the activation of the cell death [28, 50, 51, 58], which suggests that ROS could be involved in the process of cell death in astrocytes. The possibility that ROS could be required for the initiation and/or progression of cell death in these cells was further supported by the fact that the antioxidant MnTMPyP was able to rescue astrocytes from cell death induced by St. Interestingly, a nonspecific NOX inhibitor, AEBSF, was also able to significantly reduce cell death induced by St. These results suggest that astroglial cell death induced by St could be mediated, at least partially, by ROS produced by a NOX.

It is well accepted that NOX participates in several physiological and pathological processes in a wide variety of cell types. The only described function of NOX is to generate $O_2^{\bullet -}$ that can be converted to other ROS. It has been proposed that ROS generated by this complex could mediate cell death [27, 29, 31, 33, 34]. Several studies have shown extensive expression of the NOX homologues in several tissues [29, 33–35, 39]. However, not much information is available about the expression of NOX homologues in astrocytes. It was originally suggested, by indirect evidence, that NOX was present in cortical astrocytes [59]. More recently, the presence of NOX1, NOX2, NOX4, and Duox 1 in astrocytes from cerebral cortex [60] was shown. It is also known that NOX5 is not present in murines [33, 34, 61]. In this study, we show for the first time that NOX1, 2, and 4 are present in primary cultures of cerebellar astrocytes.

There are some reports suggesting that conditions that induce death of astrocytes involve the participation of NOX [62, 63]. In this study, the participation of a NOX in the cell death process induced by St was supported by the observation that this condition increases NOX activity after 2 h of St treatment. At this time, the transient ROS production induced by St was maximal. Moreover, ROS levels induced by St were significantly reduced in the presence of the NOX inhibitor

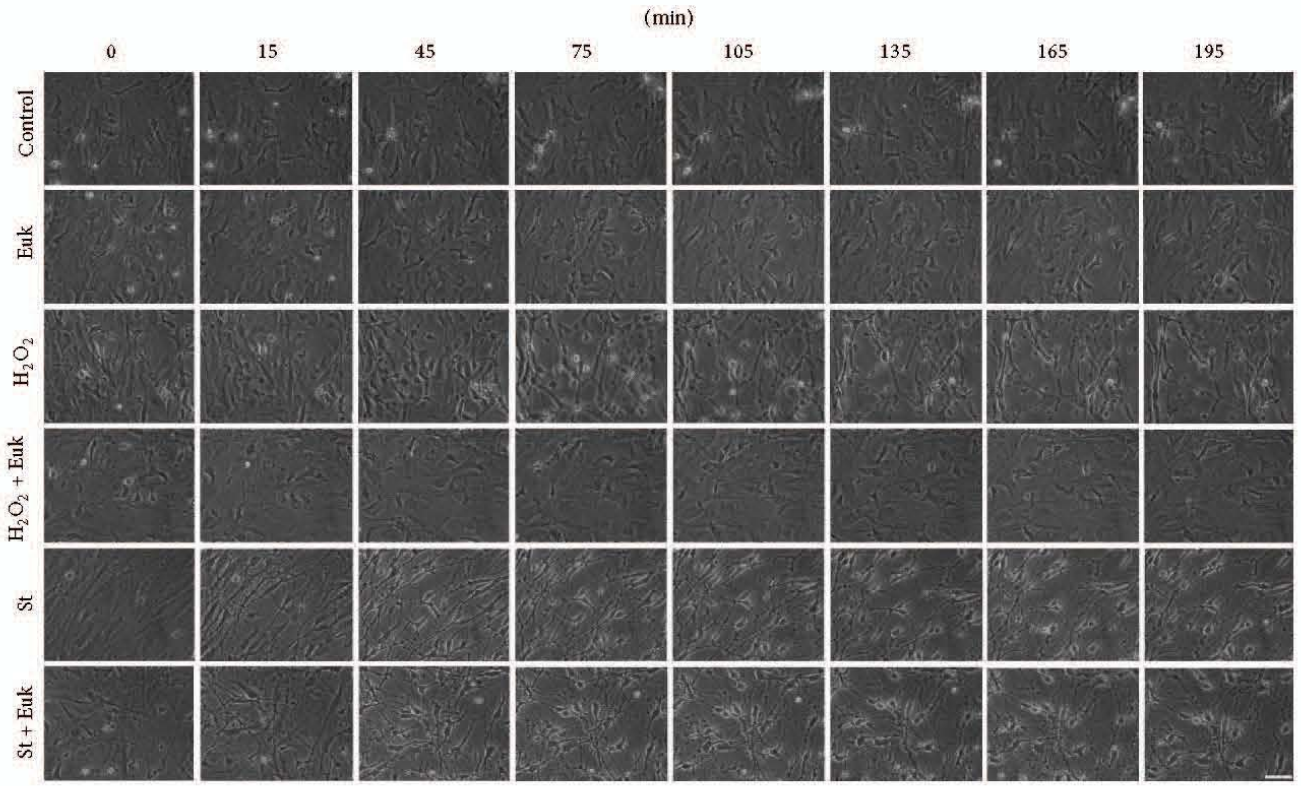

FIGURE 7: Effect of St and hydrogen peroxide on the morphology of cerebellar astrocytes. Time-lapse images of astrocytes pretreated for 2 h with Euk-134 (20 μM) in the presence or absence of hydrogen peroxide (200 μM) and St (0.5 μM) were taken from the same field. Scale bar represents 50 μM.

AEBSF. Finally, we found in mice deficient in NOX2 or NOX3 that the cell viability of astrocytes treated with St was not significantly different from astrocytes from wild type mice. This suggests that NOX other than these two homologues could be responsible for the generation of the ROS implicated in the death of astrocytes. In a previous study, we found that ROS produced by NOX2 were responsible for the death of cerebellar neurons induced by St, but not by potassium deprivation. In this regard, a possible source for ROS involved in astrocytic death by St could be NOX1 or NOX4, which was expressed in cerebellar astrocytes. An alternative explanation for the lack of effect of NOX2 or NOX3 deficiency in death induced by St is a possible compensation phenomenon that has been reported for these complexes in other preparations [64].

Apoptotic cell death is characterized by a series of morphological changes. Some of the morphological features observed during apoptosis include nuclear condensation, cell shrinkage, and retraction of cellular processes [3]. A large body of evidence suggests that the cytoskeleton is critical in the morphological changes during apoptotic progression induced in different cell death models [5, 6]; however, no information exists about the particular changes of the cytoskeletal proteins during cell death of astrocytes induced by St treatment.

In this study, we showed that St induces morphological alterations in astrocytes during the first minutes of treatment. These morphological changes could be due to a differential reorganization of cytoskeletal proteins such as actin and tubulin induced by cell death conditions. In this regard, some studies have established that during cell death there is rearrangement and accumulation of cytoskeletal proteins including actin and tubulin [65, 66]. This could be accompanied by the ability of microtubules to have spontaneous changes in the polymerization and depolymerization activities during apoptosis [67].

We observed a correlation between the morphological alterations and the cytoskeleton changes induced by the apoptotic condition. Both actin and tubulin (α-tubulin and β-tubulin) showed changes in astrocytes treated with St. This could be as a result of a dynamic behavior of actin and tubulin in apoptosis during the dismantling of the cell before the complete loss of cell viability [65]. Under these conditions, fibers of stress that determine the flattened or polygonal morphology lost their arrangement, forming small clusters. Also, the actin filaments were organized in beams. In the case of the microtubules, St treatment induced their rearrangement as diffuse networks that arise in concentrated points.

It is known that the organization of the actin cytoskeleton is a key element in the morphology of astrocytes [68] and that members of the Rho family regulate their arrangement [69–71]. The morphological changes associated with St could be mediated by an inhibition of Rho. It has been shown that

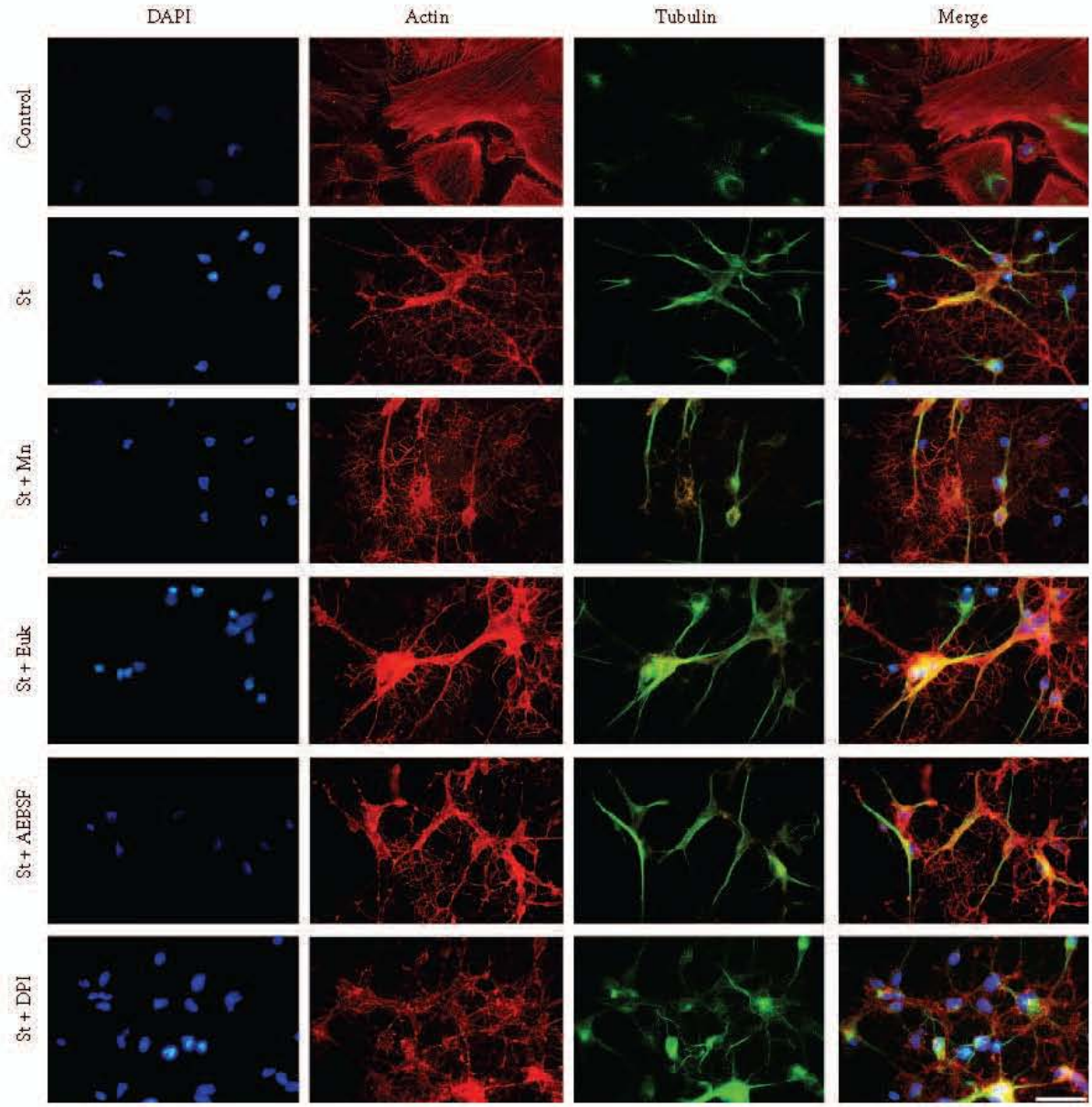

FIGURE 8: Cytoskeletal rearrangements induced by St are not mediated by ROS. Cerebellar astrocytes were treated with St (0.5 μM) for 2 h in the presence or absence of the antioxidants MnTMPyP (50 μM) and Euk-134 (20 μM) and the NOX inhibitors DPI (520 nm) and AEBSF (50 μM). Immunostaining against β-tubulin (green) and staining with rhodamine-phalloidin (red) were performed as mentioned in Section 2. Scale bar represents 50 μM.

the activity of these kinases promote the depolymerization of stress fibers, inducing the morphological change toward a stellate shape [72]. In addition, the activation of Rho stabilizes subpopulations of microtubules [73]. If the Rho pathway is inactivated, stress fibers are depolymerized and consequently a morphological change occurs. It is noteworthy to mention that no changes in the levels of actin and α-tubulin were observed at early times after St treatment, suggesting that the observed morphological alterations were due to a rearrangement of the cytoskeleton, but not due to a change in the level of expression of these proteins.

Considering that ROS could be directly or indirectly responsible for the observed morphological changes as part of the death process, we evaluated the possible involvement of ROS in this event. This idea was supported by the fact that H_2O_2 treatment induced clear morphological changes in astrocytes at early times, similarly to what was observed with St treatment. In addition, the observed changes in the morphology of astrocytes induced by St occurred early in time as it occurred for ROS production with St. However, the first noticeable morphological alterations induced by St (i.e., 15 min) (data not shown) happened at a time when ROS levels

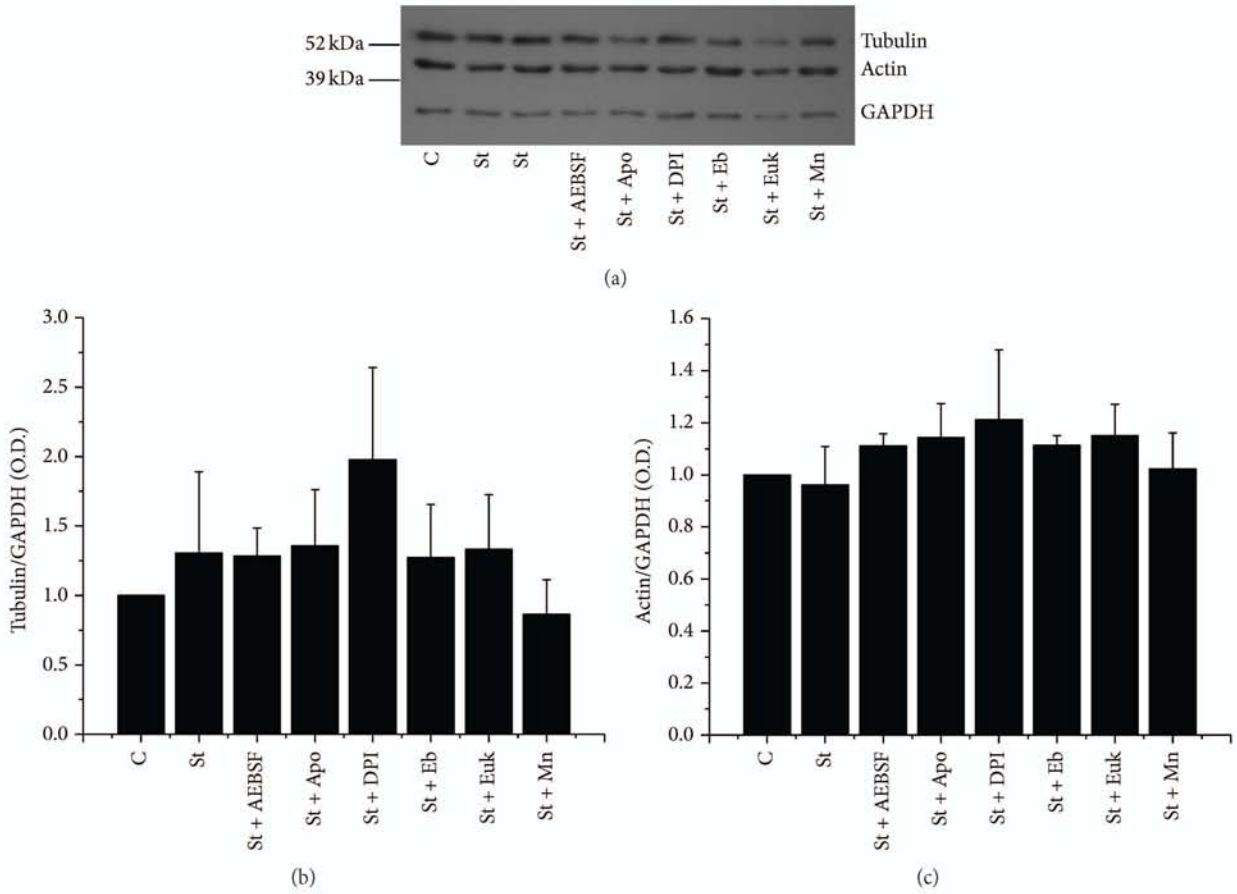

FIGURE 9: St does not induce changes in the expression of cytoskeletal proteins. Actin and α-tubulin levels were determined by Western blot assays as detailed in Section 2. Cerebellar astrocytes were treated with St (0.5 μM) in the presence or absence of the antioxidants MnTMPyP (50 μM) and Euk-134 (20 μM) and the NOX inhibitors DPI (520 nm) and AEBSF (50 μM). Data are presented as mean ± SEM of three independent experiments. No statistical differences were found among the treatments.

had not increased. More conclusive was the observation that the presence of an antioxidant in the cultures did not inhibit the morphological changes induced by St, in contrast to what was observed in astrocytes treated with H_2O_2. Similarly, the presence of a NOX inhibitor also failed to prevent the morphological changes induced by St. These results strongly suggest that neither NOX nor ROS seem to be implicated in the morphological changes induced by St. The above conclusion was further supported by the observation that both treatments with antioxidants and NOX inhibitors did not modify the described reorganization of actin and tubulin induced by St. The levels of these two proteins, which were not altered by St, were also unaffected by antioxidants.

In conclusion, we found here that ROS play a role in the death of astrocytes induced by staurosporine and that a possible source for these ROS is a member of the NOX family. We also found that NOX1, NOX2, and NOX4 are present in astrocytes, but only NOX1 and/or NOX4 could have a role in cell death of astrocytes induced by St. Finally, we showed that the actin and tubulin proteins suffer modifications related to the observed morphological changes in astrocytes treated with St, but these modifications are not dependent on NOX or ROS produced by St treatment. Overall, these results confirm the idea that NOX could contribute to death of cerebellar astrocytes.

Conflict of Interests

The authors declare that there is no conflict of interests regarding the publication of this paper.

Acknowledgments

The authors are grateful to Sitlali Olguín-Reyes for the excellent technical assistance. The authors also thank Dr. Michael Ogundele for revision of the English paper. This work was supported by DGAPA-UNAM (IN206213) and CONACYT (179234).

References

[1] R. W. Oppenheim, D. Prevette, M. Tytell, and S. Homma, "Naturally occurring and induced neuronal death in the chick embryo in vivo requires protein and RNA synthesis: evidence

for the role of cell death genes," *Developmental Biology*, vol. 138, no. 1, pp. 104–113, 1990.

[2] J. Yuan and B. A. Yankner, "Apoptosis in the nervous system," *Nature*, vol. 407, no. 6805, pp. 802–809, 2000.

[3] J. F. Kerr, A. H. Wyllie, and A. R. Currie, "Apoptosis: a basic biological phenomenon with wide-ranging implications in tissue kinetics," *British Journal of Cancer*, vol. 26, no. 4, pp. 239–257, 1972.

[4] N. A. Thornberry and Y. Lazebnik, "Caspases: enemies within," *Science*, vol. 281, no. 5381, pp. 1312–1316, 1998.

[5] L. S. Brewton, L. Haddad, and E. C. Azmitia, "Colchicine-induced cytoskeletal collapse and apoptosis in N-18 neuroblastoma cultures is rapidly reversed by applied S-100β," *Brain Research*, vol. 912, no. 1, pp. 9–16, 2001.

[6] S. B. Shelton and G. V. W. Johnson, "Tau and HMW tau phosphorylation and compartmentalization in apoptotic neuronal PC12 cells," *Journal of Neuroscience Research*, vol. 66, no. 2, pp. 203–213, 2001.

[7] T. Mashima, M. Naito, and T. Tsuruo, "Caspase-mediated cleavage of cytoskeletal actin plays a positive role in the process of morphological apoptosis," *Oncogene*, vol. 18, no. 15, pp. 2423–2430, 1999.

[8] A. Ortega and J. Morán, "Role of cytoskeleton proteins in the morphological changes during apoptotic cell death of cerebellar granule neurons," *Neurochemical Research*, vol. 36, no. 1, pp. 93–102, 2011.

[9] A. F. Castoldi, S. Barni, I. Turin, C. Gandini, and L. Manzo, "Early acute necrosis, delayed apoptosis and cytoskeletal breakdown in cultured cerebellar granule neurons exposed to methylmercury," *Journal of Neuroscience Research*, vol. 59, no. 6, pp. 775–787, 2000.

[10] J. Y. Chang and J. Z. Wang, "Morphological and biochemical changes during programmed cell death of rat cerebellar granule cells," *Neurochemical Research*, vol. 22, no. 1, pp. 43–48, 1997.

[11] E. Bonfoco, S. Ceccatelli, L. Manzo, and P. Nicotera, "Colchicine induces apoptosis in cerebellar granule cells," *Experimental Cell Research*, vol. 218, no. 1, pp. 189–200, 1995.

[12] N. Canu, L. Dus, C. Barbato et al., "Tau cleavage and dephosphorylation in cerebellar granule neurons undergoing apoptosis," *Journal of Neuroscience*, vol. 18, no. 18, pp. 7061–7074, 1998.

[13] A. M. Gorman, E. Bonfoco, B. Zhivotovsky, S. Orrenius, and S. Ceccatelli, "Cytochrome c release and caspase-3 activation during colchicine-induced apoptosis of cerebellar granule cells," *European Journal of Neuroscience*, vol. 11, no. 3, pp. 1067–1072, 1999.

[14] J. Kim, K. Mitsukawa, M. K. Yamada, N. Nishiyama, N. Matsuki, and Y. Ikegaya, "Cytoskeleton disruption causes apoptotic degeneration of dentate granule cells in hippocampal slice cultures," *Neuropharmacology*, vol. 42, no. 8, pp. 1109–1118, 2002.

[15] B. W. Kristensen, H. Noer, J. B. Gramsbergen, J. Zimmer, and J. Noraberg, "Colchicine induces apoptosis in organotypic hippocampal slice cultures," *Brain Research*, vol. 964, no. 2, pp. 264–278, 2003.

[16] E. G. Jordà, E. Verdaguer, A. Jimenez et al., "Evaluation of the neuronal apoptotic pathways involved in cytoskeletal disruption-induced apoptosis," *Biochemical Pharmacology*, vol. 70, no. 3, pp. 470–780, 2005.

[17] G. J. Müller, M. A. Geist, L. M. Veng et al., "A role for mixed lineage kinases in granule cell apoptosis induced by cytoskeletal disruption," *Journal of Neurochemistry*, vol. 96, no. 5, pp. 1242–1252, 2006.

[18] A. Bretscher, "Microfilament structure and function in the cortical cytoskeleton," *Annual Review of Cell Biology*, vol. 7, pp. 337–374, 1991.

[19] R. W. Keane, A. Srinivasan, L. M. Foster et al., "Activation of CPP32 during apoptosis of neurons and astrocytes," *Journal of Neuroscience Research*, vol. 48, no. 2, pp. 168–180, 1997.

[20] M. W. Karaman, S. Herrgard, D. K. Treiber et al., "A quantitative analysis of kinase inhibitor selectivity," *Nature Biotechnology*, vol. 26, no. 1, pp. 127–132, 2008.

[21] K. Abe, M. Yoshida, T. Usui, S. Horinouchi, and T. Beppu, "Highly synchronous culture of fibroblasts from G2 block caused by staurosporine, a potent inhibitor of protein kinases," *Experimental Cell Research*, vol. 192, no. 1, pp. 122–127, 1991.

[22] T. Okazaki, Y. Kato, T. Mochizuki, M. Tashima, H. Sawada, and H. Uchino, "Staurosporine, a novel protein kinase inhibitor, enhances HL-60-cell differentiation induced by various compounds," *Experimental Hematology*, vol. 16, no. 1, pp. 42–48, 1988.

[23] T. Yue, C. Wang, A. M. Romanic et al., "Staurosporine-induced apoptosis in cardiomyocytes: a potential role of caspase-3," *Journal of Molecular and Cellular Cardiology*, vol. 30, no. 3, pp. 495–507, 1998.

[24] A. J. Krohn, E. Preis, and J. H. M. Prehn, "Staurosporine-induced apoptosis of cultured rat hippocampal neurons involves caspase-1-like proteases as upstream initiators and increased production of superoxide as a main downstream effector," *Journal of Neuroscience*, vol. 18, no. 20, pp. 8186–8197, 1998.

[25] M. D. Jacobson, M. Weil, and M. C. Raff, "Role of Ced-3/ICE-family proteases in staurosporine-induced programmed cell death," *Journal of Cell Biology*, vol. 133, no. 5, pp. 1041–1051, 1996.

[26] H. Chae, J. Kang, J. Byun et al., "Molecular mechanism of staurosporine-induced apoptosis in osteoblasts," *Pharmacological Research*, vol. 42, no. 4, pp. 373–381, 2000.

[27] Y. Ramiro-Cortés, A. Guemez-Gamboa, and J. Morán, "Reactive oxygen species participate in the p38-mediated apoptosis induced by potassium deprivation and staurosporine in cerebellar granule neurons," *International Journal of Biochemistry and Cell Biology*, vol. 43, no. 9, pp. 1373–1382, 2011.

[28] A. Valencia and J. Morn, "Role of oxidative stress in the apoptotic cell death of cultured cerebellar granule neurons," *Journal of Neuroscience Research*, vol. 64, no. 3, pp. 284–297, 2001.

[29] A. Coyoy, A. Valencia, A. Guemez-Gamboa, and J. Morán, "Role of NADPH oxidase in the apoptotic death of cultured cerebellar granule neurons," *Free Radical Biology and Medicine*, vol. 45, no. 8, pp. 1056–1064, 2008.

[30] M. R. Sánchez-Carbente, S. Castro-Obregón, L. Covarrubias, and V. Narváez, "Motoneuronal death during spinal cord development is mediated by oxidative stress," *Cell Death and Differentiation*, vol. 12, no. 3, pp. 279–291, 2005.

[31] Y. Ramiro-Cortés and J. Morán, "Role of oxidative stress and JNK pathway in apoptotic death induced by potassium deprivation and staurosporine in cerebellar granule neurons," *Neurochemistry International*, vol. 55, no. 7, pp. 581–592, 2009.

[32] H. M. Shen and S. Pervaiz, "TNF receptor superfamily-induced cell death: redox-dependent execution," *The FASEB Journal*, vol. 20, no. 10, pp. 1589–1598, 2006.

[33] Z. Nayernia, V. Jaquet, and K. H. Krause, "New insights on NOX enzymes in the central nervous system," *Antioxidants & Redox Signaling*, vol. 20, no. 17, pp. 2815–2837, 2014.

[34] S. Sorce and K. Krause, "NOX enzymes in the central nervous system: from signaling to disease," *Antioxidants and Redox Signaling*, vol. 11, no. 10, pp. 2481–2504, 2009.

[35] D. W. Infanger, R. V. Sharma, and R. L. Davisson, "NADPH oxidases of the brain: distribution, regulation, and function," *Antioxidants and Redox Signaling*, vol. 8, no. 9-10, pp. 1583–1596, 2006.

[36] J. L. Marín-Teva, I. Dusart, C. Colin, A. Gervais, N. van Rooijen, and M. Mallat, "Microglia promote the death of developing Purkinje cells," *Neuron*, vol. 41, no. 4, pp. 535–547, 2004.

[37] J. Hur, P. Lee, M. J. Kim, Y. Kim, and Y. Cho, "Ischemia-activated microglia induces neuronal injury via activation of gp91phox NADPH oxidase," *Biochemical and Biophysical Research Communications*, vol. 391, no. 3, pp. 1526–1530, 2010.

[38] D. Zhu, C. Hu, W. Sheng et al., "NAD(P)H oxidase-mediated reactive oxygen species production alters astrocyte membrane molecular order via phospholipase A2," *Biochemical Journal*, vol. 421, no. 2, pp. 201–210, 2009.

[39] J. D. Lambeth, "NOX enzymes and the biology of reactive oxygen," *Nature Reviews Immunology*, vol. 4, no. 3, pp. 181–189, 2004.

[40] Q. Liu, J. Kang, and R. Zheng, "NADPH oxidase produces reactive oxygen species and maintains survival of rat astrocytes," *Cell Biochemistry and Function*, vol. 23, no. 2, pp. 93–100, 2005.

[41] D. G. Souza, B. Bellaver, D. O. Souza, and A. Quincozes-Santos, "Characterization of adult rat astrocyte cultures," *PLoS ONE*, vol. 8, no. 3, Article ID e60282, 2013.

[42] D. I. Brown and K. K. Griendling, "Nox proteins in signal transduction," *Free Radical Biology and Medicine*, vol. 47, no. 9, pp. 1239–1253, 2009.

[43] F. Klamt, S. Zdanov, R. L. Levine et al., "Oxidant-induced apoptosis is mediated by oxidation of the actin-regulatory protein cofilin," *Nature Cell Biology*, vol. 11, no. 10, pp. 1241–2146, 2009.

[44] M. Klemke, G. H. Wabnitz, F. Funke, B. Funk, H. Kirchgessner, and Y. Samstag, "Oxidation of cofilin mediates T cell hyporesponsiveness under oxidative stress conditions," *Immunity*, vol. 29, no. 3, pp. 404–413, 2008.

[45] S. O. Loureiro, L. Heimfarth, E. B. S. Scherer et al., "Cytoskeleton of cortical astrocytes as a target to proline through oxidative stress mechanisms," *Experimental Cell Research*, vol. 319, no. 3, pp. 89–104, 2013.

[46] D. Zhu, K. S. Tan, X. Zhang, A. Y. Sun, G. Y. Sun, and J. C.-. Lee, "Hydrogen peroxide alters membrane and cytoskeleton properties and increases intercellular connections in astrocytes," *Journal of Cell Science*, vol. 118, no. 16, pp. 3695–3703, 2005.

[47] J. Moran and A. J. Patel, "Stimulation of the N-methyl-D-aspartate receptor promotes the biochemical differentiation of cerebellar granule neurons and not astrocytes," *Brain Research*, vol. 486, no. 1, pp. 15–25, 1989.

[48] R. Balazs, O. S. Jorgensen, and N. Hack, "N-methyl-D-aspartate promotes the survival of cerebellar granule cells in culture," *Neuroscience*, vol. 27, no. 2, pp. 437–451, 1988.

[49] J. B. Schulz, M. Weller, and T. Klockgether, "Potassium deprivation-induced apoptosis of cerebellar granule neurons: a sequential requirement for new mRNA and protein synthesis, ICE-like protease activity, and reactive oxygen species," *Journal of Neuroscience*, vol. 16, no. 15, pp. 4696–4706, 1996.

[50] A. Atlante, S. Gagliardi, E. Marra, and P. Calissano, "Neuronal apoptosis in rats is accompanied by rapid impairment of cellular respiration and is prevented by scavengers of reactive oxygen species," *Neuroscience Letters*, vol. 245, no. 3, pp. 127–130, 1998.

[51] A. Valencia and J. Moran, "Reactive oxygen species induce different cell death mechanisms in cultured neurons," *Free Radical Biology and Medicine*, vol. 36, no. 9, pp. 1112–1125, 2004.

[52] J. Falsig, M. Latta, and M. Leist, "Defined inflammatory states in astrocyte cultures: correlation with susceptibility towards CD95-driven apoptosis," *Journal of Neurochemistry*, vol. 88, no. 1, pp. 181–193, 2004.

[53] R. Bertrand, E. Solary, P. O'Connor, K. W. Kohn, and Y. Pommier, "Induction of a common pathway of apoptosis by staurosporine," *Experimental Cell Research*, vol. 211, no. 2, pp. 314–321, 1994.

[54] J. Šimenc and M. Lipnik-Štangelj, "Staurosporine induces apoptosis and necroptosis in cultured rat astrocytes," *Drug and Chemical Toxicology*, vol. 35, no. 4, pp. 399–405, 2012.

[55] J. Simenc and M. Lipnik-Stangelj, "Staurosporine induces different cell death forms in cultured rat astrocytes," *Radiology and Oncology*, vol. 46, no. 4, pp. 312–320, 2012.

[56] Z. Zhu and G. Reiser, "PAR-1 activation rescues astrocytes through the PI3K/Akt signaling pathway from chemically induced apoptosis that is exacerbated by gene silencing of beta-arrestin 1," *Neurochemistry International*, vol. 67, pp. 46–56, 2014.

[57] I. D'Alimonte, P. Ballerini, E. Nargi et al., "Staurosporine-induced apoptosis in astrocytes is prevented by A1 adenosine receptor activation," *Neuroscience Letters*, vol. 418, no. 1, pp. 66–71, 2007.

[58] T. Satoh, T. Numakawa, Y. Abiru et al., "Production of reactive oxygen species and release of L-glutamate during superoxide anion-induced cell death of cerebellar granule neurons," *Journal of Neurochemistry*, vol. 70, no. 1, pp. 316–324, 1998.

[59] K. M. Noh and J. Y. Koh, "Induction and activation by zinc of NADPH oxidase in cultured cortical neurons and astrocytes," *The Journal of Neuroscience*, vol. 20, no. 23, 2000.

[60] R. Reinehr, B. Gorg, S. Becker et al., "Hypoosmotic swelling and ammonia increase oxidative stress by NADPH oxidase in cultured astrocytes and vital brain slices," *Glia*, vol. 55, no. 7, pp. 758–771, 2007.

[61] K. Bedard, V. Jaquet, and K. Krause, "NOX5: from basic biology to signaling and disease," *Free Radical Biology and Medicine*, vol. 52, no. 4, pp. 725–734, 2012.

[62] J. W. Choi, C. Y. Shin, B. K. Yoo et al., "Glucose deprivation increases hydrogen peroxide level in immunostimulated rat primary astrocytes," *Journal of Neuroscience Research*, vol. 75, no. 5, pp. 722–731, 2004.

[63] A. Guidarelli, L. Palomba, M. Fiorani, and O. Cantoni, "Susceptibility of rat astrocytes to DNA strand scission induced by activation of NADPH oxidase and collateral resistance to the effects of peroxynitrite," *Free Radical Biology and Medicine*, vol. 45, no. 4, pp. 521–529, 2008.

[64] S. Pendyala, I. A. Gorshkova, P. V. Usatyuk et al., "Role of Nox4 and Nox2 in hyperoxia-induced reactive oxygen species generation and migration of human lung endothelial cells," *Antioxidants and Redox Signaling*, vol. 11, no. 4, pp. 747–764, 2009.

[65] J. Huot, F. Houle, S. Rousseau, R. G. Deschesnes, G. M. Shah, and J. Landry, "SAPK2/p38-dependent F-actin reorganization regulates early membrane blebbing during stress-induced apoptosis," *Journal of Cell Biology*, vol. 143, no. 5, pp. 1361–1373, 1998.

[66] P. C. Endresen, J. Fandrem, T. J. Eide, and J. Aarbakke, "Morphological modifications of apoptosis in HL-60 cells: effects of

homocysteine and cytochalasins on apoptosis initiated by 3-deazaadenosine," *Virchows Archiv*, vol. 426, no. 3, pp. 257–266, 1995.

[67] M. V. Blagosklonny, P. Giannakakou, W. S. El-Deiry et al., "Raf-1/bcl-2 phosphorylation: a step from microtubule damage to cell death," *Cancer Research*, vol. 57, no. 1, pp. 130–135, 1997.

[68] V. Perez, T. Bouschet, C. Fernandez, J. Bockaert, and L. Journot, "Dynamic reorganization of the astrocyte actin cytoskeleton elicited by cAMP and PACAP: a role for phosphatidylinositol 3-kinase inhibition," *European Journal of Neuroscience*, vol. 21, no. 1, pp. 26–32, 2005.

[69] N. Rouach, A. Pébay, W. Même et al., "S1P inhibits gap junctions in astrocytes: involvement of Gi and Rho GTPase/ROCK," *European Journal of Neuroscience*, vol. 23, no. 6, pp. 1453–1464, 2006.

[70] A. Hall, "Rho GTpases and the actin cytoskeleton," *Science*, vol. 279, no. 5350, pp. 509–514, 1998.

[71] C. J. Chen, Y. C. Ou, S. Lin, S. Liao, Y. S. Huang, and A. N. Chiang, "L-glutamate activates RhoA GTPase leading to suppression of astrocyte stellation," *European Journal of Neuroscience*, vol. 23, no. 8, pp. 1977–1987, 2006.

[72] M. Burgos, S. Calvo, F. Molina et al., "PKCε induces astrocyte stellation by modulating multiple cytoskeletal proteins and interacting with Rho a signalling pathways: implications for neuroinflammation," *European Journal of Neuroscience*, vol. 25, no. 4, pp. 1069–1078, 2007.

[73] T. A. Cook, T. Nagasaki, and G. G. Gundersen, "Rho guanosine triphosphatase mediates the selective stabilization of microtubules induced by lysophosphatidic acid," *The Journal of Cell Biology*, vol. 141, no. 1, pp. 175–185, 1998.

ASN Neuro

Reactive oxygen species produced by NOX2 control cerebellar granule neurons development in vitro

Journal:	*ASN Neuro*
Manuscript ID:	ASN-14-0030.R1
Manuscript Type:	Original Papers
Keywords:	cell differentiation and migration < NEURO Development, Cell death < NEURO Degeneration, Cell survival < NEURO Repair, intracellular signaling < NEURO Signaling
Knowledge Environments:	NEURO Development, NEURO Signaling
Abstract:	Reactive oxygen species (ROS) act as signaling molecules that regulate nervous system physiology. ROS have been related to neural differentiation, neuritogenesis and programmed cell death. Nevertheless, little is known about the mechanisms involved in the regulation of ROS during neuronal development. In this study we evaluated the mechanisms by which ROS are regulated during neuronal development and the implications of these molecules in this process. Primary cultures of cerebellar granule neurons (CGN) were used to address these issues. Our results show that during the first 3 days of CGN development in vitro (DIV), the levels of ROS increased, reaching a peak at 2 and 3 DIV under depolarizing (25 mM KCl) and non-depolarizing (5 mM KCl) conditions. Subsequently, under depolarizing conditions the ROS levels markedly decreased, but in non-depolarizing conditions, the ROS levels increased gradually. This correlated with the extent of CGN maturation. Also, antioxidants and NOX inhibitors reduced the expression of Tau and MAP2. On the other hand, the levels of glutathione markedly increased at 1 DIV. We inferred that the ROS increase at this time is critical for cell survival since glutathione depletion lead to axonal degeneration and CGN death only at 2 DIV. During the first 3 DIV, NOX2 was up-regulated and expressed in filopodia and growth cones, which correlated with the H2O2 distribution in the cell. Finally, NOX2 KO CGN showed shorter neurites than wild type CGN. Taken together, these results suggest that the regulation of ROS is critical during the early stages of CGN development.

Note: The following files were submitted by the author for peer review, but cannot be converted to PDF. You must view these files (e.g. movies) online.

Supplementary video 1.mov
Supplementary video 2.mov
Supplementary video 3.mov
Supplementary video 4.mov
Supplementary video 5.mov

Reactive oxygen species produced by NOX2 control cerebellar granule neurons development *in vitro*

Mauricio Olguín-Albuerne [*] ***and Julio Morán*** [#]

Reactive oxygen species (ROS) act as signaling molecules that regulate nervous system physiology. ROS have been related to neural differentiation, neuritogenesis and programmed cell death. Nevertheless, little is known about the mechanisms involved in the regulation of ROS during neuronal development. In this study we evaluated the mechanisms by which ROS are regulated during neuronal development and the implications of these molecules in this process. Primary cultures of cerebellar granule neurons (CGN) were used to address these issues. Our results show that during the first 3 days of CGN development *in vitro* (DIV), the levels of ROS increased, reaching a peak at 2 and 3 DIV under depolarizing (25 mM KCl) and non-depolarizing (5 mM KCl) conditions. Subsequently, under depolarizing conditions the ROS levels markedly decreased, but in non-depolarizing conditions, the ROS levels increased gradually. This correlated with the extent of CGN maturation. Also, antioxidants and NOX inhibitors reduced the expression of Tau and MAP2. On the other hand, the levels of glutathione markedly increased at 1 DIV. We inferred that the ROS increase at this time is critical for cell survival since glutathione depletion lead to axonal degeneration and CGN death only at 2 DIV. During the first 3 DIV, NOX2 was up-regulated and expressed in filopodia and growth cones, which correlated with the H_2O_2 distribution in the cell. Finally, NOX2 KO CGN showed shorter neurites than wild type CGN. Taken together, these results suggest that the regulation of ROS is critical during the early stages of CGN development.

Keywords

Axonal morphogenesis, cerebellar granule neurons, glutathione, NADPH-oxidases, neuronal development, reactive oxygen species.

The development of the nervous system represents a highly coordinated event that includes different processes such as neural differentiation, neuritogenesis and programmed cell death. A primary aim of neurobiology is to unravel the molecular mechanisms that control neuronal development that is essential for the correct assembly of neuronal networks (Barnes and Polleux, 2009).

Several studies have shown in detail the extracellular mechanisms driving neuronal development, but the molecular machinery underlying the intracellular mechanisms has been less explored. Reactive oxygen species (ROS) have been implicated in several pathological condition, but they have also emerged as endogenous modulators of numerous physiological functions. ROS are formed form the univalent reduction of molecular oxygen, leading to the production of superoxide anions ($O_2^{\bullet -}$), considered the primary ROS. Subsequently, the $O_2^{\bullet -}$ is converted enzymatically and non-enzymatically into hydrogen peroxide (H_2O_2), which is considered the major ROS that regulates cell physiology (Kamata and Hirata, 1999; Droge, 2002; Valko et al., 2007; Pourova et al., 2010). In the nervous system, ROS have been mainly associated with the cause and progression of different neurologic disorders (Barnham et al., 2004; Sorce and Krause, 2009). Nevertheless, increasing evidence also support a physiological role of ROS in the developing and adult nervous systems. Some major functions of ROS in the CNS includes its involvement in hippocampal long-term potentiation, associative memory (Thiels et al., 2000), as well as its role as neuromodulator of dopamine release in the striatum (Avshalumov et al., 2005; Avshalumov et al., 2008; Sidlo et al.,2008). During nervous system development, different neurogenic regions express high levels of ROS. This expression pattern varies from one brain region to another and is also related to the developmental process at a given time -such as proliferation of neural stem cells (Yoneyama et al., 2010; Le Belle et al., 2011), neurogenesis (Tsatmali et al., 2005; Tsatmali et al., 2006; Le Belle et al., 2011) , cell migration (Le Belle et al., 2011),

División de Neurociencias, Instituto de Fisiología Celular, Universidad Nacional Autónoma de México, México City, México
* E-mail: albuerne@email.ifc.unam.mx.
# E-mail: jmoran@ifc.unam.mx.

[#]Correspondence to:
Dr. Julio Morán
División de Neurociencias,
Instituto de Fisiología Celular,
Universidad Nacional Autónoma de México,
Ap. Postal 70-253,
México, 04510, D.F., México.
Tel: 52 55/ 56-22-56-16
Fax: 52 55/ 56-22-56-07
E-mail: jmoran@ifc.unam.mx

axonal growth (Munnamalai and Suter, 2009; Munnamalai et al., 2014), axonal guidance (Morinaka et al., 2011) and programmed cell death (Valencia and Moran, 2004). The variety of ROS functions in the CNS is wide ranging from cell proliferation to cell death. Interestingly, several studies have shown that the mechanism that governs the physiological action of ROS may be similar to those underlying their pathological actions. Thus, studies pertaining to ROS actions during neuronal development may contribute to the understanding of the development and the disease of the nervous system.

NADPH-oxidases (NOX) family is one of the main ROS forming complexes in neurons. The NOX family comprises 7 homologues (NOX 1-5 and DUOX 1-2) that produce superoxide anion and hydrogen peroxide from molecular oxygen. NOX enzymes are widely expressed in most cell types, including neurons and glial cells (Bedard and Krause, 2007; Sorce and Krause, 2009). Although the physiological functions of NOX enzymes in the nervous system are largely unknown, studies have shown that NOX might be involved some processes such as the early phase of the long-term potentiation in hippocampus (Kishida et al., 2006) and neurogenesis and neuronal maturation.

The members of the NOX family can be activated by several regulators of nervous system development, including growth factors (neurotrophins and FGF), cytokines and activation of N-Methyl-D-Aspartate Receptor (NMDAR), among others (Suzukawa et al., 2000; Kim et al., 2002; Miller et al., 2007; Brennan et al., 2009). On the other hand, previous studies *in vitro* have shown that ROS produced by NOX induce neuronal differentiation of PC12 cells (Suzukawa et al., 2000; Goldsmit et al., 2001; Kamata et al., 2005), SH-SY5Y cells (Nitti et al., 2010) and P19 cells (Kennedy et al., 2010). Furthermore, it has been shown that NOX2 participates in the neurogenesis in the subventricular zone (Le Belle et al., 2011) as well as in the regulation of the actin cytoskeletal dynamics of axonal growth cones in *Aplysia* neurons (Munnamalai et al., 2014). In the developing cerebellum, we recently showed that a transient increase of ROS produced by NOX seems to be involved in the cerebellar foliation, and motor function (Coyoy et al., 2013). In view of this, the developing cerebellar cortex constitutes a suitable model for studying the mechanisms by which ROS regulate neuronal development.

The intracellular ROS levels depend not only on the ROS source, but also on the antioxidant systems in the cells. In this regard, the glutathione is a major antioxidant system in the nervous system (Dringen, 2000). Glutathione scavenges a variety of ROS and is an obligated co-substrate of glutathione peroxidase, which is a major mechanism of defense against H_2O_2 (Franco and Cidlowski, 2009; Lubos et al., 2011). In addition, changes in the reduced glutathione/oxidized glutathione complex are considered important determinants in the redox environment and redox signaling in the cells (Schafer and Buettner, 2001; Jones, 2006; Franco and Cidlowski, 2012). Therefore, the actions exerted by ROS during nervous system development may be influenced by the glutathione antioxidant system.

No much information is available on the glutathione levels during cerebellar development and the experimental evidence is rather controversial. Rice and Russo-Menna (1998), reported a subit increase in glutathione from postnatal day 12 that remianed high until the adult. However, other study indicates that the levels of glutathione transiently increase during the first week and then values return to basal levels, remaining relatively low during the subsequent stages of cerebellar development (Nanda et al., 1996).

Although some studies have established a physiological role of ROS during nervous system development, little is known about the interdependence of ROS and NOX enzymes during neuronal development. Furthermore, the mechanisms through which ROS are regulated in the developing neurons remain largely unknown. In this study, we aim to determine the physiological role of ROS in neuronal development of cerebellar granule neurons (CGN) and evaluate the role of NOX and glutathione in the regulation of ROS during this process. To address these issues, we employed cultured CGN that represents a model of study that recapitulates many of the stages of the development of the CGN in the cerebellar cortex *in vivo*. (Powell et al., 1997; Wechsler-Reya and Scott, 1999; Konishi et al., 2004; Ito and Takeichi, 2009). In the cerebellum, post-mitotic CGN precursors generate neurites and migrate to the internal granule layer, where they develop dendrites and establish synaptic contacts with mossy fibers (Solecki et al., 2006). The presynaptic inputs at this stage seem to play a key role in the maturation and survival of CGN. The state of depolarization of CGN influences their survival (Gallo et al., 1987), the activation of the enzymes involved in the synthesis of cell-specific neurotransmitters (Caballero-Benitez et al., 2004) and their dendritic pruning and maturation (Shalizi et al., 2006; Ramos et al., 2007).

Here, we determined the changes in the basal levels of ROS in CGN cultures under depolarizing and non-depolarizing conditions throughout CGN development, as well as their effects on CGN maturation. To elucidate the role of glutathione in the developing CGN, we examined the outcome of glutathione depletion on cell viability and axonal integrity. Subsequently, we measured the expression of NOX2 at different stages of CGN development and its localization in these neurons. We also explored the specific production of H_2O_2 in growth cones and filopodia. Finally, we explored the physiological relevance of ROS, glutathione and NOX2 during CGN neuritogenesis.

Materials and Methods

Materials

Fetal calf serum, penicillin and streptomycin were from Gibco® (Grand Island, NY, USA). Dihydroethidium, calcein-AM and MTT were from Molecular Probes® (Eugene, OR, USA). Trizol Reagent, M-MVL Reverse Transcriptase and oligo (dT)12-18 primer were

from Invitrogen™ (Carlsbad, CA, USA). TaqMan® Universal Master Mix II was from Applied Biosystems® (Foster City, CA, USA). Vectashield mounting media was from VECTOR LABORATORIES (Burlingame, CA, USA). Poly-L-lysine (molecular weight >300 000), trypsin, DNAse, superoxide dismutase, cytosine-D-arabino-furoanoside, DMSO, 4-(2-Aminoethyl) benzenesulfonyl fluoride hydrochloride (AEBSF), dithiobis-2-nitrobenzoic acid (DTNB), glutathione reductase, β-NADPH, glutathione reduced form, glutathione disulfide form, 2-Vinylpyridine, BSO, EDTA, propidium iodide and reagents for polyacrylamide gel electrophoresis (PAGE) were obtained from Sigma (St Louis, MO, USA). CDP-Star enhanced chemiluminescence-detecting agent for phosphatase alkaline conjugated antibodies purchased from Bio-Rad (Hercules, CA, USA). ProSiev QuadColor Protein Marker and Nucleofector VPI-1003 were from Lonza (Basel, Switzerland). Ebselen, and Euk-134 were from Cayman Chemical (Ann Arbor, MI, USA). Apocynin was from Calbiochem (La Jolla, CA, USA). Other chemicals were of the purest grade available from regular commercial sources.

Antibodies

Antibodies against GAPDH (mab374) was from Millipore (Bedford, MA, USA) and Santa Cruz Biotechnology (Santa Cruz, CA, USA), respectively. Tau (mab4019) and MAP2 (4542) were from Cell Signaling (Danvers, MA, USA). NOX2 (ab31092) was from abcam (Cambridge, MA, USA). Alexa Fluor® 488 Goat Anti-Rabbit (H+L) and Alexa Fluor® 568 Donkey Anti-Goat IgG (H+L) were from Molecular Probes® (Eugene, OR, USA).

Cell Culture

All animals used for experimentation described in the present study were treated in accordance with the accepted standards of animal care and with the procedures approved by the local Committee of Research and Ethics of the Instituto de Fisiología Celular, Universidad Nacional Autónoma de México. The protocol used followed the Guidelines for the Care and Use of Mammals in Neuroscience as well as guidelines released by the Mexican Institutes of Health Research and the National Institutes of Health guide for the care and use of laboratory animals. All efforts were made to minimize animal suffering and to reduce the number of animals used.

Cerebellar granule neurons cultures were prepared from postnatal day 8 Wistar rats and from postnatal day 7 $NOX2^{-/-}$ and wild type mice as previously described (Moran and Patel, 1989). CGN were plated at a density of 265 $\times 10^3$ cells/cm^2 in plastic dishes or coverslips coated with poly-L-lysine (5 μg/mL). Culture medium contained basal Eagle's medium supplemented with 10% (v/v) heat-inactivated fetal calf serum, 2 mM glutamine, 25 mM KCl, 50 U/mL penicillin and 50 mg/mL streptomycin. Cells were maintained under these conditions between 0 and 8 days *in vitro* (DIV). Culture dishes were incubated at 37ºC in a humidified 5% CO2/95% air atmosphere. To prevent the development of non-neuronal cells, cytosine arabinoside (10 μM) was added 24 h after seeding. At the end of the preparation, CGN cultures contained approximately 95% neurons. The colonies of NOX2 (gp91phox) knockout mice on a C57BL6 background were purchased from The Jackson Laboratory (Bar Harbor, ME, USA) and bred in our Institute.

Cell viability

CGN were incubated with calcein (10 μM) and propidium iodide (5 μM) for 15 min at 37ºC, and cells were photographed in a fluorescence microscope using filters with the following characteristics: excitation filter wavelength/dichromatic mirror cut-on wavelength/barrier filter wavelengths of 450-490/500/515 and 510-560/565/590 nm for calcein and propidium iodide respectively. Subsequent analysis involved the determination of immunopositive cells from at least two different images for each condition. Results are expressed as the percentage of viable cells (calcein-positive cells) from the total number of cells (calcein-positive cells + propidium iodide-positive cells) evaluated per field.

Metabolic activity

Mitochondrial activity was determined by the conversion of tetrazolium MTT (3-[4,5-dimethylthiazol-2-yl]-2,5 diphenyl tetrazolium bromide) into formazan crystals. CGN were seeded during different days in the same multiwell plate. MTT (0.5 mg/ml) was added to CGN for 15 min at 37ºC, the formazan crystals produced from MTT were extracted with 100% DMSO and quantified spectroscopically at 560 nm.

ROS detection

Cerebellar granule neurons were seeded during different days in the same multiwell plate. Cells were washed twice with Locke medium (154 mM NaCl, 25 or 5 mM KCl, 3.6 mM $NaHCO_3$, 2.3 mM $CaCl_2$, 5.6 mM glucose and 10 mM HEPES) and then incubated with 3.2 mM of dihydroethidium for 35 min. After that, cells were washed twice with Locke medium and images were acquired in an epifluorescence microscope using a filter with the following characteristics: excitation filter wavelength/dichromatic mirror cut-on wavelength/barrier filter wavelength of 510-560/565/590 nm. Two images from the same field were acquired, one in phase contrast and the other in fluorescence. Fluorescence measurements of the ethidium cation (E^+), which is the product of the oxidation of dihydroethidium, were performed tracing a region of interest (ROI) in the soma of fifteen cells. These ROI were considered in the fluorescence image and the mean gray intensity values were averaged. The backgrounds of two different fields were subtracted from the fluorescence values of each measured cell. At least two different images of each condition were evaluated. We measure the fluorescence of 15 cells per photograph and the average of 4 wells per experiment was considered as n=1. Results are expressed as absolute values or data were normalized with respect to 2 DIV.

Measurement of glutathione content

Glutathione was assayed using enzymatic recycling method for a 96 microwell plate (Tietze, 1969; Rahman et al., 2006). CGN were grown on 35 mm culture dishes from 0 to 5 DIV. Cells were washed in PBS and sonicated in 0.1% Triton X-100 and 0.6% sulfosalicylic acid in KPE (0.1 M potassium phosphate buffer with 5 mM EDTA disodium salt, pH 7.5). Next, samples were mixed with equal volumes of DTNB and glutathione reductase, after 30 s β-NADPH was added. Immediately, kinetic measurements of the absorbance changes at 412 nm were recorded for 15 min. Absorbance recordings and the injection of solutions were performed in the microplate reader Synergy HT (BioTek Instruments, USA). To

determine oxidized glutathione levels, the samples were pre-incubated with 2.5% vinylpyridine for 60 min and neutralized with triethanolamine prior to kinetic measurement. Glutathione and oxidized glutathione standard curves were prepared to calculate the actual concentration in the sample. Reduced glutathione was calculated from the subtraction of oxidized glutathione from the total glutathione.

Western Blot

CGN were grown on 60 cm culture dishes from 0 to 3 DIV in presence or absence of the antioxidants Ebselen (10 μM) and Euk-134 (20 μM) and the NOX inhibitors AEBSF (50 μM) and apocynin (400 μM) in 24 h treatments at the indicated times. Cells were washed twice in ice-cold PBS and homogenized in lysis buffer (25 mM Trizma, 50 mM NaCl, 2% Igepal, 0.2% SDS and Complete protease inhibitors, pH 7.4). The protein concentration of cellular homogenates was determined by using the Lowry method. A total of 60 μg of soluble protein per lane was loaded on SDS-PAGE and electrotransferred to PVDF membranes which were blocked with fat-free milk (5% in Tris-buffered saline (TBS)/Tween 20 (TTBS) buffer [100 mM Trizma, 150 mM NaCl and 0.1% Tween, pH 7.5]) and incubated overnight at 4ºC with the following specific primary antibodies: 1:3000 mouse anti-GAPDH, 1:500 mouse anti-Tau and 1:500 rabbit anti-MAP2.

Measurement of NAPDH-oxidase activity in living cells

The NAPDH-oxidase activity was determined by extracellular superoxide anion production that was measured by the reduction of cytochrome c. CGN were seeded during different days in the same multiwell plate, cells were washed twice with Locke medium and then were incubated with 100 μl of Locke media containing cytochrome c (250 μM) and β-NADPH (200 μM). Cytochrome c reduction absorbance (550 nm) was recorded at 37ºC in the microplate reader Synergy HT. The amount of superoxide anion released was calculated using an extinction coefficient of 21 mM^{-1} cm^{-1}. It was considered 300 μm as the distance that occupies a volume of 100 μl in a well plus the base of the plate.

Quantitative real-time reverse-transcription polymerase chain reaction (RT-qPCR)

Total RNA was extracted from CGN grown in depolarizing conditions from 0 to 5 DIV using Trizol Reagent according to the manufacturer's instructions. RNA quality was assessed by denaturing agarose gel electrophoresis and with NanoDro p2000 spectrophotometer (Thermo Scientific, USA). One μg of total RNA from each sample was reverse transcribed into cDNA using M-MVL Reverse Transcriptase with an oligo (dT)12-18 primer. One microgram of cDNA was used to determine the relative gene expression, which was performed in a thermal cycler Rotor-gene 6000 (Corbett Life Science), using TaqMan Universal Master Mix 2X and TaqMan Assay reagent for NOX1 (Rn00586652_m1), NOX2 (Rn00576710_m1) and GAPDH (Rn01775763_g1) (Applied Biosystems®, USA). The relative level of amplified mRNA was normalized to the expression of the housekeeping gene glyceraldehyde 3-phosphate dehydrogenase (GAPDH). The average *C*t value of the endogenous control (GAPDH) for every sample was subtracted from the *C*t value for each target gene, resulting in the ΔC_T value. Fold change was calculated using the $2^{-\Delta\Delta CT}$ method where the comparative cycle threshold ($\Delta\Delta C_T$) was defined as the difference between ΔC_T of 1 to 5 DIV minus ΔC_T of the DIV in which the expression reached its maximum.

Immunocytochemistry

CGN were plated at a density of 50×10^3 cells/cm^2 and were grown onto poly-$_L$-lysine-coated glass slides from 0 to 3 DIV. Cells were washed twice in PBS and fixed with 4% paraformaldehyde for 20 min. Subsequently, cells were blocked and permeabilized overnight at 4ºC in blocking solution (PBS containing 0.5% Triton X-100 and 10% normal goat serum) and then were incubated overnight at 4ºC in blocking solution with 1:250 (0.4 μg/ml) rabbit anti-NOX2 and 1:500 mouse anti-Tau antibodies. The primary antibody anti-NOX2 was detected with an Alexa Fluor® 488 goat anti-rabbit IgG (H+L) secondary antibody (1:1000) incubated for 2 hours at room temperature. The primary antibody anti-Tau was detected with a DyLight 594 goat anti-mouse IgG (H+L) secondary antibody (1:1000) incubated for 2 hours at room temperature. Coverslips were mounted using Vectashield mounting media with DAPI. Images were captured in the FV10i-LIV confocal microscope (Olympus, USA). Coverslips incubated without primary antibody or with 1:50 (10 μg/ml) normal rabbit IgG showed no staining. The staining for Tau detection did not affect the detection of NOX2 and vice versa.

Measurements of H_2O_2 localization in living cells

CGN were transfected before plating with 5 μg of HyPer-cyto (Evrogen, Rusia), using the Nucleofector program C-13. CGN were visualized in a microscope Axiovert 200 M (Carl Zeiss Microscopy, Germany) with a Lambda DG-4 system (Sutter Instrument, USA) and a PECON system (PECON, Germany) for cell culture and microscopy; an objective Fluar 40x/1.30 Oil M27 was used to visualize the cells. HyPer fluorescence was acquired in two different channels: CH1 (excitation 460-480 nm, beamsplitter 493 nm, emission 505-530) and CH2 (excitation 379-395 nm, beamsplitter 410 nm, emission 465-555) in time-laps imaging. The images are expressed as the ratio of CH1 to CH2 minus their respective backgrounds. A higher index corresponds to higher levels of H_2O_2. In order to determine the regions where the levels of H_2O_2 were higher, a ROI was traced and the mean fluorescence intensity was registered during different photograms, the average of these points was normalized with the average of the fluorescence in the soma. The measurements were only considered in the photograms where the region of interest was toughly in focus. The measurement of each structure represents n=1. The image analysis was performed in AxioVision 4.8.2 and Image J.

Axonal morphology

CGN were labeled with PKH67 in a proportion of 10×103 labeled cells and 18×106 non-labeled cells. PKH67 is a dye used for membrane labeling, which is composed by a green fluorescent dye with long aliphatic tales that intercalates into lipid regions of the membranes (Wallace et al., 2008) .Cells were treated with BSO (100 μM) at the time of plating and, in some experiments, the cells

were treated with Euk-134 (10 μM) 24 h after plating. Cells were visualized in a fluorescence microscope and photographed. The morphology of the axons was classified into three different categories that were: unaltered, with multiple spheroids and collapsed. The proportion of neurons categorized into these three types of morphologies was determined per experiment and averaged in independent experiments.

Axonal growth

CGN were labeled before plated with 3 μM PKH-67 at room temperature for 5 min. An equal volume of 1% BSA in PBS was then added and the cells were further incubated for 1 min to stop the staining reaction. The labeled cells were then centrifuged at 400 g for 8 min at room temperature and resuspended in culture medium in a proportion of 10×10^3 labeled cells and 18×10^6 non-labeled cells. The neurites were measured manually and only those neurites longer than the cell diameter and that did not show contacts with other neurites were considered; in the case of bipolar CGN, only the longest neurite was considered. The measurement of each neurite represents n=1. The measurements were made in Image J with the plugin Neuron J.

Statistical analysis

Statistical analysis was done by using SigmaPlot 12.1 software. Data are expressed as means ± SEM. unless otherwise indicated. Pairwise comparison within multiple groups was done by analysis of variance (ANOVA) followed by the Holm-Sidak post-hoc test; in some cases ANOVA nonparametric test was performed. The statistical significance in the comparisons between two groups were determined by the Student's t-test and by the Mann-Whitney U test. For the time course results, a Paired t-test was used. P values less than 0.05 were considered statistically significant.

Results

The levels of ROS are differentially regulated during CGN development

In order to determine the basal levels of ROS throughout CGN development, we cultured CGN in depolarizing (25 mM KCl) and non-depolarizing (5 mM KCl) concentrations of potassium chloride. This enabled us to compare two conditions of neuronal development in vitro where neurons under depolarizing conditions develops normally, while those in non-depolarizing conditions matures only partially and died by 8 days *in vitro* (DIV) in a ROS-dependent manner (Schulz et al., 1996). Under these conditions, we measured the cell viability and the metabolic activity of CGN during the first 5 DIV in order to determine the time at which cell survival is compromised during CGN development. In agreement with Gallo *et al*. (Gallo et al., 1987) and others, CGN survival measured as calcein-propidium iodide incorporation, was dependent on the state of depolarization after 3 DIV. Figure 1 shows that when CGN were cultured in non-depolarizing conditions, the cell viability diminished from 4 DIV, while in depolarizing conditions the cell viability remained unaltered (Fig. 1A and B). On the other hand, the metabolic activity, measured as MTT transformation, was reduced by 30% at 5 DIV in non-depolarizing conditions (Fig. 1C). In contrast, the metabolic activity of CGN grown in depolarizing conditions showed a sustained increase during the first 5 DIV (Fig. 1C).

We also evaluated the basal levels of ROS by the oxidation of dihydroethidium in depolarizing and non-depolarizing conditions during the first 5 DIV (Fig. 1D). When CGN were cultured in depolarizing conditions, the levels of ROS increased steadily over time from 0 to 1 DIV (160%) and from 1 to 2 DIV (110%). The maximum levels reached at 2 DIV were sustained until 3 DIV (Fig. 1E,F). Subsequently, the levels of ROS decreased to similar values to those found at 1 DIV (Fig. 1E). Then, the levels of ROS remained low until 8 DIV (Fig. 1F). On the other hand, when CGN were cultured in non-depolarizing conditions, the levels of ROS were similar to those observed in depolarizing conditions from 1 to 3 DIV (Fig. 1E); however, at 4 and 5 DIV, the levels of ROS increased gradually (Fig. 1E). Thus, under these conditions, ROS levels show two distinct phases: the first phase, from 0 to 3 DIV, which is independent of the state of depolarization, and a second phase, after 3 DIV, that is dependent on the state of depolarization.

Increased glutathione levels are required for CGN survival during early development

The levels of ROS in the cell are determined by the equilibrium between the production of ROS and the levels and activity of the antioxidants (Halliwell, 2009). Among the numerous antioxidants, we evaluated the glutathione system that is one of the most relevant antioxidant systems in neurons. Moreover, it has been reported glutathione content changes during the cerebellar cortex development (Nanda et al., 1996; Rice and Russo-Menna, 1998). Thereby, in order to evaluate a possible relationship between glutathione and ROS levels throughout CGN development, we estimated the levels of reduced and oxidized glutathione throughout CGN development in depolarizing and non-depolarizing conditions. Figure 2A shows that when CGN were grown in depolarizing conditions, the reduced glutathione content increased during the first 2 DIV. It is important to note that the most significant increase was recorded between 0-1 DIV (~90%) that was followed by a slight increase of 10% between 1-2 DIV which persisted until 5 DIV. At 8 DIV, the levels of reduced glutathione significantly decreased to values similar to those observed at 0 DIV (Fig 2B). When cells were grown in non-depolarizing conditions, the increase in the levels of reduced glutathione was similar to that in depolarizing conditions from 0 to 2 DIV; however, after 3 DIV, the level of reduced glutathione decreased significantly in CGN under non-depolarizing conditions at 5 DIV (Fig. 2A). Interestingly, the level of oxidized glutathione did not change throughout the different stages of CGN development and no significant difference was observed between depolarized and non-depolarized cells (Fig. 2A).

Considering that the levels of glutathione increase in correspondence with ROS, we hypothesized that glutathione might be involved in the actions of ROS during the first 3 DIV. This is further supported by previous studies showing that high levels of ROS induce cell death in these cells. It is possible that the observed decrease in glutathione content in CGN maintained in non-depolarizing conditions during 3 DIV could either be a cause or the result of the cell death observed at this time. In this regard, it has been shown that glutathione depletion triggers cell death and that a glutathione depletion occurs during the cell death process (Franco and Cidlowski, 2009, 2012).

Based on these evidences, we evaluated the role of glutathione in CGN survival by reducing the glutathione content in CGN cultures treated during the last 24h or 48 h of culture with buthionine sulphoximine (BSO), an inhibitor of ɣ-glutamylcysteine synthetase, which is the first and rate-limiting enzyme for the biosynthesis of glutathione. Figures 2C-F show that BSO treatment for 48 h, markedly decreased reduced glutathione content at 2, 3, 5 and 8 DIV. Similarly, oxidized glutathione content were also significantly reduced by BSO at all ages measured (Fig. 2C-F). When cell viability was evaluated we found that BSO did not affect CGN survival at any time when cultures were treated during the last 24h (Fig. 2G); however, when cultures were treated for 48 h, we observed a significant complete reduction of cell viability in CGN cultures at 2 DIV (Fig 2H). The observed effect of BSO was completely prevented by the antioxidant EUK-134 (Fig. 2I,J), suggesting that cell death induced by BSO at 2 DIV is due to an oxidative stress induced by glutathione reduction. Interestingly, under these conditions, cell viability was not affected in cultures of 3-8 DIV. These results indicate that CGN vulnerability to cell death related to oxidative stress is present only at 2 DIV, when CGN are in the process of maturation. The fact that the levels of glutathione were also completely diminished in CGN treated with BSO plus Euk-134 at 2 DIV (Fig 3C), a condition that does not affect cell viability, indicates that glutathione estimation was not affected by the antioxidant. Thus, there seems to be a narrow developmental time window where ROS seem to play a critical role not only for neuronal survival, but also for neuronal maturation. In addition, from 3-8 DIV, ROS are no longer required for cell maturation, but the lack of trophic influences (no-depolarizing conditions) could induce some mechanisms leading to an increase in ROS levels and then to cell death.

ROS promote CGN development

Previous studies suggest that ROS regulate some events of the nervous system development (Tsatmali et al., 2006; Le Belle et al., 2011; Celotto et al., 2012; Coyoy et al., 2013). In order to evaluate the relevance of ROS during CGN development, we tested the effect of two antioxidants, the mimetic of glutathione peroxidase Ebselen (Parnham and Kindt, 1984) and the mimetic of superoxide dismutase and catalase Euk-134 (Baker et al., 1998), as well as two general inhibitors of NOX1-2, AEBSF and apocynin (Diatchuk et al., 1997; Cheret et al., 2008; Hernandez-Enriquez et al., 2011; Dvoriantchikova et al., 2012; Lu et al., 2012) on the expression of Tau and MAP2 during CGN development. The expression of these proteins are indicators of neuronal maturation (Dehmelt and Halpain, 2004). First, we determined the relative levels of Tau and MAP2 from 0 to 3 DIV and, as expected, we found a correlation between the levels of these two proteins and the CGN development (Fig 3A). In both cases, the highest increase was between 1 and 2 DIV. When CGN were treated with Ebselen and Euk-134 at 0 DIV during 24 h, no effect on the levels of Tau and MAP2 were observed; however, AEBSF and apocynin significantly diminished the levels of Tau by 50%, while AEBSF, but not apocynin treatment, significantly diminished the levels of MAP2 by 70% (Fig. 3B). When CGN were treated during 24 h at 1 DIV, the antioxidants had no effect on the levels of Tau, but diminished MAP2 levels by 30%. In contrast, both AEBSF and apocynin significantly reduced the expression of Tau and MAP2 by 60% and 30%, respectively (Fig. 3C). Finally, when CGN were treated from 2 to 3 DIV, none of the treatments had any effect in the levels of Tau and MAP2 (Fig. 3D).

NADPH oxidase activity and the expression of NOX homologues change during CGN development

It has previously shown that NOX enzymes are major source of ROS in several cell types (Bedard and Krause, 2007; Sorce and Krause, 2009). Since NOX inhibitors interfere with CGN maturation, we hypothesized that members of the NOX family could be mediating ROS production during CGN development. In order to determine the relevance of ROS producing enzymes in developing CGN, we measured the NOX activity in cultured CGN by determining the extracellular reduction of cytochrome c by superoxide anion produced by NOX (Fig 4A). In CGN grown under depolarizing conditions, the NOX activity gradually increased between 1 to 3 DIV (~50%) and then the activity decreased to levels close to those found at 2 DIV, which is similar to the ROS production observed from 1 to 5 DIV (Fig 1E).

To evaluate the importance of some NOX homologues in the CGN development, we determined the expression of NOX1 and NOX2 in CGN cultured in depolarizing conditions from 0 to 5 DIV by using quantitative real time RT-PCR (Fig. 4B-E). Under these conditions, we found that NOX1 and NOX2 showed the lowest expression at 0 DIV. NOX1 reached the highest expression at 1 DIV and afterwards it gradually decreased (Fig. 4B). NOX2 presented a marked increase from 1 to 2 DIV and a minor increment between 2 and 3 DIV. Afterwards, the levels of NOX2 diminished abruptly from 3 to 4 DIV (Fig. 4C). When the relative mRNA expression of NOX1 and NOX2 were compared, we observed a higher abundance of NOX2 than NOX1 at both 1 and 3 DIV (Fig. 4D,E).

NOX2 and H_2O_2 localization in developing CGN

Some studies have highlighted the importance of the compartmentalization of ROS production in cells (Mishina et al., 2011a), which may allow ROS to activate particular redox signaling events in specific regions of the cells (Ushio-Fukai, 2009a). Accordingly, we studied the localization of NOX2 in developing CGN cultured in depolarizing conditions, based on the finding that this is one of the most abundant homologues in CGN (Fig. 4D,E). Supplementary Figure 1 shows an immunocytochemistry study at normal density, in which the mark of NOX2 is localized in the axons, but no details of the specific location of the label can be appreciated. Therefore, the immunolocalization of NOX2 was carried out in cultures with a lower density than in the rest of the experiments in order to visualize the NOX2 positive structures. This condition did not affect the cell survival (Data not shown). Figure 5 shows that NOX2 was mostly distributed in neurites and it was closely associated with the growth cones at 0 and 3 DIV. Particularly, at 0 DIV, NOX2 was preferentially concentrated in the growth cones of most developing neurites (Fig. 5A), as well as in some protrusion. In the more advanced stage of development (3 DIV), NOX2 was enriched in filopodia, axonal varicosities and growth cones (Fig. 5B); thus suggesting that ROS might be produced in specific regions of the developing neurons. The distribution of Tau, a marker of early neurites, showed a close correlation with NOX2 labeling, particularly at 3 DIV (Fig. 5).

Several studies have shown that ROS are produced in axonal growth cones during axonal outgrowth and guidance (Munnamalai and Suter, 2009; Morinaka et al., 2011; Munnamalai et al., 2014). To evaluate ROS compartmentalization we used an experimental approach that allowed the detection of variations of ROS levels in real time with a high time and spatial resolution. This was achieved by transfecting CGN with the plasmid HyPer that is a genetically encoded fluorescent sensor designed for high specific detection of cytoplasmic H_2O_2 (Belousov et al., 2006), which has been suggested to be the most suitable signaling ROS. The ratiometric sensor used has one emission peak at 516 nm and two excitation peaks at 420 nm and 500 nm. The emission fluorescence changes upon exposure to H_2O_2; while the excitation peak at 420 nm decreases, the peak at 500 nm increases, which allows us to determine the difference in H_2O_2 levels in different regions of the neuron, independently of the amount of protein expressed. We found that H_2O_2 is heterogeneously distributed throughout neurons cultured during 1 to 3 DIV under depolarizing conditions (data not shown). Since no apparent differences in the H_2O_2 localization were found at 1 to 3 DIV, we used CGN of 2 DIV. At this time ROS reach their maximum levels and the plasmid HyPer also reaches its maximum expression.

Figures 6 A-F show that, although basal level of H_2O_2 was present in all the neuronal structures, there is a clear difference in H_2O_2 levels between the soma and the axon and dendrites. H_2O_2 is evenly distributed in the soma and the levels are relatively low (Fig. 6 A,C,E). The levels of H_2O_2 in the soma did not change with time under basal conditions, but the fluorescent signal increased when cells were treated with exogenous H_2O_2 (Supp. Fig. 1A-D). In contrast, the distribution of the H_2O_2 along the axon shaft was variable under basal conditions; in some areas the concentration was slightly lower than those observed in the soma, while some other areas showed relatively higher H_2O_2 levels than in the soma. In the regions where no filopodia or varicosities are presented, the average level of H_2O_2 was approximately equal to the values recorded in the soma (Fig. A-H). Interestingly, the axonal zones showing high levels of H_2O_2 corresponded to regions with high growing and/or remodeling activity, such as axonal growth cones and filopodial regions (Fig. 6 B-D,F). In all cases, these zones showed H_2O_2 levels that doubled the levels detected in the soma or other regions of the axon (Fig. 6H). We also observed that, regardless the magnitude of movement in the axonal growth cones, these regions always showed high levels of H_2O_2 (Supplementary videos 6-9). High levels of H_2O_2 were also found in dendritic growth cones (Fig. 6 A,C,H). Not all the dynamic regions corresponded to high levels of H_2O_2, but also in the varicosities (Fig. 6D,H). The relative levels of H_2O_2 in the different regions of the axon are indicated in Table 1.

As mentioned, high levels of H_2O_2 are localized in the regions of the axon shaft where filopodia are located (Fig. 6F-H), this was more prominent in regions where filopodia are constantly remodeling (dynamic zones). In these regions we found clear variations in H_2O_2 levels that are restrained to microdomains of the axon shaft where filopodia are growing and retracting. It was generally observed an increase in H_2O_2 levels immediately before the filopodia formation, which reached its peak during the process and then it dropped to the basal value at the end of the process. In certain cases high levels of were found inside the filopodia, particularly in situations when filopodia were very motile or other protrusions were formed in the filopodia (Fig. 6G,I). These findings are illustrated in Figure 6G, in which serial images of the dynamic zone are shown.

The observed changes in H_2O_2 levels occurred in a time scale of minutes (such as in the case of axonal growth cones, the axon, the soma and varicosities) or in a range of seconds (such as in the case of dendritic growth cones, dynamic zones and filopodia). Supplementary figures 2E,F show that although H_2O_2 levels are continuously fluctuating during the period registered, the levels of H_2O_2 are always relatively high. Each image presented in this study has its corresponded supplementary video (Supplementary videos). The ratio scales bars of figures 6E,F are different than in Supplementary figures 2C,F in order to allow a proper measurement of the ratio during the H_2O_2 perfusion.

Glutathione maintains axonal integrity during the early development of CGN

High levels of ROS have been associated with an alteration of cell physiology and structural damage that leads to cell death (Ryter et al., 2007). Also, as we mentioned above, glutathione is a major antioxidant system in neurons. Thus, we evaluated the effect of glutathione depletion by BSO treatment in the structural integrity and H_2O_2 levels of CGN axons. To achieve this, we visualized a partial population of CGN stained with PKH67 dye, which allowed us to study individual axons (Supplementary figure 3). Figure 7A shows that 2 DIV CGN treated with BSO during 42 h show a clear alteration in the axonal structure. Some cells show axons with multiple spheroid-like structures (Fig. 7B). In other cells, these structures seem to increase in size and number leading to a collapse-like appearance of the axon. No evident alteration in the structure of the somas were detected. The observed effects of BSO are mediated by ROS because the presence of the antioxidant Euk-134 completely prevented the mentioned alterations (Fig. 7A,B). The quantification of the morphological alteration induced by BSO is shown in Fig. 7C. About 40% of the BSO treated cells showed a collapsed-like axon and by 50% corresponded to CGN with little spheroid-like structures. Also, about 10% of the cells with spheroids-like structures were not rescued by Euk-134 and no collapsed-like axons were observed in the presence of the antioxidant, suggesting that the formation of the small spheroids precede the formation of the collapsed-like axons and that neurons show different susceptibility to glutathione depletion. When CGN transfected with the plasmid HyPer were treated with BSO for 42 h, we found that practically all the spheroid-like structures contained high levels of H_2O_2, which was more evident in the collapsed-like axons. No evident increment in H_2O_2 levels was detected in the somas (Fig. 7D). We also observed that axonal continuity was not lost in the collapsed-like axons, since it was possible to observe the continuity of the axons in neurons transfected with HyPer (Data not shown).

NOX2 regulates neurite outgrowth of CGN

We hypothesized that NOX2 might be involved in the neurite outgrowth of CGN since NOX2 is expressed in growth cones and NOX inhibitors partially decreased the expression of Tau and MAP2. To address this, we measured the neurite outgrowth and ROS levels in CGN obtained from NOX2 KO and wild type mice (Fig. 8). Under these conditions, we found no apparent differences in wild type and NOX2 KO CGN in the phase contrast images at 1 and 2 DIV (Fig. 8C). When CGN were stained with PKH67 and the neurites were measured, we found that CGN neurites from wild type mouse showed a consistent growth that was markedly increased by about three times from 1 to 2 DIV (Fig. 8A,B). In contrast, the neurite outgrowth of NOX2 KO CGN was about 25% (at 1 DIV) and by 20% (at 2 DIV) lesser than that observed in CGN from wild type animals (Fig. 8A, B). When we measured the levels of ROS in wild type and NOX2 KO CGN, we found that ROS levels increased by two fold from 1 DIV to 2 DIV (Fig. 8C-E). When we compared the levels of ROS between wild type and NOX2 KO CGN at 1 and 2 DIV, no differences were found (Fig. 8F).

Discussion

ROS and NOX during CGN development

In this study, we found that ROS production is regulated throughout CGN development. In this regard, we propose that CGN development could be divided into two distinct phases. In the first phase, ROS increase during the first 2 DIV and remain high until 3 DIV, which is independent of the state of depolarization. In the second phase, the levels of ROS are dependent on the state of depolarization; in depolarizing conditions, ROS levels diminish at 4 DIV and then remain low during the subsequent days, while in non-depolarizing conditions, ROS levels continue increasing at 4 and 5 DIV. During these two phases, CGN undergo different developmental processes. During the first phase, CGN initiate the biochemical (Gallo et al., 1987) and morphological (Powell et al., 1997) processes of maturation and at 3 DIV most CGN have already developed the axon and multiple short dendrites (de la Torre-Ubieta et al., 2010). The second phase is coincident with a dependence of CGN survival on depolarization (Gallo et al., 1987) and dendrite maturation (Shalizi et al., 2006; Ramos et al., 2007).

Our results show that, in spite of the high levels of ROS observed at 2 and 3 DIV, CGN viability is not compromised regardless the state of depolarization. In contrast, during the second phase, our data show a correlation between low ROS levels and CGN survival in depolarizing conditions, but in non-depolarizing conditions high ROS levels are associated with a reduction of the metabolic activity and cell survival. In this regard, we have previously shown that ROS could be signals that trigger the process of apoptotic cell death of CGN at 8 DIV when CGN are switched from a depolarizing condition to a non-depolarizing condition (Ramiro-Cortes and Moran, 2009; Ramiro-Cortes et al., 2011). Together, these results suggest that the regulation of ROS during CGN development may be critical for the survival of CGN during the second phase.

Glutathione regulation during CGN development

Here, we also addressed the possibility that glutathione could be responsible for regulating the levels of ROS during development, this is supported by the idea that the balance between ROS production and the expression and activity of the antioxidant systems determine ROS levels in the cells. It is known that during nervous system development, neurons and glial cells contain glutathione and by the postnatal day 5 most neurons have decreased the levels of glutathione, while olfactory mitral and granule cells, cerebellar granule neurons, and dorsal root ganglion neurons consistently retain high levels of glutathione throughout development and in adulthood (Beiswanger et al., 1995). Moreover, glutathione deficient mice die before the embryonic day 8.5 by massive apoptosis (Shi et al., 2000) and mice lacking of glutathione

peroxidase 4 (GPx4) die before the embryonic day 8 also by an increase in apoptosis (Yant et al., 2003). Interestingly, while GPx4 is expressed in neurons, glial cells are devoid of GPx4 (Savaskan et al., 2007); furthermore, it seems that the developing brain constitutes a major site for GPx4 expression, while the specific suppression of GPx4 between the embryonic days 7.5 and 10.5 led to microcephaly and abnormal hindbrain development (Borchert et al., 2006). These studies suggest a fundamental role of glutathione during nervous system development.

In this study, we found changes in the levels of glutathione content during CGN development. In the first phase, when ROS levels are relatively high, the glutathione content increases independently of the state of depolarization; in general, during the time when ROS are in their highest levels, the glutathione content are also in its highest levels. One possibility to explain this observation could be associated with a mechanism to balance the levels of ROS required for optimal redox signaling and to prevent the deleterious effects of ROS during the first phase. The major increase of glutathione content occurred from 0 DIV to 1 DIV which precedes the major increase observed in ROS. Thereby, these results might suggest that glutathione content in CGN development responds to an internal genetic program of the cells, which is independent of the trophic conditions and ROS levels. The idea is supported by the fact that *in vivo*, the glutathione content in the developing cerebellum increases by the time when CGN precursors begin their process of differentiation CGN (Nanda et al., 1996; Rice and Russo-Menna, 1998; Komuro and Yacubova, 2003).

It is known that chronic treatments with BSO and oxygen in rat-pups lead to a high rate of apoptosis in the hippocampus, cerebellum, basal forebrain and striatum (Taglialatela et al., 1998). In this regard our results demonstrate that the increase in the glutathione content is necessary to allow CGN development since glutathione depletion at 2 DIV drastically reduces CGN survival, but it does not affect CGN survival in later stages of CGN development. This process could be explained by two major mechanisms of action of glutathione, one is the interaction of glutathione with proteins, which modifies signaling pathways during variations in ROS homeostasis (Grek et al., 2013) and by a second mechanism that involves the antioxidant actions of glutathione. The fact that the antioxidant Euk-134 completely rescues CGN viability under glutathione depletion, strongly suggests that the effect of glutathione in CGN survival is due to its antioxidant properties.

During the second phase, the levels of glutathione content are dependent on the state of depolarization. In depolarizing conditions, glutathione remains high from 3 to 5 DIV, a time when ROS levels decrease markedly. In contrast, in non-depolarizing conditions the glutathione content diminishes since 4 DIV, which correlates with the observed decrease in CGN survival and high ROS levels. This decrease in glutathione content can be considered an early hallmark of the cell death progression (Franco and Cidlowski, 2012). To rule out the possibility that the decrease of glutathione content is responsible for the cell death observed during the second phase in non-depolarizing conditions, we diminished the levels of glutathione with BSO; however, although glutathione content was importantly reduced with BSO treatment, the cell viability at the incubation tested times did not alter CGN survival at 5 DIV under depolarizing conditions, indicating that a decrease in glutathione content is not sufficient to trigger cell death in developing CGN and that the decrease in glutathione content during the second phase in non-depolarizing conditions is probably a consequence of the cell death process.

ROS and NOX in CGN maturation

The possibility that ROS are required for CGN development in the first phase is supported by our results showing that antioxidant conditions markedly diminished the levels of Tau and MAP2 proteins. Interestingly, we found that the antioxidants Ebselen and Euk-134 only reduced MAP2 expression at 2 DIV, while the NOX inhibitors, AEBSF and apocynin diminished the levels of Tau at 1 and 2 DIV, suggesting a more specific action of the ROS produced by NOX activity in this process. None of these treatments diminished the expression of these proteins at 3 DIV, which could be explained by the fact that between 2 and 3 DIV the levels of these two proteins are not significantly increased under control conditions and/or that by this time the maturational process of CGN is no longer dependent on ROS.

It is noteworthy to mention that, based on the proposed mechanism of inhibition of AEBSF and apocynin, their primary target would be the NOX1 and NOX2 homologues (Jaquet et al., 2009). However, since the effect of these inhibitors is only partial, in this study we cannot exclude the contribution of other NOX homologues and/or other sources of ROS in the CGN development. Also, although we cannot discard that part of the effects of apocynin or AEBSF could be due to unspecific actions; their effects are validated with the use of a second NOX inhibitor (apocynin or AEBSF). Thus, we think that the results obtained using separately both inhibitors with similar results may indicate that pathway Ras/Raf/MEK/ERKs (Kaplan and Miller, 2000; Patapoutian and Reichardt, 2001). Besides, NGF induces an increase in the levels of ROS produced by NOX after 10 min of treatment (Suzukawa et al., 2000). These ROS induce the phosphorylation of TrkA through the inhibition of protein tyrosine phosphatases and the formation of complexes with the scaffold proteins Shc, Grb2 and Sos, which are required for the activation of the MAPK pathway (Kamata et al., 2005). On the other hand, NGF also induces the phosphorylation of ERKs after 30 min, which induces the expression and activity of the mitochondrial super oxide dismutase (MnSOD), and the H_2O_2 resulting from the MnSOD activity induces a second phosphorylation of ERKs, which is essential for PC12 differentiation (Cassano et al., 2010).

Further studies have shown that NOX enzymes mediate the neuronal differentiation in different models (Wang et al., 2007; Kennedy et al., 2010; Nitti et al., 2010; Le Belle et al., 2011). In the present study, we found that NOX shows a pattern of activity similar to the ROS levels observed during the first and second phases of CGN development in depolarizing conditions. Different NOX homologues could contribute to the observed NOX activity, which is in line with our findings about the expression of NOX1 and NOX2 enzymes that are highly regulated throughout CGN development. Overall, in the first phase, the mRNA levels of both, NOX1 and NOX2 are up-regulated, while in the second phase they are down-regulated. Interestingly, each NOX homologue showed a slightly different pattern of expression, which suggests that these enzymes might have distinct roles during CGN development.

It is important to note that the expression of NOX2 follows more closely both the total NOX activity and the ROS levels. Furthermore, the mRNA levels of NOX2 are considerably more abundant than mRNA NOX1 levels. Thereby, we hypothesize that NOX2 could be the main source of the ROS produced during CGN development. However, we found no differences in the levels of ROS measured by dihydroethidium between NOX2 KO and wild type CGN at 1 DIV and 2 DIV. Thus, these results suggest that NOX2 is not responsible for the increase of ROS observed during the first phase of CGN development. Nevertheless, we cannot discard a possible compensatory mechanism in the NOX2 KO CGN, which has been demonstrated in other preparations where an up-regulation of NOX4 occurs in NOX2 KO mice; in cells where NOX2 gene has been silenced (Pendyala et al., 2009) or when an indirect down-regulation of NOX2 leads to an overexpression of NOX4 (Sedeek et al., 2010).

Despite the fact that ROS levels measured by dihydroethidium were not affected in NOX2 KO CGN, we found a slightly decrease in the length of CGN axons at 1 DIV and 2 DIV, which corroborates the importance of NOX2 during CGN development. Our findings that NOX2 KO CGN showed a reduction of neurite outgrow is in agreement with other studies carried out in *Aplysia* neurons that shows that NOX inhibitors reduce actin flow and its assembly at the leading edge of the axonal growth cone, leading to a decrease of the neurite outgrowth (Munnamalai and Suter, 2009). The regulation of NOX2 in the axonal growth cones of *Aplysia* neurons seems to be bidirectional, since the stimulation of NOX2 produces H_2O_2, which regulates F-actin dynamics and neurite outgrowth; on the other hand, the stimulation of neurite outgrowth induces the proximity of the cytoplasmic subunit of NOX2, p40phox, to its catalytic subunit, gp91phox, indicating that the regulation of cytoskeleton dynamics affects NOX2 activity (Munnamalai et al., 2014).

The relevance of NOX2 in the nervous system development is strengthened by the alterations of the brain physiology observed in NOX2 KO mice. These animals display deficits in hippocampal synaptic plasticity and mild impairments in cognitive function, as well a slight deficiency in motor learning (Kishida et al., 2006), which might be attributed to an altered function in either the cerebellar cortex or the deep cerebellar nuclei (Caston et al., 1995). Moreover, these mice have less proliferating cells in the subventricular zone, less migrating cells and fewer neuronal differentiation in the olfactory bulb than in wild type mice (Le Belle et al., 2011). However, it has not been reported if the alterations in motor behavior observed in NOX2 KO mice are due to aberrations in the formation of cerebellar circuits and /or alterations in the synaptic plasticity and function. In a previous study, we found that the treatment of developing rats with apocynin or with the antioxidant MnTmPyP, produced alterations in the cerebellar foliation as well as a deficiency in motor behavior, measured as alteration in the rod walking and Rotarod tests (Coyoy et al., 2013). The results obtained in the present study suggest that part of the actions of ROS and NOX could be related to neurite development during cerebellar cortex formation.

H2O2 and NOX localization

In line with the above findings, we explored the possibility that H_2O_2 were produced locally in developing CGN, as well as the possible contribution of glutathione as a regulator of H_2O_2. Although it is not completely understood how redox signaling occurs, there is increasing evidence indicating that the NOX is involved in the production of ROS required for CGN maturation.

Our results are in accordance with previous observations indicating that ROS produced by NOX enzymes may act as signaling molecules in the regulation of the neuronal differentiation of PC12 cells. In these cells, it is well known that the neurotrophin NGF induces the expression of different neuronal markers such as βIII-tubulin, GAP-43 and neurofilament L through the activation of the receptor TrkA which leads to the activation of the signaling

physiological function of ROS, and particularly H_2O_2, might occur by the activation of specific signaling pathways through reversible redox modifications of proteins in subcellular compartments (Chen et al., 2009; Ushio-Fukai, 2009b; Gough and Cotter, 2011; Mishina et al., 2011b; Kaludercic et al., 2014). Interestingly, we found different regions of the developing axons and dendrites where H_2O_2 is continuously produced. These regions apparently correspond to those regions where NOX2 is expressed. For example, NOX2 is enriched in filopodia, either in the axonal shaft where filopodia are located or inside the filopodia, coincident with the microdomains where H_2O_2 is continuously produced, which suggest that both, NOX2 and H_2O_2 might be related to filopodial dynamics. Moreover, we also observed that the increase of H_2O_2 inside the filopodia occurs previous to the filopodia elongation, and that after the process of filopodia retraction, the amount of H_2O_2 returns to basal levels. Together, these results strongly suggest that H_2O_2 is involved in filopodia formation and that NOX2 might be a possible source for the H_2O_2 produced. This idea

is supported by previous studies showing that ROS control actin dynamics (Munnamalai and Suter, 2009; Sakai et al., 2012; Lee et al., 2013; Munnamalai et al., 2014). In neutrophils, the physiological levels of H_2O_2 produced by NOX2, negatively regulate the actin polymerization by inducing actin glutathionylation, while the overexpression of glutaredoxin 1, which is the enzyme that catalyzes actin deglutathionylation, leads to multiple pseudopodia formation (Sakai et al., 2012). In macrophages, the formation of filopodia and actin polymerization is regulated by the reversible oxidation of two methionine residues by MICAL1 and MICAL2, the oxidation of these residues leads to actin disassembly, while the reduction of these residues by the methionine-R-sulfoxide reductase B1 lead actin assembly, which in conjunction orchestrate actin dynamics and macrophage function (Lee et al., 2013). Therefore, we speculate that redox reactions might control filopodia formation in developing CGN.

On the other hand, the localization of NOX2 in the axonal growth cones also correlates with the observed high levels of H_2O_2. This result suggests that H_2O_2 might be related to axonal growth cone dynamics and that H_2O_2 could be produced by NOX2, which is in line with the observation that NOX2 KO CGN showed less axonal growth than the wild type CGN. This association has been previously examined in *Aplysia* neurons, where the H_2O_2 produced by NOX2 modulates f-actin dynamics and promotes axonal growth (Munnamalai et al., 2014). On the other hand, it has also been shown that H_2O_2 negatively regulates axonal growth. In dorsal root ganglion neurons, semaphorin3A induces growth cone collapse by the regulation of cytoskeleton through CRMP2. Semaphorine3A induces the generation of H_2O_2 in the axonal growth cone through MICAL, which oxidizes CRMP2 and induces the formation of a transient disulfide-linked homodimer between the cysteines 504 of two CRMP2 proteins. Then, this homodimer is reduced by thioredoxin that forms a disulfide bond with one molecule of CRMP2. This complex is crucial for CRMP2 phosphorylation by GSK3-β, which ultimately produces the growth cone collapse of these neurons (Morinaka et al., 2011). Although it is not completely understood the regulation of the axonal growth cone dynamics by H_2O_2, it seems that multiple ROS sources are localized in this region and it is clear that ROS regulate the mechanisms responsible for the morphological organization of these structures; thereby, further studies are required to asses these issues.

Finally, we explored the possibility that axonal integrity were altered in the absence of glutathione. Interestingly, while we found no evident alterations in the neuronal soma, we observed a severe aberrant axonal alteration in CGN treated with BSO that conduces to its degeneration followed by cell death, which suggest that ROS levels are critical for both axonal formation and integrity. The spheroid-like structures formed in BSO treatments are possibly formed by the dysregulation of the H_2O_2 production in the axon, since these structures are enriched in H_2O_2 and their formation is drastically inhibited by the antioxidant treatment. The spheroid-like structures found in CGN treated with BSO, resemble the structures found in a classic model of axonal degeneration. This could have clinical implications since axons degenerate before cell bodies in different neurodegenerative diseases such as amyotrophic lateral sclerosis, Alzheimer's disease, Parkinson's disease and Huntington's disease, among others (Coleman, 2005; Conforti et al., 2014), which has been related to a process of oxidative stress (Barnham et al., 2004). Thereby we speculate that the dysregulation of the mechanisms that regulate ROS during neuronal development could be similar to those that are involved in neurodegenerative diseases.

Conclusions

In the present study we showed evidence suggesting that ROS regulate different aspects of CGN development. During the first 3 DIV, ROS increased which is necessary for CGN maturation. If the production of these molecules is not regulated in the subsequent days due to the trophic conditions (i.e., low potassium), ROS lead to CGN death. Before the peak of ROS, glutathione content increased, which seems to be required for CGN to complete their development, since the pharmacologically induced depletion of glutathione at this time conduced to CGN death. Most of the ROS produced at this stage are probably produced by NOX2, which is mainly localized in filopodia and growth cones. These regions correspond to microdomains in which H_2O_2 is continuously produced. In line with these results, neurite outgrowth is less in NOX2 KO CGN than in wild type CGN, which suggest that NOX2 is important during the early stages of CGN development. Finally, the pharmacological depletion of glutathione, demonstrated the importance of glutathione as a regulator of the H_2O_2 produced in CGN axons and the importance of ROS during the axonal morphogenesis. Together these results suggest that the H_2O_2 produced by NOX2 in combination with glutathione, control axonal morphogenesis in CGN, which contribute to our understanding about neuronal development.

Competing interests

The authors declare that they have no competing interests

Funding

This work was supported by Dirección General de Asuntos del Personal Académico-Universidad Nacional Autónoma de México [IN206213] and Consejo Nacional de Ciencia y Tecnología de México [179234]. Mauricio Olguín-Albuerne was supported by a CONACYT fellowship.

Authors' contributions

Mauricio Olguín-Albuerne carried out the experiments, contributed to analyze and interpret the data, drafted the manuscript and participated in the design of the study. Julio Morán conceived of the study, and participated in its design

and coordination and contributed to draft the manuscript. All authors read and approved the final manuscript.

References

Avshalumov MV, Patel JC, Rice ME (2008) AMPA receptor-dependent H2O2 generation in striatal medium spiny neurons but not dopamine axons: one source of a retrograde signal that can inhibit dopamine release. J Neurophysiol 100:1590-1601.

Avshalumov MV, Chen BT, Koos T, Tepper JM, Rice ME (2005) Endogenous hydrogen peroxide regulates the excitability of midbrain dopamine neurons via ATP-sensitive potassium channels. The Journal of neuroscience : the official journal of the Society for Neuroscience 25:4222-4231.

Baker K, Marcus CB, Huffman K, Kruk H, Malfroy B, Doctrow SR (1998) Synthetic combined superoxide dismutase/catalase mimetics are protective as a delayed treatment in a rat stroke model: a key role for reactive oxygen species in ischemic brain injury. The Journal of pharmacology and experimental therapeutics 284:215-221.

Barnes AP, Polleux F (2009) Establishment of axon-dendrite polarity in developing neurons. Annual review of neuroscience 32:347-381.

Barnham KJ, Masters CL, Bush AI (2004) Neurodegenerative diseases and oxidative stress. Nat Rev Drug Discov 3:205-214.

Bedard K, Krause KH (2007) The NOX family of ROS-generating NADPH oxidases: physiology and pathophysiology. Physiol Rev 87:245-313.

Beiswanger CM, Diegmann MH, Novak RF, Philbert MA, Graessle TL, Reuhl KR, Lowndes HE (1995) Developmental changes in the cellular distribution of glutathione and glutathione S-transferases in the murine nervous system. Neurotoxicology 16:425-440.

Belousov VV, Fradkov AF, Lukyanov KA, Staroverov DB, Shakhbazov KS, Terskikh AV, Lukyanov S (2006) Genetically encoded fluorescent indicator for intracellular hydrogen peroxide. Nature methods 3:281-286.

Borchert A, Wang CC, Ufer C, Schiebel H, Savaskan NE, Kuhn H (2006) The role of phospholipid hydroperoxide glutathione peroxidase isoforms in murine embryogenesis. The Journal of biological chemistry 281:19655-19664.

Brennan AM, Suh SW, Won SJ, Narasimhan P, Kauppinen TM, Lee H, Edling Y, Chan PH, Swanson RA (2009) NADPH oxidase is the primary source of superoxide induced by NMDA receptor activation. Nature neuroscience 12:857-863.

Caballero-Benitez A, Alavez S, Uribe RM, Moran J (2004) Regulation of glutamate-synthesizing enzymes by NMDA and potassium in cerebellar granule cells. The European journal of neuroscience 19:2030-2038.

Cassano S, Agnese S, D'Amato V, Papale M, Garbi C, Castagnola P, Ruocco MR, Castellano I, De Vendittis E, Santillo M, Amente S, Porcellini A, Avvedimento EV (2010) Reactive oxygen species, Ki-Ras, and mitochondrial superoxide dismutase cooperate in nerve growth factor-induced differentiation of PC12 cells. The Journal of biological chemistry 285:24141-24153.

Caston J, Vasseur F, Stelz T, Chianale C, Delhaye-Bouchaud N, Mariani J (1995) Differential roles of cerebellar cortex and deep cerebellar nuclei in the learning of the equilibrium behavior: studies in intact and cerebellectomized lurcher mutant mice. Brain research Developmental brain research 86:311-316.

Celotto AM, Liu Z, Vandemark AP, Palladino MJ (2012) A novel Drosophila SOD2 mutant demonstrates a role for mitochondrial ROS in neurodevelopment and disease. Brain and behavior 2:424-434.

Coleman M (2005) Axon degeneration mechanisms: commonality amid diversity. Nature reviews Neuroscience 6:889-898.

Conforti L, Gilley J, Coleman MP (2014) Wallerian degeneration: an emerging axon death pathway linking injury and disease. Nature reviews Neuroscience 15:394-409.

Coyoy A, Olguin-Albuerne M, Martinez-Briseno P, Moran J (2013) Role of reactive oxygen species and NADPH-oxidase in the development of rat cerebellum. Neurochemistry international 62:998-1011.

Chen K, Craige SE, Keaney JF, Jr. (2009) Downstream targets and intracellular compartmentalization in Nox signaling. Antioxid Redox Signal 11:2467-2480.

Cheret C, Gervais A, Lelli A, Colin C, Amar L, Ravassard P, Mallet J, Cumano A, Krause KH, Mallat M (2008) Neurotoxic Activation of Microglia Is Promoted by a Nox1-Dependent NADPH Oxidase. Journal of Neuroscience 28:12039-12051.

de la Torre-Ubieta L, Gaudilliere B, Yang Y, Ikeuchi Y, Yamada T, DiBacco S, Stegmuller J, Schuller U, Salih DA, Rowitch D, Brunet A, Bonni A (2010) A FOXO-Pak1 transcriptional pathway controls neuronal polarity. Genes & development 24:799-813.

Dehmelt L, Halpain S (2004) Actin and microtubules in neurite initiation: are MAPs the missing link? Journal of neurobiology 58:18-33.

Diatchuk V, Lotan O, Koshkin V, Wikstroem P, Pick E (1997) Inhibition of NADPH oxidase activation by 4-(2-aminoethyl)-benzenesulfonyl fluoride and related compounds. The Journal of biological chemistry 272:13292-13301.

Dringen R (2000) Metabolism and functions of glutathione in brain. Progress in neurobiology 62:649-671.

Droge W (2002) Free radicals in the physiological control of cell function. Physiol Rev 82:47-95.

Dvoriantchikova G, Grant J, Santos ARC, Hernandez E, Ivanov D (2012) Neuronal NAD(P)H Oxidases Contribute to ROS Production and Mediate RGC Death after Ischemia. Investigative ophthalmology & visual science 53:2823-2830.

Franco R, Cidlowski JA (2009) Apoptosis and glutathione: beyond an antioxidant. Cell death and differentiation 16:1303-1314.

Franco R, Cidlowski JA (2012) Glutathione efflux and cell death. Antioxid Redox Signal 17:1694-1713.

Gallo V, Kingsbury A, Balazs R, Jorgensen OS (1987) The role of depolarization in the survival and differentiation of cerebellar granule cells in culture. The Journal of neuroscience : the official journal of the Society for Neuroscience 7:2203-2213.

Goldsmit Y, Erlich S, Pinkas-Kramarski R (2001) Neuregulin induces sustained reactive oxygen species generation to mediate neuronal differentiation. Cell Mol Neurobiol 21:753-769.

Gough DR, Cotter TG (2011) Hydrogen peroxide: a Jekyll and Hyde signalling molecule. Cell death & disease 2:e213.

Grek CL, Zhang J, Manevich Y, Townsend DM, Tew KD (2013) Causes and consequences of cysteine S-glutathionylation. The Journal of biological chemistry 288:26497-26504.

Halliwell B (2009) The wanderings of a free radical. Free radical biology & medicine 46:531-542.

Hernandez-Enriquez B, Guemez-Gamboa A, Moran J (2011) Reactive oxygen species are related to ionic fluxes and volume decrease in apoptotic cerebellar granule neurons: role of NOX enzymes. Journal of neurochemistry 117:654-664.

Ito S, Takeichi M (2009) Dendrites of cerebellar granule cells correctly recognize their target axons for synaptogenesis in vitro. Proceedings of the National Academy of Sciences of the United States of America 106:12782-12787.

Jaquet V, Scapozza L, Clark RA, Krause KH, Lambeth JD (2009) Small-Molecule NOX Inhibitors: ROS-Generating NADPH Oxidases as Therapeutic Targets. Antioxid Redox Sign 11:2535-2552.
Jones DP (2006) Redefining oxidative stress. Antioxid Redox Signal 8:1865-1879.
Kaludercic N, Deshwal S, Di Lisa F (2014) Reactive oxygen species and redox compartmentalization. Frontiers in physiology 5:285.
Kamata H, Hirata H (1999) Redox regulation of cellular signalling. Cell Signal 11:1-14.
Kamata H, Oka S, Shibukawa Y, Kakuta J, Hirata H (2005) Redox regulation of nerve growth factor-induced neuronal differentiation of PC12 cells through modulation of the nerve growth factor receptor, TrkA. Arch Biochem Biophys 434:16-25.
Kaplan DR, Miller FD (2000) Neurotrophin signal transduction in the nervous system. Current opinion in neurobiology 10:381-391.
Kennedy KA, Ostrakhovitch EA, Sandiford SD, Dayarathna T, Xie X, Waese EY, Chang WY, Feng Q, Skerjanc IS, Stanford WL, Li SS (2010) Mammalian numb-interacting protein 1/dual oxidase maturation factor 1 directs neuronal fate in stem cells. The Journal of biological chemistry 285:17974-17985.
Kim SH, Won SJ, Sohn S, Kwon HJ, Lee JY, Park JH, Gwag BJ (2002) Brain-derived neurotrophic factor can act as a pronecrotic factor through transcriptional and translational activation of NADPH oxidase. The Journal of cell biology 159:821-831.
Kishida KT, Hoeffer CA, Hu D, Pao M, Holland SM, Klann E (2006) Synaptic plasticity deficits and mild memory impairments in mouse models of chronic granulomatous disease. Molecular and cellular biology 26:5908-5920.
Komuro H, Yacubova E (2003) Recent advances in cerebellar granule cell migration. Cellular and molecular life sciences : CMLS 60:1084-1098.
Konishi Y, Stegmuller J, Matsuda T, Bonni S, Bonni A (2004) Cdh1-APC controls axonal growth and patterning in the mammalian brain. Science 303:1026-1030.
Le Belle JE, Orozco NM, Paucar AA, Saxe JP, Mottahedeh J, Pyle AD, Wu H, Kornblum HI (2011) Proliferative neural stem cells have high endogenous ROS levels that regulate self-renewal and neurogenesis in a PI3K/Akt-dependant manner. Cell Stem Cell 8:59-71.
Lee BC, Peterfi Z, Hoffmann FW, Moore RE, Kaya A, Avanesov A, Tarrago L, Zhou Y, Weerapana E, Fomenko DE, Hoffmann PR, Gladyshev VN (2013) MsrB1 and MICALs regulate actin assembly and macrophage function via reversible stereoselective methionine oxidation. Molecular cell 51:397-404.
Lu Q, Wainwright MS, Harris VA, Aggarwal S, Hou YL, Rau T, Poulsen DJ, Black SM (2012) Increased NADPH oxidase-derived superoxide is involved in the neuronal cell death induced by hypoxia-ischemia in neonatal hippocampal slice cultures. Free Radical Bio Med 53:1139-1151.
Lubos E, Loscalzo J, Handy DE (2011) Glutathione peroxidase-1 in health and disease: from molecular mechanisms to therapeutic opportunities. Antioxid Redox Signal 15:1957-1997.
Miller EW, Tulyathan O, Isacoff EY, Chang CJ (2007) Molecular imaging of hydrogen peroxide produced for cell signaling. Nature chemical biology 3:263-267.
Mishina NM, Tyurin-Kuzmin PA, Markvicheva KN, Vorotnikov AV, Tkachuk VA, Laketa V, Schultz C, Lukyanov S, Belousov VV (2011a) Does Cellular Hydrogen Peroxide Diffuse or Act Locally? Antioxidants & redox signaling 14:1-7.
Mishina NM, Tyurin-Kuzmin PA, Markvicheva KN, Vorotnikov AV, Tkachuk VA, Laketa V, Schultz C, Lukyanov S, Belousov VV (2011b) Does cellular hydrogen peroxide diffuse or act locally? Antioxid Redox Signal 14:1-7.
Moran J, Patel AJ (1989) Effect of potassium depolarization on phosphate-activated glutaminase activity in primary cultures of cerebellar granule neurons and astroglial cells during development. Brain research Developmental brain research 46:97-105.
Morinaka A, Yamada M, Itofusa R, Funato Y, Yoshimura Y, Nakamura F, Yoshimura T, Kaibuchi K, Goshima Y, Hoshino M, Kamiguchi H, Miki H (2011) Thioredoxin mediates oxidation-dependent phosphorylation of CRMP2 and growth cone collapse. Sci Signal 4:ra26.
Munnamalai V, Suter DM (2009) Reactive oxygen species regulate F-actin dynamics in neuronal growth cones and neurite outgrowth. Journal of neurochemistry 108:644-661.
Munnamalai V, Weaver CJ, Weisheit CE, Venkatraman P, Agim ZS, Quinn MT, Suter DM (2014) Bidirectional interactions between NOX2-type NADPH oxidase and the F-actin cytoskeleton in neuronal growth cones. Journal of neurochemistry 130:526-540.
Nanda D, Tolputt J, Collard KJ (1996) Changes in brain glutathione levels during postnatal development in the rat. Brain research Developmental brain research 94:238-241.
Nitti M, Furfaro AL, Cevasco C, Traverso N, Marinari UM, Pronzato MA, Domenicotti C (2010) PKC delta and NADPH oxidase in retinoic acid-induced neuroblastoma cell differentiation. Cell Signal 22:828-835.
Parnham MJ, Kindt S (1984) A novel biologically active seleno-organic compound--III. Effects of PZ 51 (Ebselen) on glutathione peroxidase and secretory activities of mouse macrophages. Biochemical pharmacology 33:3247-3250.
Patapoutian A, Reichardt LF (2001) Trk receptors: mediators of neurotrophin action. Current opinion in neurobiology 11:272-280.
Pendyala S, Gorshkova IA, Usatyuk PV, He D, Pennathur A, Lambeth JD, Thannickal VJ, Natarajan V (2009) Role of Nox4 and Nox2 in hyperoxia-induced reactive oxygen species generation and migration of human lung endothelial cells. Antioxid Redox Signal 11:747-764.
Pourova J, Kottova M, Voprsalova M, Pour M (2010) Reactive oxygen and nitrogen species in normal physiological processes. Acta Physiol (Oxf) 198:15-35.
Powell SK, Rivas RJ, Rodriguez-Boulan E, Hatten ME (1997) Development of polarity in cerebellar granule neurons. Journal of neurobiology 32:223-236.
Rahman I, Kode A, Biswas SK (2006) Assay for quantitative determination of glutathione and glutathione disulfide levels using enzymatic recycling method. Nat Protoc 1:3159-3165.
Ramiro-Cortes Y, Moran J (2009) Role of oxidative stress and JNK pathway in apoptotic death induced by potassium deprivation and staurosporine in cerebellar granule neurons. Neurochemistry international 55:581-592.
Ramiro-Cortes Y, Guemez-Gamboa A, Moran J (2011) Reactive oxygen species participate in the p38-mediated apoptosis induced by potassium deprivation and staurosporine in cerebellar granule neurons. Int J Biochem Cell Biol 43:1373-1382.
Ramos B, Gaudilliere B, Bonni A, Gill G (2007) Transcription factor Sp4 regulates dendritic patterning during cerebellar maturation. Proceedings of the National Academy of Sciences of the United States of America 104:9882-9887.
Rice ME, Russo-Menna I (1998) Differential compartmentalization of brain ascorbate and glutathione between neurons and glia. Neuroscience 82:1213-1223.

Ryter SW, Kim HP, Hoetzel A, Park JW, Nakahira K, Wang X, Choi AM (2007) Mechanisms of cell death in oxidative stress. Antioxid Redox Signal 9:49-89.

Sakai J, Li J, Subramanian KK, Mondal S, Bajrami B, Hattori H, Jia Y, Dickinson BC, Zhong J, Ye K, Chang CJ, Ho YS, Zhou J, Luo HR (2012) Reactive oxygen species-induced actin glutathionylation controls actin dynamics in neutrophils. Immunity 37:1037-1049.

Savaskan NE, Borchert A, Brauer AU, Kuhn H (2007) Role for glutathione peroxidase-4 in brain development and neuronal apoptosis: specific induction of enzyme expression in reactive astrocytes following brain injury. Free radical biology & medicine 43:191-201.

Schafer FQ, Buettner GR (2001) Redox environment of the cell as viewed through the redox state of the glutathione disulfide/glutathione couple. Free Radical Bio Med 30:1191-1212.

Schulz JB, Weller M, Klockgether T (1996) Potassium deprivation-induced apoptosis of cerebellar granule neurons: a sequential requirement for new mRNA and protein synthesis, ICE-like protease activity, and reactive oxygen species. The Journal of neuroscience : the official journal of the Society for Neuroscience 16:4696-4706.

Sedeek M, Callera G, Montezano A, Gutsol A, Heitz F, Szyndralewiez C, Page P, Kennedy CR, Burns KD, Touyz RM, Hebert RL (2010) Critical role of Nox4-based NADPH oxidase in glucose-induced oxidative stress in the kidney: implications in type 2 diabetic nephropathy. American journal of physiology Renal physiology 299:F1348-1358.

Shalizi A, Gaudilliere B, Yuan Z, Stegmuller J, Shirogane T, Ge Q, Tan Y, Schulman B, Harper JW, Bonni A (2006) A calcium-regulated MEF2 sumoylation switch controls postsynaptic differentiation. Science 311:1012-1017.

Shi ZZ, Osei-Frimpong J, Kala G, Kala SV, Barrios RJ, Habib GM, Lukin DJ, Danney CM, Matzuk MM, Lieberman MW (2000) Glutathione synthesis is essential for mouse development but not for cell growth in culture. Proceedings of the National Academy of Sciences of the United States of America 97:5101-5106.

Sidlo Z, Reggio PH, Rice ME (2008) Inhibition of striatal dopamine release by CB1 receptor activation requires nonsynaptic communication involving GABA, H2O2, and KATP channels. Neurochemistry international 52:80-88.

Solecki DJ, Govek EE, Tomoda T, Hatten ME (2006) Neuronal polarity in CNS development. Genes & development 20:2639-2647.

Sorce S, Krause KH (2009) NOX enzymes in the central nervous system: from signaling to disease. Antioxid Redox Signal 11:2481-2504.

Suzukawa K, Miura K, Mitsushita J, Resau J, Hirose K, Crystal R, Kamata T (2000) Nerve growth factor-induced neuronal differentiation requires generation of Rac1-regulated reactive oxygen species. The Journal of biological chemistry 275:13175-13178.

Taglialatela G, Perez-Polo JR, Rassin DK (1998) Induction of apoptosis in the CNS during development by the combination of hyperoxia and inhibition of glutathione synthesis. Free radical biology & medicine 25:936-942.

Thiels E, Urban NN, Gonzalez-Burgos GR, Kanterewicz BI, Barrionuevo G, Chu CT, Oury TD, Klann E (2000) Impairment of long-term potentiation and associative memory in mice that overexpress extracellular superoxide dismutase. The Journal of neuroscience : the official journal of the Society for Neuroscience 20:7631-7639.

Tietze F (1969) Enzymic method for quantitative determination of nanogram amounts of total and oxidized glutathione: applications to mammalian blood and other tissues. Anal Biochem 27:502-522.

Tsatmali M, Walcott EC, Crossin KL (2005) Newborn neurons acquire high levels of reactive oxygen species and increased mitochondrial proteins upon differentiation from progenitors. Brain research 1040:137-150.

Tsatmali M, Walcott EC, Makarenkova H, Crossin KL (2006) Reactive oxygen species modulate the differentiation of neurons in clonal cortical cultures. Molecular and cellular neurosciences 33:345-357.

Ushio-Fukai M (2009a) Compartmentalization of Redox Signaling Through NADPH Oxidase-Derived ROS. Antioxid Redox Sign 11:1289-1299.

Ushio-Fukai M (2009b) Compartmentalization of redox signaling through NADPH oxidase-derived ROS. Antioxid Redox Signal 11:1289-1299.

Valencia A, Moran J (2004) Reactive oxygen species induce different cell death mechanisms in cultured neurons. Free Radical Bio Med 36:1112-1125.

Valko M, Leibfritz D, Moncol J, Cronin MT, Mazur M, Telser J (2007) Free radicals and antioxidants in normal physiological functions and human disease. Int J Biochem Cell Biol 39:44-84.

Wang N, Xie K, Huo S, Zhao J, Zhang S, Miao J (2007) Suppressing phosphatidylcholine-specific phospholipase C and elevating ROS level, NADPH oxidase activity and Rb level induced neuronal differentiation in mesenchymal stem cells. J Cell Biochem 100:1548-1557.

Wechsler-Reya RJ, Scott MP (1999) Control of neuronal precursor proliferation in the cerebellum by Sonic Hedgehog. Neuron 22:103-114.

Yant LJ, Ran Q, Rao L, Van Remmen H, Shibatani T, Belter JG, Motta L, Richardson A, Prolla TA (2003) The selenoprotein GPX4 is essential for mouse development and protects from radiation and oxidative damage insults. Free radical biology & medicine 34:496-502.

Yoneyama M, Kawada K, Gotoh Y, Shiba T, Ogita K (2010) Endogenous reactive oxygen species are essential for proliferation of neural stem/progenitor cells. Neurochemistry international 56:740-746.

Table 1. . Frequency counts of structures with low or high levels of H2O2

	Frequency counts (%)						
	0 – 0.5	0.5 – 1	1 – 1.5	1.5 – 2	2 – 2.5	2.5 – 3	3 – 3.5
Axons	4.761	50	38.095	7.142	0	0	0
AGC	0	0	0	26.923	42.307	28.846	1.923
DGC	0	0	41.666	33.333	25	0	0
DZ	0	0	14.285	35.714	14.285	35.714	0
ASF	0	1.886	19.811	36.792	36.792	3.773	0.943
Filopodia	0	0	3.846	50	34.615	11.538	0
Varicosities	0	0	16.129	33.333	36.559	13.978	0

CGN of 2 DIV were transfected with the plasmid HyPer and H_2O_2 levels were detected as detailed in Methods. The levels of H2O2 were normalized with respect to the soma. The frequency of different neuronal structures with low or high levels of H2O2 was counted. Low levels of H2O2 were considered as those levels that were at least 50% less than the levels of the soma, while high levels of H_2O_2 were considered as those levels that exceeded at least 50% the levels of the soma. n=42 (Axons), n=52 (axonal growth cone, AGC), n=12 (dendritic growth cone, DGC), n=14 (dynamic zone, DZ), n=106 (axonal shaft in filopodium, ASF), n=26 (Filopodia), n=93 (Varicosities). Data were acquired from 42 neurons registered in time-lapse imaging.

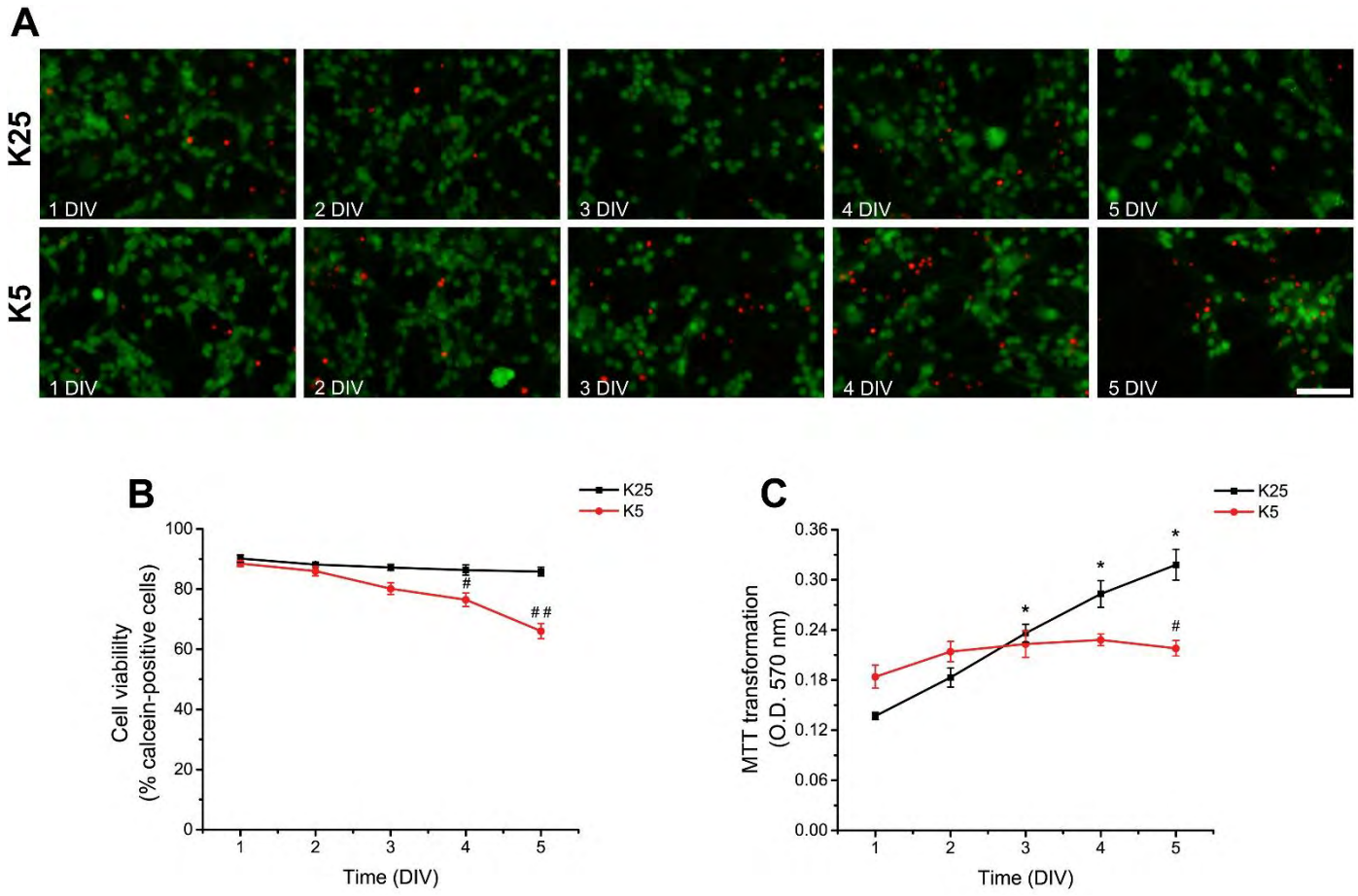

Figure 1. ROS are differentially produced during CGN development.

(A) Representative micrographs of CGN grown in depolarizing conditions (K25) and non-depolarizing conditions (K5) from 1 to 5 DIV. Calcein-positive cells are marked in green and propidium iodide-positive cells are marked in red. (Scale bar, 100 µm). (B) Cell viability is expressed as the percentage of calcein-positive cells from the total number of cells, which was estimated as the sum of calcein-positive cells plus propidium iodide-positive cells. In CGN grown in K5, cell viability was lower at 4 and 5 DIV compared to 4 and 5 DIV CGN grown in K25 (# $P<0.01$, ## $P<0.001$, ANOVA, n=6). Data are mean ± SEM. (C) Metabolic activity was determined by MTT transformation of CGN grown in K25 or K5 from 1 to 5 DIV. In CGN grown in K25, metabolic activity increased at 3, 4 and 5 DIV compared to 1 DIV (⋆ $P<0.001$, ANOVA, n=6). In CGN grown in K5, mitochondrial activity was lower at 5 DIV compared to 5 DIV K25 (# $P<0.001$, ANOVA, n=6). Data are mean ± SEM. (D) Phase contrast and fluorescence micrographs of CGN grown in K25 or K5 during 1 to 5 DIV. (Scale bar, 100 µm). (E) ROS levels of CGN grown in K5 or K25 from 1 to 5 DIV. ROS levels are expressed as mean values of the mean fluorescence intensity of ethidium cation, which is the product of the dihydroethidium oxidation. In CGN grown in K25, the levels of ROS produced at 2 and 3 DIV increased compared to 1 DIV (⋆ $P<0.05$, ANOVA, n=4). In CGN grown in K5, the levels of ROS produced at 4 and 5 DIV were higher compared to 4 and 5 DIV CGN grown in K25 (# $P<0.001$, ANOVA, n=4). Data are mean ± SEM. (F) ROS levels of CGN grown in K25 from 1 to 8 DIV. ROS levels produced from 1 to 8 DIV were higher compared to 0 DIV ($P<0.001$, ANOVA, n=3-9). ROS levels produced at 2 and 3 DIV were higher compared to 0, 1, 4-8 DIV ($P<0.001$, ANOVA, n=3-9). Data are normalized with respect to 2 DIV and are presented as mean ± SD.

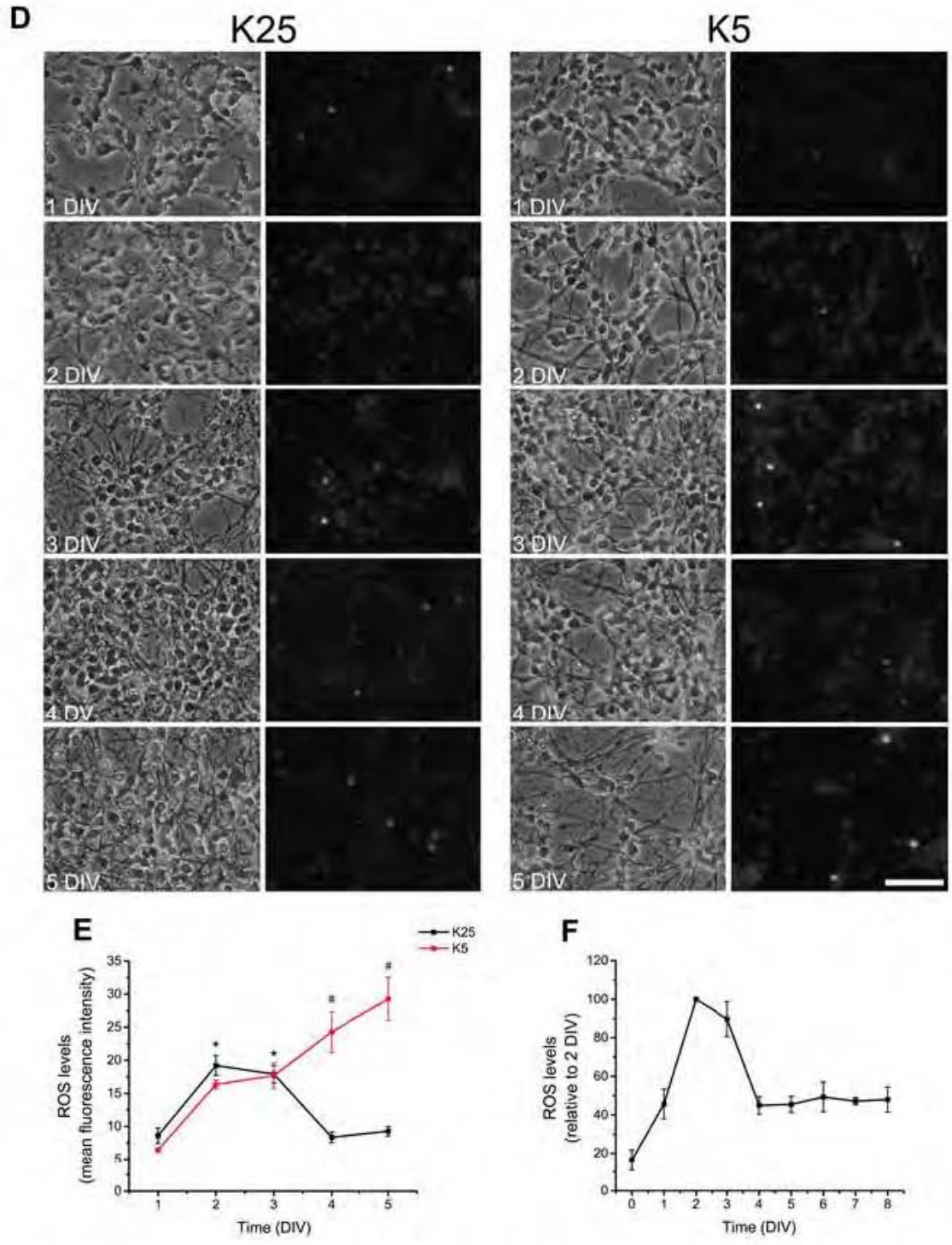
D
K25
K5
1 DIV
2 DIV
3 DIV
4 DIV
5 DIV
E
K25
K5
ROS levels
(mean fluorescence intensity)
Time (DIV)
F
ROS levels
(relative to 2 DIV)
Time (DIV)

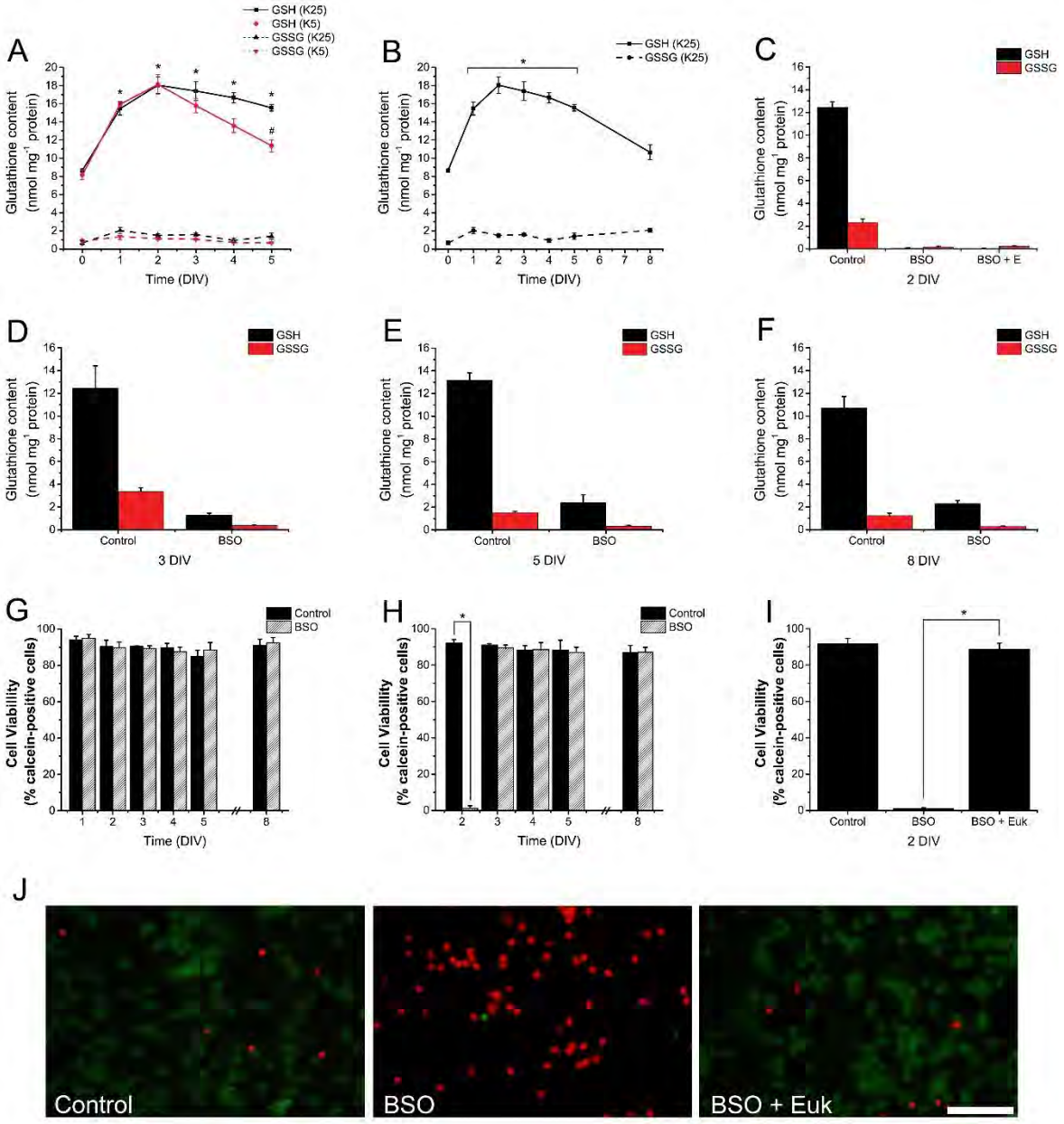

Figure 2. Glutathione is differentially produced and is necessary for CGN survival

(A,B) Reduced glutathione (GSH) and oxidized glutathione (GSSG) content were determined in CGN grown in K25 and K5 from 0 to 8 DIV by a modification of the Tietze recycling assay as detailed in Methods. (A) In CGN grown in K25, the levels of GSH from 1 to 5 DIV were higher compared to 0 DIV (⋆ $P<0.001$, ANOVA, n=4). In CGN grown in K5, the levels of GSH at 5 DIV were lower with respect to 5 DIV K25 (# $P<0.001$, ANOVA, n=4). Data are mean ± SEM. (B) In CGN grown in K25 from 0 to 8 DIV the levels of GSH from 1 to 5 DIV were higher compared to 0 DIV (⋆ $P<0.001$, ANOVA, n=4). Data are mean ± SEM. (C) GSH and GSSG were determined in CGN grown in K25 at 2 DIV and treated with BSO (100 µM) for 48 h and Euk-134 (20 µM) for 24 h. BSO treatments reduced the levels of GSH and GSSG ($P<0.05$, ANOVA nonparametric test, n=5). Data are mean ± SEM. (D-F) GSH and GSSG were determined in CGN grown in K25 at 3, 5 and 8 DIV and treated with BSO (100 µM) for 48 h. BSO treatments reduced the levels of GSH and GSSG in all cases ($P<0.001$, Student's t-test, n=5, n=4, n=4 respectively). (G-I) Cell viability was determined by calcein and propidium iodide. Data are expressed as the percentage of calcein-positive cells from the total number of cells, which was estimated as the sum of calcein-positive cells plus propidium iodide-positive cells. (G) Cell viability was determined in CGN grown in K25 and treated with BSO (100 µM) for 24 h at 1, 2,

3, 4, 5 and 8 DIV (no statistical differences were found, ANOVA, n=4). (H) Cell viability was determined in CGN grown in K25 and treated with BSO (100 μM) for 48 h at 2, 3, 4, 5 and 8 DIV. BSO reduced cell viability at 2 DIV (⋆ P<0.001, ANOVA, n=4). (I) Cell viability was determined in CGN grown in K25 at 2 DIV and treated with BSO (100 μM) for 48 h and Euk-134 (20 μM) for 24 h. Cell viability was diminished by BSO but was completely rescued by Euk-134 (⋆ P<0.001, ANOVA, n=4). Data are mean ± SEM. (J) Representative micrographs of CGN grown in K25 and treated with BSO (100 μM) for 48 h and Euk-134 (20 μM) for 24 h. Calcein-positive cells are marked in green and propidium iodide-positive cells are marked in red. (Scale bar, 100 μm).

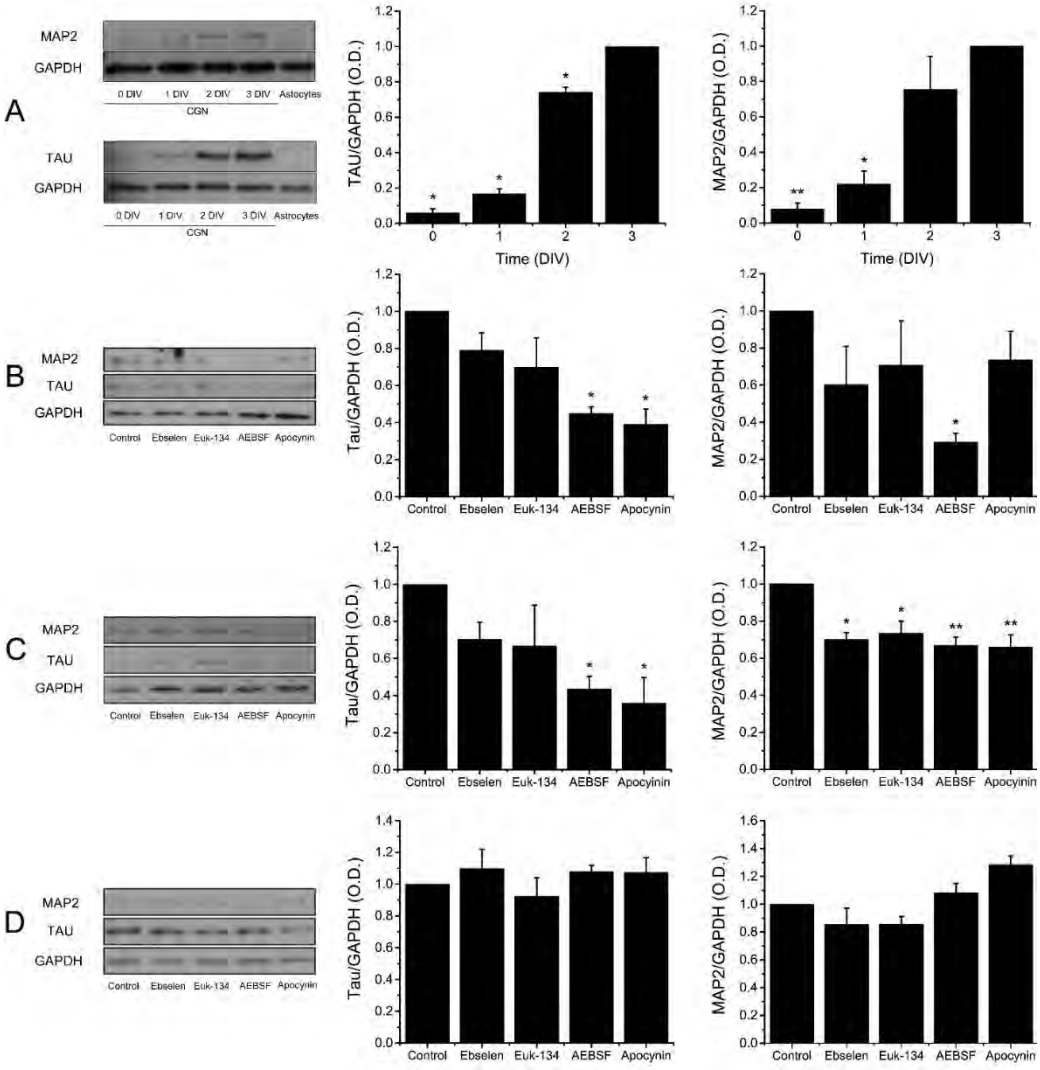

Figure 3. NOX-produced ROS promote CGN maturation

The levels of Tau and MAP2 were determined by Western blot in homogenates of CGN grown in K25 from 0 to 3 DIV and cultured cerebellar astrocytes. (A) Representative blots of Tau (~70 kDa) and MAP2 (~280 kDa) with their respective densitometric analysis of Tau (⋆ P<0.001, ANOVA, n=3) and MAP2 (⋆⋆ P<0.005, ⋆ P<0.001, ANOVA, n=4). Data are normalized with respect to 3 DIV and are mean ± SEM. (B-D) Representative blots of Tau and MAP2 with their respective densitometric analysis of CGN treated with the antioxidants ebselen (10 μM) or Euk-134 (20 μM) or the NOX inhibitors AEBSF (50 μM) or apocynin (400 μM) for 24 h. (B) CGN at 1 DIV, Tau (⋆ P<0.001, ANOVA, n=5), MAP2 (⋆ P=0.007, ANOVA, n=4). (C) CGN at 2 DIV, Tau (⋆ P<0.05, ANOVA, n=4) and MAP2 (⋆ P<0.01, ⋆⋆ P<0.001, ANOVA, n=4). (D) CGN at 3 DIV, Tau (P=0.604, ANOVA, n=5) and MAP2 (P=0.004, ANOVA, n=5). Densitometric values are the ratio of Tau/GADPH or MAP2/GAPDH and are normalized with respect to control. Data are mean ± SEM.

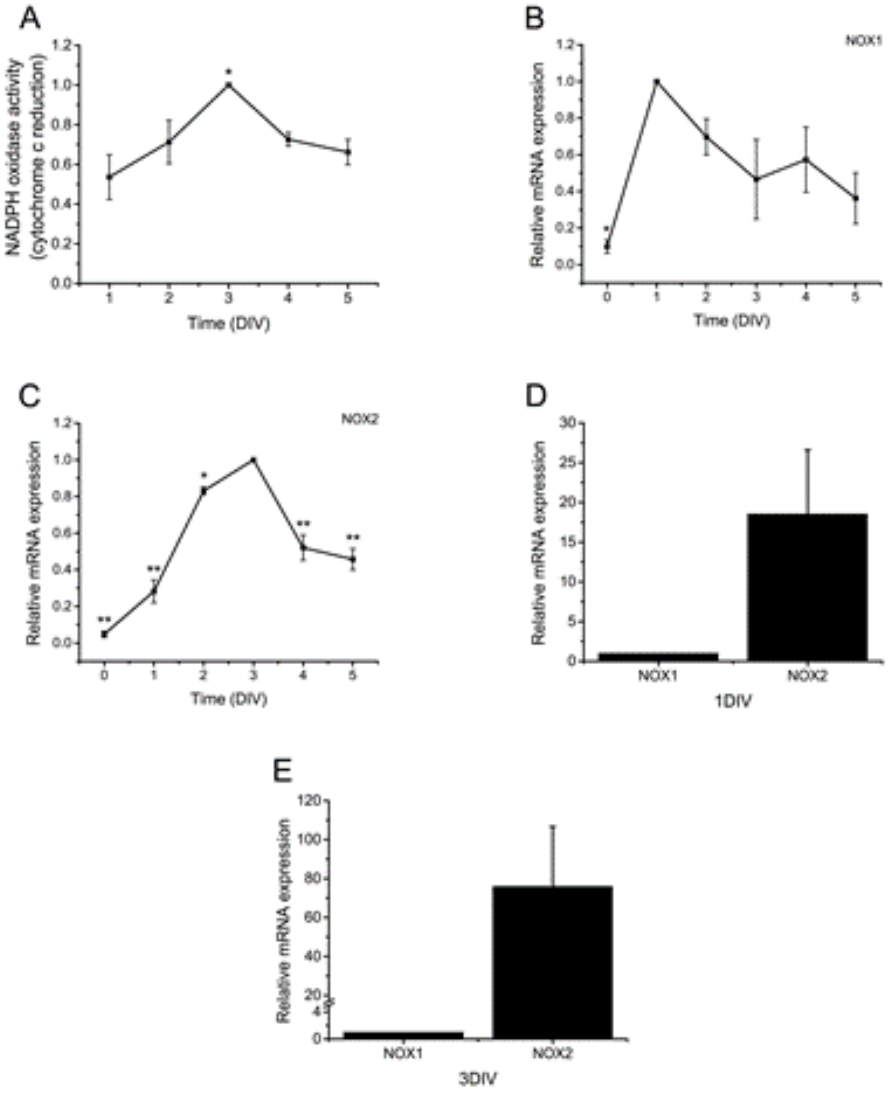

Figure 4. NOX1 and NOX2 are differentially expressed during CGN development

(A) NOX activity was determined in CGN from 1 to 5 DIV by cytochrome c reduction as detailed in Methods. NOX activity significantly increased at 3 DIV as compared to 1 DIV ($P<0.01$, ANOVA, n=5). Data were calculated as nmol min^{-1} per mg protein and are normalized with respect to 3 DIV and are presented as mean ± SEM. (B-E) Relative mRNA levels of NOX1 and NOX2 were determined in CGN from 0 to 5 DIV by the $2^{-\Delta\Delta Ct}$ method of relative quantification as detailed in Methods. Data were normalized with respect to the time in which the expression reaches its maximum level. (B) NOX1 mRNA levels at 0 DIV were significantly different with respect to 1 DIV (⋆ $P=0.007$, ANOVA, n=3). Data are mean ± SEM. (C) NOX2 mRNA levels at 0, 1, 2, 4 and 5 DIV were significantly different with respect to 3 DIV (⋆ $P=0.047$, ⋆⋆ $P<0.001$, ANOVA, n=3). Data are mean ± SEM. (D) NOX2 mRNA levels at 1 DIV were higher as compared to NOX1 mRNA levels (⋆ $P<0.05$, Mann-Whitney U Test, n=4). Data are mean ± SEM. (E) NOX2 mRNA levels at 3 DIV were higher as compared to NOX1 (⋆ $P<0.05$, Mann-Whitney U Test, n=4). Data are mean ± SEM.

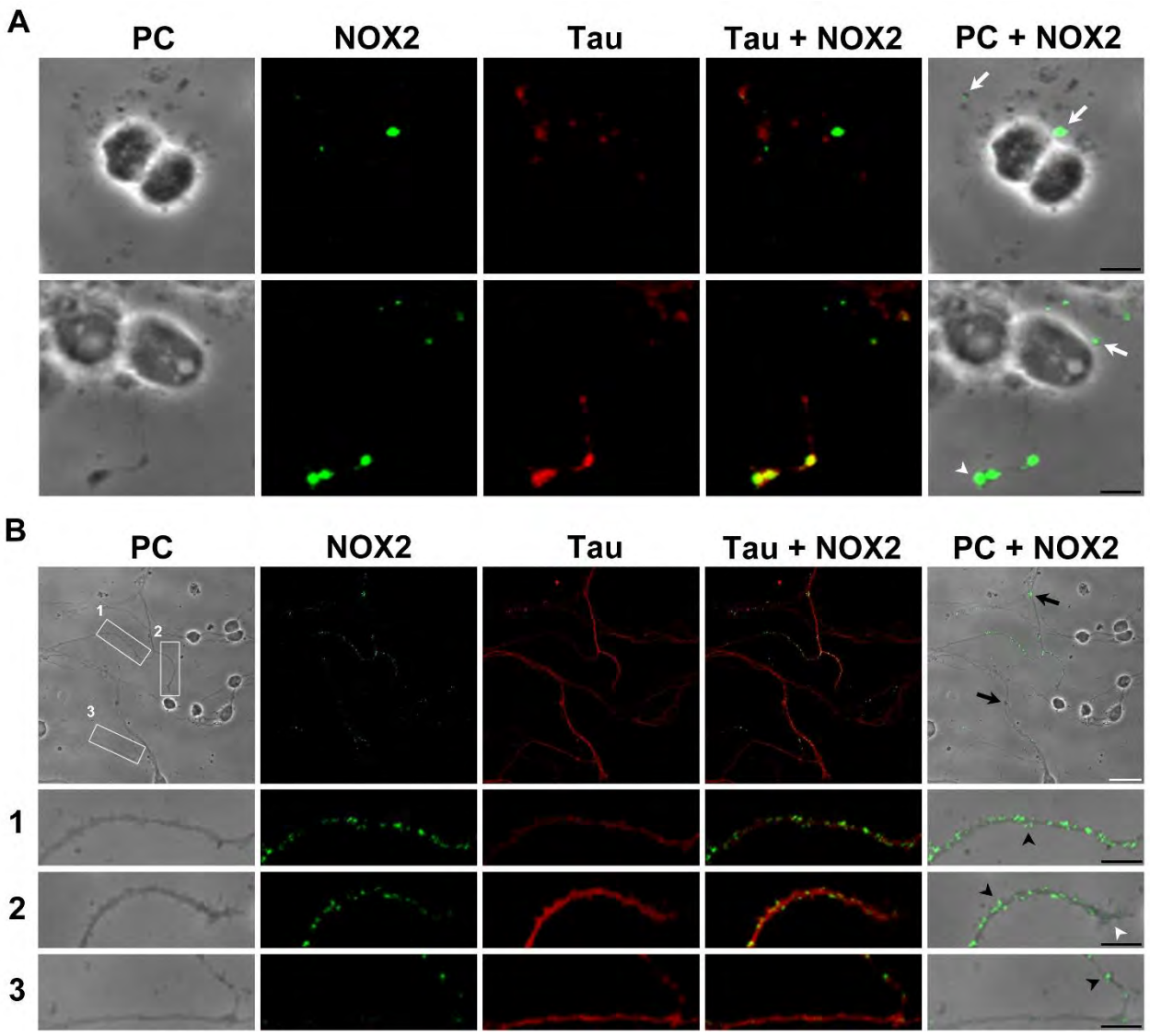

Figure 5. NOX2 is expressed in filopodia and axonal growth cones in developing CGN

Representative confocal micrographs of NOX2 (green) and Tau (red) distribution and phase contrast (PC) micrographs at 0 and 3 DIV. (A) Two representative images of CGN at 0 DIV. White arrows indicate small protrusions and white arrowheads indicate growth cones. (B) A representative micrograph of CGN at 3 DIV. White squares (1-3) are shown below as magnified images. CGN were seeded at low density. White arrowheads indicate growth cones, black arrowheads indicate filopodia and black arrows indicate varicosities. (White scale bars, 20 µm; black scale bars, 5 µm).

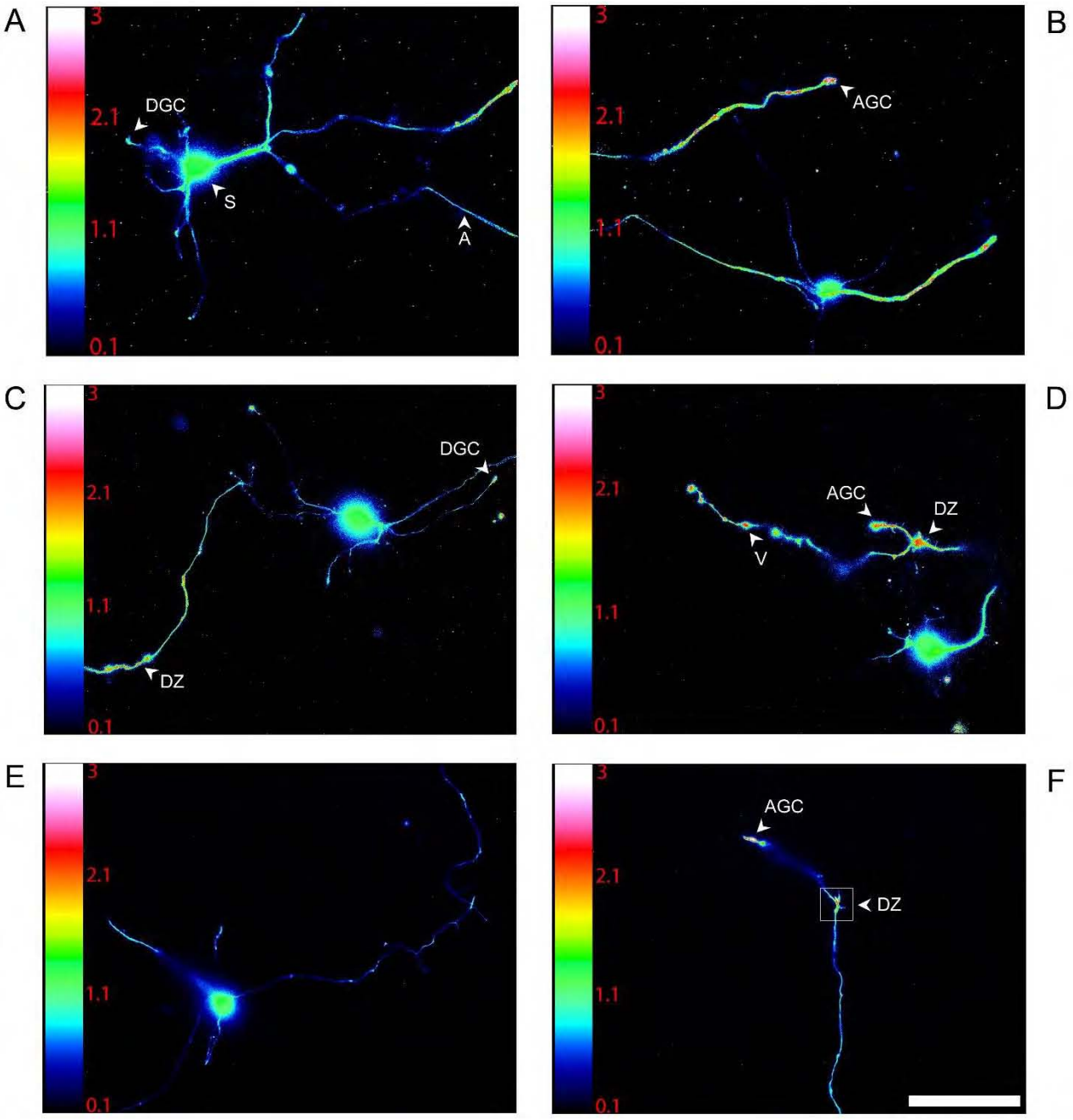
A
3
2.1
1.1
0.1
DGC
S
A
B
AGC
C
DGC
DZ
D
AGC
DZ
V
E
F
AGC
DZ

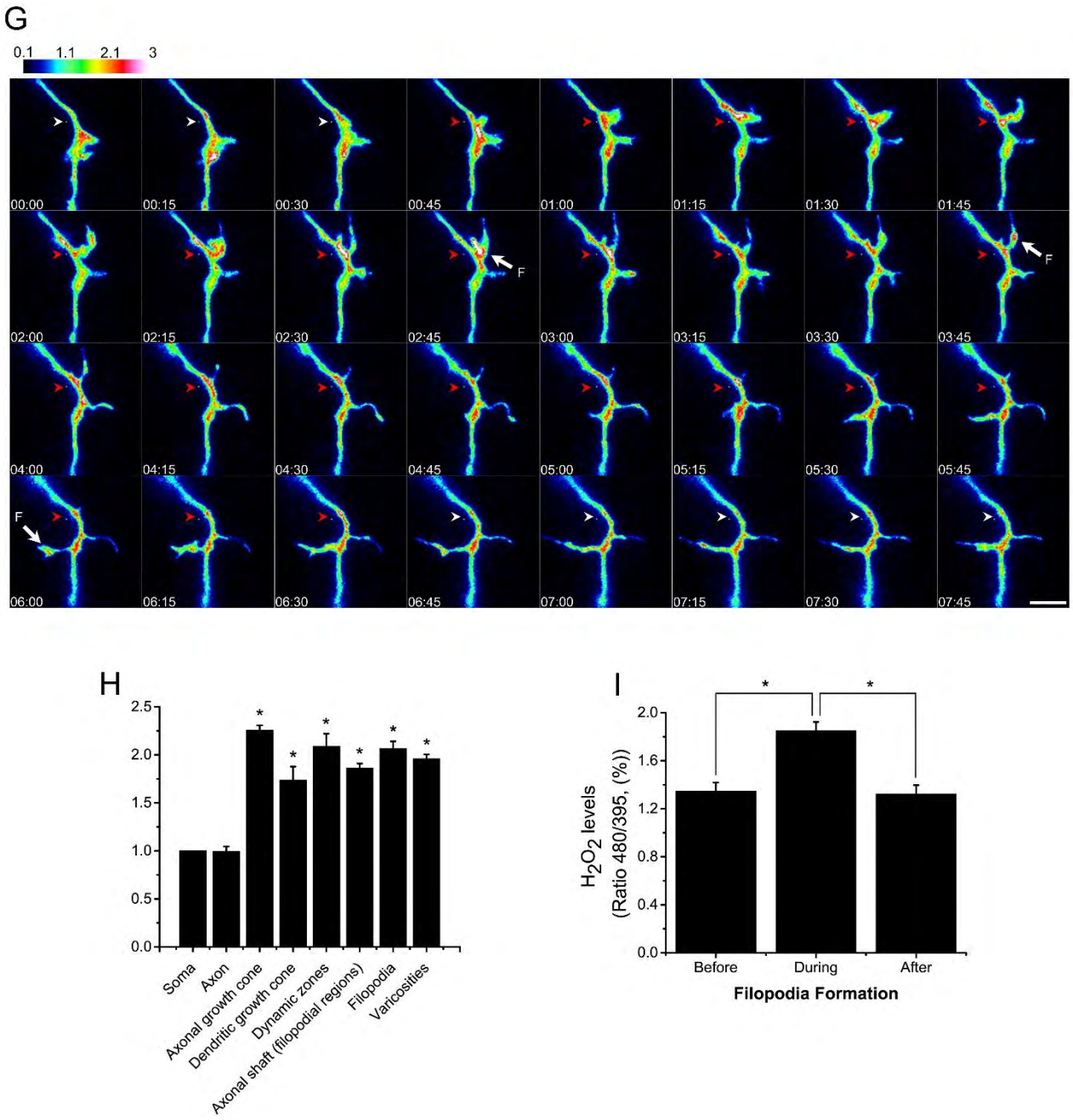

Figure 6. H_2O_2 is produced in specific regions of developing CGN

(A-F) Representative micrographs of CGN of 2 DIV transfected with the plasmid HyPer and H_2O_2 levels were detected as detailed in Methods. The emission fluorescence was recorded from the excitation wavelengths 480 nm and 395 nm in time-lapse imaging (supplementary videos). Color scale bars represent the ratio between the excitation wavelengths 480 nm and 395 nm, which represents the regions in the cell where H_2O_2 is being produced. Arrowheads indicate: soma (S), axon (A), axonal growth cone (AGC), dendritic growth cone (DGC), dynamic zone (DZ) and varicosities (V) (Scale bar, 50 µm). (G) Magnified time-lapse images of the dynamic zone marked in (F). (A) Cell soma of (B). (E) Cell soma of (F). (F) Was captured previously (E) to allow H_2O_2 (500 µM) perfusion shown in (F). White arrowheads indicate a region of the axonal shaft previous or posterior to the filopodium formation. Red arrowheads indicate a region of the axonal shaft where a filopodium is present (ASF) and also corresponds to a relative high H_2O_2 production area. Arrows indicate filopodia (F) with relative high H_2O_2 production (Scale bar, 5 µm). (H) Quantification of H_2O_2 levels normalized with respect to the soma (⋆ $P<0.05$, ANOVA nonparametric test, n=42 (A), n=52 (AGC), n=12 (DGC), n=14 (DZ), n=106 (ASF), n=26 (F), n=93 (V)). Data are mean ± SEM of 42 neurons registered in time-lapse imaging. (I) Quantification of the fluorescence recorded during filopodia formation normalized with respect to the soma. The fluorescence was measured in ASF during the time before to filopodium formation, during the time the filopodium is present and after filopodia retraction. The mean fluorescence in ASF during filopodium formation is higher than the mean fluorescence recorded in ASF after and before filopodium formation (⋆ $P<0.001$, Paired t-test, n=21).

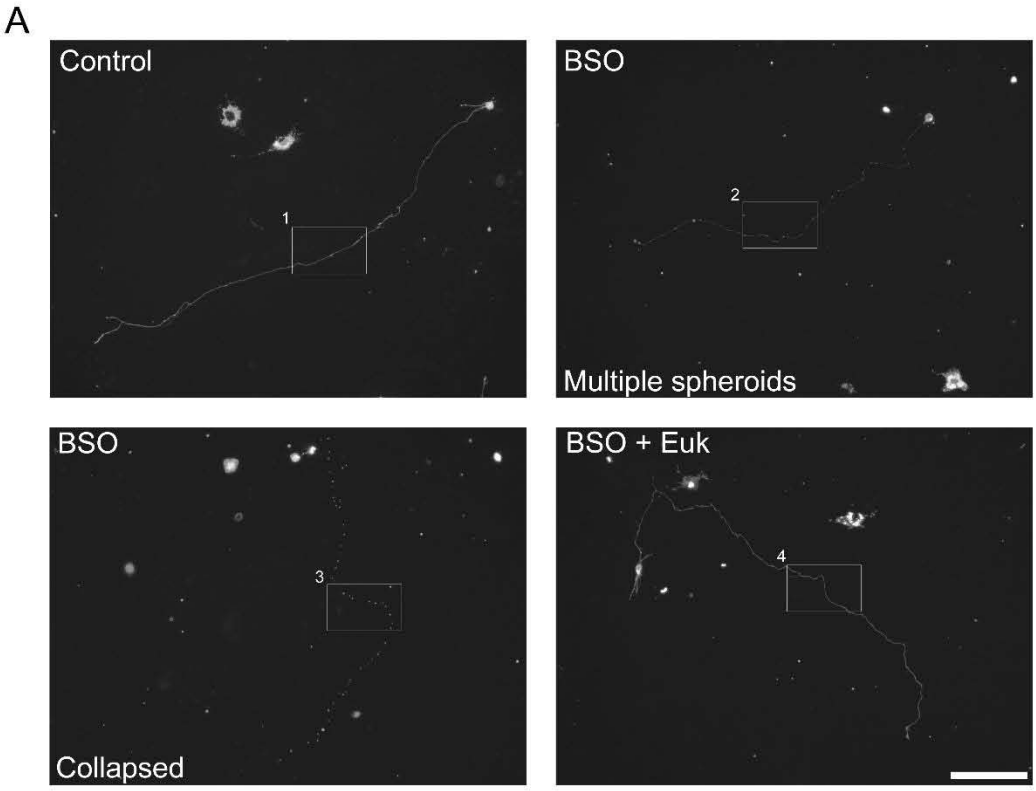
A
Control
1
BSO
2
Multiple spheroids
BSO
3
Collapsed
BSO + Euk
4
B
1
2
3
4

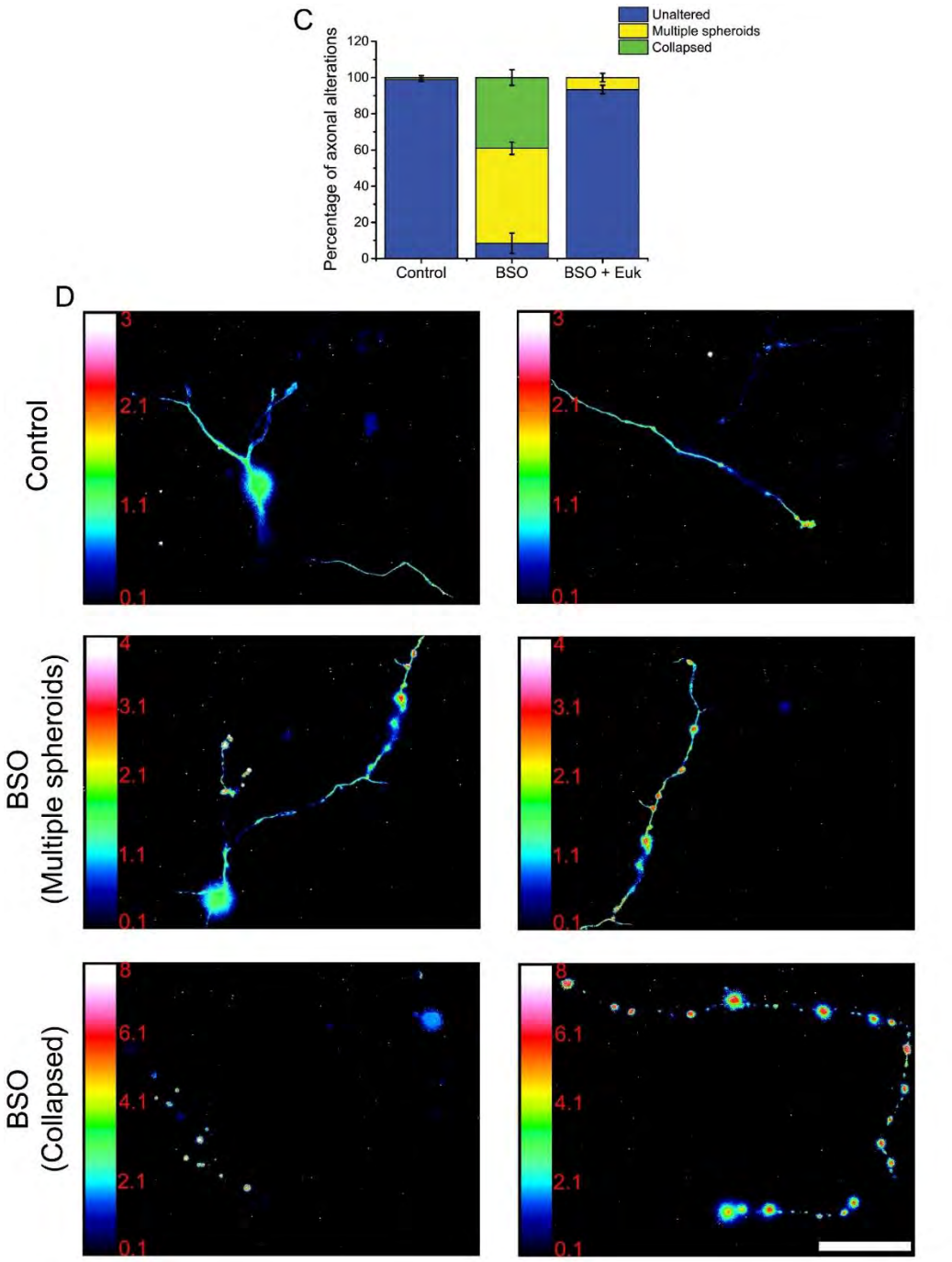

Figure 7. Axonal morphology is altered by glutathione depletion

(A) Representative micrographs of CGN at 2 DIV treated with BSO (100 µM) for 42 h or with Euk-134 (20 µM) for 18 h. Cells were labelled with PKH67 (3 µM) before plating and neurites were visualized as detailed in Methods. Two different axonal morphologies were found in CGN treated with BSO, axons containing multiple spheroids and collapsed axons. (Scale bar, 100 µm). (B) Magnified images of the indicated areas by white squares in A. (Scale bar, 20 µm). (C) Quantification of axons with morphology altered by BSO treatments. CGN treated with BSO showed a higher percentage of axons with alterations as compared to Control and BSO + Euk-134 ($P<0.05$, ANOVA nonparametric test, n=4). (D) Representative micrographs of CGN transfected with the plasmid HyPer as detailed in methods. CGN were treated with BSO (100 µM) for 42 h and then cells were recorded in time-lapse imaging (Scale bar, 50 µm).

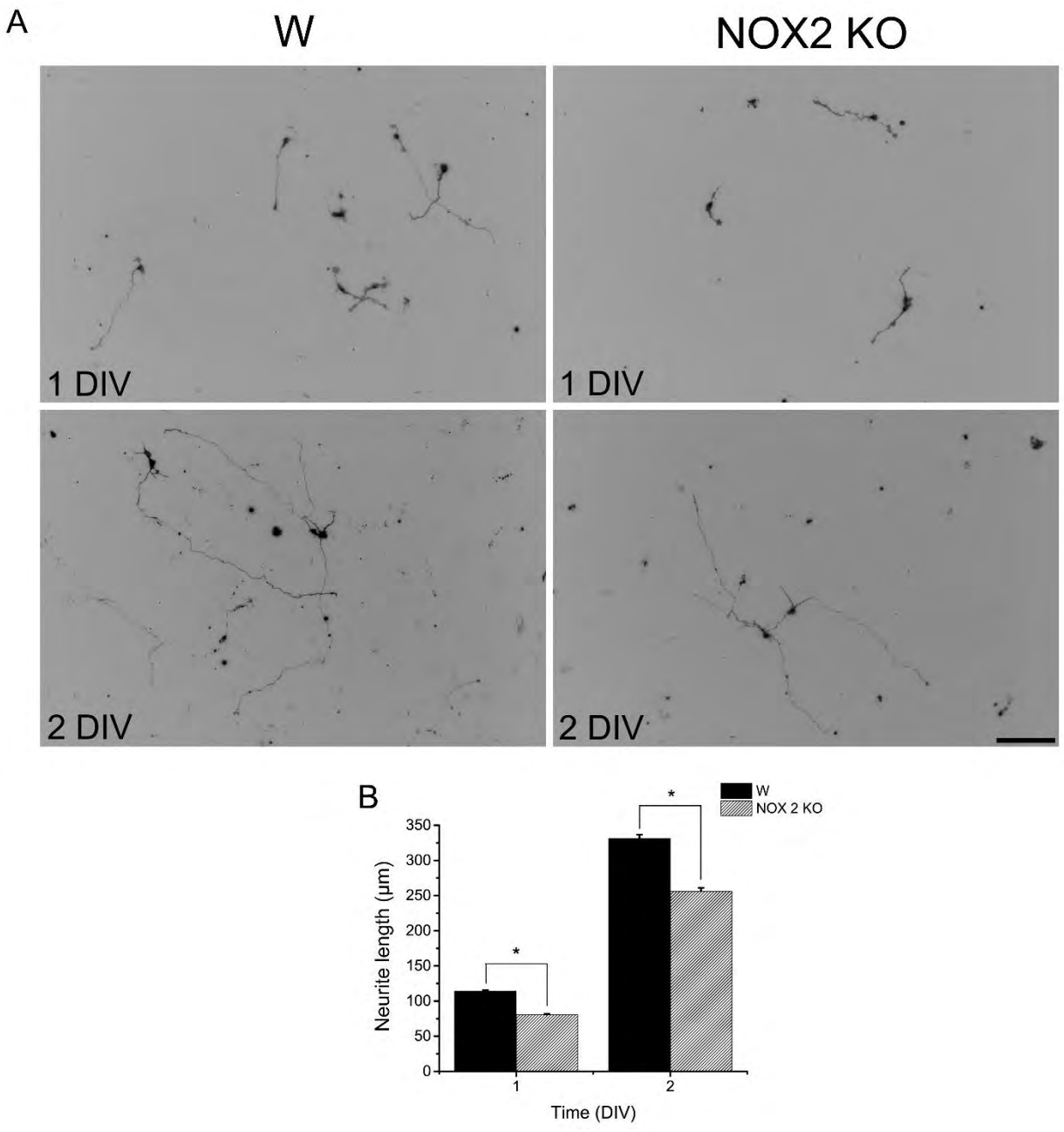
A
W
NOX2 KO
1 DIV
1 DIV
2 DIV
2 DIV
B
W
NOX 2 KO
Neurite length (µm)
350
300
250
200
150
100
50
0
1
2
Time (DIV)
*
*

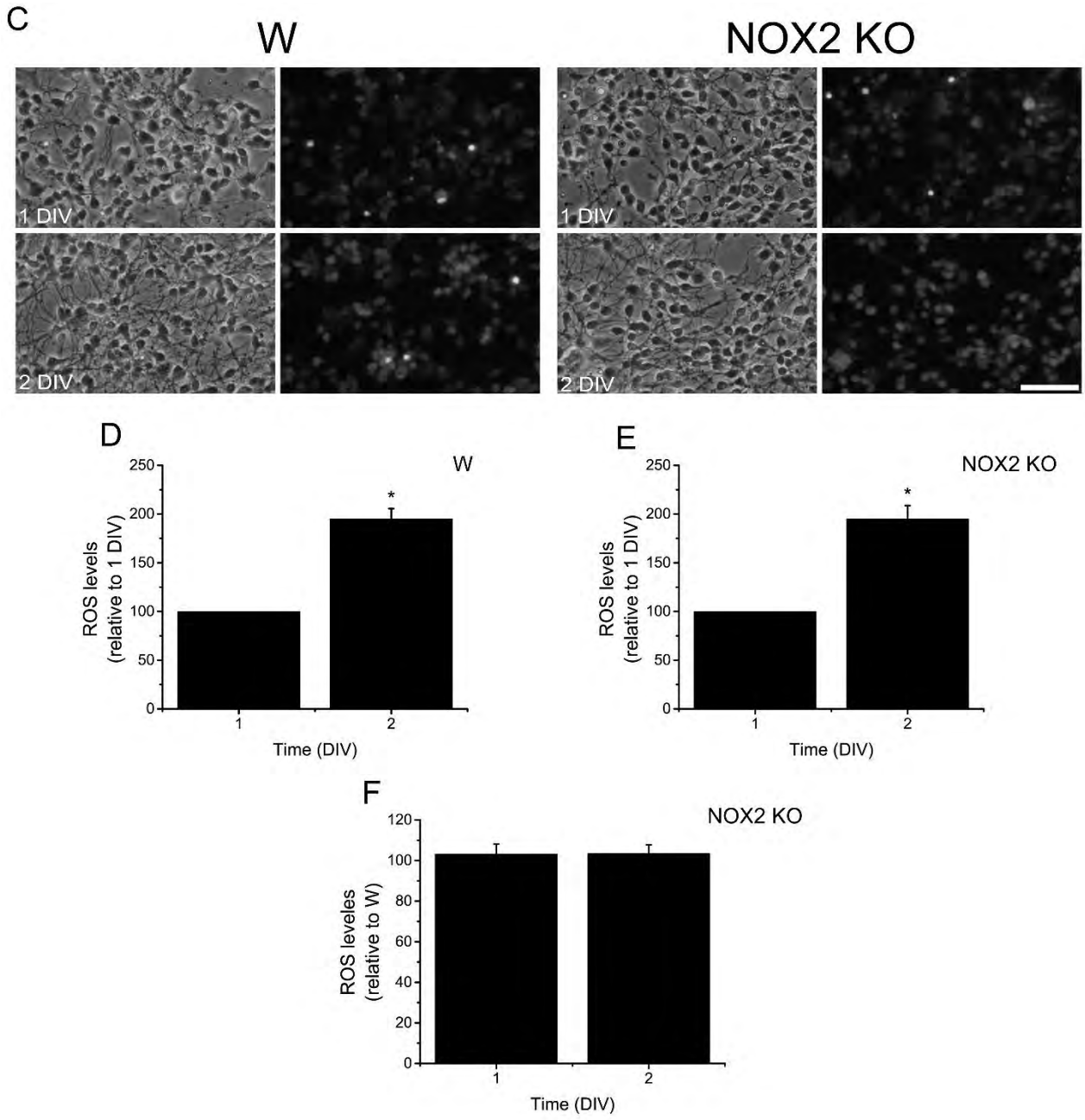

Figure 8. NOX2 regulates axon formation

(A, B) Wild type (W) and NOX2 KO CGN were labelled with PKH67 (3 µM) before plating and neurites were visualized at 1 and 2 DIV as detailed in Methods. (A) Representative micrographs of CGN labeled with PKH67 at 1 and 2 DIV. (Scale bar, 100 µm). (B) Quantification of neurite outgrowth of W and NOX2 KO CGN was performed as detailed in Methods. The neurite outgrowth in NOX2 KO CGN at 1 and 2 DIV was lower with respect to W CGN (⋆ $P<0.001$, Mann-Whitney U Test, n=2067 and n=1151, respectively). Data are mean ± SEM. (C) Representative micrographs of W and NOX2 KO CGN cultured for 1 and 2 DIV. (Scale bar, 100 µm). (D, E) Quantification of ROS levels in W and NOX2 KO CGN cultured from 1 and 2 DIV (⋆ $P<0.05$, Mann-Whitney U Test, n=4). Data were normalized with respect to 1 DIV and are mean ± SEM. (F) ROS levels of NOX2 KO CGN at 1 and 2 DIV were compared with respect to W. (No statistical differences were found, Mann-Whitney U Test, n=5). Data were normalized with respect to W and are presented as mean ± SEM.

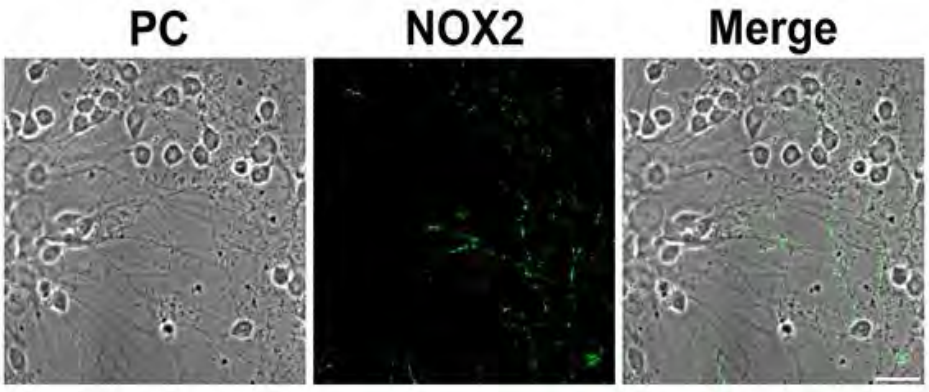

Supplementary figure 1.
Representative confocal micrographs of NOX2 (green) and phase contrast (PC) micrographs of CGN at 3 DIV. CGN were seeded at normal density. (White scale bar, 20 μm.

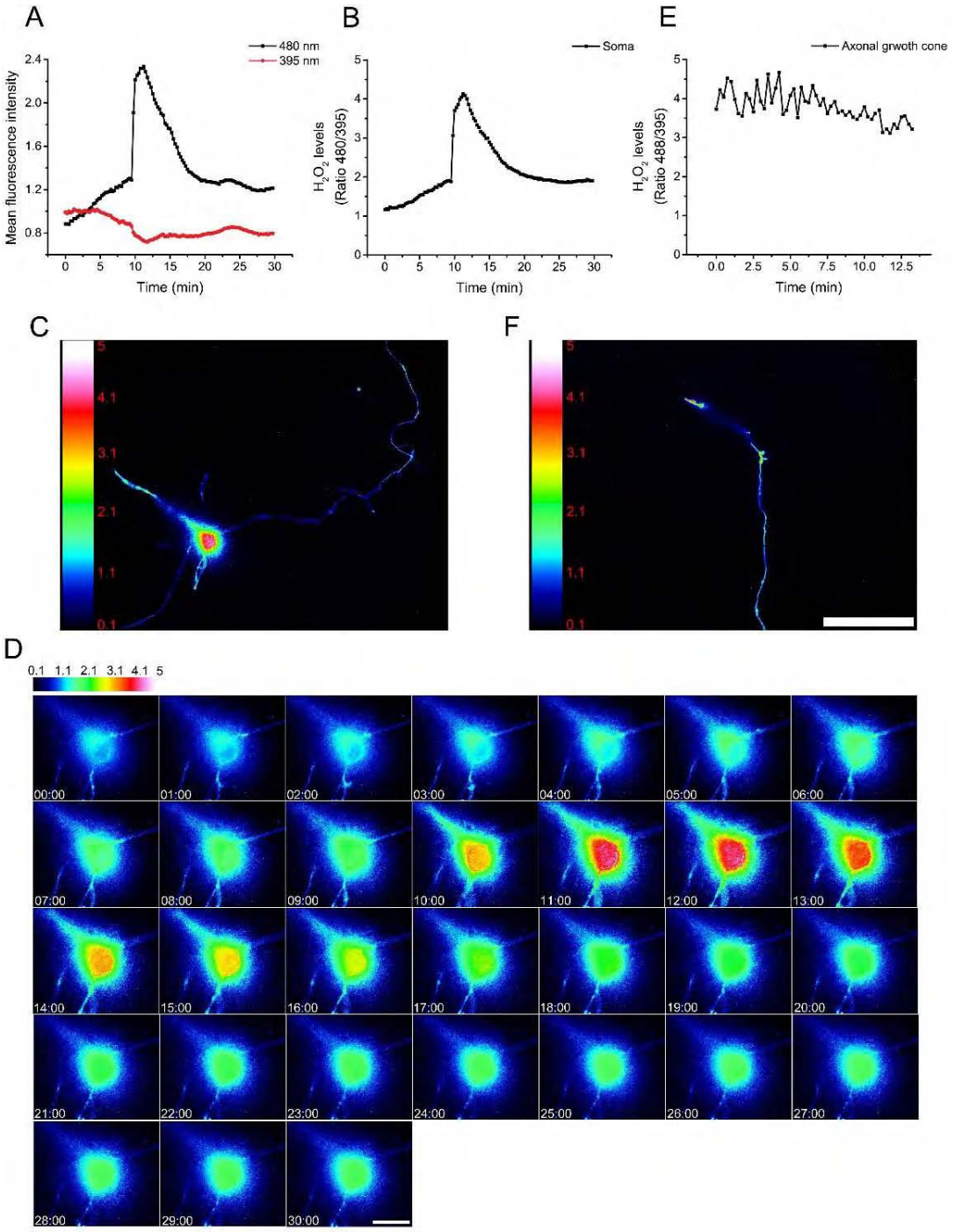

Supplementary figure 2. Changes in HyPer fluorescence during H_2O_2 perfusion

(A-F) CGN of 2 DIV were transfected with the plasmid HyPer and H_2O_2 levels were detected as detailed in Methods. (A) The emission fluorescence of the excitation wavelengths 480 nm and 395 nm corresponding to a ROI traced inside the soma of a neuron perfused with H_2O_2. Data are normalized with respect to the average of the first 10 points registered. H_2O_2 (500 µM) was perfused after 10 min. (B,E) The fluorescence ratio of the excitation wavelengths 480 nm and 395 nm of a ROI traced inside the soma (B) or the axonal growth cone (E) of the same neuron. (C,F) Are micrographs of cell soma and axon of the same neuron transfected with the plasmid HyPer. (F) Was recorded before H_2O_2 perfusion (Scale bar, 50 µm). (D) Series of magnified images of the soma shown in (C) during H_2O_2 perfusion. (Scale bar, 10 µm).

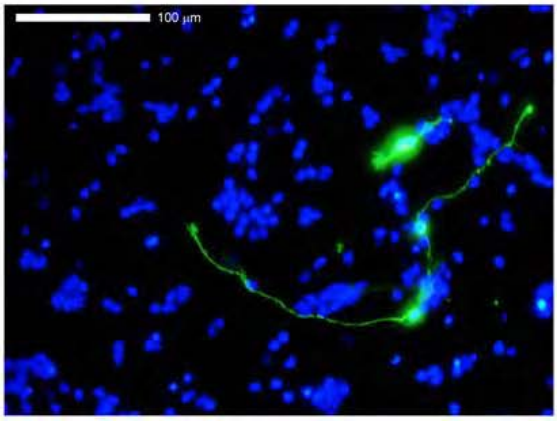

Supplementary figure 3. PKH67 stain . CGN at 1 DIV showing neurites stained with the dye PHK67 (green) and nuclei stained with DAPI (blue).

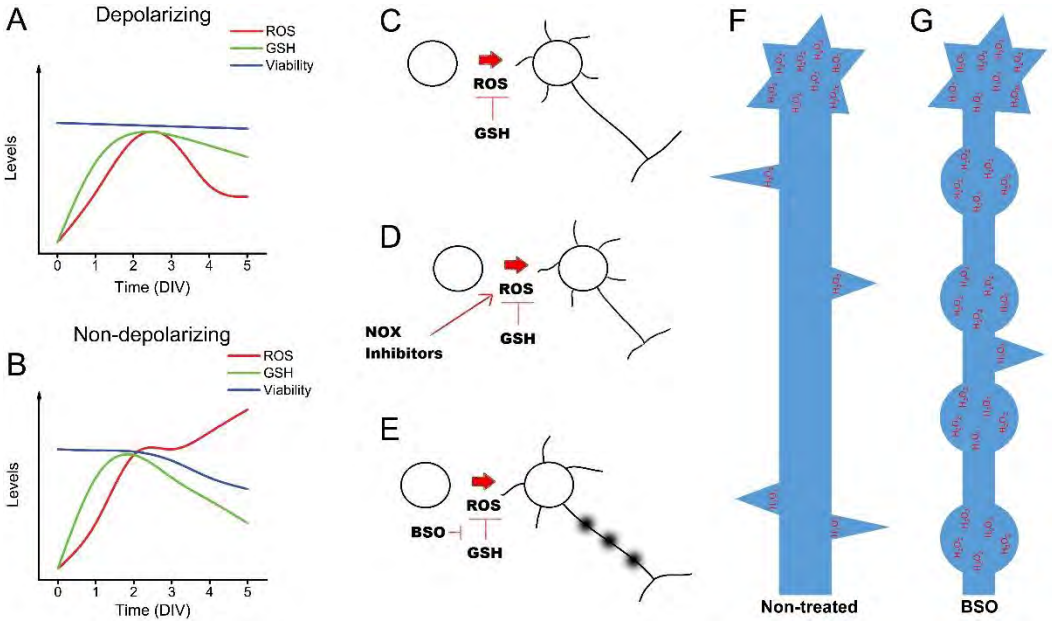

Schematic diagram. Summary of the principal findings

(A,B) Relationship between the levels of ROS, reduced glutathione and cell survival in CGN under depolarizing and non-depolarizing conditions. During the first 3 DIV, ROS and reduced glutathione increase, reaching the highest levels around 2 DIV. By the third DIV, CGN maintained under depolarizing conditions (A) show a significant decrease in the ROS levels, as well as a moderate reduction of glutathione levels. Cell viability remains unaltered. In CGN cultured in non-depolarizing conditions (B), the levels of ROS remain increasing while the levels of reduced glutathione decrease and the cell survival is compromised. (C-E) Effect of ROS in the development of CGN. (C) During normal development, the levels of ROS are regulated by reduced glutathione. Also, (D) when ROS production is decreased by NOX2 inhibition, the development of CGN is altered, as indicated by a low expression of the neuronal markers, Tau and MAP2, as well as a reduced axonal growth. (E) In contrast, the reduction of the levels of glutathione leads to an alteration in the axonal development and cell death. (F) The H_2O_2 produced in CGN is mainly localized in the axons; this H_2O_2 is associated with the formation of filopodia and with axonal growth cone dynamics. (G) Glutathione depletion leads to the formation of multiple spheroid-like structures in the axon that are rich in H_2O_2.

Chapter

ROLE OF REACTIVE OXYGEN SPECIES AS SIGNALING MOLECULES IN THE REGULATION OF PHYSIOLOGICAL PROCESSES OF THE NERVOUS SYSTEM

Mauricio Olguín-Albuerne[1,*], Marco Antonio Zaragoza-Campillo[1,#] and Julio Morán[1,•]

[1]División de Neurociencias, Instituto de Fisiología Celular,
Universidad Nacional Autónoma de México,
México City, México

ABSTRACT

In the nervous system, reactive oxygen species (ROS) have been implicated in several physiological and pathological events. It has been suggested that the members of the family of the NADPH-oxidases (NOX) could be a source of ROS involved in many of these processes. In hippocampus, ROS produced by NOX are required for the NMDA receptor-dependent long-term potentiation (LTP), thereby regulating hippocampal synaptic plasticity and memory formation. In developing neurons, ROS regulate the dynamics of the axonal growth cone during the establishment of neuronal networks and, in neurons from *Aplysia*, ROS produced by NOX promote axonal growth. In addition, ROS produced by NOX critically influence the neuronal proliferation and neurogenesis and they have been implicated in the progression of the programmed cell death of neurons during cerebellar development.

Most of the physiological and pathological actions of ROS are mediated by modification of the redox state of several proteins. The oxidation of these proteins occurs in specific amino acid residues such as cysteine, tyrosine and tryptophan. In particular, the oxidation of cysteine residues is a major mechanism for the control of several proteins.

[*] E-mail: albuerne@email.ifc.unam.mx.
[#] E-mail: zaragoza@email.ifc.unam.mx.
[•] Tel.: (5255) 56 22 56 16, Fax: (5255) 56 22 56 07, E-mail: jmoran@ifc.unam.mx.
Both (I and II) authors contributed equally to this work.

These molecules include channels, enzymes and proteins from the cytoskeleton. For example, in the striatum, the hydrogen peroxide modulates dopamine release by the oxidation of the ATP-sensitive K^+ channels and, in dorsal root ganglion neurons, ROS induce the growth cone collapse by the oxidation of CRMP2.

It has been proposed that ROS also alter the redox state of the proteins of the signaling pathways. For example, ROS produced in response to growth factors control the proliferation and neurogenesis of neural precursor cells through the redox regulation of PI3K/Akt pathway. On the other hand, the oxidation of thioredoxins (Trx) and glutaredoxins (Grx1) leads to their dissociation from ASK1 that dephosphorylates and promotes its activation and the consequent stimulation of JNK and p38, which are involved in several physiological processes such as apoptosis. Other proteins such as thioredoxin-interacting protein (TXNIP) negatively regulates Trx1 and controls the cellular redox state. Finally, Akt has also been reported to be inactivated by direct oxidation, but it can also be activated by the oxidation of PTEN.

In this chapter, we review the experimental evidences supporting a role for ROS in cell signaling in the nervous system and we discuss the interactions of ROS with several proteins as part of the mechanisms that regulates neuronal physiology.

ABBREVIATIONS

AMPA: α-amino-3-hydroxy-5-methyl-4-isoxazole propionic acid
AP5: 2-amino-5-phosphonopentanoic acid
apCAM: *Aplysia* cell adhesion molecule
ASK1: Apoptosis signal-regulating kinase 1
Bcl-X_L: B-cell lymphoma-extra large
CNS: Central Nervous System
CRMP2: Collapsin response mediator protein 2
DPI: Diphenyleneiodonium chloride
EGF: Epidermal growth factor
ERK1/2: Extracellular signal-regulated kinases-1/2
FGFR: Fibroblast growth factor receptor
GAP-43: Growth-associated protein-43
Grx: Glutaredoxin
GST: Glutathione S-Transferase
H_2O_2: Hydrogen peroxide
JNK: Jun N-terminal kinase
MAPK: Mitogen-activated protein kinase
MAPKK: Mitogen-activated protein kinase kinase
MAPKKK: Mitogen-activated protein kinase kinase kinase
MSN: Medium spiny neurons
NADPH: Nicotinamide adenine dinucleotide phosphate
NGF: Nerve Growth Factor
NMDA: N-methyl-D-aspartate
NOX: NADPH oxidase
OPA1: Optic atrophy 1
PDGF: Platelet-derived growth factor
PDK1: Phosphoinositide dependent kinase 1

PI3K: Phosphatidylinositol 3-kinase
PIP_2: Phosphatidylinositol (4, 5)-bisphosphate
PIP_3: Phosphatidylinositol (3, 4, 5)-triphosphate
PKCε: Protein kinase C ε
PTEN: Phosphatase and tensin homolog deleted on chromosome ten
ROMO1: Reactive oxygen species modulator 1
ROS: Reactive oxygen species
RTK: Receptor tyrosine kinase
SCG10: Superior cervical ganglion-10
TNF-α: Tumor necrosis factor-α
Trk: Tropomyosin-related receptor kinase
Trx: Thioredoxin
TrxR1: Thioredoxin reductase 1
TXNIP: Thioredoxin-interacting protein
USP9X: Ubiquitin-specific peptidase 9, X-linked
VEGFR: Vascular endothelial growth factor receptor

INTRODUCTION

It is well known that reactive oxygen species (ROS) are important regulators of numerous cellular functions. Many advances in the field have been achieved in recent years due in part to the advances in the methodologies employed for the study of the actions of ROS. This has allowed to increase our knowledge about the role of ROS as mediators of different physiological events. In the nervous system, the majority of these studies have focused on elucidating the role of ROS in the neuropathologies and neurodegenerative diseases, which have contributed to the understanding of the mechanisms by which the ROS are produced and regulate these processes. Although there have been important advances in the field, there are still many gaps in our knowledge about the role of ROS in the physiology of the nervous system. In this chapter we will detail some studies on the nervous system in which the ROS play a role as regulators of cellular function in the physiology, as well as the generation and progress of certain pathological conditions of the nervous system.

GENERAL MECHANISMS OF ROS ACTIONS

Several studies have described different physiological processes in which ROS act as cellular regulators through the oxidation of specific proteins, leading to a modification of their state of activation and influencing specific signaling pathways and cell function. This occurs mainly through the oxidation of proteins in specific amino acid residues such as cysteine, tyrosine and tryptophan [1]. Particularly, the oxidation of cysteines is a major target to control protein functions. For example, it is well known that ROS, particularly H_2O_2, induce the activation of several protein kinases, as well as the activation or inactivation of several protein phosphatases mediated by the oxidation of cysteines [2-5]. Hydrogen peroxide exerts different modifications depending on the type of reaction. In this chapter we review different examples

in which H_2O_2 alters the function of the proteins through the modification of cysteine residues of different proteins, as well as the protein-glutathione and protein-thioredoxin complexes.

CYSTEINE MODIFICATIONS

The functionality of a wide variety of proteins depends on a series of reversible reactions that are controlled by the redox state of the cell. In this regard, the oxidation of cysteines by hydrogen peroxide is a main mechanism. Once the thiolate group of reactive cysteines interacts with H_2O_2, it is converted to sulfenic acid (R-SOH). At this point, different reactions may occur in the absence of glutathione, thioredoxin and glutaredoxin. The highly reactive sulfenic acid can reduce an adjacent thiol group, and a disulfide bond will be formed. Alternatively, sulfenic acid can further be oxidized by hydrogen peroxide, forming sulfinic acid ($R\text{-}SO_2H$). This group is important in the redox regulation of some proteins such as peroxiredoxins. Despite its stability, sulfinic acid can be reduced by sulfiredoxins and sestrins to sulfenic acid [6, 7], or it can be oxidized by hydrogen peroxide forming sulfonic acid ($R\text{-}SO_3H$); so far it is not known any enzymatic reaction to reduce the sulfonic acid [8, 9]. On the other hand, sulfenic acid can also form a disulfide link between reduced glutathione and the cysteine residue of another protein, forming a glutathionylated protein; however, if glutathione is in an oxidized form, it can be established a bond with the thiolate group of a cysteine residue. In addition, the disulfide bonds formed between cysteines can be reduced by thioredoxin or glutaredoxin, forming a disulfide bond between the protein and any of these proteins. Both processes may be important for the regulation of the activity of several proteins, as is the case for ASK1 and CRMP2. The bond formed between protein-thioredoxin and protein-glutaredoxin can be broken by hydrogen peroxide (Figure 1) [10-12].

OXIDATIVE MODIFICATIONS OF SIGNALING PROTEINS

It is known that the oxidation of proteins involved in cellular signaling represents a critical posttranslational regulatory mechanism [13]. The redox regulation of intracellular signals involved in physiological processes requires efficient cellular sources of ROS (NADPH-oxidase, electron chain transport, etc.), as well as proteins sensitive to the redox state. There are several examples that fulfill these features and that involve not only signaling proteins, but also other type of proteins such as receptors.

Most of these studies have been focused on the regulation of signaling molecules through the oxidation of cysteine residues. In this chapter, we describe some examples.

a) Trx /Grx and ASK1

The reductive activity of Trx1 thiols depends on the cysteine 32 (Cys32) and 35 (Cys35), while that from the mitochondrial isoform (Trx2) depends on Cys90 and Cys93 [14], which constitute a redox catalytic CGPC motif [15, 16].

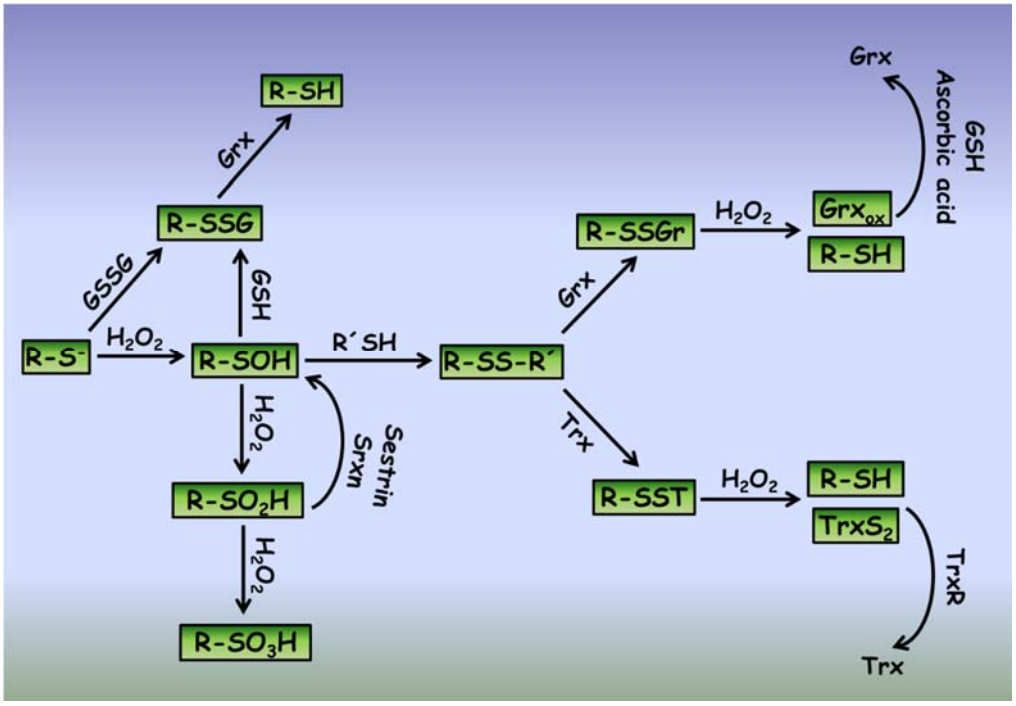

Figure 1. *Mechanisms of cysteine oxidation involved in redox signaling.* The reaction between hydrogen peroxide and the reactive cysteine thiolate group ($R\text{-}S^-$) produces sulfenic acid (R-SOH), which increases the probability to generate a disulfide bridge (R-SS-R´) with an adjacent thiol group (R´SH). If R-SOH is oxidized by H_2O_2 then sulfinic acid ($R\text{-}SO_2H$) is formed, which is a reaction that can be reduced by sestrin and sulfiredoxin (Srxn). When H_2O_2 oxidizes $R\text{-}SO_2H$ then sulfonic acid ($R\text{-}SO_3H$) is formed. The presence of reduced glutathione (GSH) and proteins containing an R-SOH group generates glutathionylated proteins (R-SSG), but if glutathione is in the oxidized form (GSSG), it binds to the thiolate group of cysteine residues, forming R-SSG. Thioredoxins and glutaredoxins can reduce the disulfide bonds between oxidized proteins through the formation of intermolecular disulfide bonds, which can be dissociated by H_2O_2.

Proline is the key amino acid for the reductive action of the CGPC motif. In Trx1, when proline is replaced by serine or threonine, the protein experiences marked changes in its redox properties, as well as in the stability between the oxidized and reduced forms [17]. Similarly, the active catalytic site CPYC of Grx contains two cysteine residues (Cys22 y Cys25) susceptible to be oxidized [18]. In contrast to Trx that forms an intramolecular disulfide bond between the cysteines of its catalytic site Trx-[S-S], Grx specifically form disulfide bonds with glutathione. During its catalytic cycle a covalent intermediary is formed between the Cys22 of Grx and glutathione (Grx-S-S-glutathione) [19]. During oxidative stress, Grx-S-S-glutathione seems to be the predominant form, instead of Grx-[S-S] [20, 21].

It is suggested that the Cys250 of ASK1 binds to the Cys32 or Cys35 of Trx1 via an intermolecular disulfide bridge, which can be broken by ROS [14, 22]. This interaction can also be eliminated by TXNIP, which binds to the Cys 32 of Trx1 therefore reducing the ability of Trx1 to bind ASK1 [23]. It has been shown that the Cys30 of ASK1 forms an intermolecular disulfide bridge with the Cys90 of Trx2 [14]. On the other hand, the cysteines of the active site of Grx (Cys22 and Cys25) are responsible for the interaction between Grx and ASK1, probably through the formation of an intramolecular disulfide bond in Grx [24].

b) Trx and PTEN

PTEN is a tumor suppressor protein that can be reduced by intracellular agents, supporting the idea that the reversible oxidation and reduction of cysteines in the active site represents a key mechanism for PTEN regulation [25]. It is known that H_2O_2 oxidizes Cys124 in the active site of PTEN that forms an intramolecular disulfide bond with Cys71, leading to PTEN inactivation [25].

The binding of Trx1 to PTEN is mediated by the formation of a disulfide bridge between the Cys32 of the Trx1 active site and the Cys212 from the C2 domain of PTEN, which induces a steric effect in the catalytic site of PTEN and the C2 domain that binds to membrane lipids. This condition obstructs the access of the substrate to the catalytic site of the PTEN phosphatase domain as well as the binding of the C2 domain to the inner side of the plasmatic membrane [26]. Due to the fact that Trx directly interacts with PTEN, it has been suggested that the reduction of PTEN is carried out by the binding of oxidized PTEN to Trx1 in a reduced state. It is unknown whether the reductase TrxR1 reverts the interaction between Trx1 and PTEN and cannot be excluded that glutathione and Grx break this union.

c) Trx and TXNIP

It has been shown that during oxidative conditions, TXNIP contains an intramolecular disulfide bond formed by Cys63 and Cys247, which is able to interact with the reduced form of Trx by forming an intermolecular disulfide bond between Cys247 from TXNIP and Cys32 from Trx [27]. Hwang *et al.* [28] recently showed that ROS can oxidize the intermolecular disulfide bond between TXNIP and Trx leading to their dissociation. After restoration of the redox potential by antioxidant conditions, the Trx reactive cysteines interact with the bond formed between Cys63 and Cys247 from two TXNIP molecules. After that, these two TXNIP molecules undergo a structural rearrangement that involves the exchange of the former disulfide bond to a new one between the Cys63 and Cys190 from two TXNIP molecules and then the *novo* formation of the intermolecular disulfide bond between the Trx Cys32 and the Cys247 from TXNIP [28].

d) Akt

Murata *et al*. [29] reported that the exposure of cardiac cells to H_2O_2 induces the formation of an intramolecular disulfide bond between Cys297 and Cys311 of the Akt kinase domain, which leads to its dephosphorylation. These cysteines are conserved in the three Akt isoforms. By using site-directed mutagenesis, they also showed that the formation of this bond leads to Akt proteasomal degradation [29]. It has been shown that the PDGF induces ROS generation in smooth muscle cells [30] and that the Akt2 redox-regulation participates in the glucose consumption induced by PDGF. In this regard, it was recently reported by Wani *et al*. [31] that ROS induced by PDGF cause the oxidation of the Cys124 of Akt2, modulating its inactivation... Cys124 is not conserved in Akt1 and Akt3. These results point to the Cys124-Cys297 or Cys124-Cys311 intramolecular bonds as responsible for the Akt2 inhibition by oxidation [31]. Interestingly, the exogenous H_2O_2 administration activated Akt1 y Akt2, but intracellular

accumulation of H_2O_2 resulted in the inactivation of Akt2 only, suggesting a differential action of the ROS source on Akt isoforms activation. It is proposed that the activation of Akt2 by phosphorylation is inhibited by oxidation. This highlights that Akt signaling can be modulated by physiological levels of ROS with functional consequences on the cellular and molecular processes induced by PDGF [31].

e) MAPKs (JNK, p38 and ERK)

JNK activity can be modulated by ROS by an indirect way. For example, it has been shown that GSTπ is inactivated in vitro by H_2O_2 by forming both an intramolecular disulfide bond between the Cys47 and the Cys101 and an intermolecular bond between the Cys47 of two monomers of GST [32]. On the other hand, it is known that the binding of the monomeric GSTπ to JNK inhibits the activation of JNK. Therefore, ROS allow the JNK activation by favoring the formation of GSTπ oligomers that are unable to bind JNK. This has been shown in cultured mouse fibroblasts exposed to pro-oxidant conditions. Under these conditions it is observed the formation of dimers and larger aggregates of GSTπ, JNK activation and the consequent phosphorylation of c-Jun and apoptosis [33].

It was recently reported that p38 is oxidized upon exposure to exogenous H_2O_2 or prostaglandin J2 (an inflammatory mediator), resulting in the inactivation of its kinase activity despite of being phosphorylated. Both, the Cys119 and the Cys162 of p38 were identified as sites of oxidation, with no formation of disulfide bridges. As p38 can be oxidized under micromolar concentrations of the prostaglandin J2, this could represent a signaling event physiologically relevant during inflammation [34].

ROS may exert different actions on the signaling molecules depending on their concentration. In a previous study [35], it was reported that low concentrations of H_2O_2 (0.1 μM) oxidize the Cys38 and Cys214 of ERK2, which does not occur with higher concentrations (10 μM). It was also found that the Cys162 of p38 was also oxidized, but only at a concentration of 20 μM of H_2O_2. In the case of JNK2, several cysteines are directly oxidized with 1 μM of H_2O_2: Cys41, Cys116, Cys137, Cys177 and Cys222, but none of these are oxidized at a concentration of 0.1 μM of H_2O_2. These variable actions of ROS in the oxidation of MAPKs could contribute to the differential control of events such as proliferation and disruption of the cell cycle in some cells [35]. This is an example that low and high concentrations of ROS may produce opposite effects depending on the cysteines oxidized.

f) Receptor Tyrosine Kinase

It is known that one of the consequences of an increase in ROS levels is the inhibition of protein phosphatases, which regulate the activity of several intracellular signaling pathways, including the PI3K/Akt, PLCγ, MAPK and JAK/STAT pathways. For example, some of the physiological and pathological effects of the inhibition of protein tyrosine phosphatases induced by ROS is the activation of cell signals mediated by the receptor tyrosine kinase (RTKs) [36, 37]. Recently, several studies have implicated ROS in the transactivation of RTKs, i.e. in the activation of the receptor independent of its ligand [38-40].

Among the three types of Trk receptors, the BDNF receptor, TrkB, is the most studied RTK in the CNS of mammals. This receptor is widely expressed in both mature and developing neurons and participates in various biological processes such as survival and neuronal differentiation, as well as the physiology, structure and plasticity of synapses [41]. Recently, it was reported in cortical neurons that endogenous and exogenous ROS directly activate TrkB receptor by a mechanism that requires the Src family kinases, i.e., TrkB is activated by a transactivation mechanism mediated by physiological levels of ROS without the participation of BDNF. One of the functional consequences of this ROS-mediated TrkB transactivation is an increase of the survival of cultured neurons [40]. In addition, both the H_2O_2 and BDNF induced the activation of ERK1/2, a signaling protein downstream of TrkB receptors [40].

Furthermore, a recent study in mouse cortical neurons showed that ROS and the NADPH-oxidase (NOX) activity are required for the transactivation of TrkB and PDGFβ by serotonin (5-HT) [42]. This study suggests that serotonin activates their Gαi coupled receptors, leading to PLC activation, which induces calcium release from the endoplasmic reticulum and the activation of PKC. It is suggested that PKC activates NOX, resulting in ROS production. This condition or the exogenous application of H_2O_2 can induce the phosphorylation/activation of the TrkB receptors and PDGFβ. [42]. In the case of the NGF receptor, TrkA, it has also been reported that the redox state regulates its activity through tyrosine phosphatases [43]. There is no much evidence to explain the mechanism by which ROS promote the phosphorylation of TrkA, TrkB and PDGFβ receptors. In the case of the PDGFβ receptor, it has been identified two conserved cysteine residues, which are critical for the RTK kinase activity: Cys822 and Cys940. In this regard, it has been observed that the kinase activity of the receptor is not due to the formation of a disulfide bond between these cysteines, and that the Cys940 mutation only induces a conformational change in the protein [44].

It is known that ROS can also transactivate the EGF receptor [45] and that the activation of this receptor induces an increase in the endogenous levels of H_2O_2 [46], suggesting that the EGF receptor is sensitive to the redox state, and that it induces the generation of ROS. In this context, it was recently demonstrated in cells stimulated with EGF that the Cys797 of the catalytic site of the EGF receptor is directly oxidized by endogenous H_2O_2 that further increases its kinase activity. ROS are apparently produced through the association of EGF receptor with NOX2, one of the 7 homologues of NOX. This highlights the importance of endogenous H_2O_2 in the signaling of the EGF receptor as a result of the activation of NOX [47].

The VEGF receptor (VEGFR) is another example of an RTK that is regulated by direct oxidation of cysteines. In particular, a recent study in endothelial cells showed that VEGFR-2 activity is negatively regulated by the reversible formation of a disulfide bond between the Cys1199 and Cys1206, where the Cys1206 is the direct target of the oxidation by ROS in the absence of the antioxidant enzyme PrxII. Therefore, under physiological conditions, PrxII preserves the reduced state of VEGFR-2 by blocking its oxidative inactivation by H_2O_2 [48].

The FGF type 1 receptor (FGFR-1) also contains a cysteine (Cys488) that is susceptible to be oxidized. This residue was first characterized in the corresponding Cys277 of Src kinase [49]. This study showed that Src in its reduced form is fully active, but it becomes partially inactivated under oxidizing conditions. It is known that the oxidation of the Src Cys277 generates an intermolecular disulfide bond with the Cys277 of other monomer of Src, forming a dimer linked by the disulfide bridge Cys277-Cys277. However, other study shows that H_2O_2

induces Src activation through the formation of an intramolecular disulfide between Cys245 and Cys487, which takes place during cell adhesion [50]. The Cys277 of Src is located in the sequence GQGCFG of its catalytic domain called "Gly loop". Similarly, FGFR-1 contains the Cys488 in the corresponding conserved sequence. In this regard, FGFR-1 is also inactivated by oxidation of the Cys488, which also generates a dimer linked by an intermolecular disulfide bridge; although, in this case, other cysteines seem to participate to stabilize the dimer by oxidation [49].

All these studies suggest that ROS represent a key component for the transactivation pathways in neurons and highlight the physiological relevance of ROS in the mechanisms of transactivation, where ROS could activate multiple RTKs through the inactivation of phosphatases of tyrosine, rather than the transactivation of RTK by GPCR. Table 1 shows the redox sensitive cysteines of some signaling proteins.

PHYSIOLOGICAL ROLE OF ROS IN THE NERVOUS SYSTEM

ROS act as signal molecules that regulate different processes in the adult and developing brain [64-68]. Coincidently, it is in the neurogenic regions of the developing and adult brain where ROS are relatively elevated in physiological conditions [65, 66, 69]. Particularly, during nervous system development, ROS have been shown to regulate the proliferation of neural stem cells and the neuronal differentiation [64-68]. ROS have also been shown to act as morphogens during brain development. For example, it has been observed an increased mitochondrial ROS levels, aberrant axonal targeting and abnormal brain formation when the mitochondrial SOD of the fruit fly *Drosophila* is mutated.

Table 1. Cysteine oxidation with physiological relevance in cell signaling

Protein	Cysteine	Oxidative modification	Physiological result	Refs
Trx1	Cys32 and Cys35	Intramolecular disulfide bond	Dissociates from ASK1 in the cytosol inducing apoptosis	**[15, 51, 52]**
	Cys32 or Cys35	Intermolecular disulfide bond with Cys250 of ASK1	Inhibits the activity of ASK1 in the cytosol	**[14, 22]**
Trx2	Cys90 and Cys93	Intramolecular disulfide bond	Dissociates from ASK1 in the mitochondrion inducing apoptosis	**[14]**
	Cys90	Intermolecular disulfide bond with Cys30 of ASK1	Inhibits the activity of ASK1 in the mitochondrion	**[14, 53, 54]**
Grx	Cys22 and Cys25	Glutathionylation and/or intramolecular disulfide bond	Dissociates from ASK1 inducing apoptosis	**[18, 24, 55]**

Table 1. Cysteine oxidation with physiological relevance in cell signaling (continued)

Protein	Cysteine	Oxidative modification	Physiological result	Refs
TXNIP	Cys63 and Cys247 Cys247	Intramolecular disulfide bond Intermolecular disulfide bond with Cys32 of Trx1	Interaction with Trx1 Inhibition of reducing activity of Trx1 inducing cell death	**[27]** **[27, 28, 56]**
Akt	Cys297 and Cys311	Intramolecular disulfide bond	Binding of PP2A and inhibition of cell survival	**[29, 57, 58]**
Akt2	Cys124	Intramolecular disulfide bond with Cys297 o Cys311	Inactivation of Akt2, glucose uptake	**[31]**
JNK	Cys41, Cys162, Cys137, Cys177, Cys222	Direct oxidation	Cell cycle arrest	**[35]**
p38	Cys119 and Cys162	Direct oxidation	Inactivation of p38, inflammation	**[34, 35]**
ASK1	Cys250	Conformational change by direct oxidation	Formation of multimers of ASK1 which activates cell apoptosis	**[59, 60]**
PTEN	Cys124 and Cys71 Cys212	Intramolecular disulfide bond Intermolecular disulfide bond with Cys32 of Trx1	Inactivation of PTEN Inhibition of the phosphatase activity of PTEN inducing proliferation and cell survival	**[25, 61, 62]** **[26]**
ERK2	Cys38 and Cys214	Direct oxidation	Promotes proliferation	**[35]**
PKC	Cysteine-rich regions	Direct oxidation	Neuronal differentiation	**[63]**
Src	Cys277 Cys245 and Cys487	Intermolecular disulfide bond with Cys277 between two Src Intramolecular disulfide bond	Inactivation by the formation of a dimer Activation of Src in cell adhesion events	**[49]** **[50]**
EGFR	Cys797	Direct oxidation	Activation of EGFR	**[47]**
VEGFR-2	Cys1199 and Cys1206	Intramolecular disulfide bond	Inactivation kinase of VEGFR-2	**[48]**
FGFR-1	Cys488	Direct oxidation	Inactivation by the formation of a dimer	**[49]**
GSTπ	Cys47 and Cys101	Intramolecular disulfide bond	Formation of oligomers of GSTπ that cannot bind to JNK inducing apoptosis	**[32, 33]**
CRMP2	Cys540	Intermolecular disulfide bond with Cys540 between two CRMP2	Induce growth cone collapse	**[64]**

These flies also present clusters of nuclei located in the neuropile of the central brain, where normally does not contain these organelles [70].

In mammals, during the postnatal development of rat cerebellum, ROS is transiently produced at different stages of development and is restricted to specific regions of the developing cerebellar cortex. In addition, different members of the NOX family are differentially expressed during cerebellar development. The inhibition of ROS during rat development, leads to changes in cerebellar folia formation, as well as an alteration in motor behavior [65]. These studies suggest that the proper regulation of ROS during critical periods of time is required for normal brain development.

Little is known about the mechanisms related to the physiological actions of ROS in the nervous system, but three different conditions have been identified in these processes: 1) ROS are produced in response to a physiological stimulus induced by a growth factor or a neurotransmitter and the most likely source is a NOX and/or the mitochondria. 2) It is necessary a target protein with specific chemical features that allow to interact with ROS, as it was previously described. 3) These events should occur restrained in time and space in order to be specific; otherwise ROS could trigger unspecific responses, including cell death. In this chapter we describe some studies that exemplify the physiological actions of ROS in the nervous system.

a) Proliferation

A growing body of experimental evidence suggests that ROS induce proliferation of neural cells. It has been shown that the neural progenitor cells derived from embryonic hippocampus generate ROS under basal conditions and that the antioxidants and inhibitors of the ROS-producing enzyme NOX reduce their proliferation [71]. In these cells, it has been observed a correlation between the levels of ROS and proliferation [72]. Furthermore, *in vivo* administration of the antioxidant α-lipoic acid reduced cell proliferation in the dentate subgranular zone of the hippocampus [72].

Le Belle and collaborators [66] demonstrated in neurosphere cultures obtained from the subventricular zone that H_2O_2 promoted self-renewal of neural progenitor cells. Also, when ROS levels were lowered, the number of neurospheres was decreased and restored by exogenous addition of H_2O_2. Consistent with these studies, high levels of ROS have been detected in the neurogenic regions of the subventricular zone, the glomerular layer of the olfactory bulb and the subgranular zone [66, 69]. In addition, BDNF also increased the levels of ROS and self-renewal of progenitor cells; however, none of these effects were observed in BDNF-treated cells derived from KO NOX2 mice. Besides, the KO NOX2 mice have less proliferating cells in the subventricular zone than wild type mice and the pharmacological inhibition of NOX diminished both the generation of ROS and proliferation in the subventricular zone. These results suggest that the ROS produced by BDNF are implicated in the proliferation and that the ROS source is NOX2.[66]. Furthermore, H_2O_2 also induced the oxidation of PTEN in these cells.

Finally, H_2O_2 activates the pathway PI3K/Akt/mTOR through the inactivation of PTEN [73]. In KO PTEN mice neither H_2O_2 nor BDNF were able to stimulate neurosphere formation. Thus, the effect of ROS in neural precursor cells seems to be mediated by the redox inactivation of PTEN [66].

b) Neuronal Differentiation

It has been found that ROS are critical determinants of neuronal differentiation in several experimental models. Part of this idea is supported by the *in vivo* observations of a transient ROS production in response to trophic conditions that induce neuronal differentiation in specific neurogenic regions of the brain [65, 66, 69]. Under these conditions, the differentiation process is delayed or diminished when ROS are decreased by antioxidants or inhibitors of the ROS sources.

Many of the studies on neuronal differentiation have been performed in the PC12 cell line. When these cells are treated with the neurotrophin NGF, these cells develop neurites (neuritogenesis) and express different neuronal markers, including βIII-tubulin, GAP-43 and neurofilament L, among others. This process begins with the activation of TrkA, which leads to the activation of PLCγ-PKC-Raf and the subsequent activation of the signaling pathway Ras-Raf-MEK-ERK. The sustained activity of ERK is necessary for the achievement of the neuronal-like characteristics of PC12 cells. Finally, TrkA also activates the PI3K-Akt signaling pathway that promotes cell survival [74, 75].

In this regard, neuronal differentiation of PC12 is ROS dependent. For example, hyperoxia and xanthine/xanthine oxidase activation induce the formation of neurites trough a sustained activation of ERKs in a process that is mediated by ROS production [76]. In particular, the activation of ERKs is affected by ROS in different points of the signaling cascade. In PC12 cells it has been demonstrated that ROS induce the phosphorylation of TrkA through the inhibition of PTPs (protein tyrosine phosphatases), and also promote the activation of PLCγ and PI3K, as well as the formation of the receptor complexes with the scaffold proteins Shc, Grb2 and Sos, which are indispensable for the activation of the MAPK pathway [77]. Although it is not clear how ROS induce the formation of the complex formed by the TrkA receptor and the scaffold proteins, it has been proposed that H_2O_2 induces the activation of ERKs by Src through the Ras-Raf pathway [78] and by Fyn through the Jak2-Shc-Grb2-Sos-Ras pathway [79]. Furthermore, neurite outgrowth of PC12 induced by NGF is mediated by Fyn [80], while Src is required for neurite outgrowth induced by cAMP, but not by NGF [81]. Thereby these kinases seem to be involved in the neuronal differentiation of PC12 induced by ROS and one of the possible targets of ROS produced by NGF might be Fyn that acts upstream ERKs activation.

It is not conclusive the role played by the different sources of ROS during the differentiation processes; however, it seems that different sources might have different effectors, which could have diverse effects in cells. For example, in PC12 cells, NGF induces a peak of ROS levels after 10 min of treatment. This production of ROS is inhibited by DPI, an inhibitor of NOX, suggesting that NOX is the ROS source induced by NGF at this time [82]. On the other hand, the NGF treatment produces a time dependent reduction of the expression of NOX2 at 48 h, with a concomitant increase in the expression of NOX1. After 72 h, there is a second peak of ROS, which is produced by NOX1, since the elimination of NOX1 abolishes this peak. Under this scenario, the inhibition of ROS production by NOX inhibitors and a mimetic of catalase after 48 h of NGF treatment, increases the neurite length and the expression of βIII-tubulin. However, when catalase is applied together with NGF from the beginning, the differentiation of PC12 cells is reduced [83]. These results suggest that ROS produced by different sources at different stages of PC12 cells differentiation have different effects in the differentiation process. The first peak of ROS, probably produced by NOX2, is critical to

initiate the observed changes, while the second peak of ROS, which is produced by NOX1, negatively regulate neurite outgrowth of differentiated PC12 cells.

The counterpart of ROS produced are the antioxidant systems. In this regard, it has been reported in PC12 cells that NGF induces the expression of the antioxidants glutathione peroxidase and catalase after 3 days of treatment [84]. This regulation of the antioxidant systems allows the cells to contend with the H_2O_2 chronically produced by NGF [85]. However, the role of the antioxidant systems in neuronal differentiation has not been completely determined. When PC12 cells are treated with NGF, there is an induction of the phosphorylation of ERKs from 5 min to 30 min, which is crucial to induce the expression and activity of the mitochondrial MnSOD that is necessary to induce differentiation. MnSOD is required to induce a second peak of the phosphorylation of ERKs at 180 min after NGF treatment. If MnSOD is overexpressed, it is induced the neural specific transcription of NGF1a in the absence of NGF; while MnSOD silencing leads to a reduction in the phosphorylation of ERKs. It is proposed that the mechanism by which MnSOD induces the phosphorylation of ERKs at 180 min is through the conversion of superoxide anion into H_2O_2, which is indispensable to induce the long term phosphorylation of ERKs. When H_2O_2 is reduced by the mimetic of glutathione peroxidase Ebselen, the second peak of ERKs phosphorylation is also inhibited and the neurite outgrowth is completely prevented [86].

It is not completely understood how ROS participate in the activation of ERKs. Gopalakrishna *et al*. [63] employed the xanthine/xanthine oxidase system and $CoCl_2$ as pro-oxidants to induce cell differentiation. Both oxidants were able to induce neuronal differentiation of PC12 measured as neurite outgrowth, the expression of neurofilament-L, GAP-43 and SCG10. The differentiation induced by oxidants was mediated by PKC, since the non-selective inhibitors of PKC, calphostin C and chelerythrine, reduced neurite outgrowth. Also, $CoCl_2$ induced the translocation of PKC from the cytosol to the membrane. During the period of activation the capacity of PKC to bind phorbol esters was reduced, suggesting that there is a redox modification of the regulatory domain of PKC. Further exposure to higher concentrations of $CoCl_2$ induced the inactivation of PKC. The exposure of cells to $CoCl_2$ oxidized 7 of the 18 sulfhydryls detected in PKC and exposure to higher concentrations of $CoCl_2$ induced the oxidation of 3 more PKC sulfhydryls. Thus, the increasing oxidation of sulfhydryls residues decreases PKC activity. In this study, the MEK inhibitor PD98059 did not affect the activation of PKCε, but substantially decreased the activation of ERKs, CREB and neurite outgrowth induced by CoCl2. This suggests that PKCε couples the oxidative signal to the final activation of ERKs, and that there are more possible targets of oxidative modification upstream of MEK. Finally, in a context of NGF treatment, ROS produced during the first minutes activate PKCε [63], indicating that the oxidation of PKCε is an important event in the neuronal differentiation induced by NGF (Figure 2).

In primary cultures of neural precursor cells obtained from cerebral cortex, ROS control neuronal fate. In this model, those cells producing high levels of ROS were differentiated to neurons [87]. The same occurs in primary cultures of neural precursor cells obtained from the subventricular zone, where exogenous administration of H_2O_2 produced more differentiated neurons. Conversely, the inhibition of NOX or PI3K diminished the number of neurons, while the effect of the exogenous administration of H_2O_2 was abolished by the pharmacological inhibition of PI3K. Furthermore, cultures derived from KO NOX2 mice produced significantly lesser neurons than those from wild type animals [66].

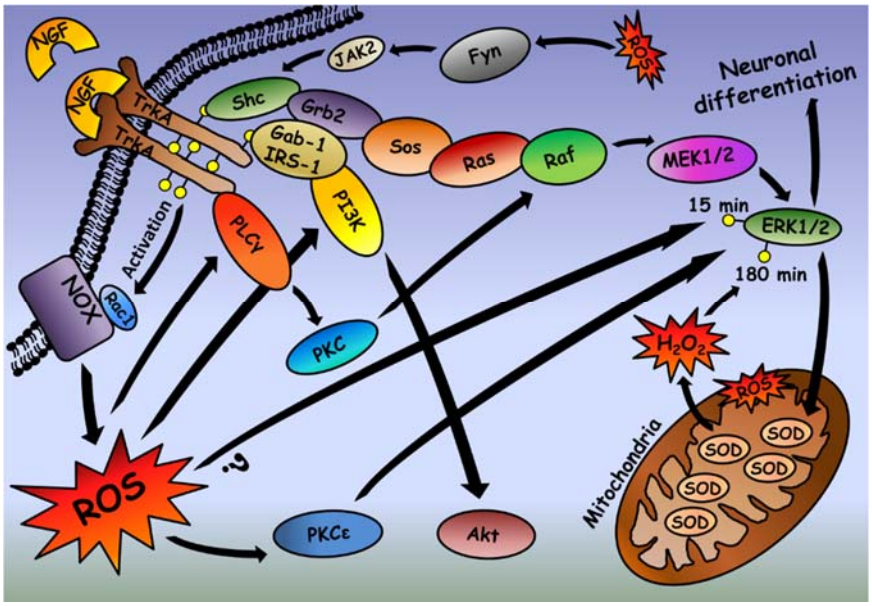

Figure 2. *Redox regulation of PC12 cells differentiation.* When PC12 cells are treated with NGF, there occurs a TrkA transphosphorylation, which induces the recruitment of adapter proteins leading to the activation of the signaling pathway Ras-Raf-MEK1/2-ERK1/2 that promotes differentiation. On the other hand, it is proposed that ROS produced by NOX induce a maximal phosphorylation of ERK at 15 min, which is crucial to induce the expression and activity of the mitochondrial MnSOD required for the conversion of superoxide anion into H2O2. The generation of H_2O_2 is necessary to generate a second peak of the phosphorylation of ERKs at 180 min. ROS generated by NOX may also induce the activation of PKC, coupling the oxidative signal to ERK activation. NGF binding to TrkA also leads to the activation of the signaling pathway PLCγ-PKC-Raf and the subsequent activation of ERK. ROS may also activate Fyn, coupling the signaling pathway Shc-Ras-Raf-MEK1/2-ERK1/2. It has also been suggested that PKC and Akt induce the activation of NOX.

Tsatmalli *et al.* also demonstrated that neuronal differentiation of neural precursor cells from cortex are influenced by ROS in multiple aspects. When neural precursor cells are selected according to their ROS production, it was found that high ROS producer cells generated neurons, while low ROS producer cells generated astrocytes, oligodendrocytes and a different type of neurons. These former neurons were classified in two types: the type 1 neurons were predominant in number (around 65%) and had pyramidal morphology, multiples neurites and fired a single action potential, while the type 2 neurons were less in proportion (around 35%), had rounded soma, less neurites and fired repetitive action potentials. When low ROS producer cells are treated with antioxidants, the proportion of the generated neurons are reverted, increasing the number of neurons type 2 (around 80%) [69]. Overall, these results strongly suggest that ROS promotes neuronal differentiation of neural precursor cells in different regions of the brain.

c) Axonal Growth and Guidance

The participation of the ROS in axonal growth is a process that has extensively been studied in the axon growth cones of *Aplysia* neurons. Munnammalai *et al*. [67] found in this model that

axonal growth cones have high concentrations of ROS, which favor the axonal growth, since the decrease of ROS by treatments with antioxidants, inhibitors of NOX or lipoxygenase decreased the axonal growth. ROS modulate different aspects of the dynamics of the actin cytoskeleton. This regulation is determined by both the ROS levels and its source, which could define the compartmentalization of ROS. For example, physiological levels of ROS promote the assembly and protrusion of the actin filaments, while the inhibition of NOX prevents this process. On the other hand, lipoxygenase inhibition influences the assembly of actin in the actin arches, but not in the filopodia [67].

In further studies, Munnammalai *et al.* [68] determined that NOX2 is localized in the plasma membrane of the axonal growth cones. The activation of NOX2 increased the levels of ROS in the P domain, while the pharmacological inhibition of NOX2 impaired actin dynamics and axonal growth. Interestingly, the localization of active NOX2 was elevated in F-actin bundles in non-stimulated growth cones, which was reduced when F-actin bundles were disrupted with cytochalasin B treatments. Finally, the activity of NOX2 was increased when neurons were grown in beds of apCAM (*Aplysia* cell adhesion molecule), which evoke growth in the apCAM zones [68], indicating that the dynamics of the axonal growth cones are importantly affected by a bidirectional relationship between actin cytoskeleton and NOX2 [68].

As mentioned, the specific localization of ROS in the axonal growth cone might affect different aspects of axonal growth cone dynamics. In this regard, Zhang *et al.* [88] characterized in *Aplysia* neurons the relationship between ROS production and calcium. In this model, calcium is elevated in the axonal growth cone in response to serotonin, which is dependent on ROS produced by NOX. This relationship involves the regulation of microtubule dynamics and ROS production dependent on Rac1. Under control conditions, nearly 13% of the neurons showed increased levels of calcium, which was increased by 80% when the constitutive active form of Rac1 was injected into the cells. This constitutive active form of Rac1 promoted the movement of microtubules and endoplasmic reticulum Ca^{2+} stores towards the P-domain of the axonal growth cone. On the other hand, the constitutive active form of Rac1 promoted ROS formation in response to serotonin, while the dominant-negative form had the opposite effect. When ROS were inhibited by antioxidants in the presence of the constitutive active form of Rac1, the observed increase of calcium release evoked by serotonin was completely blocked. Conversely, the dominant-negative of Rac1, restored calcium release when low concentration of exogenous H_2O_2 was added. This effect of ROS is dependent on IP_3 receptors, since the blockade of these receptors with xestopongin C did not restore calcium release [88]. This is in line with the idea that ROS oxidizes the IP_3 receptors, which favor calcium release [89]. Furthermore, the regulation of calcium release by ROS in the axonal growth cone might regulate axonal growth cone dynamics, since calcium has pleiotropic effects in the growth cone motility [90].

During nervous system development, neurons tend to establish the proper contact with specific targets through a complex process that is regulated by extracellular cues that guide the axons. A group of proteins that guide the axonal growth cone are the semaphorins, whose mechanisms of action requires the activation of their receptors [91], which couple specific signaling pathways that regulate repulsive axon guidance and cell migration. In dorsal root ganglion neurons, semaphorin3A induces growth cone collapse by the cytoskeleton regulation through the collapsin response mediator protein 2 (CRMP2). The phosphorylation of CRMP2 by GSK3-β and Cdk5 promotes microtubule disassembly, which produces the growth cone

collapse [92]. In these cells, Morinaka *et al.* [64] found that the phosphorylation of CRMP2 is specifically regulated by ROS. Semaphorine3A induces the generation of H_2O_2 in the axonal growth cone through the participation of the Molecule Interacting with CasL (MICAL), which oxidizes CRMP2 and induces the formation of a transient disulfide-linked homodimer between the cysteines 504 of two CRMP2 proteins. Then, this homodimer is reduced by Trx that forms a disulfide bond with one molecule of CRMP2. This complex is crucial for CRMP2 phosphorylation by GSK3-β, which ultimately produces the growth cone collapse of these neurons [64]. Together, these studies demonstrate the importance of local ROS production in developing neurons, which can affect nervous system development and the proper establishment of neuronal circuits.

d) Apoptosis and Survival

i) Trx, Grx and the MAPK Pathway,

During the last decade there has been a remarkably advance in the knowledge of the role of ROS as signal molecules involved in programmed cell death. Oxidative stress can alter the cell homeostasis at different level. For example, ROS can induce modifications of the sulfhydryl groups leading to modifications of the functional characteristics of proteins with reactive cysteine residues. This condition might be strengthened if ROS also inhibit the thioredoxin (Trx) and/or glutaredoxin (Grx) system, which are responsible for reversing the inter- or intramolecular disulfide bonds, as well as the S-glutathionylation of proteins, respectively [93].

As all redox proteins, both Trx and Grx can exist in an oxidized or reduced form, which accounts a critical feature for their interaction with other proteins. One of these proteins is ASK1, a member of the MAPKKK, which is expressed in the cytosol and mitochondria [14] and that is involved in the signaling initiated by oxidative stress that leads to apoptosis [94, 95]. Although ASK1 is involved in proliferation and differentiation in several cell types, its role in apoptosis has been the most widely characterized [96-99]. It has been proposed that ASK1 regulates the intrinsic, extrinsic and caspase-independent apoptotic pathways, which can be induced by conditions such as stimulation of death receptors, DNA damage, oxidative stress and stress of the endoplasmic reticulum [99]. ASK1 is also the target of many proteins related to survival, which bind to different domains of ASK1. Trx and Grx are part of this group of proteins. Trx binds to the N-terminal domain, while the Grx binds to the C-terminal domain of ASK1, inhibiting the activity of ASK1 [15, 24, 51].

Trx1 was the first identified negative regulator of the activity of ASK1 [15]. It has been described that under basal conditions, ASK1 forms homo-oligomers through their coiled-coil domains in the carboxyl terminal (CCC). Also, both Trx1 and 14-3-3 proteins, bind to ASK1 forming what is called the signalosome that negatively regulates ASK1 activity [52]. The 14-3-3 proteins bind to ASK1 in the phosphorylated Ser967 [94]. In response to ROS generation, Trx1 is oxidized and Cys35 and Cys32 form an intramolecular disulfide bridge with the consequent conformational change of Trx1 leading to its dissociation from ASK1 and the release of 14-3-3 proteins. Subsequently, TRAF2 and/or TRAF6, which act as positive regulators, are recruited to ASK1, which promotes the interaction between ASK1 molecules through their domains coiled-coil in the amino terminal (NCC) and allows the autophosphorylation of T845 in ASK1 and completing the ASK1 activation triggered by the

oxidative stimulus [52]. Under oxidative stress ASK1 is ubiquitinated and may be degraded; however, the peptidase USP9X promotes the deubiquitination of active ASK1 to counteract its proteasome-dependent degradation. In this way, USP9X stabilizes the activity of ASK1 [100]. Once active, ASK1 activates JNK and p38, which triggers the apoptotic cell death.

Alternatively, Nadeau *et al*. [59, 60] proposed another mechanism for Trx1 in the regulation of ASK1 in response to H_2O_2. They showed that H_2O_2 induces ASK1 oxidation leading to the formation of multimers of ASK1 linked by disulfide bonds. They also identified the Cys250 in ASK1 as the critical residue for JNK activation in response to H_2O_2-induced oxidative stress. When they mutated the Cys250 of ASK1, the binding of ASK1 to Trx1 was blocked; however, although the ASK1 multimers linked by disulfide bridges are still formed, no longer phosphorylation in T845 (related to activation) and downstream activation of the MAPKs pathway is observed.

These results suggest that the dissociation of ASK1 from Trx1 is not enough to promote ASK1 signaling, but it is required the oxidation of the Cys250 of ASK1 to induce a conformational change that allows the activation of the protein [59, 60]. It is necessary more experimental evidences to understand the role that plays the Cys250 in the activation of ASK1 in response to H_2O_2.

In cerebellar granule neurons it has been shown that staurosporine (Sts) and potassium deprivation (K5) cause apoptotic death [101, 102]. In addition, both K5 and Sts induce the generation of ROS, which is transient and occurs during the 4 h after treatment [101, 103]. In this regard, it was found that K5 activated both ASK1-JNK-cJun and ASK1-p38-ATF2 pathways, where ROS acted upstream ASK1 [101, 102]. On the other hand, Sts induced apoptotic death only through the ASK1-p38-ATF2 pathway, indicating that ROS generated by Sts seems to act at a different level [102].

On the other hand, it has been observed that the overexpression of Grx protects cells from metabolic oxidative stress induced by glucose deprivation by a mechanism that suppresses the redox activation of ASK1 and its targets downstream, including the JNK pathway [24, 55]**.** These results support the hypothesis that the Grx-ASK1 interaction sensitive to the redox state is regulated by the Grx through the regulation of the intracellular glutathione-dependent redox reactions that involve the participation of H_2O_2 [24]. The oxidative stress induced by glucose deprivation can activate ASK1 through two different pathways: the glutathione-dependent Grx-ASK1 and the Trx-ASK1 independent of glutathione. It is proposed that the release of either Grx or Trx is sufficient for activating ASK1 [55].

It has been observed that the knockdown of ASK1 protects the neuronal cells SHSY5Y from L-DOPA-induced apoptosis [104, 105]. These results support the idea that the possible regulation of Grx of apoptosis induced by oxidants in neurons is mediated via ASK1. However, there are many potential effectors for ASK1 activation and many of them are also sensitive to oxidation and potential targets of Grx; therefore, additional studies are needed to outline the specific role of Grx under this condition [106].

The reversible inactivation of PTEN has also been described in studies using H_2O_2 or ROS produced by NOX in macrophages [61, 62]. As already mentioned, Trx1, in its reduced state, directly binds to PTEN in a redox-dependent way to inhibit its phosphatase activity on PIP_3, resulting in an increase in the activity of Akt [26]. Akt binds to PIP_3 through their PH domains (domains of homology to pleckstrine), which allows that PDK1 phosphorylates Akt T803 (PDK2 phosphorylates the Ser473), leading to full Akt activation. In this regard, it is proposed that under basal conditions PTEN is active, carrying out the dephosphorylation of PIP_3, and

therefore decreasing the Akt activity. Under oxidative stress, Trx1 binds PTEN avoiding PIP_3 dephosphorylation and inducing a constitutive activation of Akt, which triggers the antiapoptotic signals.

As mentioned previously, under oxidative stress, Trx1 oxidizes and releases from ASK1. Therefore it is possible that Trx1, once reduced by the Thioredoxin reductase 1 (TrxR1), binds PTEN generating survival signals to counteract the apoptotic signals triggered by ASK1. The inhibition of ROS-dependent phosphatase activity of PTEN also suggests that ROS produced under pathological conditions could contribute to the apoptosis inhibition and subsequent formation of tumors in the nervous system.

ii) Redox Regulation of Akt

As mentioned above, it is known that Akt is sensitive to the redox state and that the oxidative modification of the Akt reactive cysteines are critical for its activity [29, 31, 57, 58]. Also, H_2O_2 induces the formation of disulfide bridges between Cys297 and Cys311 in Akt, as well as the subsequent dephosphorylation mediated by PP2A. Overexpression of Grx reduces Akt, which abolishes its binding to PP2A, then allowing a sustained Akt phosphorylation, inducing an inhibition of apoptosis in cardiac cells [29], indicating an antiapoptotic action of Grx through a redox regulation of Akt. Interestingly, it has been found that inactive Akt is fully oxidized, while the active form is only partially oxidized. In this regard, it was recently reported that ROS produced by NOX1 oxidize the Akt reactive cysteines promoting its interaction with PP2A, which inhibits Akt and therefore induces apoptosis in cardiomyocytes [57].

In the nervous system, it has been found that mice treated with MPTP, a neurotoxin which selectively damage dopaminergic neurons from the ventral midbrain, the critical cysteines of Akt are oxidized, increasing its association with PP2A, and therefore lowering the levels of Akt selectively phosphorylated. The presence of antioxidants fully reversed these effects [58]. Grx1 overexpression in primary neurons derived from human stem cells maintains the reduced state of Akt and inhibits the MPTP-mediated loss of phosphorylation [58], indicating that the preservation of the redox homeostasis by the overexpression of Grx1 can preserve the levels of phosphorylated Akt.

On the other hand, the inhibition of Akt induces an activation of p38 and JNK that promotes apoptosis, whereas active Akt directly phosphorylates ASK1 Ser83, which leads to apoptosis inhibition [107]. Min and collaborators [108] proposed that the regulation of Akt on ASK1 for the control of apoptosis occurs through the interaction between Hsp90, Akt and ASK1 to keep ASK1 in an inactive state. They suggest that this interaction allows Akt to be in the proximity of the N-terminal domain of ASK1 to phosphorylate it in the Ser83. In response to an apoptotic condition, such as H_2O_2, the Hsp90-Akt-ASK1 complex becomes more stable, since Akt moves to the ASK1 C-terminal domain, which causes a decrease in the phosphorylation of the Ser83 and the subsequent activation of ASK1 that activates p38 pathways and/or JNK leading to apoptosis.

In this model, Hsp90 would serve as a protein scaffold to keep Akt and ASK1 in proximity. Unlike Trx and Grx, Hsp90-Akt complex does not dissociate from ASK1 in response to oxidative stress, but it undergoes a conformational change that generates a more stable complex [108]. Thus, the regulation of apoptotic death through the ROS-mediated ASK1 activation is complex and represents an active research field (Figure 3).

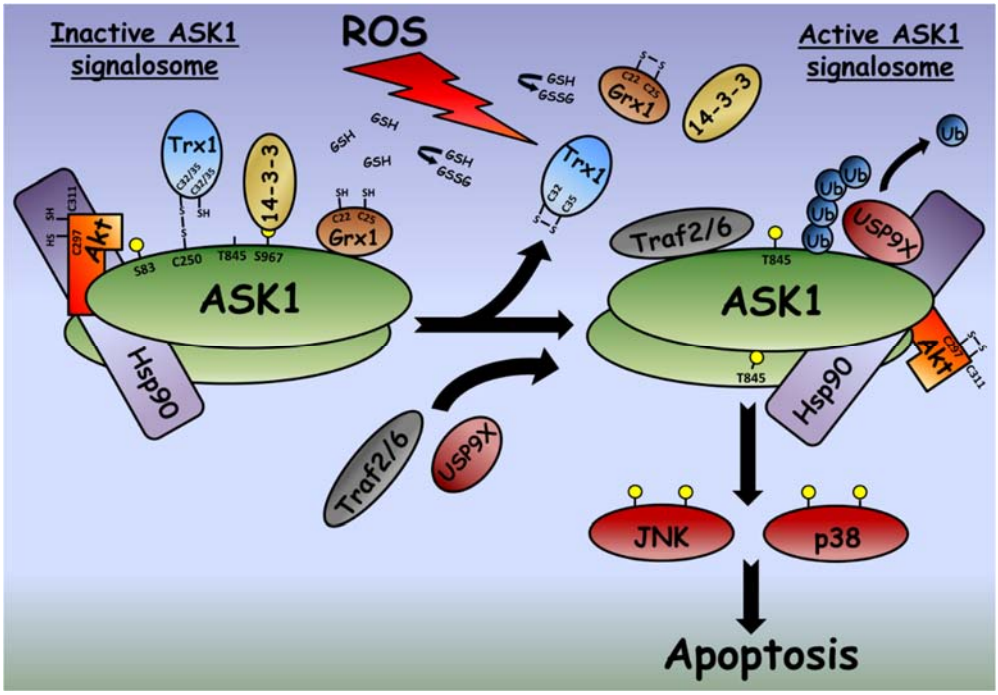

Figure 3. *Participation of the reactive oxygen species in the activation of ASK1 through its different redox sensitive controllers.* During the inactive condition, ASK1 forms homo-oligomers through their CCC domains. Each monomer binds Trx1, Grx1, 14-3-3 proteins, Akt, and Hsp90, which negatively regulate the activation of ASK1, forming the so called signalosome. HSP90 acts as a scaffold protein that maintains ASK1 bound to Akt, allowing the Ser83 ASK1 phosphorylation by Akt. Trx1 forms an intermolecular disulfide bridge with the Cys250 of ASK1, while Grx1 is attached to the c-terminus of ASK1 and 14-3-3 protein binds to the phosphorylated Ser967 of ASK1. In response to ROS generation, Trx1, Grx1 and 14-3-3 protein dissociate from ASK1 and Hsp90 and Akt undergoes a conformational rearrangement with respect to ASK1, which physically prevents that Akt negatively phosphorylates ASK1. Akt is inactivated when it forms an intramolecular disulfide bridge between the Cys297 and Cys311. Meanwhile, TRAF2 and/or TRAF6 join ASK1, which results in the homophilic interaction between the two ASK1 proteins through their NCC, allowing the autophosphorylation of T845 in ASK1. USP9X joins the signalosome and stabilizes active ASK1 by avoiding its proteasomal degradation by deubiquitination. Once ASK1 is totally active, it phosphorylates MAPKK, which in turn phosphorylates JNK and p38 MAPK, inducing apoptosis. See text for more details.

iii) TXNIP and TRX

Although most of the studies have focused on the interaction between Trx1 and cytosolic ASK1, it is also known that the mitochondrial isoform of thioredoxin (Trx2) also interacts with the mitochondrial ASK1 and inhibits its activity preventing the apoptosis induced by ASK1 in endothelial cells and hepatocytes [14, 53]**.** Trx2 has a critical role in the control of mitochondrial oxidative stress and mitochondria-dependent apoptosis [54]. Thus, Trx2 helps to repair the oxidative damage of proteins by reducing the disulfide bonds formed by the cysteines oxidation.

Unlike Trx1, Trx2 specifically regulates the JNK-independent apoptotic intrinsic pathway in vascular endothelial cells, suggesting that Trx1 and Trx2 control different apoptotic pathways [14].

On the other hand, TXNIP also known as VDUP1 (vitamin D3 up-regulated protein-1) or TBP2 (thioredoxin-binding protein-2), is a redox protein ubiquitously expressed that promotes apoptosis [56]. In mouse pancreatic beta cells, it has been described that under basal conditions, TXNIP is predominantly located in the nucleus. In response to oxidative stress, TXNIP translocates from the nucleus to the mitochondria, where it forms a complex with Trx2, removing Trx2 from ASK1. The Trx2-mediated inhibition of ASK1 elimination leads to cytochrome c release, caspase-3 activation and apoptosis [56]. The TXNIP translocation to the mitochondria induced by oxidative stress fits well with the role that TXNIP has as regulator of the redox state and the mitochondrial death pathway.

It is believed that under physiological levels of ROS, the TXNIP-Trx1 complex formation is favored. In endothelial cells, this complex translocates from the nucleus to the plasmatic membrane, activating the inflammatory processes and promoting cell survival. In this context, TXNIP acts as a scaffold protein for the transport of Trx1 to the membrane. This translocation is required, for example, to carry out the trans-activation of the VEGF type 2 receptor (VEGFR-2) mediated by H_2O_2 and the subsequent activation of ERK1/2. Here, the TXNIP-Trx1 complex acts as a redox sensitive mediator for the control of VEGFR-2 signaling, which promotes cell survival under physiological ROS levels [109]. Thus, TXNIP can function as an intermediary in the signaling depending on the cell compartment and can be proapoptotic under high concentrations of ROS or a survival protein in cells with physiological levels of ROS (Figure 4). Recently, it has been proposed the concept of "Redoxisome" to refer to the complex Trx-TXNIP as a signaling transducer relative to the redox state under normal and pathological conditions [110].

In the nervous system, the role played by these molecules and their interaction with ROS in the apoptotic death has not been explored in detail. It has been reported that the activation of ASK1 is involved in neuronal apoptosis, as occurs in NGF-deprived sympathetic neurons [111]. In addition, Trx attenuates neuronal damage [112], regulates the MAPK cascade through the suppression of ASK1 activation and increases the transcription factors activation [15]. In cerebellar granule neurons, it has been described that the TXNIP gene corresponds to the early response genes whose expression is directly regulated by the flow of calcium during neuronal apoptosis [32]. Therefore, it is possible that TXNIP regulates the MAPKs pathway forming a complex net of signal transduction in neuronal apoptosis. It is likely that these mechanisms have variations due to the fact that in other cell types TXNIP has been described as a cytosolic protein [23, 113, 114].

It is known that the overstimulation of NMDA receptors (NMDAR) leads to the generation of free radicals in neurons that causes an oxidative damage associated with neuronal death and several neurodegenerative diseases [115]. On the other hand, it has been reported that physiological synaptic activity increases the expression of antioxidant defenses (thioredoxin, peroxiredoxin and sulfiredoxin) in neurons. It was found that the blockade of the NMDAR under basal conditions promoted an increased vulnerability to oxidative insults [116].

The stimulation of the NMDAR activates the PI3K/Akt pathway leading to the phosphorylation of the transcription factor FOXO in the nucleus, causing its dissociation from the TXNIP promoter and inducing the release of FOXO from the nucleus, reducing TXNIP levels. Thus, a low TXNIP transcription results in less inhibition of Trx, and therefore promotes a neuroprotective action against oxidative damage under physiological conditions [116].

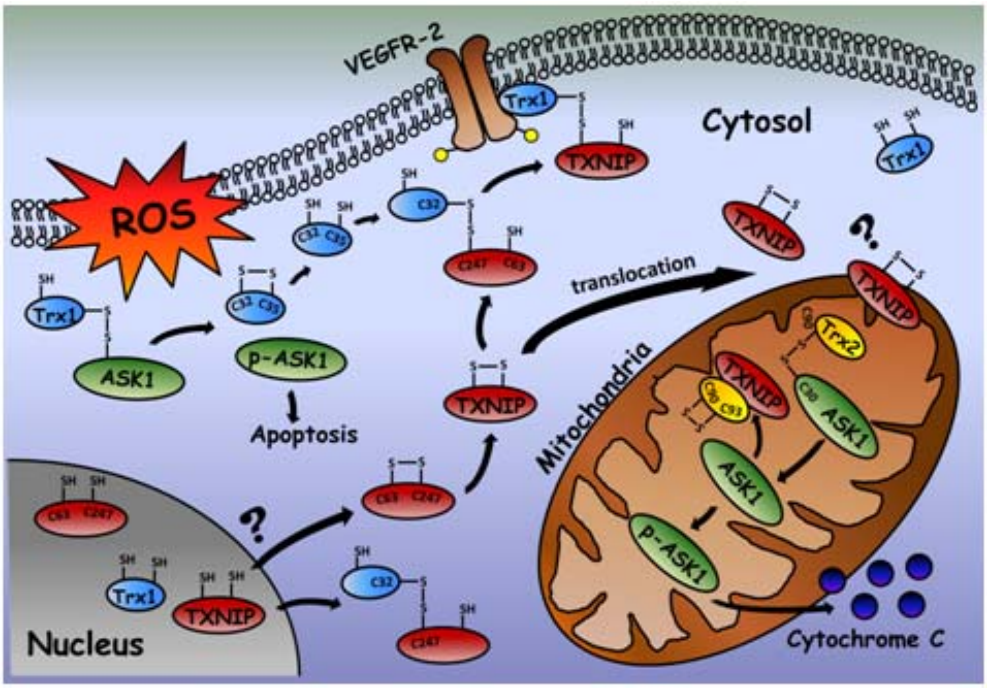

Figure 4. *Participation of TXNIP in the cascade of signal transduction that promotes survival and cell death.* Under basal conditions, TXNIP is located in the nucleus, while Trx1 is found both in the cytosol and the nucleus and Trx2 is located only in the mitochondria. The inactive form of ASK1 is located both in the cytosol (interacting with reduced Trx1), and in the mitochondria (bound to reduced Trx2). In response to oxidative stress, TXNIP translocates from the nucleus to the mitochondria, where it binds Trx2, which relieves the inhibition of ASK1 by Trx2 that is now in its oxidized form. This allows ASK1 activation in the mitochondria inducing signals that lead to apoptotic death. Meanwhile, Trx1 is oxidized and released from ASK1, which activates and induces apoptotic death. The antioxidant mechanisms activated by ROS can reduce the levels of oxidized Trx1. On the other hand, under physiological levels of ROS, the formation of the TXNIP-Trx1 complex is induced in the nucleus and in the cytosol. In the case of the VEGF receptor (VEGFR-2), this complex translocates to the membrane, where it carries out the trans-activation of the receptor, which activates ERK1/2 that promotes cell survival. See text for more details.

iv) ROS, Mitochondria and Apoptosis

The mitochondrion is one of the main sources of ROS in the cell. It has been suggested that the mitochondrial ROS are involved in several pathologies, including neurodegenerative diseases [117]. Interestingly, new mechanisms have been proposed to explain how changes in the redox state of a mitochondrial protein may lead to cell death/survival through a mechanism associated with changes in the mitochondrial morphology. It is known that dynamics of mitochondrial fusion and fragmentation regulates many mitochondrial functions necessary for cell physiology. Although the machinery that catalyzes these processes has been described, little is known about the signaling components that regulate these phenomena [118]. In this regard, in the nervous system, it is known that the inhibition of mitochondrial fission in cortical neurons blocks the ROS production and cell damage produced by inhibitors of the electron transport chain [119]. Also, the ROS overproduction observed in a condition of hyperglycemia requires an increase in mitochondrial fission [120].

Recently, it has been described that Romo1 (reactive oxygen species modulator 1) represents a fundamental element in the generation of mitochondrial ROS. Romo1 is a 79 amino acids transmembrane protein, which is located in the mitochondria and that induces the production of mitochondrial ROS through the complex III of the electron transport chain [121-123]. In this regard, Screaton and cols. [118] reported that Romo1 is sensitive to the redox state and that this molecule represents a molecular switch (or redox switch) that links ROS and the mitochondrial morphology by modulating the mitochondrial fusion and the remodeling of the mitochondrial crests. This group found that the loss of Romo1 induces the deoligomerization of OPA1 (optic atrophy 1), which is required for mitochondrial fusion. Under this condition occurs a mitochondrial crests remodeling, which increases the probability of cytochrome c release and apoptosis [124]. In spite of the evidences of Romo1 as a protein involved in the morphological modeling of mitochondria and sensitive to the redox state, there is no enough information about the direct regulation of ROS on the components of the machinery responsible for the mitochondrial fission and fusion, therefore further research on this field is required.

In addition to its role in mitochondrial fusion, it has also been suggested that Romo1 may serve as a molecular link between TNF-α and the mitochondrial ROS during TNF-α-mediated apoptosis. In this regard, the complex II of TNF-α binds to the C-terminus of Romo1, which recruits Bcl-X_L and reduces the mitochondrial membrane potential, resulting in ROS production and apoptotic cell death [125]. Since Romo1 seems to participate in the modulation of the intrinsic pathway of apoptosis, its inhibition might have therapeutic applications by promoting the apoptotic death of cancer cells and by disrupting the ROS production involved in the signaling pathways responsible for cell proliferation.

ROS AND BRAIN FUNCTION

ROS play an important role in the regulation of normal brain function. For example, ROS is a regulator of dopamine release in the striatum and in the long term potentiation (LTP) and plasticity in the hippocampus. However, the underlying mechanisms by which ROS regulate these functions are not fully understood.

a) ROS as Neuromodulator

The group of Rice has significantly contributed to the understanding of the ROS function as neuromodulators of dopamine release in nigrostriatal pathway [126-130]. This system regulates motor movement [131-134], receives synaptic inputs from the cerebral cortex, thalamus and substantia nigra [135] and the degeneration of neurons from the substantia nigra has been related to Parkinson's disease [136, 137]. Avshalumov *et al.* [126] demonstrated in coronal striatal slices that endogenous glutamate release produces H_2O_2 under physiological conditions and that the blockade of glutamate receptors produced an increase in the release of dopamine by these neurons. The effect of glutamate on dopamine release seems to be indirect [126, 127], probably mediated by H_2O_2. This is supported by the fact that dopamine release was prevented in the presence of catalase or glutathione peroxidase. On the other hand, the effect of GABA-dependent modulation of dopamine release is also mediated by H_2O_2 since

catalase completely prevented the effect of picrotoxin (a blocker of $GABA_A$ receptors). On the other hand, when endogenous glutathione peroxidase was inhibited by mercaptosuccinate, the increased H_2O_2 markedly inhibits dopamine release, an effect that was blocked by catalase [126].

The modulation of H_2O_2 on dopamine release occurs in a physiological time scale. In experiments where a single pulse of electrical stimulation elicited dopamine release, glutathione peroxidase inhibition did not have any effect on dopamine release; however, if subsequent pulses are applied, it can be appreciated a decrease in dopamine release by decreasing glutathione peroxidase with mercaptosuccinate within the first three to five electrical pulses train. Thus, H_2O_2 produced during the first pulse seems to be responsible for dopamine release inhibition elicited by the subsequent pulses. The effect of glutamate and GABA occurs in the same neurons that produce H_2O_2 since the activation of $GABA_A$ receptors has no effect when glutamate receptors are blocked, which indicates that GABA has no effect on dopamine release. Since the antioxidant enzymes catalase and glutathione peroxidase are not expected to enter the cells, their effect most be in the extracellular space. Thus the release of H_2O_2 produced by neurons in the striatum diffuse from the postsynaptic sites to inhibit the presynaptic dopamine release [126].

The activity-dependent production of H_2O_2 also occurs in neurons from substantia nigra pars compacta (SNpc). An increase in the firing rate of these neurons by depolarizing current injection induces elevated H_2O_2 levels. The presence of catalase produced an increase in the firing rate. In contrast, high concentrations of mercaptosuccinate (1 mM) produced a marked hyperpolarization and cease of firing in one population of dopamine neurons. These results can be mimicked by adding exogenous H_2O_2 (1.5 mM) which also inhibits dopamine release [128]. Thus, two groups of SNpc neurons can be distinguished by their capacity to respond to H_2O_2 [129]. Avshalumov and collaborators [129, 130] also determined that the target upon which H_2O_2 acts to modulate dopamine release are the ATP-sensitive K^+ channels (K_{ATP}). These channels are activated by a decrease in the ATP/ADP ratio and are composed by inwardly rectifying pore-forming subunits ($K_{ir}6.2$ in neurons) and sulfonylurea receptor subunits (SUR1/SUR2) [138-140].

Mitochondria seem to be the source of H_2O_2 that regulates the dopamine release in the dorsal striatum. Bao *et al.* [141] demonstrated that inhibiting mitochondrial ROS by using succinate and rotenone inhibits glutamate-dependent regulation of dopamine release. The already mentioned increased of dopamine release induced by the blockade of glutamate receptors was completely prevented in the presence of succinate and rotenone. On the other hand, an increase the levels of H_2O_2 by mercaptosuccinate produced the typical 35% decrease in the evoked dopamine release, which was completely prevented by succinate and rotenone. Together, these results indicate that mitochondria are a primary source of ROS in the glutamate-dependent modulation of dopamine release [141].

b) ROS as Regulators of Synaptic Plasticity

ROS have also been identified as regulators of synaptic plasticity. Neurons have the ability to change their activity in response to experience through a modification in the efficiency of the synapses. Long-term potentiation (LTP) and long-term depression (LTD) are two elements of synaptic plasticity in hippocampus that have been proposed as the cellular processes that are

essential for the memory and learning. LTP is a long-lasting strengthening in the efficacy of synaptic transmission, while LTD is an activity-dependent reduction in synaptic efficiency [142, 143]

The molecular mechanisms of the LTP have been widely described in the CA1 region of hippocampus. In this region, the dendrites of pyramidal neurons receive synaptic inputs from the Shaffer collaterals of the CA3 region. Different studies have addressed the effects of ROS in LTP, which are diverse and seem to be related to the concentration of H_2O_2 and/or superoxide anion. In this regard, Kamsler *et al.* [43] demonstrated that H_2O_2 (20 µM) prevented the establishment of new LTP and enhanced LTD, while H_2O_2 (1 µM) markedly increased LTP and suppressed LTD [43]. On the other hand, brief incubations of hippocampal slices with H_2O_2 promoted LTP [144], while long time incubations prevented LTP [145]. In addition, the administration of antioxidants such as catalase or cell-permeable scavengers of superoxide or H_2O_2 impaired LTP [146, 147]. These experiments demonstrate that ROS are strong regulators of LTP.

Based on different models of transgenic mice, it has been possible to comprehend more about the role of ROS in synaptic plasticity. KO NOX2 mice have deficient LTP and suffer hippocampus-dependent memory impairments, as well as a slight motor coordination impairment and motor memory alterations [148]. On the other hand, in a mouse model that overexpresses extracellular superoxide dismutase (EC-SOD), hippocampal slices fail to show LTP and the contextual fear conditioning is markedly impaired as compared to wild type mice [149]. These evidences demonstrate that the regulation of ROS during LTP is related to the consolidation of hippocampus-dependent memories. Interestingly, these findings are reverted during aging, since hippocampal slices obtained from aged EC-SOD mice exhibit an enhanced LTP in comparison with wild type mice. Furthermore, aged EC-SOD mice exhibit better hippocampus-dependent spatial learning and better cerebellum-dependent learning than in aged wild type mice, which correlates with lower levels of ROS in hippocampus and cerebellum in aged EC-SOD mice [150]. These results emphasize the changes in ROS production during the lifespan and their implications in learning and memory.

CONCLUSION

Reactive oxygen species play a critical role in cellular physiology. An increasing body of evidence supports a role of ROS as signaling agents. The regulation of physiological and pathologic processes by ROS is mediated by specific proteins mainly involved in intracellular signaling. The mechanisms by which ROS modulate these processes involve the direct oxidation of cysteine residues of several proteins involved in redox signaling. This generates disulfide bonds between cysteine residues in the same protein or between two proteins. It is noteworthy to mention that ROS actions depend on the cellular context, as well as the specific time and particular location of ROS produced. This represents a very fine mechanism of regulation that also involves the antioxidant systems, the ROS sources and the target proteins. Direct oxidative modification of cysteines leads to the activation of specific signaling pathways that modify different physiological processes such as proliferation, neuronal differentiation, axonal growth and guidance and apoptosis. This can occur in a time scale that goes from minutes to hours, but also in the order of seconds, as it occurs in the oxidation of receptors and

channels. The importance of these studies underlie in our comprehension of nervous system function, as well as the redox biology. There are still many gaps in our knowledge about the mechanisms of action involving ROS as signaling molecules. Thus, many studies should be addressed to solve these subjects.

ACKNOWLEDGMENTS

This work was partially supported by a grant from DGAPA-PAPIIT, UNAM, México (IN206213) and from CONACYT, México (179234).

REFERENCES

[1] Droge W. Free radicals in the physiological control of cell function. *Physiological reviews,* 2002;82(1):47-95.

[2] Valko M., Leibfritz D., Moncol J., Cronin M. T., Mazur M., Telser J. Free radicals and antioxidants in normal physiological functions and human disease. *The international journal of biochemistry and cell biology,* 2007;39(1):44-84.

[3] Tonks N. K. Redox redux: revisiting PTPs and the control of cell signaling. *Cell,* 2005;121(5):667-70.

[4] Pourova J., Kottova M., Voprsalova M., Pour M. Reactive oxygen and nitrogen species in normal physiological processes. *Acta physiologica,* 2010;198(1):15-35.

[5] Kamata H., Hirata H. Redox regulation of cellular signalling. *Cellular signalling,* 1999;11(1):1-14.

[6] Day A. M., Brown J. D., Taylor S. R., Rand J. D., Morgan B. A., Veal E. A. Inactivation of a peroxiredoxin by hydrogen peroxide is critical for thioredoxin-mediated repair of oxidized proteins and cell survival. *Molecular cell,* 2012;45(3):398-408.

[7] Jonsson T. J., Lowther W. T. The peroxiredoxin repair proteins. *Sub-cellular biochemistry,* 2007;44:115-41.

[8] Finkel T. Signal transduction by reactive oxygen species. *The Journal of cell biology,* 2011;194(1):7-15.

[9] Lo Conte M., Carroll K. S. The redox biochemistry of protein sulfenylation and sulfinylation. *The Journal of biological chemistry,* 2013;288(37):26480-8.

[10] Rinna A., Torres M., Forman H. J. Stimulation of the alveolar macrophage respiratory burst by ADP causes selective glutathionylation of protein tyrosine phosphatase 1B. *Free radical biology and medicine,* 2006;41(1):86-91.

[11] Forman H. J., Fukuto J. M., Torres M. Redox signaling: thiol chemistry defines which reactive oxygen and nitrogen species can act as second messengers. *American journal of physiology Cell physiology,* 2004;287(2):C246-56.

[12] Forman H. J., Ursini F., Maiorino M. An overview of mechanisms of redox signaling. *Journal of molecular and cellular cardiology,* 2014.

[13] Cross J. V., Templeton D. J. Regulation of signal transduction through protein cysteine oxidation. *Antioxidants and redox signaling,* 2006;8(9-10):1819-27.

[14] Zhang R., Al-Lamki R., Bai L., Streb J. W., Miano J. M., Bradley J., et al. Thioredoxin-2 inhibits mitochondria-located ASK1-mediated apoptosis in a JNK-independent manner. *Circulation research,* 2004;94(11):1483-91.

[15] Saitoh M., Nishitoh H., Fujii M., Takeda K., Tobiume K., Sawada Y., et al. Mammalian thioredoxin is a direct inhibitor of apoptosis signal-regulating kinase (ASK) 1. *The EMBO journal,* 1998;17(9):2596-606.

[16] Holmgren A. Thioredoxin structure and mechanism: conformational changes on oxidation of the active-site sulfhydryls to a disulfide. *Structure,* 1995;3(3):239-43.

[17] Roos G., Garcia-Pino A., Van Belle K., Brosens E., Wahni K., Vandenbussche G., et al. The conserved active site proline determines the reducing power of Staphylococcus aureus thioredoxin. *Journal of molecular biology,* 2007;368(3):800-11.

[18] Chrestensen C. A., Eckman C. B., Starke D. W., Mieyal J. J. Cloning, expression and characterization of human thioltransferase (glutaredoxin) in E. coli. *FEBS letters,* 1995;374(1):25-8.

[19] Yang Y., Jao S., Nanduri S., Starke D. W., Mieyal J. J., Qin J. Reactivity of the human thioltransferase (glutaredoxin) C7S, C25S, C78S, C82S mutant and NMR solution structure of its glutathionyl mixed disulfide intermediate reflect catalytic specificity. *Biochemistry,* 1998;37(49):17145-56.

[20] Chai Y. C., Ashraf S. S., Rokutan K., Johnston R. B., Jr., Thomas J. A. S-thiolation of individual human neutrophil proteins including actin by stimulation of the respiratory burst: evidence against a role for glutathione disulfide. *Archives of biochemistry and biophysics,* 1994;310(1):273-81.

[21] Ciriolo M. R., Palamara A. T., Incerpi S., Lafavia E., Bue M. C., De Vito P., et al. Loss of GSH, oxidative stress, and decrease of intracellular pH as sequential steps in viral infection. *The Journal of biological chemistry,* 1997;272(5):2700-8.

[22] Liu Y., Min W. Thioredoxin promotes ASK1 ubiquitination and degradation to inhibit ASK1-mediated apoptosis in a redox activity-independent manner. *Circulation research,* 2002;90(12):1259-66.

[23] Junn E., Han S. H., Im J. Y., Yang Y., Cho E. W., Um H. D., et al. Vitamin D3 up-regulated protein 1 mediates oxidative stress via suppressing the thioredoxin function. *Journal of immunology,* 2000;164(12):6287-95.

[24] Song J. J., Rhee J. G., Suntharalingam M., Walsh S. A., Spitz D. R., Lee Y. J. Role of glutaredoxin in metabolic oxidative stress. Glutaredoxin as a sensor of oxidative stress mediated by H2O2. *The Journal of biological chemistry,* 2002;277(48):46566-75.

[25] Lee S. R., Yang K. S., Kwon J., Lee C., Jeong W., Rhee S. G. Reversible inactivation of the tumor suppressor PTEN by H2O2. *The Journal of biological chemistry,* 2002;277(23):20336-42.

[26] Meuillet E. J., Mahadevan D., Berggren M., Coon A., Powis G. Thioredoxin-1 binds to the C2 domain of PTEN inhibiting PTEN's lipid phosphatase activity and membrane binding: a mechanism for the functional loss of PTEN's tumor suppressor activity. *Archives of biochemistry and biophysics,* 2004;429(2):123-33.

[27] Patwari P., Higgins L. J., Chutkow W. A., Yoshioka J., Lee R. T. The interaction of thioredoxin with Txnip. Evidence for formation of a mixed disulfide by disulfide exchange. *The Journal of biological chemistry,* 2006;281(31):21884-91.

[28] Hwang J., Suh H. W., Jeon Y. H., Hwang E., Nguyen L. T., Yeom J., et al. The structural basis for the negative regulation of thioredoxin by thioredoxin-interacting protein. *Nature communications,* 2014;5:2958.

[29] Murata H., Ihara Y., Nakamura H., Yodoi J., Sumikawa K., Kondo T. Glutaredoxin exerts an antiapoptotic effect by regulating the redox state of Akt. *The Journal of biological chemistry,* 2003;278(50):50226-33.

[30] Sundaresan M., Yu Z. X., Ferrans V. J., Irani K., Finkel T. Requirement for generation of H2O2 for platelet-derived growth factor signal transduction. *Science,* 1995;270(5234):296-9.

[31] Wani R., Qian J., Yin L., Bechtold E., King S. B., Poole L. B., et al. Isoform-specific regulation of Akt by PDGF-induced reactive oxygen species. *Proceedings of the National Academy of Sciences of the United States of America,* 2011;108(26):10550-5.

[32] Bernardini S., Bernassola F., Cortese C., Ballerini S., Melino G., Motti C., et al. Modulation of GST P1-1 activity by polymerization during apoptosis. *Journal of cellular biochemistry,* 2000;77(4):645-53.

[33] Adler V., Yin Z., Fuchs S. Y., Benezra M., Rosario L., Tew K. D., et al. Regulation of JNK signaling by GSTp. *The EMBO journal,* 1999;18(5):1321-34.

[34] Templeton D. J., Aye M. S., Rady J., Xu F., Cross J. V. Purification of reversibly oxidized proteins (PROP) reveals a redox switch controlling p38 MAP kinase activity. *PloS one,* 2010;5(11):e15012.

[35] Galli S., Antico Arciuch V. G., Poderoso C., Converso D. P., Zhou Q., Bal de Kier Joffe E., et al. Tumor cell phenotype is sustained by selective MAPK oxidation in mitochondria. *PloS one,* 2008;3(6):e2379.

[36] Trachootham D., Lu W., Ogasawara M. A., Nilsa R. D., Huang P. Redox regulation of cell survival. *Antioxidants and redox signaling,* 2008;10(8):1343-74.

[37] Groeger G., Quiney C., Cotter T. G. Hydrogen peroxide as a cell-survival signaling molecule. *Antioxidants and redox signaling,* 2009;11(11):2655-71.

[38] Liu Y., Li M., Warburton R. R., Hill N. S., Fanburg B. L. The 5-HT transporter transactivates the PDGFbeta receptor in pulmonary artery smooth muscle cells. *FASEB journal : official publication of the Federation of American Societies for Experimental Biology,* 2007;21(11):2725-34.

[39] Moody T. W., Osefo N., Nuche-Berenguer B., Ridnour L., Wink D., Jensen R. T. Pituitary adenylate cyclase-activating polypeptide causes tyrosine phosphorylation of the epidermal growth factor receptor in lung cancer cells. *The Journal of pharmacology and experimental therapeutics,* 2012;341(3):873-81.

[40] Huang Y. Z., McNamara J. O. Neuroprotective effects of reactive oxygen species mediated by BDNF-independent activation of TrkB. *The Journal of neuroscience : the official journal of the Society for Neuroscience,* 2012;32(44):15521-32.

[41] Huang E. J., Reichardt L. F. Neurotrophins: roles in neuronal development and function. *Annual review of neuroscience,* 2001;24:677-736.

[42] Kruk J. S., Vasefi M. S., Heikkila J. J., Beazely M. A. Reactive oxygen species are required for 5-HT-induced transactivation of neuronal platelet-derived growth factor and TrkB receptors, but not for ERK1/2 activation. *PloS one,* 2013;8(9):e77027.

[43] Kamsler A., Segal M. Hydrogen peroxide modulation of synaptic plasticity. *The Journal of neuroscience : the official journal of the Society for Neuroscience,* 2003;23(1):269-76.

[44] Lee J. W., Kim J. E., Park E. J., Kim J. H., Lee C. H., Lee S. R., et al. Two conserved cysteine residues are critical for the enzymic function of the human platelet-derived growth factor receptor-beta: evidence for different roles of Cys-822 and Cys-940 in the kinase activity. *The Biochemical journal*, 2004;382(Pt 2):631-9.

[45] Goldkorn T., Balaban N., Matsukuma K., Chea V., Gould R., Last J., et al. EGF-Receptor phosphorylation and signaling are targeted by H2O2 redox stress. *American journal of respiratory cell and molecular biology*, 1998;19(5):786-98.

[46] Bae Y. S., Kang S. W., Seo M. S., Baines I. C., Tekle E., Chock P. B., et al. Epidermal growth factor (EGF)-induced generation of hydrogen peroxide. Role in EGF receptor-mediated tyrosine phosphorylation. *The Journal of biological chemistry*, 1997; 272(1): 217-21.

[47] Paulsen C. E., Truong T. H., Garcia F. J., Homann A., Gupta V., Leonard S. E., et al. Peroxide-dependent sulfenylation of the EGFR catalytic site enhances kinase activity. *Nature chemical biology*, 2012;8(1):57-64.

[48] Kang D. H., Lee D. J., Lee K. W., Park Y. S., Lee J. Y., Lee S. H., et al. Peroxiredoxin II is an essential antioxidant enzyme that prevents the oxidative inactivation of VEGF receptor-2 in vascular endothelial cells. *Molecular cell*, 2011;44(4):545-58.

[49] Kemble D. J., Sun G. Direct and specific inactivation of protein tyrosine kinases in the Src and FGFR families by reversible cysteine oxidation. *Proceedings of the National Academy of Sciences of the United States of America*, 2009;106(13):5070-5.

[50] Giannoni E., Buricchi F., Raugei G., Ramponi G., Chiarugi P. Intracellular reactive oxygen species activate Src tyrosine kinase during cell adhesion and anchorage-dependent cell growth. *Molecular and cellular biology*, 2005;25(15):6391-403.

[51] Liu H., Nishitoh H., Ichijo H., Kyriakis J. M. Activation of apoptosis signal-regulating kinase 1 (ASK1) by tumor necrosis factor receptor-associated factor 2 requires prior dissociation of the ASK1 inhibitor thioredoxin. *Molecular and cellular biology*, 2000;20(6):2198-208.

[52] Shiizaki S., Naguro I., Ichijo H. Activation mechanisms of ASK1 in response to various stresses and its significance in intracellular signaling. *Advances in biological regulation*, 2013;53(1):135-44.

[53] Lim P. L., Liu J., Go M. L., Boelsterli U. A. The mitochondrial superoxide/thioredoxin-2/Ask1 signaling pathway is critically involved in troglitazone-induced cell injury to human hepatocytes. *Toxicological sciences : an official journal of the Society of Toxicology*, 2008;101(2):341-9.

[54] Tanaka T., Hosoi F., Yamaguchi-Iwai Y., Nakamura H., Masutani H., Ueda S., et al. Thioredoxin-2 (TRX-2) is an essential gene regulating mitochondria-dependent apoptosis. *The EMBO journal*, 2002;21(7):1695-703.

[55] Song J. J., Lee Y. J. Differential role of glutaredoxin and thioredoxin in metabolic oxidative stress-induced activation of apoptosis signal-regulating kinase 1. *The Biochemical journal*, 2003;373(Pt 3):845-53.

[56] Saxena G., Chen J., Shalev A. Intracellular shuttling and mitochondrial function of thioredoxin-interacting protein. *The Journal of biological chemistry*, 2010;285(6):3997-4005.

[57] Matsuno K., Iwata K., Matsumoto M., Katsuyama M., Cui W., Murata A., et al. NOX1/NADPH oxidase is involved in endotoxin-induced cardiomyocyte apoptosis. *Free radical biology and medicine*, 2012;53(9):1718-28.

[58] Durgadoss L., Nidadavolu P., Valli R. K., Saeed U., Mishra M., Seth P., et al. Redox modification of Akt mediated by the dopaminergic neurotoxin MPTP, in mouse midbrain, leads to down-regulation of pAkt. *FASEB journal : official publication of the Federation of American Societies for Experimental Biology*, 2012;26(4):1473-83.

[59] Nadeau P. J., Charette S. J., Landry J. REDOX reaction at ASK1-Cys250 is essential for activation of JNK and induction of apoptosis. *Molecular biology of the cell*, 2009;20(16):3628-37.

[60] Nadeau P. J., Charette S. J., Toledano M. B., Landry J. Disulfide Bond-mediated multimerization of Ask1 and its reduction by thioredoxin-1 regulate H(2)O(2)-induced c-Jun NH(2)-terminal kinase activation and apoptosis. *Molecular biology of the cell*, 2007;18(10):3903-13.

[61] Kwon J., Lee S. R., Yang K. S., Ahn Y., Kim Y. J., Stadtman E. R., et al. Reversible oxidation and inactivation of the tumor suppressor PTEN in cells stimulated with peptide growth factors. *Proceedings of the National Academy of Sciences of the United States of America*, 2004;101(47):16419-24.

[62] Leslie N. R., Bennett D., Lindsay Y. E., Stewart H., Gray A., Downes C. P. Redox regulation of PI 3-kinase signalling via inactivation of PTEN. *The EMBO journal*, 2003;22(20):5501-10.

[63] Gopalakrishna R., Gundimeda U., Schiffman J. E., McNeill T. H. A direct redox regulation of protein kinase C isoenzymes mediates oxidant-induced neuritogenesis in PC12 cells. *The Journal of biological chemistry*, 2008;283(21):14430-44.

[64] Morinaka A., Yamada M., Itofusa R., Funato Y., Yoshimura Y., Nakamura F., et al. Thioredoxin mediates oxidation-dependent phosphorylation of CRMP2 and growth cone collapse. *Science signaling*, 2011;4(170):ra26.

[65] Coyoy A., Olguin-Albuerne M., Martinez-Briseno P., Moran J. Role of reactive oxygen species and NADPH-oxidase in the development of rat cerebellum. *Neurochemistry international*, 2013;62(7):998-1011.

[66] Le Belle J. E., Orozco N. M., Paucar A. A., Saxe J. P., Mottahedeh J., Pyle A. D., et al. Proliferative Neural Stem Cells Have High Endogenous ROS Levels that Regulate Self-Renewal and Neurogenesis in a PI3K/Akt-Dependant Manner. *Cell Stem Cell*, 2011;8(1):59-71.

[67] Munnamalai V., Suter D. M. Reactive oxygen species regulate F-actin dynamics in neuronal growth cones and neurite outgrowth. *Journal of neurochemistry*, 2009; 108(3): 644-61.

[68] Munnamalai V., Weaver C. J., Weisheit C. E., Venkatraman P., Agim Z. S., Quinn M. T., et al. Bidirectional interactions between NOX2-type NADPH oxidase and the F-actin cytoskeleton in neuronal growth cones. *Journal of neurochemistry*, 2014.

[69] Tsatmali M., Walcott E. C., Makarenkova H., Crossin K. L. Reactive oxygen species modulate the differentiation of neurons in clonal cortical cultures. *Molecular and cellular neurosciences*, 2006;33(4):345-57.

[70] Celotto A. M., Liu Z., Vandemark A. P., Palladino M. J. A novel Drosophila SOD2 mutant demonstrates a role for mitochondrial ROS in neurodevelopment and disease. *Brain and behavior*, 2012;2(4):424-34.

[71] Yoneyama M., Kawada K., Gotoh Y., Shiba T., Ogita K. Endogenous reactive oxygen species are essential for proliferation of neural stem/progenitor cells. *Neurochemistry international*, 2010;56(6-7):740-6.

[72] Limoli C. L., Rola R., Giedzinski E., Mantha S., Huang T. T., Fike J. R. Cell-density-dependent regulation of neural precursor cell function. *Proceedings of the National Academy of Sciences of the United States of America,* 2004;101(45):16052-7.

[73] Leslie N. R. The redox regulation of PI 3-kinase-dependent signaling. *Antioxidants and redox signaling,* 2006;8(9-10):1765-74.

[74] Patapoutian A., Reichardt L. F. Trk receptors: mediators of neurotrophin action. *Current opinion in neurobiology,* 2001;11(3):272-80.

[75] Kaplan D. R., Miller F. D. Neurotrophin signal transduction in the nervous system. *Current opinion in neurobiology,* 2000;10(3):381-91.

[76] Katoh S., Mitsui Y., Kitani K., Suzuki T. Hyperoxia induces the neuronal differentiated phenotype of PC12 cells via a sustained activity of mitogen-activated protein kinase induced by Bcl-2. *The Biochemical journal,* 1999;338 (Pt 2):465-70.

[77] Kamata H., Oka S., Shibukawa Y., Kakuta J., Hirata H. Redox regulation of nerve growth factor-induced neuronal differentiation of PC12 cells through modulation of the nerve growth factor receptor, TrkA. *Archives of biochemistry and biophysics,* 2005;434(1):16-25.

[78] Aikawa R., Komuro I., Yamazaki T., Zou Y., Kudoh S., Tanaka M., et al. Oxidative stress activates extracellular signal-regulated kinases through Src and Ras in cultured cardiac myocytes of neonatal rats. *The Journal of clinical investigation,* 1997;100(7): 1813-21.

[79] Abe J., Berk B. C. Fyn and JAK2 mediate Ras activation by reactive oxygen species. *The Journal of biological chemistry,* 1999;274(30):21003-10.

[80] Dey N., Howell B. W., De P. K., Durden D. L. CSK negatively regulates nerve growth factor induced neural differentiation and augments AKT kinase activity. *Experimental cell research,* 2005;307(1):1-14.

[81] Obara Y., Labudda K., Dillon T. J., Stork P. J. PKA phosphorylation of Src mediates Rap1 activation in NGF and cAMP signaling in PC12 cells. *Journal of cell science,* 2004;117(Pt 25):6085-94.

[82] Suzukawa K., Miura K., Mitsushita J., Resau J., Hirose K., Crystal R., et al. Nerve growth factor-induced neuronal differentiation requires generation of Rac1-regulated reactive oxygen species. *The Journal of biological chemistry,* 2000;275(18):13175-8.

[83] Ibi M., Katsuyama M., Fan C., Iwata K., Nishinaka T., Yokoyama T., et al. NOX1/NADPH oxidase negatively regulates nerve growth factor-induced neurite outgrowth. *Free radical biology and medicine,* 2006;40(10):1785-95.

[84] Sampath D., Jackson G. R., Werrbach-Perez K., Perez-Polo J. R. Effects of nerve growth factor on glutathione peroxidase and catalase in PC12 cells. *Journal of neurochemistry,* 1994;62(6):2476-9.

[85] Jackson G. R., Sampath D., Werrbach-Perez K., Perez-Polo J. R. Effects of nerve growth factor on catalase and glutathione peroxidase in a hydrogen peroxide-resistant pheochromocytoma subclone. *Brain research,* 1994;634(1):69-76.

[86] Cassano S., Agnese S., D'Amato V., Papale M., Garbi C., Castagnola P., et al. Reactive oxygen species, Ki-Ras, and mitochondrial superoxide dismutase cooperate in nerve growth factor-induced differentiation of PC12 cells. *The Journal of biological chemistry,* 2010;285(31):24141-53.

[87] Tsatmali M., Walcott E. C., Crossin K. L. Newborn neurons acquire high levels of reactive oxygen species and increased mitochondrial proteins upon differentiation from progenitors. *Brain research,* 2005;1040(1-2):137-50.

[88] Zhang X. F., Forscher P. Rac1 modulates stimulus-evoked Ca(2+) release in neuronal growth cones via parallel effects on microtubule/endoplasmic reticulum dynamics and reactive oxygen species production. *Molecular biology of the cell,* 2009;20(16): 3700-12.

[89] Joseph S. K., Nakao S. K., Sukumvanich S. Reactivity of free thiol groups in type-I inositol trisphosphate receptors. *The Biochemical journal,* 2006;393(Pt 2):575-82.

[90] Henley J., Poo M. M. Guiding neuronal growth cones using Ca2+ signals. *Trends in cell biology,* 2004;14(6):320-30.

[91] Sharma A., Verhaagen J., Harvey A. R. Receptor complexes for each of the Class 3 Semaphorins. *Frontiers in cellular neuroscience,* 2012;6:28.

[92] Zhou Y., Gunput R. A., Pasterkamp R. J. Semaphorin signaling: progress made and promises ahead. *Trends in biochemical sciences,* 2008;33(4):161-70.

[93] Mieyal J. J., Gallogly M. M., Qanungo S., Sabens E. A., Shelton M. D. Molecular mechanisms and clinical implications of reversible protein S-glutathionylation. *Antioxidants and redox signaling,* 2008;10(11):1941-88.

[94] Goldman E. H., Chen L., Fu H. Activation of apoptosis signal-regulating kinase 1 by reactive oxygen species through dephosphorylation at serine 967 and 14-3-3 dissociation. *The Journal of biological chemistry,* 2004;279(11):10442-9.

[95] Ichijo H., Nishida E., Irie K., ten Dijke P., Saitoh M., Moriguchi T., et al. Induction of apoptosis by ASK1, a mammalian MAPKKK that activates SAPK/JNK and p38 signaling pathways. *Science,* 1997;275(5296):90-4.

[96] Chang H. Y., Nishitoh H., Yang X., Ichijo H., Baltimore D. Activation of apoptosis signal-regulating kinase 1 (ASK1) by the adapter protein Daxx. *Science,* 1998;281(5384):1860-3.

[97] Hatai T., Matsuzawa A., Inoshita S., Mochida Y., Kuroda T., Sakamaki K., et al. Execution of apoptosis signal-regulating kinase 1 (ASK1)-induced apoptosis by the mitochondria-dependent caspase activation. *The Journal of biological chemistry,* 2000;275(34):26576-81.

[98] Charette S. J., Lambert H., Landry J. A kinase-independent function of Ask1 in caspase-independent cell death. *The Journal of biological chemistry,* 2001;276(39): 36071-4.

[99] Nishitoh H., Matsuzawa A., Tobiume K., Saegusa K., Takeda K., Inoue K., et al. ASK1 is essential for endoplasmic reticulum stress-induced neuronal cell death triggered by expanded polyglutamine repeats. *Genes and development,* 2002;16(11):1345-55.

[100] Nagai H., Noguchi T., Homma K., Katagiri K., Takeda K., Matsuzawa A., et al. Ubiquitin-like sequence in ASK1 plays critical roles in the recognition and stabilization by USP9X and oxidative stress-induced cell death. *Molecular cell,* 2009;36(5):805-18.

[101] Ramiro-Cortes Y., Moran J. Role of oxidative stress and JNK pathway in apoptotic death induced by potassium deprivation and staurosporine in cerebellar granule neurons. *Neurochemistry international,* 2009;55(7):581-92.

[102] Ramiro-Cortes Y., Guemez-Gamboa A., Moran J. Reactive oxygen species participate in the p38-mediated apoptosis induced by potassium deprivation and staurosporine in cerebellar granule neurons. *The international journal of biochemistry and cell biology,* 2011;43(9):1373-82.

[103] Valencia A., Moran J. Role of oxidative stress in the apoptotic cell death of cultured cerebellar granule neurons. *Journal of neuroscience research,* 2001;64(3):284-97.

[104] Sabens E. A., Distler A. M., Mieyal J. J. Levodopa deactivates enzymes that regulate thiol-disulfide homeostasis and promotes neuronal cell death: implications for therapy of Parkinson's disease. *Biochemistry*, 2010;49(12):2715-24.

[105] Liedhegner E. A., Steller K. M., Mieyal J. J. Levodopa activates apoptosis signaling kinase 1 (ASK1) and promotes apoptosis in a neuronal model: implications for the treatment of Parkinson's disease. *Chemical research in toxicology*, 2011;24(10): 1644-52.

[106] Allen E. M., Mieyal J. J. Protein-thiol oxidation and cell death: regulatory role of glutaredoxins. *Antioxidants and redox signaling*, 2012;17(12):1748-63.

[107] Kim A. H., Khursigara G., Sun X., Franke T. F., Chao M. V. Akt phosphorylates and negatively regulates apoptosis signal-regulating kinase 1. *Molecular and cellular biology*, 2001;21(3):893-901.

[108] Zhang R., Luo D., Miao R., Bai L., Ge Q., Sessa W. C., et al. Hsp90-Akt phosphorylates ASK1 and inhibits ASK1-mediated apoptosis. *Oncogene*, 2005;24(24): 3954-63.

[109] World C., Spindel O. N., Berk B. C. Thioredoxin-interacting protein mediates TRX1 translocation to the plasma membrane in response to tumor necrosis factor-alpha: a key mechanism for vascular endothelial growth factor receptor-2 transactivation by reactive oxygen species. *Arteriosclerosis, thrombosis, and vascular biology*, 2011;31(8):1890-7.

[110] Yoshihara E., Masaki S., Matsuo Y., Chen Z., Tian H., Yodoi J. Thioredoxin/Txnip: Redoxisome, as a Redox Switch for the Pathogenesis of Diseases. *Frontiers in immunology*, 2014;4:514.

[111] Kanamoto T., Mota M., Takeda K., Rubin L. L., Miyazono K., Ichijo H., et al. Role of apoptosis signal-regulating kinase in regulation of the c-Jun N-terminal kinase pathway and apoptosis in sympathetic neurons. *Molecular and cellular biology*, 2000;20(1): 196-204.

[112] Takagi Y., Mitsui A., Nishiyama A., Nozaki K., Sono H., Gon Y., et al. Overexpression of thioredoxin in transgenic mice attenuates focal ischemic brain damage. *Proceedings of the National Academy of Sciences of the United States of America*, 1999; 96(7): 4131-6.

[113] Schulze P. C., Yoshioka J., Takahashi T., He Z., King G. L., Lee R. T. Hyperglycemia promotes oxidative stress through inhibition of thioredoxin function by thioredoxin-interacting protein. *The Journal of biological chemistry*, 2004;279(29):30369-74.

[114] Schulze P. C., De Keulenaer G. W., Yoshioka J., Kassik K. A., Lee R. T. Vitamin D3-upregulated protein-1 (VDUP-1) regulates redox-dependent vascular smooth muscle cell proliferation through interaction with thioredoxin. *Circulation research*, 2002;91(8):689-95.

[115] Lipton S. A. NMDA receptor activity regulates transcription of antioxidant pathways. *Nature neuroscience*, 2008;11(4):381-2.

[116] Papadia S., Soriano F. X., Leveille F., Martel M. A., Dakin K. A., Hansen H. H., et al. Synaptic NMDA receptor activity boosts intrinsic antioxidant defenses. *Nature neuroscience*, 2008;11(4):476-87.

[117] Federico A., Cardaioli E., Da Pozzo P., Formichi P., Gallus G. N., Radi E. Mitochondria, oxidative stress and neurodegeneration. *Journal of the neurological sciences*, 2012;322(1-2):254-62.

[118] Norton M., Ng A. C., Baird S., Dumoulin A., Shutt T., Mah N., et al. ROMO1 is an essential redox-dependent regulator of mitochondrial dynamics. *Science signaling*, 2014;7(310):ra10.

[119] Liot G., Bossy B., Lubitz S., Kushnareva Y., Sejbuk N., Bossy-Wetzel E. Complex II inhibition by 3-NP causes mitochondrial fragmentation and neuronal cell death via an NMDA- and ROS-dependent pathway. *Cell death and differentiation*, 2009; 16(6): 899-909.

[120] Yu T., Robotham J. L., Yoon Y. Increased production of reactive oxygen species in hyperglycemic conditions requires dynamic change of mitochondrial morphology. *Proceedings of the National Academy of Sciences of the United States of America*, 2006;103(8):2653-8.

[121] Chung Y. M., Kim J. S., Yoo Y. D. A novel protein, Romo1, induces ROS production in the mitochondria. *Biochemical and biophysical research communications*, 2006; 347(3): 649-55.

[122] Chung Y. M., Lee S. B., Kim H. J., Park S. H., Kim J. J., Chung J. S., et al. Replicative senescence induced by Romo1-derived reactive oxygen species. *The Journal of biological chemistry*, 2008;283(48):33763-71.

[123] Lee S. B., Kim J. J., Kim T. W., Kim B. S., Lee M. S., Yoo Y. D. Serum deprivation-induced reactive oxygen species production is mediated by Romo1. *Apoptosis : an international journal on programmed cell death*, 2010;15(2):204-18.

[124] Scorrano L., Ashiya M., Buttle K., Weiler S., Oakes S. A., Mannella C. A., et al. A distinct pathway remodels mitochondrial cristae and mobilizes cytochrome c during apoptosis. *Developmental cell*, 2002;2(1):55-67.

[125] Kim J. J., Lee S. B., Park J. K, Yoo Y. D. TNF-alpha-induced ROS production triggering apoptosis is directly linked to Romo1 and Bcl-X(L). *Cell death and differentiation*, 2010;17(9):1420-34.

[126] Avshalumov M. V., Chen B. T., Marshall S. P., Pena D. M., Rice M. E. Glutamate-dependent inhibition of dopamine release in striatum is mediated by a new diffusible messenger, H2O2. *The Journal of neuroscience : the official journal of the Society for Neuroscience*, 2003;23(7):2744-50.

[127] Avshalumov M. V., Patel J. C., Rice M. E. AMPA receptor-dependent H2O2 generation in striatal medium spiny neurons but not dopamine axons: one source of a retrograde signal that can inhibit dopamine release. *Journal of neurophysiology*, 2008;100(3):1590-601.

[128] Chen B. T., Avshalumov M. V., Rice M. E. H(2)O(2) is a novel, endogenous modulator of synaptic dopamine release. *Journal of neurophysiology*, 2001;85(6):2468-76.

[129] Avshalumov M. V., Chen B. T., Koos T., Tepper J. M., Rice M. E. Endogenous hydrogen peroxide regulates the excitability of midbrain dopamine neurons via ATP-sensitive potassium channels. *The Journal of neuroscience : the official journal of the Society for Neuroscience*, 2005;25(17):4222-31.

[130] Avshalumov M. V., Rice M. E. Activation of ATP-sensitive K+ (K(ATP)) channels by H2O2 underlies glutamate-dependent inhibition of striatal dopamine release. *Proceedings of the National Academy of Sciences of the United States of America*, 2003;100(20):11729-34.

[131] Gruber A. J., McDonald R. J. Context, emotion, and the strategic pursuit of goals: interactions among multiple brain systems controlling motivated behavior. *Frontiers in behavioral neuroscience*, 2012;6:50.

[132] Yin H. H., Knowlton B. J. The role of the basal ganglia in habit formation. *Nature reviews Neuroscience*, 2006;7(6):464-76.

[133] Palmiter R. D. Dopamine signaling in the dorsal striatum is essential for motivated behaviors: lessons from dopamine-deficient mice. *Annals of the New York Academy of Sciences*, 2008;1129:35-46.

[134] Balleine B. W., Delgado M. R., Hikosaka O. The role of the dorsal striatum in reward and decision-making. *The Journal of neuroscience : the official journal of the Society for Neuroscience*, 2007;27(31):8161-5.

[135] Nakano K., Kayahara T., Tsutsumi T., Ushiro H. Neural circuits and functional organization of the striatum. *Journal of neurology*, 2000;247 Suppl. 5:V1-15.

[136] Hernandes M. S., Britto L. R. NADPH oxidase and neurodegeneration. *Current neuropharmacology*, 2012;10(4):321-7.

[137] Valencia A., Sapp E., Kimm J. S., McClory H., Reeves P. B., Alexander J., et al. Elevated NADPH oxidase activity contributes to oxidative stress and cell death in Huntington's disease. *Human molecular genetics*, 2013;22(6):1112-31.

[138] Stephan D., Winkler M., Kuhner P., Russ U., Quast U. Selectivity of repaglinide and glibenclamide for the pancreatic over the cardiovascular K(ATP) channels. *Diabetologia*, 2006;49(9):2039-48.

[139] Ashcroft S. J., Ashcroft F. M. Properties and functions of ATP-sensitive K-channels. *Cellular signalling*, 1990;2(3):197-214.

[140] Babenko A. P., Aguilar-Bryan L., Bryan J. A view of sur/KIR6.X, KATP channels. *Annual review of physiology*, 1998;60:667-87.

[141] Bao L., Avshalumov M. V., Patel J. C., Lee C. R., Miller E. W., Chang C. J., et al. Mitochondria are the source of hydrogen peroxide for dynamic brain-cell signaling. The *Journal of neuroscience : the official journal of the Society for Neuroscience*, 2009;29(28):9002-10.

[142] Dan Y., Poo M. M. Spike timing-dependent plasticity of neural circuits. *Neuron*, 2004;44(1):23-30.

[143] Raymond C. R. Different requirements for action potentials in the induction of different forms of long-term potentiation. *The Journal of physiology*, 2008;586(7):1859-65.

[144] Katsuki H., Nakanishi C., Saito H., Matsuki N. Biphasic effect of hydrogen peroxide on field potentials in rat hippocampal slices. *European journal of pharmacology*, 1997; 337(2-3):213-8.

[145] Auerbach J. M., Segal M. Peroxide modulation of slow onset potentiation in rat hippocampus. *The Journal of neuroscience : the official journal of the Society for Neuroscience*, 1997;17(22):8695-701.

[146] Thiels E., Urban N. N., Gonzalez-Burgos G. R., Kanterewicz B. I., Barrionuevo G., Chu C. T., et al. Impairment of long-term potentiation and associative memory in mice that overexpress extracellular superoxide dismutase. *The Journal of neuroscience : the official journal of the Society for Neuroscience*, 2000;20(20):7631-9.

[147] Klann E. Cell-permeable scavengers of superoxide prevent long-term potentiation in hippocampal area CA1. *Journal of neurophysiology*, 1998;80(1):452-7.

[148] Kishida K. T., Hoeffer C. A., Hu D., Pao M., Holland S. M., Klann E. Synaptic plasticity deficits and mild memory impairments in mouse models of chronic granulomatous disease. *Molecular and cellular biology*, 2006;26(15):5908-20.

[149] Thiels E., Klann E. Hippocampal memory and plasticity in superoxide dismutase mutant mice. *Physiology and behavior*, 2002;77(4-5):601-5.

[150] Hu D., Serrano F., Oury T. D., Klann E. Aging-dependent alterations in synaptic plasticity and memory in mice that overexpress extracellular superoxide dismutase. The *Journal of neuroscience: the official journal of the Society for Neuroscience*, 2006; 26(15):3933-41.